Engineering and functional characterisation of pentameric concatenated $(\alpha4)_2(\beta2)_3$ and $(\alpha4)_3(\beta2)_2$ nicotinic acetylcholine receptors

Anna Lisa Carbone

A thesis submitted in partial fulfilment of the requirements of Oxford Brookes University for the degree of Doctor of Philosophy

PhD Thesis
May 2009

THE FOLLOWING HAVE NOT BEEN COPIED ON INSTRUCTION FROM THE UNIVERSITY

Illustrations on pages

7

9

12

19

28

45

Vado
con l'anima prona
e incerta
a fendere l'aria
che mi separa dal mondo,
incontro ai misteri
lasciati dal vento
e distendo le ali
per lidi ignoti,
per nuovi approdi.

Vincenzo Carbone

To my family
and all the special people
who have supported me
in these years

List of Publications

Carbone AL, Moroni M, Groot-Kormelink P, Bermudez I. (2009)
'Pentameric concatenated $(\alpha4)_2(\beta2)_3$ and $(\alpha4)_3(\beta2)_2$ nicotinic acetylcholine receptors: position of β2_α4 interfaces in the concatamers determines functional expression. Br J Pharmacol. 156(6):970-81.

Moroni M, Vijayan R, **Carbone A**, Zwart R, Biggins PC, Bermudez I. (2008)
Non-agonist-binding subunit interfaces confer distinct functional signatures to the alternate stoichiometries of the alpha4beta2 nicotinic receptor: an alpha4-alpha4 interface is required for Zn^{2+} potentiation. J Neurosci. 28(27):6884-94.

Zwart R, **Carbone AL**, Moroni M, Bermudez I, Mogg AJ, Folly EA, Broad LM, Williams AC, Zhang D, Ding C, Heinz BA, Sher E. (2008)
Sazetidine-A is a potent and selective agonist at native and recombinant alpha 4 beta 2 nicotinic acetylcholine receptors. Mol Pharmacol. 73(6):1838-43

Manuscripts in preparation:

Carbone AL, Moroni M, Bermudez I. ADNFLE-linked mutations alter the stoichiometry of α4β2 nAChRs

Poster Presentations:

- Ligand-gated ion channels – 18th neuropharmacology conference, Washington DC, USA, November 2008

  'Alternate α4β2 nicotinic acetylcholine receptors of defined subunit composition and arrangement'.

- Society for Neuroscience Meeting, Washington DC, USA, 2008

  'Effect of nitration on cytisine at central nicotinic acetylcholine receptors'.

- Nicotinic Acetylcholine Receptor Meeting, Cambridge, UK, 2008

  'Alternate α4β2 nicotinic acetylcholine receptors of defined subunit composition and arrangement'.

- British Pharmacological Society Winter Meeting, Brighton, UK, 2007

  'Alternate alpha4beta2 nicotinic acetylcholine receptors of defined subunit composition and arrangement'.

- Society for Neuroscience Meeting, S. Diego, CA, 2007

  Sfn Satellite Symposium - Nicotinic Acetylcoline Receptors as a Therapeutic Targets – Emerging Frontiers in Basic Research and Clinical Science, San Diego, CA 2007

  'Functional and radioligand binding properties of alternative stoichiometries of human alpha4beta2 nAChRs'.

- Ion Channels and Diseases of Electrically Excitable Cells, The Fifth Oxion Day, September 2007, Oxford, University of Oxford, UK

- 16th BNA National Meeting, Harrogate, UK 2007

  'Functional and radioligand binding properties of alternative stoichiometries of human alpha4beta2 nAChRs'. British Neusci. Assoc. Abstr., Vol 19 P29.06, 2007

- Ion Channels and Diseases of Electrically Excitable Cells, The fourth Oxion Day, September 2006, Oxford, University of Oxford, UK

Abstract

Neuronal nicotinic acetylcholine receptors (nAChRs) are ligand-gated ion channels that influence neurotransmitter release, hence constituting a key component of the physiological mechanisms of neuronal signalling. This thesis is concerned with the properties of the α4β2 nAChR, the most abundant nAChR in the brain, and the major contributor to the central effects of nicotine. The α4β2 nAChR is made up of five subunits, which in heterologous systems can assemble into at least two different stoichiometries: the high sensitivity (HS) $(\alpha4)_2(\beta2)_3$ stoichiometry and the low sensitivity (LS) $(\alpha4)_3(\beta2)_2$ stoichiometry, which might both exist in native tissues. Despite the attractiveness of the α4β2 nAChR as a target for therapeutic intervention, progress in the development of α4β2 nAChR-selective drugs has been slowed, partly because of the lack of stoichiometric-specific receptor models.

This study presents a strategy to express homogenous populations of α4β2 nAChRs with fixed stoichiometry. By using standard molecular biological techniques, pentameric concatenated $(\alpha4)_2(\beta2)_3$ and $(\alpha4)_3(\beta2)_2$ nAChRs were engineered. These receptors were expressed in *Xenopus laevis* oocytes and functional studies showed that their functional properties resembled those of their non-linked counterparts. Subsequent site-directed mutagenesis in combination with functional analysis allowed the identification of the agonist-binding subunits in both concatamers.

Concatenated receptors proved to be suitable for comparative studies of the effects of receptor mutation linked to autosomal dominant nocturnal frontal lobe epilepsy. Studies carried out on non-linked receptors, showed that the properties of the $(\alpha4)_3(\beta2)_2$ stoichiometry were affected more markedly than those of the $(\alpha4)_2(\beta2)_3$ stoichiometry. Insertion of the mutation in concatenated receptors revealed that the mutation not only affected the functional properties of α4β2 nAChRs but also altered the subunit composition of the receptor.

These studies show that pentameric concatenated constructs are a powerful tool to study the function and structure of receptors that assemble in multimeric types in expression systems.

CHAPTER 1. INTRODUCTION 1

1.1 Synaptic transmission 2

1.2 Nicotinic acetylcholine receptors 6

1.3 Structure of *Torpedo* nAChRs 6

1.4 The acetylcholine binding site 8

1.5 Gating of the nAChR channel 13

1.6 The ion channel pore 17

1.6.1 Charge selectivity filter 19

1.7 Desensitisation of nAChRs 21

1.8 Role of the M3-M4 intracellular loop 22

1.9 Neuronal nAChRs 23

1.10 Subunit assembly and receptor diversity 24

1.11 Stoichiometry of neuronal nAChRs 25

1.12 Distribution of nAChRs in the mammalian brain 27

1.13 Non-neuronal localisation of nAChRs 31

1.14 Biophysical properties of neuronal nAChRs 32

1.15 Pharmacology of neuronal nAChR 33

1.15.1 Agonists 34

1.15.2 Competitive antagonists 35

1.15.3 Allosteric modulators 37

1.16 Physiological functions of native nAChRs 39

1.16.1 Neuronal nAChR are predominantly presynaptic receptors 40

1.16.2 Postsynaptic receptors 41

1.16.3 Role of neuronal nAChR in non-neuronal cells 42

1.17 Upregulation of nAChRs 42

1.18 nAChRs and nicotine addiction 44

1.19 nAChRs in ageing and neurodegenerative diseases 46

1.20 nAChRs in schizophrenia and mood and attention disorders 47

1.21 nAChRs and nociception 48

1.22. Role of nAChRs in epilepsy 48

1.23 The α4β2 nAChR 49

1.24 Concatenation of subunit for the study of LGICs 51

THESIS SYNOPSIS 53

AIM OF THE THESIS 54

CHAPTER 2. MATERIALS AND METHODS 55

2.1 Reagents 56

2.2 Animals 56

2.3 Molecular Biology 56

2.4 Single Point Mutations 57

2.5 Construction of concatenated receptors 58

2.6 Insertion of mutations in concatenated receptors 59

2.7 *In vitro* transcription of concatenated receptors 59

2.8 *Xenopus laevis* oocytes preparation 60

2.9 Microinjection of cDNA and cRNA 60

2.10 Electrophysiological Recordings 61

2.11 Time course of desensitisation 62

2.12 Study of Zn^{2+} sensitivity and Ca^{2+} permeability 62

2.13 Western Blot Assay 63

2.14 Data Analysis 64

CHAPTER 3. PENTAMERIC CONCATENATED $(\alpha4)_2(\beta2)_3$ AND $(\alpha4)_3(\beta2)_2$ NICOTINIC ACETYLCHOLINE RECEPTORS: SUBUNIT ARRANGEMENT DETERMINES FUNCTIONAL EXPRESSION 66

3.1 Introduction 67

3.2 Experimental procedures 69

3.2.1 Overall strategy 70

3.2.2 Modification of plasmid expression vectors to host pentameric constructs 70

3.2.3 Subcloning of single subunits into modified pcDNA3.1 Hygro(-) 71

3.2.4 cDNA and cRNA injection in *Xenopus* oocytes. 74

3.3 Results 75

3.3.1 The pharmacological profile of $\beta2_{(Q8)}\beta2_{(Q8)}\alpha4_{(Q8)}\beta2_{(Q8)}\alpha4$ and $\beta2_{(Q8)}\alpha4_{(Q8)}\alpha4_{(Q8)}\beta2_{(Q8)}\alpha4$ is different from that of their non-linked counterpart 76

3.3.2 $\beta2_{(Q8)}\beta2_{(Q8)}\alpha4_{(Q8)}\beta2_{(Q8)}\alpha4$ and $\beta2_{(Q8)}\alpha4_{(Q8)}\alpha4_{(Q8)}\beta2_{(Q8)}\alpha4$ receptors are degraded during synthesis 80

3.3.3 Functional expression of $\beta2_{(AGS)}\beta2_{(AGS)}\alpha4_{(AGS)}\beta2_{(AGS)}\alpha4$ and $\beta2_{(AGS)}\alpha4_{(AGS)}\alpha4_{(AGS)}\beta2_{(AGS)}\alpha4$ concatamers is very poor 81

3.3.4 β2_α4_β2_α4_β2 and β2_α4_β2_α4_α4 concatamers recapitulate non-linked $(\alpha4)_2(\beta2)_3$ or $(\alpha4)_3(\beta2)_2$ properties 82

3.3.5 Sensitivity of β2_α4_β2_α4_β2 and β2_α4_β2_α4_α4 concatenated receptors to Zn^{2+} activation and Ca^{2+} permeability 90

3.3.6 Chaperone 14-3-3 increases functional expression of β2_α4_β2_α4_α4 and β2_α4_β2_α4_β2 constructs 92

3.4 Discussion 94

CHAPTER 4. IDENTIFICATION OF AGONIST BINDING SUBUNITS IN LINKED $(\alpha4)_2(\beta2)_3$ AND $(\alpha4)_3(\beta2)_2$ RECEPTORS 100

4.1 Introduction 101

4.2 Experimental procedures 102

4.2.1 cDNA constructs and mutagenesis 102

4.2.2 Injection of cDNAs constructs into *Xenopus* oocytes 102

4.2.3 Electrophysiological protocols 102

4.3 Results 104

4.3.1 Effect of mutations implicated in agonist binding on non-linked $(\alpha4)_2(\beta2)_3$ and $(\alpha4)_3(\beta2)_2$ nAChRs 105

4.3.2 Agonist binding β2 subunits in β2_α4_β2_α4_β2 receptors 109

4.3.3 Localisation of the agonist binding α4 subunits in β2_α4_β2_α4_α4 nAChRs 111

4.4 Discussion 114

CHAPTER 5. ADNFLE-LINKED MUTATIONS ALTER THE STOICHIOMETRY OF α4β2 nAChRs 118

5.1 Introduction 119

5.2 Experimental procedures 121

5.2.1 cDNA constructs and mutagenesis 121

5.2.2 Injection of cDNAs constructs into *Xenopus* oocytes 121

5.2.3 Electrophysiological protocols 121

5.3 Results 123

5.3.1 Effect of a leucine insertion in the M2 domain of the α4 subunit on the expression of α4β2 nAChRs 124

5.3.2 $\alpha4^{776insL}$ mutation increases sensitivity to ACh of the $(\alpha4)_3(\beta2)_2$ stoichiometry 125

5.3.3 Desensitisation of $\alpha4^{776insL}$ mutant α4β2 nAChRs 126

5.3.4 $\alpha4^{776insL}$ mutation decreases the Ca^{2+} permeability of the $(\alpha4)_3(\beta2)_2$ nAChR 128

5.3.5 Agonists efficacy at $\alpha4^{776insL}$ mutant receptors 128

5.3.6 Use of the L9'T reporter mutation to determine the stoichiometry of mutant receptors 129

5.3.7 Expression of the $\alpha4^{776insL}$ mutation in concatenated $(\alpha4)_2(\beta2)_3$ and $(\alpha4)_3(\beta2)_2$ receptors 131

5.4 Discussion 134

GENERAL DISCUSSION 140

References 144

Appendix 1 179

List of Tables

Chapter 3

Table 3.1	Functional properties of glutamine-linked $(\alpha4)_2(\beta2)_3$ and $(\alpha4)_3(\beta2)_2$ receptors	79
Table 3.2	Functional properties of β2_α4_β2_α4_β2 and non-linked $(\alpha4)_2(\beta2)_3$ nAChRs	88
Table 3.3	Functional properties of β2_α4_β2_α4_α4 and non-linked $(\alpha4)_3(\beta2)_2$ nAChRs	189

Chapter 4

Table 4.1	Functional effects of alanine mutants of conserved aromatic residues in non-linked $(\alpha4)_2(\beta2)_3$ and $(\alpha4)_3(\beta2)_2$ receptors	108

Chapter 5

Table 5.1	Time constant of current decay of wild type and $\alpha4^{776insL}$ α4β2 nAChRs	127
Table 5.2	Effects of TM2 L9'T mutation on the functional effects of ACh on wild type and mutant $(\alpha4)_2(\beta2)_3$ and $(\alpha4)_3(\beta2)_2$ receptors	131

Appendix 1

Table A.1	Primers used for concatenation of $\beta2_{(Q8)}\beta2_{(Q8)}\alpha4_{(Q8)}\beta2_{(Q8)}\alpha4$ and $\beta2_{(Q8)}\alpha4_{(Q8)}\alpha4_{(Q8)}\beta2_{(Q8)}\alpha4$ receptors	179
Table A.2	Primers for concatenation of $\beta2_{(AGS)}\beta2_{(AGS)}\alpha4_{(AGS)}\beta2_{(AGS)}\alpha4$ and $\beta2_{(AGS)}\alpha4_{(AGS)}\alpha4_{(AGS)}\beta2_{(AGS)}\alpha4$ receptors	182
Table A.3	Primers for concatenation of $\beta2_{(AGS)}\alpha4_{(AGS)}\beta2_{(AGS)}\alpha4_{(AGS)}\beta2$ and $\beta2_{(AGS)}\alpha4_{(AGS)}\beta2_{(AGS)}\alpha4_{(AGS)}\alpha4$ receptors	185

List of Figures

Chapter 1

Fig. 1.1	Electron microscopy structure of *Torpedo* nAChR at 4 Å resolution. Side view of the α1 subunit	7
Fig. 1.2	Top view of the extracellular domain involved in the ACh binding site in the muscle-type nAChR	9
Fig. 1.3	Crystal structure of *Lymnaea stagnalis* AChBP at 2.7 Å resolutior Side view of AChBP protomer from outside the pentameric ring	12
Fig. 1.4	A model for the structural and functional organization of the ion channel	19
Fig. 1.5	Distribution of nAChR subtypes in the nervous system	28
Fig. 1.6	Modulation of DA release in the VTA by nAChRs	45

Chapter 3

Fig. 3.1	Diagram showing the experimental approach used to create concatenated α4β2 receptors	73
Fig. 3.2	Expression of pentameric concatamers with subunit order of $\beta2_{(Q8)}\beta2_{(Q8)}\alpha4_{(Q8)}\beta2_{(Q8)}\alpha4$ and $\beta2_{(Q8)}\alpha4_{(Q8)}\alpha4_{(Q8)}\beta2_{(Q8)}\alpha4$ in *Xenopus* oocytes	76
Fig. 3.3	$\beta2_{(Q8)}\beta2_{(Q8)}\alpha4_{(Q8)}\beta2_{(Q8)}\alpha4$ and $\beta2_{(Q8)}\alpha4_{(Q8)}\alpha4_{(Q8)}\beta2_{(Q8)}\alpha4$ receptors have ACh sensitivity similar to that of receptors expressed from monomeric constructs	77
Fig. 3.4	The pharmacological profile of $\beta2_{(Q8)}\beta2_{(Q8)}\alpha4_{(Q8)}\beta2_{(Q8)}\alpha4$ and $\beta2_{(Q8)}\alpha4_{(Q8)}\alpha4_{(Q8)}\beta2_{(Q8)}\alpha4$ receptors is different from that of non-linked α4β2 receptors	78
Fig. 3.5	Western blot analysis of $\beta2_{(Q8)}\beta2_{(Q8)}\alpha4_{(Q8)}\beta2_{(Q8)}\alpha4$ and $\beta2_{(Q8)}\alpha4_{(Q8)}\alpha4_{(Q8)}\beta2_{(Q8)}\alpha4$ receptors shows the presence of breakdown products	80
Fig. 3.6	Western blot analysis of $\beta2_{(AGS)}\beta2_{(AGS)}\alpha4_{(AGS)}\beta2_{(AGS)}\alpha4$ and $\beta2_{(AGS)}\alpha4_{(AGS)}\alpha4_{(AGS)}\beta2_{(AGS)}\alpha4$ receptors	82
Fig. 3.7	Expression level of β2_α4_β2_α4_β2 and β2_α4_β2_α4_ α4 pentameric in *Xenopus* oocytes	83
Fig. 3.8	Western blot analysis of β2_α4_β2_α4_β2 and β2_α4_β2_α4_α4 expressed in *Xenopus* oocytes	84
Fig. 3.9	$(\alpha4)_3(\beta2)_2$ and $(\alpha4)_2(\beta2)_3$ nAChRs expressed from the pentameric construct have ACh similar to those of receptors expressed from monomeric constructs	85
Fig. 3.10	Functional sensitivity of concatenated and non-linked $(\alpha4)_2(\beta2)_3$ and $(\alpha4)_3(\beta2)_2$ nAChR to α4β2-preferring ligands	87

Fig. 3.11	Concentration-response curves of the α4β2-preferring antagonist DhβE on the function of concatenated α4β2 receptors	90
Fig. 3.12	Zn^{2+} sensitivity of concatenated $(\alpha4)_3(\beta2)_2$ and $(\alpha4)_2(\beta2)_3$ nAChRs expressed heterologously in *Xenopus* oocytes	91
Fig. 3.13	Ca^{2+} permeability of concatenated $(\alpha4)_3(\beta2)_2$ and $(\alpha4)_2(\beta2)_3$ nAChRs expressed heterologously in *Xenopus* oocytes	92
Fig. 3.14	Chaperone 14-3-3 increases functional expression of concatenated $(\alpha4)_3(\beta2)_2$ and $(\alpha4)_2(\beta2)_3$ nAChRs	93
Chapter 4		
Fig. 4.1	ACh I_{max} currents in wild-type (w.t.) or mutant non-linked $(\alpha4)_2(\beta2)_3$ and $(\alpha4)_3(\beta2)_2$ nAChRs	106
Fig. 4.2	Effects of alanine mutants of conserved aromatic residues on the sensitivity of non-linked to activation by ACh	106
Fig. 4.3	Effects of alanine mutants of conserved aromatic residues on the sensitivity of non-linked α4β2 nAChRs to activation by epibatidine	107
Fig. 4.4	Effects of $\beta2^{W82A}$ on ACh sensitivity of β2_α4_β2_α4_β2 receptors	110
Fig. 4.5	Functional effects of $\alpha4^{Y230A}$ on the sensitivity to activation of β2_α4_β2_α4_α4 concatamers by epibatidine	111
Fig. 4.6	Zn^{2+} sensitivity of wild type and mutant β2_α4_β2_α4_α4 receptors	113
Fig. 4.7	Effects of $\alpha4^{E224A}$ on the ACh sensitivity of wild type and mutant β2_α4_β2_α4_α4 receptors	113
Chapter 5		
Fig. 5.1	Expression levels of mutant $(\alpha4^{776insL})_2(\beta2)_3$ and $(\alpha4^{776insL})_3(\beta2)_2$ receptors in *Xenopus* oocytes	124
Fig. 5.2	Western blot analysis of total expression levels of α4 and β2 nAChR subunits in wild type and mutant receptors	125
Fig. 5.3	The mutation affect the ACh sensitivity of the two stoichiometries to a different extent	126
Fig. 5.4	ACh evoked inward currents in wild type and mutant non-linked α4β2 nAChR	127
Fig. 5.5	Ca^{2+} permeability of non-linked $(\alpha4^{776insL})_3(\beta2)_2$ and $(\alpha4^{776insL})_2(\beta2)_3$ nAChRs expressed heterologously in *Xenopus* oocytes	128
Fig. 5.6	Effect of the $\alpha4^{776insL}$ mutation on agonists efficacies of α4β2 receptors	129
Fig. 5.7	Effect of inserting a L9'T mutation in the β2 subunit in$(\alpha4^{776insL})_3(\beta2)_2$ and $(\alpha4^{776insL})_2(\beta2)_3$ nAChRs	131

Fig. 5.8 Expression level of concatenated $(\alpha4^{776insL})_2(\beta2)_3$ and $(\alpha4^{776insL})_3(\beta2)_2$ receptors in *Xenopus* oocytes 132

Fig. 5.9 ACh concentration-response curves for concatenated $\alpha4^{776insL}\beta2$ receptors 133

List of abbreviations

α-Btx	α-bungarotoxin
α-Ctx	α-conotoxin
5-HT	serotonin
ACh	acetylcholine
AChBP	acetylcholine binding protein
AD	Alzheimer's disease
ADNFLE	autosomal dominant nocturnal frontal lobe epilepsy
AMP	adenosine monophosphate
APL	allosterically potentiating ligands
C-terminus	carboxy-terminus
cDNA	complementary deoxyribose nucleic acid
CI	confidence interval
CNS	central nervous system
cRNA	complementary ribonucleic acid
DA	dopamine
dNTP	deoxyribonucleotide triphosphate
DhβE	dihydro-β-erythroidine
DMSO	dimethylsulphoxide
d-TC	*d*-tubocurarine
EC_{50}	concentration producing half maximal effect
ECD	extra-cellular domain
EDTA	ethylenediaminetetraacetic acid
FRET	fluorescence resonance energy transfer
GABA	γ-aminobutyric acid
HEPES	N-2-hydroxyethylpiperazine-N'-2-ethansulphonic acid
HS	high sensitivity
IC_{50}	concentration producing half maximal inhibition
LGIC	ligand gated ion channel
LS	low sensitivity
MCS	multiple cloning site
MLA	methylycaconitine
N-terminus	amino-terminus
NA	noradrenaline
nAChR	nicotinic acetylcholine receptor
NBM	nucleus basalis of Meyer
NCI	non-competitive inhibitors
nHill	Hill coefficient
NMDA	n-methyl-D-aspartic acid
OCB	open channel blocker
PBS	phosphate buffer saline
PCR	polymerase chain reaction
PD	Parkinson's disease
PKA	protein kinase A
PMSF	phenylmethanesulfonyl fluoride
PNS	peripheral nervous system
VGCC	voltage-gated calcium channel
VTA	ventral tegmental area
ZAC	zinc-activated channels

CHAPTER 1

INTRODUCTION

1.1 Synaptic transmission

Nerve cells differ from other cells in the body in their ability to communicate rapidly with one another, sometimes over great distances and with great precision. Communication between neurons and communication between neurons and their non-neuronal targets occur at specialised junctions called synapses. The term synapse (from the greek *synapsis*, junction) was introduced in 1897 by Charles Sherrington (Sherrington, 1897) to refer to the specialised contact zone, described histologically by Ramon y Cajal two centuries ago (Ramón y Cajal, 1888), where one neuron communicates with another. The normal direction of signal transmission is from the axon terminal to the target cell; thus, the axon terminal is called presynaptic terminal and the target cell is called postsynaptic cell. Although synapses come in many forms and shapes, we can distinguish between two main types: electrical and chemical synapses.

The electrical synapse, extremely rare in vertebrate brains, is the simplest form of synapse. This type of connection occurs at specialised sites called gap-junctions. At a gap-junction, the presynaptic and postsynaptic membranes are separated by only about 3 nm, and this narrow gap is spanned by special proteins called connexins. Six connexins assemble together to form a channel called connexon, which allows ions to pass directly from the cytoplasm of one cell to the cytoplasm of the other. Unlike most chemical synapses, electrical synapses are bi-directional; ionic currents pass equally well in both directions. Transmission at electrical synapses is very fast. Thus, an action potential in the presynaptic cell can produce, almost instantaneously, an action potential in the postsynaptic neuron. In addition to electrical signals, because the connexon is about 2 nm in diameter, many small organic molecules such as second messengers, can pass from one cell to the other. This may have important, but to date probably still underappreciated, consequences for cellular signalling in the brain (reviewed in Eccles, 1964; Katz, 1966).

Chemical synapses are what we would view as a proper synapse. In the chemical synapse, also called unbridged junction, the pre- and postsynaptic neurons are not contiguous. There is a discrete separation, called synaptic cleft, between the presynaptic and postsynaptic element. In addition, the pre- and postsynaptic membranes are morphologically strikingly different. The presynaptic terminal is characterised by a high density of vesicles, called synaptic vesicles, which contain the chemical messenger, called neurotransmitter; the postsynaptic membrane presents clustering of neurotransmitter receptors and other molecules. Presynaptic signals are transmitted via the release of

neurotransmitters from the presynaptic neuron, which bind to receptors located on the postsynaptic membrane. What triggers the release of neurotransmitter from vesicles is an elevation of the intracellular Ca^{2+} ($[Ca^{2+}]_i$). The arrival of action potentials at the presynaptic terminal results in the opening of voltage-gated Ca^{2+}channels, which rapidly increases $[Ca^{2+}]_i$ from about 30 nM to 10-30 μM in the vicinity of the presynaptic membrane. Calcium ions then trigger a biochemical cascade that stimulates the movement of the neurotransmitter containing vesicles towards the nerve terminal ending, where they fuse with the plasma membrane to release their neurotransmitter content into the synaptic cleft by exocytosis. The released transmitter then diffuses into the synaptic cleft and binds to specific postsynaptic receptors, which results in a postsynaptic cellular response. The type of response generated depends on both the type of neurotransmitter released by the presynaptic cell and the type of receptors present on the postsynaptic membrane (reviewed in Eclles, 1964; Katz, 1966).

There are many different types of neurotransmitter, and typically a neuron releases only one type. Most neurotransmitters fall into one of the following three chemical classes: a) amino acids such as glutamate, glycine and γ-aminobutyric acid (GABA); b) amines such as acetylcholine (ACh), dopamine (DA), noradrenaline (NA) and serotonin (5-HT); and c) peptides such as dynorphin, enkephalins, substance P and neuropeptide Y (reviewed in Triggle and Triggle, 1976).

Postsynaptic membrane receptors can be ionotropic and metabotropic receptors. Ionotropic receptors generate faster and shorter responses than metabotropic receptors. Typically, ionotropic receptors are activated by amino acid and amine neurotransmitters, whereas all three types of neurotransmitters can activate metabotropic receptors (reviewed in Kandel, 2000).

Ionotropic receptors are ligand-gated ion channels (LGICs), which, upon activation, directly open a channel, which is more or less selective for certain ion species. This results in a very fast alteration of the permeability of the postsynaptic membrane and causes a change in the transmembrane potential of the cell, called postsynaptic potential. If the postsynaptic potential is of sufficient high amplitude, an action potential may be elicited and this will be transmitted to the end of the axon of the postsynaptic cell thus perpetuating the electrical signal to the adjacent cell. The signal can be either excitatory in the case of depolarising currents, or inhibitory in the case of hyperpolarising currents. What determines whether synaptic signals produce excitation or inhibition is the type of ions that can pass through the ion channel of the postsynaptic receptors. For example, ACh-gated

ion channels at the neuromuscular junction are highly permeable to Na^+ and thus, when they open, the net effect is a depolarisation of the postsynaptic membrane. If, however, the transmitter-gated channels are permeable to Cl^-, because the chloride equilibrium potential is negative, the net effect of transmitter-dependent activation of the ion channel will be to hyperpolarize the postsynaptic cell from the resting membrane potential (reviewed in Kandel, 2000).

Metabotropic receptors are associated to G-proteins and they generate slower and longer-lasting signals than their ionotropic counterparts. The type of signals generated by this type of postsynaptic receptors involves three steps: 1) binding of the neurotransmitter to metabotropic receptors embedded in the postsynaptic membrane; 2) activation of G-proteins by the bound-receptors; 3) activation of effector proteins by the activated G-proteins. Effector proteins can be G-protein-gated ion channels embedded in the postsynaptic membrane, or they can be enzymes that synthesise second messengers that diffuse away in the cytosol (e.g., cyclic AMP, inositol triphosphate) or stay within the membrane compartment (e.g., diacylglycerol). Second messengers can activate additional enzymes in the cytosol or plasma (reviewed in Kandel, 2000).

Different neurones release different neurotransmitters and they are often grouped according to the neurotransmitter that they release. For example, neurones that release the neurotransmitter ACh are called cholinergic neurones. The cholinergic system is one of the most important and phylogenetically oldest pathways in the nervous system. Cholinergic neurons communicate by releasing ACh and the key molecules that transduce the ACh message are the muscarinic and nicotinic acetylcholine receptors (nAChRs). The nAChR in the central nervous system (CNS) is a key molecule involved in the propagation of signals between nerve cells and their targets at the CNS and peripheral synapses and it appears to exert a predominantly modulatory influence on brain mechanisms. The cholinergic innervation acting via nAChRs regulates processes such as neurotransmitters release, cell excitability and neuronal integration. nAChRs have been identified as crucial elements in CNS functions such as consciousness, attention, and memory. Dysfunction of nAChRs leads to a perturbation of the cholinergic system causing various diseases during development, adulthood and aging (Gotti *et al.*, 1997; Lindstrom, 1997; Changeux and Edelstein, 2001; Hogg *et al.*, 2003).

This study is concerned with the pharmacological and structural properties of a particular subtype of nAChRs, the $\alpha4\beta2$ receptor. This protein belongs to the Cys-loop

superfamily of LGIC and is an important target for therapeutic intervention in a number of diseases of the brain such as age-related cognitive impairment and neurodegenerative diseases, epilepsy, schizophrenia, mood disorders, chronic pain, attention deficits, and nicotine addiction.

1.2 Nicotinic acetylcholine receptors

nAChRs are cation-selective ion channels which generate fast cationic currents upon binding to ACh. nAChRs belong to the Cys-loop superfamily of LGIC which also includes serotonin type 3A ($5HT_{3A}$), glycine, γ-aminobutyric acid type A ($GABA_A$), $GABA_C$ and zinc-activated channels (ZAC), and invertebrate glutamate-, histamine-, and 5HT-gated chloride channels (Karlin, 2002; Jones and Sattelle, 2006). nAChRs were first identified and characterised at the vertebrate neuromuscular junction and in the *Torpedo californica* electric organ. The muscle nAChR of *Torpedo* is the prototype for all the nAChRs and indeed for all the members of the Cys-loop family of receptors.

1.3 Structure of *Torpedo* nAChRs

nAChRs are transmembrane proteins composed of five subunits arranged around a central water-filled pore (McGehee and Role, 1995; Jones *et al.*, 1999). To date 17 nAChR subunits have been cloned. The subunits have been divided into muscle-type (α1, β1, δ, γ, and ε) and neuronal-type (α2-α10 and β2-β4) subunits. The α subunits, both the muscle- and the neuronal-type, possess two adjacent cysteines essential for ACh binding, whereas the non-α subunits do not. The muscle-type nAChR is the best studied, as it can be found in large amounts in the *Torpedo* electric organ, from which it is easily extracted and purified. The receptor is composed of two α1 subunits and β1, δ and ε (γ in the foetus) subunits organised in a clockwise α1γα1β1δ arrangement. In contrast, the 12 neuronal subunits can form a number of different nAChR subtypes, which can be either homomeric, made of only one type of subunit (e.g., α7 receptors) or heteromeric, made of two or more distinct subunits (e.g., α4β2, α9β10, α6β2β3α4).

All nAChR subunits are similar in amino acid sequence and have the same membrane topology. Each subunit comprises: 1) a large extracellular amino-terminal domain (ECD), which contains the agonist binding site, several glycosylation sites, and at least one highly conserved cysteine bridge. In addition to its role in competitive ligand binding the ECD is essential for the correct assembly of the receptor (Chavez and Hall, 1992; Verral and Hall, 1992). This region also contains sites that interact with allosteric modulators as well as an immunogenic region, against which a large fraction of autoantibodies against nAChR is directed in the autoimmune disease myasthenia gravis

(Tzartos *et al.*, 1998); 2) three hydrophobic membrane-spanning segments (M1-M3) separated by short loops; 3) a large and variable intracellular domain, which contains putative phosphorylation sites for serine/threonine kinases; 4) a fourth transmembrane segment M4 with a relatively short extracellular carboxy-terminal end (Galzi and Changeux, 1995). Also common to all the α-subunits is the presence in the first extracellular domain of a cysteine-loop (Cys-loop) defined by two cysteines (Cys) that in the mammalian subunits are separated by 13 amino acids. The Cys-Cys pair is required for agonist binding (Fig. 1.1).

Fig. 1.1. Ribbon diagram of the α1 subunit. The figure shows the side view of the α1 subunit. Locations of the functionally important A, B, C, β1 β2 and Cys loops in the N-terminal domain of the subunit are indicated. The transmembrane domains (M1-4) and the intracellular M3-M4 loop are shown in yellow. (From Unwin, 2005).

At low resolution the *Torpedo* nAChR appears as an integral elongated transmembrane protein, ~160 Å long, that protrudes by ~60 and ~20 Å into the synaptic and intracellular compartments, respectively, composed of five similar rod-shaped subunits

arranged around the central axis, with a symmetry perpendicular to the membrane. It creates a central pore, with a diameter of ~25 Å at the synaptic entrance, which becomes narrower at the transmembrane level, and makes a narrow water-filled path across the membrane (Unwin *et al.*, 1988). The ion conducting pathway, which is ~40 Å long, is bounded by two large vestibules, which serve as pre-selectivity filters for ions (Unwin *et al.*, 2002; Unwin, 2005). The presence of charged groups at the mouth and on the inner wall concentrate the ions the vestibules select for (cations), while screening out the ions they discriminate against (anions). The cation conductance is increased by rings of negative charges located at the mouth of the pore. These rings have been shown to influence channel conductance (Imoto *et al.*, 1988).

1.4 The acetylcholine binding site

Early electrophysiological studies on *Torpedo* or mammalian muscle nAChRs indicated that nAChRs contains two ACh binding sites located in the ECD (Galzi *et al.*, 1990). The ligand-binding domain shapes a long, ~20 Å diameter central vestibule and the two binding sites are about 40 Å from the membrane surface and 45 Å from the gate, on opposite sides of the pore (Unwin, 2005). The receptor subunits in the ligand-binding domain are each organized around two sets of β-sheets joined through a disulphide bridge forming a Cys-loop, as was shown by the structure of the closely related soluble protein, the snail acetylcholine binding protein (AChBP) (Brejc *et al.*, 2001). The agonist binding site is a hydrophobic pocket located at the interface between adjacent subunits (Karlin, 2002; Sine, 2002). Several lines of evidence have demonstrated that, in the case of both the *Torpedo* electric organ and muscle nAChR, the binding sites for nicotinic agonists and competitive antagonists are located at the α1/δ and α1/γ subunit interfaces (Fig. 1.2). The most compelling supporting findings are: (a) affinity labelling experiments performed with a series of competitive antagonists of different chemical structure which showed that the chemical probes labelled primarily the α1 subunit, and to a lesser extent the γ and δ subunits (Oswald and Changeux, 1982; Dennis *et al.*, 1988; Langenbuch-Cachat *et al.*, 1988; Pedersen and Cohen, 1990; Middleton and Cohen, 1991); (b) expression in cell lines of the α1 subunit with either the γ or δ subunits which yielded an ACh binding pocket with native pharmacology, whereas all other pairwise coexpressions or single expressions of subunit failed to give ACh binding sites (Blount and Merlie, 1989). The much stronger

labelling of α1 compared with that of the γ and δ subunits suggests an asymmetric location of the binding site with respect to the interfaces. It has thus been proposed to refer to the α1 subunit as carrying the 'principal component', and the δ or γ subunit as contributing to the 'complementary component' of the nicotinic binding site (Corringer *et al.*, 1995).

Photo-affinity labelling, proteolysis, and mutational studies (Kao and Karlin, 1986; Dennis *et al.*, 1988; Galzi *et al.*, 1990; Galzi *et al.*, 1991) made it possible the identification of the various residues that compose the principal component of the α1 subunit of the *Torpedo* receptor. The ligand binding site is formed by the contribution of residues highly conserved throughout the LGIC family. These residues are located in three separate loops of the polypeptide chain of the principal side of the binding site (Corringer *et al.*, 2000), designated A, B and C. The complementary side contributes to the binding site with less conserved residues located in loops D, E and F (Fig. 1.2).

Fig. 1.2. Top view of the extracellular domain involved in the ACh binding site in the muscle-type nAChR. The ACh binding sites are located at the α/γ and α/δ interfaces. The principal component of the ACh binding site is located in the α subunit which contributes with loops A, B, and C. The residues involved in the binding site are represented by small spheres. Loop A is formed by residue Tyr^{93} (Y), loop B Loop by the amino acid Trp^{149} (W) and loop C by residues Tyr^{190} (Y), Cys^{192} (C), Cys^{193} (C) and Tyr^{198} (Y). The disulfide bond in the α subunit is indicated as S—S—. The complementary component of the high-affinity ACh binding site is located in the δ or γ subunit which contributes with loops D, E, and F. (From Arias, 1997).

Most of the residues which contribute to the binding pocket are located in loop C in the α subunit that at its apex contains the Cys-Cys pair (α1Cys192 - α1Cys193 in *Torpedo*). In addition to these, the most important residues required for ligand binding are

predominantly hydrophobic aromatic amino acids, including α1Tyr93 (loop A), α1Trp149 (loop B), α1Tyr190 and α1Tyr198 (loop C), which connect β-strands in the α subunit (Sine, 2002) (Fig. 1.2). All these residues were identified as being near the agonist binding site by labelling with a small photo-activable ligand that covalently reacts with the receptor and acts as a competitive antagonist (Dennis *et al.*, 1988), and the first three are highly conserved in the muscle and neuronal nAChR subunits. Studies in which a series of unnatural tryptophan derivatives were substituted in place of the natural residues, suggested that the side chain of α1Trp149 is in Van der Waals contact with the quaternary ammonium group of ACh in the bound state of the receptor (Zhong *et al.*, 1998). A single channel study by Akk (2001) showed that mutation of this residue affected binding but mainly caused impairment of gating. Mutations of α1Tyr93, α1Tyr190 and α1Tyr198 affect in the same way the apparent affinity of ACh, which suggests that these tyrosine residues contribute to stabilization of the quaternary ammonium portion of ACh (Sine *et al.*, 1994). Incorporation of unnatural amino acids at these positions revealed a prominent role of the hydroxyl group and of the aromatic ring of α1Tyr93 and α1Tyr198, respectively (Nowak *et al.*, 1995). Chemical labelling also showed that the pair of adjacent cysteines (Cys192 and Cys193) is likely to be close to the binding site (Kao and Karlin, 1986). The most important residues in neighbouring subunits that influence ACh binding are Trp57 of the δ subunit and the homologous Trp55 of the γ subunit, localized in the loop D (Chiara *et al.*, 1998). Moreover, mutation of δAsp180 (loop F) to asparagine, and of the homologous γAsp174 was found to decrease the affinity for ACh (Martin *et al.*, 1996).

The crystal structure of nAChR, and indeed of any of the members of the Cys-loop family of receptors, has not yet been resolved. However, in the last decade two breakthrough studies have made it possible to glimpse the three-dimensional structure of this important signalling protein. The first breakthrough was the resolution of the crystal structure of the fresh water snail protein, the ACh binding protein (AChBP) (Brejc *et al.*, 2001; Smit *et al.*, 2001). AChBP is a soluble protein found in fresh water snails that is produced and stored in glial cells and released in an ACh-dependent manner into the synaptic cleft, where it modulates synaptic transmission. Mature AChBP is a homopentamer. Each protomer is 210 amino acids long and has 20 - 23 % sequence identity with the ECD of nAChR and 15 - 18 % with the ECD of other LGICs (Smit *et al.*, 2001). The crystal structure of the AChBP showed that the protein subunits in the ligand binding domain are each organised around two sets of ten β-sheets forming a β-sandwich and joined through the disulphide bridge forming the Cys-loop (Fig. 1.3, Brejc *et al.*,

2001). This disulfide bond is conserved in the superfamily of pentameric LGICs and is important for the assembly of the receptor (Blount and Merlie, 1990; Green and Wanamaker, 1997). Nearly all residues that are conserved within the nAChR family are present in the AChBP, including those that are relevant for ligand binding. Moreover, AChBP binds known nAChR agonists and competitive antagonists such as ACh, nicotine, *d*-tubocurarine (dTC) and α-bungarotoxin (α-Btx) (Smit *et al.*, 2001). As mentioned above, in the nAChR residues important for binding are clustered in loop regions (A-F). In the AChBP structure, these loop regions form a single pocket region at the subunit interface, with loops A-C contributed from one subunit and D-F from another. Loop C is particularly prominent in the AChBP and it contains several conserved residues involved in ACh binding, including two adjacent cysteins (homologous of *Torpedo* α1Cys192 and α1Cys193) and two tyrosines (homologous of *Torpedo* α1Tyr190 and α1Tyr198). Subsequent crystallization of the AChBP in the presence of nicotinic agonists and antagonists (Celie *et al.*, 2004; Celie *et al.*, 2005; Ulens *et al.*, 2006) provided atomic resolution details on the atomic interactions between ligands and specific residues in the ligand binding site.

Crystal structures of AChBP bound to agonists (Celie *et al.*, 2004; Hansen *et al.*, 2005) showed that agonists are fully enveloped by the protein. Trp143 (corresponding to *Torpedo* α1Trp148) makes strong π-cation interactions with the agonist (Zhong *et al.*, 1998); the other four aromatic residues that form the remainder of the binding cavity, direct their π electrons or hydroxyl groups toward the agonist. Asp85, situated behind the central Trp, forms hydrogen bonds with the main chain to optimize the Trp for interaction with agonists (Lee and Sine, 2004). Hydrogen bonds also form between polar moieties of the agonist and the protein main or side chains from both faces of the binding site, and in some cases include a bridging water molecule. Hydrophobic residues from both faces further stabilize agonists through van der Waals contacts. Finally, loop C caps the entrance to the binding cavity, trapping the agonists.

Fig. 1.3. Ribbon representation of the of *Lymnaea stagnalis* AChBP. Side view of AChBP protomer from outside the pentameric ring. The side of the protomer, bearing the conserved Cys loop is called the principal (plus) side. Disulphide bridges are indicated in green ball-and-stick representation. (From Brejc *et al.*, 2001)

The second breakthrough in the elucidation of the molecular structure of nAChRs and Cys-loop receptors in general was the attainment of electron microscopy images of full-length *Torpedo* nAChRs at a resolution of 4 Å. These images revealed the overall organisation of the pentameric assembly in its closed form, the architecture of the ECD and the pore region of each subunit (Miyazawa *et al.*, 2003; Unwin, 2005). The ECD of the α subunit of the *Torpedo* nAChR was shown to contain ten β-strands (six inner sheets and four outer sheets) and one major α-helix, like AChBP protomers. This portion also contains several loop regions (i.e., the loops A, B and C, the Cys loop and the β1–β2 loop), which are critical for receptor function. The subunits in the ligand-binding domain interact mainly through polar side-chains. Similar sets of interactions occur in the AChBP (Brejc *et al.*, 2001). The β9–β10 hairpin of the α subunit incorporates loop C, which is implicated in ACh binding. The side-chains of Tyr190, Tyr198 and Cys192 in loop C and Trp149 in loop B are conserved in nAChR α subunits and co-ordinate to the bound ACh analogue, carbamylcholine, in the complex with AChBP (Celie *et al.*, 2004). Thus, this whole region, including the loop A and the adjacent strands β5 and β6 of the γ (or δ) subunit, is involved in shaping the ACh-binding pocket of the receptor.

Recently Dellisanti *et al.* (2007) resolved the crystal structure of the ECD of the mouse α1 subunit bound to the toxin α-Btx at high-resolution (1.94 Å), providing new insights in the structure-function relationships of the nAChR. The new structure confirmed what was already known, but it also revealed the presence of a water-filled hydrophilic cavity in the core of the subunit, close to the transmembrane domain, which is thought to be important for gating in the intact receptor. These hydrophilic residues are not present in the AChBP, which could explain why AChBP is not particularly efficient in gating when fused to a transmembrane domain (Bouzat *et al.*, 2004).

1.5 Gating of the nAChR channel

Ligand binding induces rapid conformational changes in the receptor, which in turn are converted into channel opening within microseconds. The receptor in the closed state switches to the open state in a reversible process called gating. In the absence of agonist, the nAChR channel can open but with very low probability, whereas in the presence of ACh the channel opens with a probability approaching unit. Activation by ACh can therefore be viewed as an amplification process in which the probability that the channel will open is greatly increased (Jackson, 1986). For all Cys-loop receptors, binding of two agonist molecules is required for full amplification. When two molecules of agonist bind to the receptor, the channel opens, with an equilibrium constant that increases with increasing number of bound agonist. Channel opening is driven by higher affinity of the agonist for the open than for the closed state. According to this mechanism the transition from the closed to the open state occurs in one step. Recently, a new gating mechanism has been suggested for the heteromeric glycine α1β receptor, which, like the nAChR, belongs to the Cys-loop superfamily of LGICs. According to this model, gating may be divided into two steps: a flip pre-open state, with the channel still closed, and the open state. The flipped receptor has higher affinity for the agonist, which could result from domain closure around the bound agonist (Burzomato et al, 2004). Subsequent studies showed that the flip mechanism also fits nicotinic data very well and it describes more accurately the gating behaviour of the receptor (Lape *et al.*, 2008). The flip mechanism could also explain the nature of partial agonism in the nAChR family. It has been shown that partial agonists have lower affinity for the flipped state rather than low affinity for the open state; it was

therefore suggested that partial agonism originates from a reduced ability to flip rather than a reduced ability to open (Lape *et al.*, 2008).

The gating mechanism described above infers a conformational change in the ligand binding domain of the nAChR induced by agonist binding. The first structural evidence for such transitions came from cryo-electron microscopy of the *Torpedo* nAChR following rapid application of ACh (Unwin, 1995). These experiments showed that binding of ACh initiates two connected events in the ligand binding domain. One is a local structural rearrangement of the ACh-binding site, and the other a larger scale conformational change, involving rotational movements predominantly in the two α subunits. Subsequent analysis revealed agonist-dependent rotation of the inner β-sheets of the binding domain, and tilting of the peripheral β-sheets toward the central water-filled vestibule (Unwin *et al.*, 2002). The crystal structure of AChBP showed a similar tilting of a peripheral β-hairpin, known as loop C (Celie *et al.*, 2004; Hansen *et al.*, 2005). Comparison of agonist-free and agonist-bound crystal structures and molecular dynamics simulations (Gao *et al.*, 2005) of the AChBP also revealed agonist-dependent motion of loop C. These observations were further supported by the refined cryo-electron microscopic structure of the *Torpedo* at 4 Å resolution (Unwin, 2005) and the crystal structures of the nAChR-like bacterial channels ELIC (Hilf and Dutzler, 2008) and GLIC (Bocquet *et al.*, 2009). In the agonist-free receptor loop C is in an 'open' or 'uncapped' configuration, which corresponds to the closed or resting state of the channel; in the agonist-bound receptor loop C is in a 'closed' or 'capped' configuration, which corresponds to the open or desensitise state of the receptor. The capped conformation with bound agonist suggests that binding flips loop C from uncapped to capped, thus initiating the structural changes that lead to channel opening.

A coupled triad of residues, αTyr190, αAsp200 and αLys145, was identified as physically linked to loop C and it is thought to trigger early steps in the activation process. Mutation of any of these three residues markedly impairs channel gating, and all three are interdependent in contributing to gating (Mukhtasimova *et al.*, 2005). In the uncapped configuration of loop C generated by molecular dynamics simulation of AChBP (Gao *et al.*, 2005), the conserved Tyr185 (equivalent to α1Tyr190 in *Torpedo*) is 8 Å away from the conserved Lys139 (α1Lys145 in *Torpedo*) in β-strand 7, which forms a salt bridge with the conserved Asp194 (αAsp200 in *Torpedo*) in β-strand 10. In agonist-bound crystal structures of AChBP (Celie *et al.*, 2004), loop C tilts inwards and Tyr185 moves closer to Lys139 (2 - 3 Å), displacing Asp194 from the Tyr/Lys pair. The recent structure of the

ligand-binding domain of the α1 muscle subunit confirms that α1Lys145 and α1Asp200 form a salt bridge which stabilizes β-strand 7 and 10 (Dellisanti *et al.*, 2007). When the agonist binds to the receptor, capping of loop C weakens the αLys145/αAsp200 salt bridge as αTyr190 establishes contact with αLys145. These local changes displace β-strands 7 and 10, which transmit further changes to the junction of the binding and pore domains.

Three structural elements of the binding-channel domain interface, the β1-β2, Cys- and β8-β9 loops from the ligand-binding domain, and the M2-M3 loop from the channel domain, transmit structural changes from the ligand-binding domain to the pore. The importance of these loops for coupling binding to gating has been demonstrated by generating a chimera receptor in which AChBP was substituted for the binding domain of the $5HT_{3A}$ (Bouzat *et al.*, 2004) receptor, as well as by mutational studies (Lyford *et al.*, 2003; Bouzat *et al.*, 2004; Chakrapani *et al.*, 2004; Sala *et al.*, 2005).

Mutational-functional studies subsequent to the publication of the structural model of the *Torpedo* receptor at 4 Å resolution (Unwin, 2005) have largely confirmed the findings of Unwin (2005). Thus, analysis of the receptor structure revealed a molecular pathway from the binding site to the top of the channel-forming M2 domain, in which the pre-M1 domain is functionally coupled to the M2-M3 linker through the β1-β2 loop. αArg209 and αGlu45 have been identified as key elements of this pathway (Lee and Sine, 2005). The side chain of αArg209 from the pre-M1 strand forms a salt bridge with αGlu45 from the β1-β2 loop, aligning these residues with αPro272 and αSer269 of the M2-M3 loop to create an assembly that interconnects the ligand binding domain with the pore domain (Lee and Sine, 2005). Both Arg209 and Glu45 are present in every member of the Cys-loop receptor family (Le Novere and Changeux, 2001), suggesting a common transduction mechanism between ligand binding and channel gating (Corringer *et al.*, 2000; Absalom *et al.*, 2003; Kash *et al.*, 2003; Kash *et al.*, 2004; Xiu *et al.*, 2005). Mutation of any of these residues of the principal pathway markedly alters channel gating, suggesting that they couple binding to gating. A strong physical interdependence was found for the pair Arg209/Glu45 and also for the triads Glu45/Val46/Pro272 and Val46/Pro272/Ser269 providing compelling evidence for physical interactions between these residues. In addition, for the $5HT_{3A}$ receptor it was proposed that structural changes induced by ligand binding lead to cis/trans isomerisation of Pro272 in the M2-M3, which may bend the M2-M3 loop and facilitate rotation of M2 into the open channel conformation (Lummis *et al.*, 2005). Comparison of x-ray structures of ELIC in the inactive state and GLIC in the active state suggests that agonist binding causes translation of the β1-β2 loop against the M2-M3

linker, displacing the tops of the M2 and M3 α-helices away form the central axis, thus initiating ion conduction (Hilf and Dutzler, 2008; Bocquet *et al.*, 2009).

More recently, a parallel coupling pathway has been identified, in which the pre-M1 domain is coupled to the M2-M3 linker through the Cys-loop (Lee *et al.*, 2009). Strong energetic coupling has been revealed among αPhe135 and αPhe137 from the Cys-loop, αLeu210 from the pre-M1 domain, and αLeu273 from the M2-M3 linker. The high-resolution structures of the bacterial homologs ELIC and GLIC confirm the interaction of the Cys-loop with the pre-M1 domain and the M2-M3 loop revealed form the cryo-electron structure of the *Torpedo* AChR. In both *Torpedo* and bacterial structures, the C-terminal half of the Cys-loop associates with the pre-M1 domain, the N-terminal half associates with the M2-M3 linker and the prevalent inter-residue contacts are hydrophobic. Studies of linear free energy relationship of channel gating suggested that the β1-β2 and the Cys-loops change conformation at the same time (Jha *et al.*, 2007). A coordinated movement of the two loops would displace the linker away from the central axis, moving the tops of the M2 and M3 α-helices in the same direction, dilating the top of the pore (Bocquet *et al.*, 2009; Hilf and Dutzler, 2009).

Gating of the AChR channel requires global structural changes, yet how these changes propagate between subunits remains largely unknown. Low-resolution cryo-electron microscopy images detected agonist-mediated changes in the α-subunits but not in the other subunits (Unwin *et al.*, 2002). However, several lines of evidence show that the non-α subunits contribute profoundly to channel gating (Bouzat *et al.*, 2002; Mitra *et al.*, 2004; Mukhtasimova and Sine, 2007); the non-α subunits may move as rigid bodies in response to the α subunits or as part of an intersubunit network. αTyr127, εAsn39 and δAsn41 are good candidates for intersubunit linkages. These residues show the characteristics expected of structures that couple agonist binding to channel gating: residue proximity, residue conservation, impaired channel gating by single mutations and nonadditive changes in gating by double mutations. αTyr127 and εAsn39 or δAsn41 were shown to associate in the diliganded closed state but they dissociate in the open state (Mukhtasimova and Sine, 2007).

Electron microscopy of the *Torpedo* AChR at a resolution of 0.9 nm suggested that channel gating primarily involves rotation of the M2 helices (Unwin, 1995). Different movements were proposed for the M2 helices: computational studies suggested both a twisting and tilting of the M2s (Taly *et al.*, 2005; Cheng *et al.*, 2006a; Cheng *et al.*, 2007); lysine substitution along M2 suggested a simple dilation rather than twisting of the M2s

(Cymes *et al.*, 2005); molecular dynamic simulations of the neuronal α7 nAChR suggested both rotation and tilting (Cheng *et al.*, 2006b); finally, recent studies of molecular dynamic simulation of the *Torpedo* AChR suggested peristaltic motions of M2 and may account for all the proposed motions (Wang *et al.*, 2008). The M2 helices from the five subunits form a narrow constriction, called resting gate, which represents the barrier to the ion flow. Motion of the M2 helices during gating leads to a transient removal of this barrier. In the resting gate, the narrow constriction has a diameter of about 3 Å, which increases to about 8 Å when the gate opens (Wang and Imoto, 1992). Finally, simulation of the α7 receptor motion during gating showed that the M4 domain bends significantly outward during relief of the gate (Law *et al.*, 2005).

The mechanisms described so far centre on stable states of the receptor, open and close, but equally important is the transition state that connects them. The transition state is important because its free energy relative to closed and open states determines the channel gating rate constants. The rate constant for channel opening is high, allowing opening of the ACh-occupied channel within tens of microseconds, and also allowing repeated opening during each occupancy. The rate constant for channel closing is about 20-fold slower, yielding an open-state lifetime of around half a millisecond. Recent studies indicated that, after binding, nAChRs move through a number of brief intermediate shut states, a 'conformational wave', before the channel opens (Grosman *et al.*, 2000; Chakrapani *et al.*, 2004; Auerbach, 2005; Zhou *et al.*, 2005; Purohit *et al.*, 2007).

1.6 The ion channel pore

The ion channel domain of the *Torpedo* nAChR is 40 Å long and has a diameter of 20 Å (Miyazawa *et al.*, 2003). The ion channel was initially identified by photoaffinity labelling using the open-channel blocker chlorpromazine. Chlorpromazine was found to label, in an agonist dependent manner, a unique high-affinity site located within the M2 transmembrane domain, to which all five the subunits of the *Torpedo* receptor contribute (Heidmann and Changeux, 1984; Giraudat *et al.*, 1986). Studies using chimeras between *Torpedo* ray and bovine nAChR δ subunits have confirmed the role of the M2 domain in formation of the ion conducting pore, revealing an involvement of the M2 domain and the M2-M3 linker in determining the rate of ion transport through the channel (Imoto *et al.*, 1988). Furthermore, affinities of voltage-dependent blockers were found to be susceptible

to mutations within the nAChR M2 domain (Leonard *et al.*, 1988) and changes in conductance were observed when charged residues in the linkers near the M2 domain were mutated (Imoto *et al.*, 1988). Subsequent photoaffinity labelling studies and substituted cysteine accessibility (SCAM) experiments identified further amino acids located in the M2 domain of the receptor which were shown to be lining the pore (Hucho *et al.*, 1986; Pedersen *et al.*, 1992; Karlin and Akabas, 1995). The pattern of labelling supports the folding of M2 into an α-helix, in agreement with secondary structure predictions (Le Novere *et al.*, 1999) and high-resolution images of the ion channel of the *Torpedo* nAChR (Unwin, 2005), with the water accessible amino acid residues all being positioned on the same side of the helix. Electron microscopy images of the open conformation of the channel identified five rods bordering the ion channel, attributed to the M2 segment (Unwin, 1995). In the closed form of the receptor, these rods bend inwards, towards the central axis, making the lumen of the pore narrower near the middle of the membrane. However, the exact location of the constriction point has not been identified yet, and different experimental approaches have led to different conclusions: residues at positions 9' and 13' of M2 that form a hydrophobic girdle (Panicker *et al.*, 2002; Miyazawa *et al.*, 2003); residues at positions 2' through 6' near the intracellular end of M2 (Wilson and Karlin, 1998; Karlin, 2002; Paas *et al.*, 2005); or a location closer to the extracellular entrance of the channel (Labarca *et al.*, 1995; England *et al.*, 1999). The diameter of the α-helical component is consistent with the notion that ions cross the membrane at this level in a fully hydrated state, whereas the narrower diameter of the loop component is expected to accommodate only partially dehydrated ions. The critical role of the loop component in cation discrimination as well as charge selectivity further supports its contribution to the selectivity filter of the channel by specific dehydration of ions. Accordingly, the α-helical component would select on the basis of stabilization of hydrated ions within the membrane, and the several phenotypes observed at this level could be explained in a first attempt on the basis of a structural reorganization of this portion of the channel.

The M2 helix seems to have minimal contacts with M1, M3 and M4, which form an outer scaffold around the ion pore. Overall, the ion channel appears to be composed of two distinct structural domains: an upper 'alpha-helical component', which delimits both the wide portion of the pore and the pharmacological site for non-competitive blockers; and a lower 'loop component', which contributes to the narrowest portion of the channel (Fig. 1.4) (Dani, 1989; Villarroel and Sakmann, 1992; Wang and Imoto, 1992).

Fig. 1.4. A model for the structural and functional organization of the ion channel. The contribution of two subunits is shown to illustrate the ion channel, which is actually formed by homologous regions from the five subunits of the pentamer. The residues with numbers correspond to the rings involved in ion selectivity (*circles*). (From Corringer *et al.*, 2000)

1.6.1 Charge selectivity filter

When a channel activates, permeant ions flow passively down their electrochemical gradient, changing the membrane potential and allowing communication between extra- and intracellular environments. nAChRs are cation-selective ion channels. In most nAChRs the dominant ion flux is carried by Na^+ and K^+ but in receptors such as α7 nAChRs Ca^{2+} permeability is more significant (Bertrand *et al.*, 1993). The permeability of monovalent cations increases with their radius, whereas there is an inverse correlation between radius and permeability for divalent cations (Keramidas *et al.*, 2004). Cations enter the pore through the extracellular vestibule formed by the N-terminal domain or through lateral openings, located at the subunit interfaces. Several studies have located the 'charge selectivity filter' of the Cys-loop LGICs at the intracellular border of M2 (Keramidas *et al.*, 2004).

Sequence analysis of consensus amino acids facing the ionic pore between different LGICs showed a remarkable homology, even between cationic and anionic channels. Selectivity for cations is determined by conserved rings of residues located on either side of the channel mouth (Imoto *et al.*, 1988) and in fenestrated structures in the cytoplasmic domain (Kelley *et al.*, 2003), which stabilise cations and concentrate them relative to bulk solution. Mutational studies and molecular dynamics simulations revealed the contribution of several residues to ionic selectivity: two rings of polar Ser/Thr, in positions 6' and 12' in

the M2 domain (the prime numbering starts at the beginning of the M2); three rings of hydrophobic Leu/Val in positions 9', 13' and 16'. The Leu residue located in 9' position is the only fully conserved residue and is considered a signature for this class of receptors; and three rings of charged Asp/Glu residues, in positions -5', -1' and 20', called cytoplasmic, intermediate and extracellular ring, respectively. Equivalent residues have been found in the prokaryotic homolog GLIC (Bocquet *et al.*, 2009). Mutations in any of the residues that form these rings were found to alter all aspects of ionic selectivity of the channel. In the muscle type receptor, residues equivalent to α7Ser240 and α7Glu237 were found to be involved in the selectivity and permeability of monovalent cation (Imoto *et al.*, 1988; Cohen *et al.*, 1992; Villaroel and Sakmann, 1992; Wang and Imoto 1992). In contrast, mutation of the residue Glu237 in the α7 receptor abolished calcium permeability but preserved that to monovalent cations (Bertrand *et al.*, 1993). In the α7 nAChR, insertion of a proline residue between positions 234 and 237, along with the introduction of a polar or even charged residue in position Leu247 and Val251 and the mutation Glu237A, was shown to convert the receptor from cationic to anionic (Galzi *et al.*, 1992; Corringer *et al.*, 1999a; Corringer *et al.*, 1999b) and the reciprocal mutations convert the α1 glycine receptor from an anionic to a cationic channel (Keramidas *et al.*, 2002). Large hydrophobic residues in the centre of the pore play an important role in channel closing in nAChRs (Revah *et al.*, 1991; Wilson and Karlin, 2001; Miyazawa *et al.*, 2003). It was proposed that these hydrophobic residues would impede ion permeation by a process called 'hydrophobic gating' as long as the channel does not exceed a certain size (Beckstein and Sansom, 2006). Unlike in the structure of nAChR, in the bacterial nAChR-like channel ELIC these residues physically obstruct the pore in the closed conformation of the channel, thus preventing diffusion of ions.

Molecular dynamics simulations studies of the muscle nAChR (Wang *et al.*, 2008) and co-crystallization of AChBP with sulphate anions (Hansen *et al.*, 2008) suggested that three more rings of functional analogous polar or negatively charged residues within the central vestibule of the ligand binding domain, corresponding to αAsn47, αGlu83 and αAsp97, are important for ion conductance.

1.7 Desensitisation of nAChRs

In the mammalian nervous system, nAChRs can be broadly classified as either α7-containing receptors that desensitise rapidly (in milliseconds) or non-α7 receptors that desensitise slowly (in seconds). When a medium to high (μM to mM) concentration of agonist is applied, nAChRs are first activated and then desensitise, entering a bound, non-conductive state, with subsequent recovery after agonist removal. This process, called 'classical desensitisation', develops usually in the range of tens of milliseconds, although different subtypes of nAChRs have differential susceptibility to desensitisation. Furthermore, different agonists have different ability to desensitise nAChRs.

Low agonist concentrations can induce desensitisation even without apparent receptor activation. This process is called 'high-affinity desensitisation' (Paradiso and Steinbach, 2003). High-affinity desensitisation is a slow process (taking seconds to minutes), and therefore is more likely than classical desensitisation to be generated during chronic exposure to agonists. High-affinity desensitisation is also receptor-subtype specific, affecting preferentially α4β2 rather than α7 or α3β4 nAChRs. Together with desensitisation, long exposure to an agonist (e.g. nicotine) can produce sustained changes in receptor sensitivity due to upregulation of the receptors (Buisson and Bertrand, 2002).

Recent findings suggested that recovery from desensitisation is agonist-dependent (Mike *et al.*, 2000; Meyer *et al.*, 2001; Paradiso and Steinbach, 2003). For example, when the onset and extent of desensitisation are similar, the recovery of α4β2 receptors after the removal of nicotine requires much more time than recovery after the removal of ACh (Paradiso and Steinbach, 2003). Desensitised receptors are characterised by high affinity for agonists indicating that they might be potential traps for unbound agonist molecules (Giniatullin *et al.*, 1997; Giniatullin *et al.*, 2001).

Although identification of the molecular structures underlying desensitisation is still incomplete, site-directed mutagenesis within receptor subunits revealed that replacement of certain elements can transform the desensitisation properties of the receptor when expressed in heterologous systems. However, if mutant receptors display altered desensitisation, this does not necessarily prove that the mutated sites are the structural motifs responsible for this process. In fact, because desensitisation is a function of agonist binding and receptor activation, any mutant expressing changes in these parameters could show changes in the properties of desensitisation. Furthermore, receptor properties might be influenced by the expression system itself (Lewis et al., 1997).

A single-point mutation (Ser284Leu) in the second transmembrane domain (M2) of the α4 subunit strongly increased the rate of onset of classical desensitisation without effect on agonist affinity (Matsushima *et al.*, 2002). Other M2 mutations in the α4 subunit can produce similar effects whereas mutations in M2 of the β2 subunit slow desensitisation. Single-point mutations in M2 of α7 receptors can greatly decrease the desensitisation onset and strongly increase agonist affinity (Revah *et al.*, 1991; Placzek *et al.*, 2004). The dissociation between changes in agonist affinity and desensitisation onset suggests that there are independent sites for receptor activation and desensitisation (Lopez-Hernandez *et al.*, 2004). In addition to single amino acids, larger subunit domains have a role in desensitisation. In fact, large regions of the extracellular N-terminal domain of the β2 subunit (when combined with the α3 subunit) are important to ensure the fast onset of classical desensitisation (Bohler *et al.*, 2001), whereas the N-terminal domain of the α4 subunit, along with the first three transmembrane domains, appears responsible for high-affinity desensitisation (Kuryatov *et al.*, 2000).

Desensitisation is a plastic process, rapidly adapting to changes in neuronal activity through modulation by local factors. One of these is the endogenous peptide substance P, which powerfully facilitates desensitisation by binding to an allosteric site distinct from the ACh-recognition sites (Di Angelantonio *et al.*, 2003). Other modulators are intracellular messengers (e.g., Ca^{2+}) that primarily target the recovery from, rather than the onset of, desensitisation (Khiroug *et al.*, 1998; Quick and Lester, 2002; Khiroug *et al.*, 2003).

1.8 Role of the M3-M4 intracellular loop

The amino acid sequence of the large cytoplasmic loop between M3 and M4 shows considerable diversity among different nAChR subunits. The functions of the large cytoplasmic loop, however, have not been studied as extensively as the functions of the extracellular or transmembrane domains. The structure of this loop was not seen in the 4 Å structure of *Torpedo* nAChR and was presumed to be disordered (Unwin, 2005).

Residues in the large cytoplasmic loop near the intracellular end of M4 affect assembly of subunits and electrophysiological properties of nAChRs (Yu and Hall, 1994; Valor *et al.*, 2002; Kuo *et al.*, 2005; Castelan *et al.*, 2007). Because of the sequence diversity of the large cytoplasmic loop, this region might be important for subunit specific behaviour and interactions with cellular components and physiology. The large

cytoplasmic loop interacts with cytoplasmic transport machinery for trafficking nAChRs to synapses (Williams *et al.*, 1998; Temburni *et al.*, 2000; Keller *et al.*, 2001; Ren *et al.*, 2005; Xu *et al.*, 2006) and residues at the cytoplasmic and extracellular ends of M4 (Roccamo and Barrantes, 2007) of α1 affect assembly and targeting to the cell surface. At the cell membrane, the large cytoplasmic loop interacts with the cytoskeleton (Bencherif and Lukas, 1993; Yu and Hall, 1994; Shoop *et al.*, 2000). Phosphorylation of the large cytoplasmic loop (Pacheco *et al.*, 2003; Wiesner and Fuhrer, 2006) was shown to affect desensitisation (Huganir *et al.*, 1986; Fenster *et al.*, 1999), expression (Wang *et al.*, 2004; Cho *et al.*, 2005) and cytoskeleton interactions (Colledge and Froehner, 1997).

1.9 Neuronal nAChRs

Neuronal nAChR are widely expressed in both the central (CNS) and peripheral (PNS) nervous systems. To date, nine α (α2-α10) and three β (β2- β4) nicotinic subunits have been identified in the nervous system, cochlea and a number of non-neuronal tissues (Hogg *et al.*, 2003; Gotti and Clementi, 2004). Neuronal nAChRs can be divided into two main classes: the αBgtx-sensitive receptors, which contain α7, α8, α9 and/or α10 subunits and can form homomeric or heteromeric receptors; and αBgtx-insensitive receptors, which are heteromeric receptors containing the α2-α6 and β2-β4 subunits, and bind many nicotinic agonists with high affinity but not α-Bgtx (Lindstrom, 2000; Gotti and Clementi, 2004).

The ACh or agonist binding site lies at the interface between an α and an adjacent subunit which may be the same α subunit in homomeric receptors (α7, α8), a different α subunit in heteromeric αBtx-sensitive receptors (α7-α8 or α9-α10) or a β subunit in heteromeric αBtx-insensitive receptors (Gotti *et al.*, 2006). In heteromeric αBtx-insensitive nAChRs, the primary component of the binding site is carried by the α2, α3, α4 or α6 subunits and the complementary component by the β2 or the β4 subunits whereas, in homomeric receptors each subunit contribute to both the primary and complementary components of the binding site (reviewed in Changeux *et al.*, 1998; Corringer *et al.*, 2000). The α5 and β3 subunits carry neither the primary nor the complementary component, but form functional channels in heterologous systems when expressed with another ligand binding subunit and a complementary β subunit. The α5 and the β3 subunits do not participate directly in the formation of the binding site but may contribute to the receptor

targeting and localisation in neuronal plasma membrane domains (Le Novere *et al.*, 2002; Gotti *et al.*, 2005).

1.10 Subunit assembly and receptor diversity

Studies on the *Torpedo* nAChR showed that the assembly of the pentameric receptor occurs in the endoplasmic reticulum and it requires the coordinate expression of all the receptor subunits and their subsequent oligomerisation before transport through the Golgi apparatus to the plasma membrane is signalled (Smith *et al.*, 1987; Blount *et al.*, 1990; Green and Claudio, 1993). Appropriate nAChR assembly requires the correct number of subunits to combine in the correct order. Studies of muscle nAChR assembly suggested two possible models: 1) the assembly proceeds in the endoplasmic reticulum where specific subunits are added sequentially to the receptor complex according to the conformation the complex assumes (Paulson *et al.*, 1991; Green and Claudio 1993; Wanamaker *et al.*, 2003); 2) α-γ and α-δ dimers are formed before these paired subunits subsequently interact with the β subunit to assemble the mature pentamer (Smith *et al.*, 1987; Blount and Merlie, 1990; Wang *et al.*, 1996). Specific subunit associations are defined primarily by sequences located in the N-terminal domain (Verrall and Hall, 1992; Yu and Hall, 1994; Kreienkamp *et al.*, 1995). Recent studies showed that the variable and large cytoplasmatic domain between M3 and M4 also contributes to protein-protein interactions involved in nAChR assembly, subcellular localisation and stability (Kukhtina *et al.*, 2006; Kracun *et al.*, 2008).

Diverse combinations of neuronal subunits can assemble into diverse types of nAChRs each with different functional properties (Moroni *et al.*, 2006). Moreover, subunit composition of nAChRs changes during development (Moretti *et al.*, 2004). Studies of recombinant nAChRs have revealed how neuronal nAChR subunits can assemble in order to form functional receptors. α7 is the only mammalian subunit which appears to preferentially form homomeric, rather than heteromeric, receptors in heterologous expression systems (Couturier *et al.*, 1990; Gerzanich *et al.*, 1994). This is consistent with evidence that this subunit forms homomeric receptors in native systems (Keyser *et al.*, 1993; Chen and Patrick, 1997; Drisdel and Green, 2000). There is also evidence that α7 can co-assemble with β2 to form a functional heteromeric receptor (Khiroug *et al.*, 2002). The nAChR α9 subunit can generate homomeric receptors when expressed in *Xenopus*

oocytes (Elgoyhen *et al.*, 1994), but it forms a functional nAChR very much more efficiently when it is co-expressed with the α10 subunit (Elgoyhen *et al.*, 2001; Sgard *et al.*, 2002). This finding is consistent with evidences that indicate that native α9-containing nAChRs are heteromeric complexes with α10 (Elgoyen *et al.*, 2001; Katz *et al.*, 2004; Vetter *et al.*, 2007). The neuronal α2-α6 and β2-β4 subunits fail to generate functional receptors when expressed individually in *Xenopus* oocytes (Boulter *et al.*, 1987; Duvoisin *et al.*, 1989; Luetje and Patrick, 1991), results that are consistent with studies performed in cultured cell lines (Whiting *et al.*, 1991; Rogers *et al.*, 1992; Wong *et al.*, 1995; Ragozzino *et al.*, 1997). Despite their inability to form homomeric nAChRs, these subunits are able to form functional receptors when expressed as pairwise combinations of one α and β subunit, such as α2β4, α3β2, α3β4, α4β2 and α4β4 (Duvoisin *et al.*, 1989; Papke *et al.*, 1989). Subunits like the α6 subunit assemble with other α and β subunits to form complex heteromeric receptors such as the α4β2α6β2β3 receptor or α6β3β4 (Kuryatov *et al.*, 2000) or much simpler receptors such as α6β2 or α6β4 (Gerzanich *et al.*, 1997; Fucile *et al.*, 1998). Several triplet subunit combinations containing α5 have been distinguished from heteromeric 'pair' subunit combinations on the basis of altered electrophysiological properties. These include: α3α5β2 (Wang *et al.*, 1996b; Gerzanich *et al.*, 1998), α3α5β4 (Wang *et al.*, 1996; Fucile *et al.*, 1997; Gerzanich *et al.*, 1998) and α4α5β2 (Ramirez-Latorre *et al.*, 1996). The β3 subunit was shown to co-assemble with several nAChR subunits, but in most of the combinations it appears to have a dominant-negative effect which results in a lack of functional expression of the β3-containig receptor. Co-assembly of β3 into functional α3β3β4 nAChRs was, however, demonstrated by heterologous expression in *Xenopus* oocytes by using a reporter mutation approach (Groot-Kormelink *et al.*, 1998). Heterologous expression studies also demonstrated the preferential co-assembly of α6 into triplet subunit combinations, which include α6β3β4 (Kuryatov *et al.*, 2000; Tumkosit *et al.*, 2006) and also α3α6β4 and α3α6β2 (Fucile *et al.*, 1998; Kuryatov *et al.*, 2000).

1.11 Stoichiometry of neuronal nAChRs

As mentioned above, some nAChR subunits (such as α7) are able to form functional homomeric receptors (Couturier *et al.*, 1990). In contrast, most nAChR subtypes form heteromeric receptors, containing at least one type of α subunit and one type of non-α

subunit. The different combinations of α and α/β subunits give receptors which differ in terms of cation permeability, activation and desensitisation kinetics, and ligand pharmacology.

The *Torpedo* muscle-type ACh receptor has been well characterized and shown to be a pentameric protein composed of two ACh-binding α1 subunits and one of each of three structural subunits, β1, γ, and δ. The stoichiometry of most other nAChRs, on the other hand, remains to be fully elucidated.

nAChRs purified from chick brain (Whiting and Lindstrom, 1986; Whiting *et al.* 1987), rats (Whiting and Lindstrom, 1987), and cattle (Whiting and Lindstrom, 1988) have shown to be composed of only two types of subunits: ACh-binding α subunits, and structural β subunits. Biochemical and electrophysiological studies showed that both chick α4β2 (Anand *et al.*, 1991; Cooper *et al.*, 1991) and human α3β4 subtypes have a stoichiometry of 2α and 3β when heterologously expressed in *Xenopus* oocytes injected with cRNAs or cDNAs ratio of 1/1 (α/β). Studies conducted in *Xenopus* oocytes also showed that α9 and α10 co-assemble with the stoichiometry $(\alpha9)_2(\alpha10)_3$ (Plazas *et al.*, 2005).

However, more recent data indicate that this is an oversimplification. Several lines of evidence show that some neuronal nAChR subunit can assemble into receptors with alternate stoichiometries and that this can influence the pharmacological and functional properties of the receptor. Several studies showed that in heterologous systems the human α4 and β2 subunits can assemble in at least two different stoichiometries (Zwart and Vijveberg, 1998; Nelson *et al.*, 2003; Moroni *et al.*, 2006; Zwart *et al.*, 2006) and strong evidences suggested that α4β2 nAChRs may exist in at least two different stoichiometries in the mammalian brain (Marks *et al.*, 1999; Butt *et al.*, 2002; Gotti *et al.*, 2008). In heterologous systems the predominant stoichiometries are $(\alpha4)_3(\beta2)_2$ and $(\alpha4)_2(\beta2)_3$ (Nelson *et al.*, 2003; Moroni *et al.*, 2006) but other stoichiometric arrangements cannot be excluded (Zwart and Vijveberg, 1998).

Recent studies of more complex nAChRs using reporter mutations showed that receptors containing the α3, β3 and β4 subunits assemble with a stoichiometry of $(\alpha3)_2\beta3(\beta4)_2$ (Boorman *et al.*, 2000).

1.12 Distribution of nAChRs in the mammalian brain

The brain cholinergic system is made up of a series of closely and connected subsystems consisting of overlapping groups of cells, whose dendrites contact those of many other cells. However, each cell innervates a discrete area and establishes its own discrete connections. Each cholinergic neuron receives only a small number of innervating fibers, which come from different areas of the brain. Each cholinergic subsystem receives therefore a large and complete set of information.

The major cholinergic subsystems in the brain are located in the: 1) magnocellular basal complex, which provides the greatest cortical and hippocampal input; 2) peduncolopontine-laterodorsal tegmental complex, the second most important cholinergic subsystem in the brain. It projects to the thalamic nuclei and midbrain dopamine neurons; 3) striatum, densely innervated by cholinergic fibers that originate from the intrinsic cholinergic neurons and do not project beyond the borders of the striatum; 4) lower brain stem, which innervates the superior colliculus, cerebellar nuclei and cortex; 5) habenula-interpeduncular system, an important station through which the lymbic system can influence the brainstem reticular formation; 6) autonomic nervous system. Parasympathetic preganglionic cells, located in the encephalic trunk in the sacral segments S2-S4 of the spinal cord, project long neuritis to the parasympathetic ganglia located in or near the target organs; sympathetic preganglionic neurons, located in the thoracic and lumbar segments (from T1 to L3), which project to paravertebral sympathetic ganglia (reviewed in Gotti and Clementi, 2004).

Neuronal nAChRs are expressed in relatively low density in the human brain. In addition, their pattern of distribution is relatively homogenous and is not restricted to the well-defined brain cholinergic pathways mentioned above. The elucidation of nAChR subunits distribution is currently based on a combination of technical approaches and the availability of knock-out or knock-in mice. The neuroanatomical distribution of various nAChR subtypes and subunit mRNAs in rodent and chick brain has been well known for some years but it has been less well characterised in human brain. The majority of studies performed to date, have mapped the distribution of high affinity nAChR sites utilising labelled nicotinic agents in homogenates of discrete brain areas or histological brain sections. This method is very sensitive, but its specificity for nAChR subtypes is not very high because no subtypes-specific ligands are as yet available: [^{3}H]-nicotine and [^{3}H]-epibatidine labels all nAChRs; [^{3}H]-cytisine labels the receptors containing the α3, α4

and β2 or β4 subunits; [^{3}H]-α-conotoxin-MII labels α3 and α6 containing receptors; and [^{125}I]-αBtx labels α7 and α9/10 receptors (reviewed in Gotti and Clementi, 2004). Evaluation of the distribution of specific nAChR subunit, rather than subtypes, expression in the human brain has been achieved by *in situ* hybridisation, quantitative RT-PCR, and the use of subunit specific antibodies in immunohistological and immunoblotting studies, which give good results in term of specificity and sensitivity. The distribution of receptors has also been described *in vivo* in the human brain using positron emission tomography (PET) analysis, a non-invasive imaging technique. Despite the incomplete nature and the limitations of the studies performed to date, it is possible to draw a map of nAChRs distribution in the human brain (Fig. 1.5).

Fig. 1.5. Distribution of nAChR subtypes in the nervous system. Sagittal brain Section showing nAChR subtypes expressed in different areas of the central nervous system (upper panel) and in the visual pathway, superior cervical ganglia and cochlea (lower panel). (From Millar and Gotti, 2009).

nAChRs are present in a variety of brain structures, in particular the thalamic, neocortical and striatal regions. High affinity nAChR sites as mapped by the binding of [^{3}H]-nicotine in both homogenate and autoradiographic studies display a distinct pattern in the human brain. The highest levels of binding are observed in the thalamus and nucleus basalis of Meynert (NBM) with relatively lower levels in the hippocampus, cortex and

caudate putamen (Adem *et al.*, 1987; Perry *et al.*, 1992; Court *et al.*, 1995). High levels of binding are observed in the majority of thalamic nuclei with greatest density observed in the lateral dorsal nuclei, medial and lateral geniculate nuclei and anterior thalamic nuclei (Adem *et al.*, 1988; Spurden *et al.*, 1997). Cortical nAChRs are concentrated in the entorhinal cortex and the subicular complex (Court and Clementi, 1995). However, regional differences in [^{3}H]-nicotine binding are observed throughout the cortex, with distinct laminar distribution of ligand in individual regions. In the somatosensory cortex, highest levels are observed in the uppermost and innermost layers with significantly less binding observed in layer IV. In contrast, in the primary motor and temporal cortices, ligand binding was observed to be considerably denser in the outer layers than in the inner layers with a distinct high density and observed in layer III of the temporal cortex. Greatest levels of cortical [^{3}H]-nicotine binding are observed in the subicular complex, in particular, the presubiculum and entorhinal cortex. In the hippocampus [^{3}H]-nicotine binding is generally low in the CA1-4 and dentate gyrus, but is greater in the *lacunosum moleculare* in CA2-3 (Perry *et al.*, 1992). This distribution of high affinity nAChR sites in human brain has recently been confirmed by autoradiographic studies comparing [^{3}H]-nicotine and [^{3}H]-epibatidine (Marutle *et al.*, 1998; Sihver *et al.*, 1998). Two high affinity binding sites in the temporal cortex, thalamus and cerebellum of human brain have been identified with [^{3}H]-epibatidine (Houghtling *et al.*, 1995; Marutle *et al.*, 1998). These sites are likely to represent binding to α4β2 and α3 nAChRs. However, differences in regional binding between [^{3}H]-nicotine and [^{3}H]-epibatidine were observed with a proportionally higher level of [^{3}H]-epibatidine binding in the thalamus and cerebellum, possibly reflecting selectivity for different nAChR subtypes between nicotine and epibatidine - i.e., greater selectivity of [^{3}H]-epibatidine for α3 nAChRs.

The pattern of nAChR sites in the cortex of human brain with regard to their laminar distribution has also been determined with the use of [^{3}H]-nicotine, [^{3}H]-cytisine and [^{3}H]-epibatidine and autoradiographic analysis of whole human brain hemispheres (Sihver *et al.*, 1998). The laminar distribution of all three ligands was generally similar to the highest levels of binding observed in layers I, III and V, and particularly high levels observed in layer III of the primary sensory motor cortex and inferior frontal sulcus. However, examination of the regional distribution of the three ligands suggests the presence of three different binding sites within the human cortex. The first site is thought to be a common site for [^{3}H]-nicotine, [^{3}H]-cytisine and [^{3}H]-epibatidine, and is likely to represent binding to α4 subunits in the brain. The morphological distribution of

[^{3}H]-nicotine and [^{3}H]-epibatidine indicate that they bind to an additional site specifically noticeable in the primary motor cortex, layer IIIb of the occipital cortex and layer V of the superior temporal sulcus, as their binding in these regions is significantly greater than that of [^{3}H]-cytisine. Although more detailed, these observations are generally consistent with the regional laminar distribution of [^{3}H]-nicotine binding sites as described by Perry *et al.* (1992). Although relatively few [^{125}I]-αBtx binding studies have been performed on human brain, comparison of [^{125}I]-αBtx and [^{3}H]-nicotine autoradiography reveals a distinct pattern of binding for the two ligands. A single high affinity [^{125}I]-αBgtx site is identified in human brain, with the highest density of binding observed in the hippocampus contrasting to the relatively sparse concentration of [^{3}H]-nicotine binding sites in this region (Rubboli *et al.*, 1994; Court *et al.*, 1995; Breese *et al.*, 1997a). [^{125}I]-αBtx and [^{3}H]-nicotine also show a distinct pattern of distribution in the thalamus. A recent study compared the relative distribution of the two ligands in this brain region (Spurden *et al.*, 1997). Consistent with previous reports [^{3}H]-nicotine binding was high in the majority of thalamic nuclei, particularly the lateral dorsal, medial geniculate, lateral geniculate and anterior nuclei. In contrast, the relative level of [^{125}I]-αBtx binding is lower in all of these nuclei, with the highest level of binding observed in the reticular nucleus, NBM and the horizontal limb of the diagonal band of Broca (Breese *et al.*, 1997a).

On the basis of the results of *in situ* hybridisation studies, it seems that the most important and diffused receptor subtype in the human brain is the α4β2 type, but the α4β4/β2 subtype is also present in important regions such as the striatum, hippocampus habenula and cortex (Fig. 1.5). The α3β4 receptor is the major subtype in the autonomic ganglia and adrenal medulla as well as in subset on CNS neurones in the medial habenula, dorsal medulla, pineal gland and retina (reviewed in Gotti and Clementi, 2004). Both the α4β2 and the α3β4 subtypes may also contain the α5 subunit, whose presence is believed to increase the rate of channel desensitisation and calcium permeability (Lindstrom, 2000; Gentry and Lukas, 2002). In addition to these major central and peripheral nAChR subtypes, many other native subtypes with more complex subunit compositions have been recently identified in the CNS. *In situ* hybridisation experiments and immunopurification and immunoprecipitation studies have shown the presence of α6 mRNA in the substantia nigra and ventral tegmental area (VTA), the locus coeruleus and retina, as well as in rodent striatum, the superior colliculus and nucleus genicolatus lateralis (Champtiaux *et al.*, 2003; Moretti *et al.*, 2004). The primate brain has also a substantial presence of α2β2, which may be an important subtype in particular brain regions (Han *et al.*, 2000). α7-containing

receptors are highly expressed in the cortex, hippocampus and subcortical limbic regions of the brain, and at low levels in the thalamic nuclei (reticular, geniculate), in the cerebellum, pituitary and pineal glands, and basal ganglia. mRNA for α9 subunits has been detected in sensory end organs, such as cochlear hair cells (Vetter *et al.*, 1999), nasal epitelium, skeletal muscle of the tongue and in the pitituary gland (Hiel *et al.*, 2000). The α10 has also been identified in the lymphoid tissue (Kawashima *et al.*, 2007). α6-containing nAChRs are expressed at higher concentrations on nerve terminals than in the cell body/dendrite compartment, suggesting that the α6 subunit, or another subunit regularly associated with α6 (such as β3), plays a targeting role (Gotti *et al.*, 2005).

1.13 Non-neuronal localisation of nAChRs

It is now well-estabilished that in addition to neurotransmission ACh is involved in cell-to-cell communication in various non-neuronal systems as well as in many aspects of cell biology and homeostasis (Grando et al., 2007). Moreover non-neuronal cholinergic communication and regulation have been demonstrated not only in mammalian cells but also in primitive uni- and multicellular organisms such as bacteria, algae, protozoa, sponge and primitive plants and fungi (Wessler *et al.*, 1999; Wessler *et al.*, 2001; Wessler *et al.*, 2003; Horiuchi *et al.*, 2003).

mRNAs coding for the α4, α5, α7, β4 and β2 subunits have been found in vertebrate adult muscle (Corriveau *et al.*, 1995; Sala *et al.*, 1996; Maelicke *et al.*, 2000). α7 is highly expressed in mammalian muscle during development and the perinatal period, and decreases later on in adult life (Maelicke *et al.*, 2000). The function of neuronal nAChRs in muscle is not known, but it is possible that they may control various metabolic and trophic functions, and perhaps gene expression. Nicotinic binding sites are also present on lymphoid cells (reviewed in Kawashima and Fujii, 2000); the receptor subtypes likely to be expressed are α3β4, α4β2 and α7. It has long been known that also macrophages express nAChRs and in particular the α7 subtype. Human epidermal keratinocytes express nAChRs that have the biophysical properties of a α3 subtype (Grando *et al.*, 1995), but the presence of other subtypes has also been shown. α3, α5 and α7 nAChR subunits are present in bronchial epithelial cells (Zia *et al.*, 1997) and α4, α7 and β2 in neuroepithelial bodies (Fu *et al.*, 2003). The vascular system contains a number of nAChR subunits in endothelial cells (α3, α5, α7, α10, β2, β3, and β4) and vascular smooth muscle (α2, α3, α4, α5, α7 and

α10) (Macklin *et al.*, 1998; Brugmann *et al.*, 2003), which probably play a role in controlling angiogenesis and cell proliferation. nAChRs expressed in astrocytes (Sharma and Vijayaraghavan, 2002; Graham *et al.*, 2003) seem to be involved in modulation of synaptic activity.

1.14 Biophysical properties of neuronal nAChRs

The most basic conformational states of nAChRs are the closed state at rest, the open state, and the desensitised state (Dani, 2001). In the closed state the channel is not conducting, but the receptor can bind ligands. Upon binding ACh, the receptor undergoes an allosteric transition from the closed, resting conformation to the open state. The nAChR ion channel is stabilized in the open conformation for several milliseconds. The continued presence of agonist leads to ion channel closure and receptor desensitisation, which lasts for many milliseconds or more. In this condition, the receptor is refractory to activation although it displays higher affinity for agonist binding (Dani, 2001).

As mentioned before, nAChRs form cation-selective ion channels. When a pulse of ACh is released at the synapse, the channels in the post-synaptic membrane open, and the initial electrochemical driving force is mainly for sodium ions to pass from the extracellular space into the interior of the cell. As the membrane depolarises, the driving force increases for potassium ions to go in the opposite direction. Although sodium and potassium carry most of the nAChR current, calcium can also make a significant contribution (Decker and Dani, 1990; Castro and Albuquerque, 1995). Calcium ions entry through nAChRs can be biologically important because of the intracellular signalling functions of free Ca^{2+}.

The rate at which the nAChRs proceed through the various conformational states and the selectivity with which it conducts cations in the open state, depend on many factors, including the subunit composition, and is influenced, in particular, by the exact amino acid sequence of the subunits. Therefore, the diversity of nAChR types has the potential to produce many different responses to endogenous or exogenous agonists. The speed of activation, the intensity of membrane depolarisation, the size of the ionic signal, the rate of desensitisation and recovery from desensitisation, the pharmacology, and the regulatory control of the ACh response will all depend from the subunit composition of the receptor, as well as other local factors (Dani, 2001).

1.15.1 Agonists

Nicotinic agonists interact with the ACh-binding site on the nAChR to produce channel activation. They are generally charged ammonium compounds, as electrostatic interactions with the receptors favour compounds with a positively charged core (Swanson and Albuquerque, 1992). By homology to the *Torpedo* nAChR, heteromeric nAChR are believed to possess two binding sites that act in a positively co-operative manner, thus both sites must be occupied by agonists to induce receptor-channel activation. For homomeric nAChRs, agonists are believed to occupy all five binding sites present in the pentameric molecule, however it remains unclear whether complete occupancy of all binding sites is required for receptor activation.

The major agonist identified and routinely used as probes for neuronal nAChRs are: nicotine, cytisine, anatoxin and the highly potent alkaloid epibatidine. Nicotinic agonists display a limited subtype-selectivity, however, there is a difference in rank order of potency for each compound that depends on the specific combination of α and β subunits and on the species studied, as described below.

The neurotransmitter ACh is the endogenous agonist for nAChRs. ACh binds with high affinity at α4β2 receptors but its lack of selectivity for nicotinic versus muscarinic receptors limits its utility as a nicotinic ligand.

The prototype agonist for nAChRs is nicotine, an alkaloid isolated from the plant *Nicotiana tabacum*. This classical agonist is most commonly employed to distinguish the ligand-gated nAChRs from the muscarinc G-protein coupled ACh binding receptors. Nicotine binds with high affinity to heteromeric neuronal nAChRs and with lower affinity to the muscle and homomeric neuronal receptors. The α4β2 receptor appears to show the highest sensitivity towards nicotine (Flores *et al.*, 1992). Nicotine is widely used in behavioural studies.

Cytisine is a toxic alkaloid, isolated from *Cytisina laburnum*. Cytisine is an agonist at most nAChR but its affinity for neuronal β2- or β4-containing nAChR (Luetje and Patrick, 1991; Papke and Heinemann, 1994) is about 100-fold higher than that for neuronal homomeric or muscle nAChR (Chavez-Noriega *et al.*, 1997; Slater *et al.*, 2003). The functional efficacy of this agonist depends on the identity of the β subunit present in the receptor; cytisine has full efficacy at β4-containing nAChRs, whilst its efficacy is greatly reduced at β2-containing receptors (Luetje and Patrick, 1991). At the α4β2 nAChR cytisine

displays stoichiometry-dependent efficacy, which may be potentially useful in drug design (Moroni *et al.*, 2006).

Anatoxin-A is a natural alkaloid produced by the freshwater cyanobacterium *Anabaena flos-aque*. Studies using recombinant α4β2 and α7 nAChRs showed anatoxin-A to be considerably more potent than nicotine, with greater action at the α4β2 receptor than at the homomeric α7 receptor (Thomas *et al.*, 1993).

Epibatidine is an azabycycloheptane alkaloid isolated from the skin of the Ecuadorian poisonous frog *Epipedobates tricolour*. Epibatidine is the most potent natural agonist at nAChRs yet known (Spande *et al.*, 1992) and it is structurally similar to nicotine and ACh. It activates all nAChRs with high potency, but it shows highest potency for the α4β2 receptor.

1.15.2 Competitive antagonists

Competitive antagonists are compounds that interact with the ACh-binding site on the nAChR, stabilising the receptor in the closed conformation and preventing access for agonists. In general, competitive antagonists are larger compounds than agonists and they are more likely to interact with a larger area of the receptors (Swanson and Albuquerque, 1992). As for agonist alkaloids, most competitive antagonists originate from a wide variety of natural sources. Unfortunately, the number of subtype-selective antagonists is very limited and not all are commercially available.

The classic competitive antagonist is dTC, obtained from the South American shrub *Chondrodendron tomentosum*, and well known as one of the neurotoxic components of the South American Indians' arrow poison. It has been identified as having cholinergic properties for almost 100 years (Chiappinelli, 1985). dTC binds non specifically to all nAChR with similar low micromolar sensitivity and it is able to fully antagonise functional responses mediated by a wide variety of nAChRs (Chavez-Noriega *et al.*, 1997). However, at the muscle nAChR it shows differential affinity for the two agonist binding sites. A high affinity site lies at the interface formed by the α and ε or γ subunits and a low affinity site is present at the α and δ subunit interface (Blount and Merlie, 1989; Sine and Claudio, 1991).

Dihydro-β-erythroidine (DhβE) is a purely competitive antagonist for neuronal nAChRs isolated from *Erythrina americana* seeds. DhβE is a potent alkaloid that blocks heteromeric and homomeric nAChR subfamilies at sub-micromolar concentrations,

although it appears to be a more efficient antagonist at α4β2 and α3β2 nAChRs (Decker *et al.*, 1995).

The snake toxin α-Btx, isolated from the venom of the Taiwanese banded krait, *Bungarus multicinctus*, is the most well-established subtype-selective nicotinic antagonist. It has been widely employed in the identification and characterization of nAChR and in displacement binding studies to define novel nicotinic compounds. α-Btx binds to skeletal muscle and homomeric neuronal nAChR with high-affinity and specificity; however it does not block any of the α/β heteromeric nAChRs (Chiappinelli, 1985; McGehee and Role, 1995). Neuronal-Btx (n-Btx), also extracted from the venom of *Bungarus multicinctus*, is a potent blocker of many of the heteromeric nAChRs. It produces pseudo-irreversible blockade of α3β2 receptors in the nanomolar range and of α4β2 nAChRs in the micromolar range. However, receptor conformations containing the α2 subunit appear to be almost insensitive to n-Btx (Luetje *et al.*, 1990).

The α-conotoxins are small peptide toxins purified from the venom of *Conus* snails, with specificity for nAChR subtypes (McIntosh *et al.*, 1999). Three well characterise α-conotoxins are specific for neuronal nAChRs. α-Conotoxins MII blocks ACh-mediated responses in heteromeric receptors, displaying highest affinity (nanomolar range) for the α3β2-containing subtype and least affinity for the muscle nAChR (Cartier *et al.*, 1996; Harvey *et al.*, 1997; McIntosh *et al.*, 1999). The α-conotoxin ImI reversibly blocks the homomeric α7 receptors with nanomolar affinity, but it is even more potent at the α9 receptor (Johnson *et al.*, 1995). In comparison, this neurotoxin has no effect on any heteromeric nAChR subtypes containing pair wise combinations of α2-α4 with either β2 or β4 subunits. α-conotoxins AuIB is a selective antagonist of α3β4 nAChRs (Luo *et al.*, 1998; Grady *et al.*, 2001) but it is less potent than α-Conotoxin MII.

Methylcaconitine (MLA) is an alkaloid isolated from the seeds of *Delphinium brownie* and it is capable of specifically and potently producing blockade of α7 nAChRs in brain and membrane preparations at low nanomolar concentrations (Alkondon *et al.*, 1992). MLA also blocks α3β2 and α4β2 nAChRs, although at concentrations greater than 100 nM (Eaton *et al.*, 2003).

Strychnine is a colorless crystalline alkaloid isolated form the seed of the *Strychnos nux vomica* tree. Strychnine is a competitive antagonist of glycine receptors but it has also been shown to block homomeric α7 nAChRs at micromolar concentrations (Albuquerque *et al.*, 1998; Garcia-Colunga and Miledi, 1999) and homomeric α9 and heteromeric α9/α10 receptors at nanomolar concentrations (Elgoyhen *et al.*, 2001).

1.15.3 Allosteric modulators

The function of neuronal nAChRs is influenced by a variety of modulatory compounds, including physiostigmine, steroids, ethanol and Ca^{2+} ion channel blockers, that do not bind to the classical ACh sites, but to a number of structurally distinct allosteric sites, which are in turn insensitive to ACh.

Noncompetitive allosteric activator sites are located on the α subunit of the receptor. Compounds that bind to this site, called allosterically potentiating ligands (APLs), enhance channel opening and ion conductance (Pereira *et al.*, 1993). When tested alone, generally, they tend to behave in an agonist-manner with low efficacy at low doses and as open-channel blockers (OCB) at high doses. When co-applied with ACh or nicotine, however, they potentiate agonist-induced activation, indicating that agonists and APLs can bind simultaneously to the receptor, interacting at different sites. APLs include the cholinesterase inhibitor physiostigmine (Seerden *et al.*, 1998), tacrine, galanthamine (Badio *et al.*, 1997; Smulders *et al.*, 2005), the alkaloid codeine (Che *et al.*, 2001) and the neurotransmitter serotonin at low doses (Albuquerque *et al.*, 1996). More recently, activating properties have been reported for 17β-estradiol on human α4β2 nAChR (Curtis *et al.*, 2002) and for cocaine methiodide on α7 receptors (Francis *et al.*, 2001).

In contrast, compounds that bind to the non competitive negative allosteric sites, called non-competitive inhibitors (NCIs) or OCBs, inhibit ion channel function. These include chloropromazine, local anaesthetics, ethanol and barbiturates (Lena and Changeux, 1993). NCIs act on two distinct sites: the high affinity site is thought to be located within the ion channel, in the M2 transmembrane domain. Binding to this site is facilitated by agonist activation of the receptor and produce a rapid reversible ion channel blockade with ion conductance blocked by simple steric hindrance; the second site binds ligand with low affinity and it is thought to be located at the interface between the receptor and the lipid membrane.

It is important to notice that many substances show a dual mode of action, being competitive/non-competitive blockers, or activators/blockers, depending on the dose employed, on the receptor subtype, or on the introduction of certain mutations in the channel pore. For instance, serotonin applied at subnanomolar concentration behaves as an APL, whereas at micromolar concentrations it inhibits the activation of the channel in a voltage dependent manner and at α7 receptors containing the mutation L248T (Fucile *et al.*, 2002a). The $GABA_A$ receptor antagonist bicuculline shows a similar behaviour, being

a non-competitive antagonist on heteromeric receptors, a competitive antagonist on the wild-type α7 receptor, and an agonist on the L248T mutant α7 receptor (Demuro *et al.*, 2001).

Muscarinic receptor antagonists such as atropine and scopolamine and the acetylcholine esterase inhibitors physostigmine, tacrine and galanthamine, at concentrations between 1 and 100 μM, enhance ion currents evoked by low concentrations of ACh in oocytes expressing human α4β2 nAChRs. However, at saturating ACh concentrations the same range of concentrations of these compounds inhibits the function of the receptors (Smulders *et al.*, 2005). Insights on the mode and site of action of this class of APLs were recently given by Hansen and Taylor (2007), who showed that APLs such as galanthamine and cocaine bind to sites located at interfaces contributed by conserved hydrophobic residues. This site resembles the benzodiazepine site of the $GABA_A$ receptor in the sense that both contain residues that occupy positions homologous to residues contributing to the agonist site.

Steroids have the ability to desensitise nAChRs by action at a site located in the extracellular hydrophilic domain that is distinct from the ACh site (Bertrand *et al.*, 1991; Inoue and Kuriyama, 1991). Progesterone, corticosterone and dexamethasone are potent inhibitors of α3-containing receptors expressed in SH-SY5Y cell lines at nanomolar to micromolar concentrations, without affecting ACh binding (Ke and Lukas, 1996). Moreover, corticosterone is known to desensitise nicotinic receptors and to produce tolerance to the effect of nicotine (Grun *et al.*, 1992; Pauly and Collins, 1993; Robinson *et al.*, 1996).

L-type Ca^{2+} channel antagonists such as nimodipine and nifedipine are capable of blocking agonist induced activation of nicotinic receptors (Lopez *et al.*, 1993) and are able to inhibit noradrenaline release from chromaffin cells in a non-reversible dependent manner (Gandia *et al.*, 1996). The mechanism of action of these compounds is unknown but the binding site is proposed to be located within the ion channel. Interestingly, Ca^{2+} ions themselves modulate the function of the receptor. Multiple Ca^{2+} binding sites exist on both muscle and neuronal receptors (Fairclough *et al.*, 1993), which when activated produce a voltage sensitive decrease in conductance. A further category of Ca^{2+} binding sites, present only in neuronal nicotinic receptors, potentiates agonist activation of ion currents in a voltage insensitive manner (Mulle *et al.*, 1992).

Recently, a new class of selective nicotinic allosteric potentiators was identified (Broad *et al.*, 2006; Timmermann *et al.*, 2007). Three novel (2-amino-5-keto)thiazole

compounds were reported to act as selective modulators of central but not ganglionic or neuromuscular nAChRs. These compounds selectively potentiate human recombinant α7, α2β4, α4β2, and α4β4, but not α3- or α1- containing nAChRs or other ion channels (Broad *et al.*, 2006). The allosteric modulator 1-(5-chloro-2-hydroxy-phenyl)-3-(2-cloro-5-trifluoromethyl-phenyl)-urea is a selective potentiator of the α7 homomeric receptor and it was shown to produce cognitive enhancement in vivo (Timmermann *et al.*, 2007). The discovery of these compounds may have a profound impact on the treatment of cognitive dysfunctions.

1.16 Physiological functions of native nAChRs

Although the molecular structure and biochemistry of neuronal nAChRs have been extensively characterised, less is known about their functional significance, especially in view of the diverse receptor subunit combinations that appear to exist. The various locations of neuronal nAChRs at the pre-, peri-, and extra-synaptic sites, in addition to the post-synaptic sites, provide also a variety of means of modulating neuronal function (Lindstrom, 1997). nAChRs have an important role in ganglionic transmission and control of the peripheral autonomic system (Ascher *et al.*, 1979), but their role in the CNS has not yet been fully elucidated. They are known to be implicated in various complex cognitive functions, such as attention, learning, memory consolidation, arousal, sensory perception, and in the control of locomotor activity, pain, perception and body temperature regulation (reviewed in Gotti *et al.*, 1997). Most of the data supporting these functions came from gene knockout experiments or from behavioural studies performed with nicotine or nicotinic receptor antagonists in humans or animals, and natural models of nicotinic denervation, such as degenerative brain diseases.

nAChRs were first localised at presynaptic sites in the PNS and CNS during the late 1980's. Studies using nerve terminal preparations (e.g., synaptosomes) in recent years have demonstrated that presynaptic nAChRs enhance the release of a wide variety of neurotransmitters, including glutamate, noradrenaline, dopamine, GABA and serotonin, suggesting that the main function of these receptors in the brain is to regulate neurotransmitter release by presynaptic action (Wonnacott, 1997). Thus, in contrast to the muscle nAChR, known to mediate fast synaptic transmission, neuronal nACh receptors conduct their functional effects mostly through modulation of synaptic transmission. It has

Another characteristic feature of neuronal nAChRs is that they display current rectification for transmembrane potentials above -40 mV. First reported for the α4β2 nAChR, this functional feature was also described at other receptor subtypes (Couturier *et al.*, 1990; Haghighi and Cooper, 2000). This receptor property allows current flow when the cell is hyperpolarised, but the current is progressively reduced when the transmembrane potential is more positive than -40 mV. Mutation of a single charged residue (Glu-to-Asp) at the inner mouth of the pore of the α7 receptor abolishes rectification (Forster and Bertrand, 1995; Haghighi and Cooper, 2000), which arises from a voltage-dependent progressive reduction of the channel mean open time. The nAChRs pass current and provide Ca^{2+} influx at highly negative membrane potentials, which provide strong driving forces for inward currents. At very active depolarised postsynaptic membranes, nAChRs make a progressively smaller contribution because of the voltage-dependent rectification. Similarly, nAChRs that are expressed presynaptically contribute best to signal transmission when the synaptic boutons are hyperpolarised.

1.15 Pharmacology of neuronal nAChR

In order to effectively control different nicotinic brain functions through pharmacological action, it is essential to identify drugs that act selectively on different receptor subtypes, in order to maximise the desired effects and minimise the unwanted effects (e.g. on muscle-type receptors). The pharmacology of nAChR has always been selective, but this was confined to the discrimination between ligands having an effect on muscle and neuronal types, such as the blocking compounds, hexamethonium (more effective on neuronal subtypes) and decamethonium (more effective on muscle nAChR). However, with the increasing awareness of the functional and pharmacological diversity within the neuronal subtypes, it has become essential to develop drugs that selectively discriminate neuronal receptor subtypes. Much of the discovery process has been based on templates from the wide variety of natural sources present in animals and plants. The most established ligands that interact with neuronal nAChRs are described in the next Sections.

been therefore proposed that the role of nAChR in the brain is to modulate neuronal excitability (McGehee and Role, 1995). However, postsynaptic CNS nAChRs also play important roles, the most clearly demonstrated being the control of ganglionic transmission and fast ACh-mediated synaptic transmission in the hippocampus and in the sensory cortex (Jones *et al.*, 1999).

The role of the most predominant nAChR in the brain, α4β2, is not fully understood. A possible function for this subtype in associative memory was suggested by gene knockout, which demonstrated that mice lacking the β2 subunit lose high affinity CNS binding sites, do not produce electrophysiological responses to nicotine in thalamic neurons, and fail to exhibit nicotine-enhanced performance in a passive model of cognitive function (Picciotto *et al.*, 1995). α4β2 is clearly the main target of nicotine and therefore is likely to be important in the reward function, or feeling of pleasure. It also appears to be involved in the feeling of pain. In addition, β2 knockout mice displayed accelerated signs of ageing, which implies that this subunit may have a protective role against ageing (Zoli *et al.*, 1999).

nAChRs have also a role during development and neuronal plasticity (Role and Berg, 1996; Broide and Leslie, 1999), probably by contributing to calcium-dependent activities. nAChRs are expressed in the early stages of foetal life (Court *et al.*, 1997) and their density varies during the course of development. Their involvement in axon guidance (Pugh and Berg, 1994) suggests that they could be involved in shaping and maintaining neuronal circuitries.

1.16.1 Neuronal nAChR are predominantly presynaptic receptors

Given the high homology between muscle and neuronal nAChRs, a role in fast synaptic transmission in the CNS was anticipated for neuronal nAChRs. However, there are only a few examples of this role in the mammalian CNS (Alkondon *et al.*, 1998; Frazier *et al.*, 1998), where nAChRs have a more modulatory influence (McGehee *et al.*, 1995; Role and Berg., 1996). Physiological studies in the early 1990s led to the hypothesis that nAChRs in the brain could modulate neuronal function by regulating neurotransmitter release (Wonnacott, 1997). Nicotine is known to elicit the release of a wide range of neurotransmitters such as DA, NA, glutamate, serotonin and GABA, commonly by acting at presynaptic nAChRs, which is consistent with such a modulatory activity. nAChRs are located presynaptically on somatodendritic regions of neurones (Clarke, 1993) where they act as autoreceptors or heteroreceptors, regulating transmitter release by influencing the

levels of neuronal excitability, or on the presynaptic terminal itself where they can initiate transmitter release by themselves.

Depolarisation of presynaptic terminals induced by ACh binding to presynaptic nAChRs activates voltage-gated Ca^{2+} channels (VGCCs), and the intra-terminal Ca^{2+} triggers neurotransmitter release. Vescicular release can also occur stochastically in an action potential-independent manner. The cationic current through the presynaptic nAChRs can both depolarise membranes and raise intracellular Ca^{2+} levels due to the intrinsic Ca^{2+} permeability of the receptor, and nAChRs can directly influence neurotransmitter release. There is evidence suggesting that neurotransmitter release is influenced by both mechanisms. DA release from striatal synaptosomes is mediated by non-α7 neuronal nAChR subtypes functionally coupled to VGCCs (Soliakov and Wonnacott, 1996; Kulak *et al.*, 2001; Turner 2004), whereas, at rat hippocampal glutamatergic terminals, Ca^{2+} entry through α7 nAChRs initiates calcium induced calcium release, from presynaptic stores, inducing glutamate release and eventually eliciting bursts of miniature excitatory postsynaptic currents (Sharma and Vijayaraghavan, 2003).

nAChRs located on the axonal arbour immediately before the synaptic terminal can also affect the release of various neurotransmitters. Particularly at GABAergic synapses, activation of preterminal nAChRs has been found to depolarise the membrane locally, leading to activation of voltage-dependent channels that directly mediate the synaptic calcium influx underlying enhanced GABA release (Lena *et al.*, 1993; Alkondon *et al.*, 1997). Axonal nAChRs may also modulate transmitter release and local excitability in another way. These receptors might enable an action potential to invade only a portion of the axonal arbour. By directly exciting or by shunting the progress of an action potential at a bifurcation, axonal nAChRs could initiate or alter the spread of neuronal excitation.

1.16.2 Postsynaptic receptors

nAChRs located on postsynaptic terminals mediate fast synaptic transmission. Fast synaptic nicotinic transmission has been detected at small excitatory input at several neuronal areas, but the low density of nicotinic synapses makes it difficult to locate them in the brain. In the hippocampus, fast nicotinic transmission onto GABAergic interneurons has been reported (Alkondon *et al.*, 1998; Frazier *et al.*, 1998; Hefft *et al.*, 1999). In developing visual cortex, nicotinic transmission can be evoked onto both glutamatergic pyramidal cells and GABAergic interneurons (Roerig *et al.*, 1997). Although direct

nicotinic excitation of a neuron usually does not predominate, it could influence the excitability of a group of neurons owing to the broad cholinergic projections into an area. Thus, beyond their specific roles at discrete synapses, nAChRs also modulate neuronal circuits in a broader sense. An example of nicotinic modulation of circuit excitability was seen in hippocampal neurons, where application of nicotinic agonists on interneurons caused both inhibition and disinhibition, thus modulating the rhythmic activity in the hippocampus (Ji and Dani, 2000).

1.16.3 Role of neuronal nAChR in non-neuronal cells

Neuronal nAChRs are also expressed in non-excitable cells, such as lymphocytes, monocytes, macrophages, dendritic cells, adipocytes, keratinocytes, endothelial cells and epithelial cells of the intenstine and lung (Whaley *et al.*, 1981; Skok *et al.*, 2001; Sharma and Vijayaraghavan, 2002). The role of neuronal-type nAChRs in the periphery is complex and different nAChR types are responsible for different functions. Among these, the role of nAChRs in inflammation has stimulated great interest in the field of anti-inflammatory therapeutics. The nAChR subtype involved in the anti-inflammatory pathway was recently identified. Stimulation of the α7 nAChR present on the membrane of tissue macrophages controls the production of inflammatory cytokines acting at the post-transcriptional level (Wang *et al.*, 2003).

1.17 Upregulation of nAChRs

Nicotinic receptors go against the generally accepted paradigm in cell membrane receptor studies that over-exposure to agonists produces receptor down regulation whereas prolonged inactivation by antagonists has the opposite effect (Gentry and Lukas, 2002). Studies of the brain of tobacco smokers and animals chronically exposed to nicotine have in fact showed that long term exposure to nicotine, at concentrations found in the blood of smokers, results in an increase in the number of nAChRs (called up-regulation) (Gentry and Lukas, 2002; Perry *et al.*, 1999). This particular effect might be due to the fact that nicotine also acts as a time-averaged antagonist, as demonstrated by functional studies of native and transfected nAChRs in which the constant presence of an agonist leads to desensitisation (Picciotto, 2003).

The molecular mechanism underlying the up-regulation of nAChRs was investigated both *in vitro* and *in vivo*. Prolonged nicotine exposure induces up-regulation of homomeric α7 and heteromeric α3β2, α4β2, α6β2 and α3β4 receptors expressed in heterologous systems. Moreover, it was recently shown that the presence of the β3 subunit in α6β2β3 and α6β4β3 subtypes produces greater nicotine-induced up-regulation than that observed in the same receptors lacking the β3 subunit (Broadbent *et al.*, 2006). This is probably due to a direct effect of the β3 subunit on subtype assembly. Both α7- and α3-containing receptors are up-regulated by chronic nicotine treatment, but to a different extent and at higher doses than those necessary to up-regulate the α4β2 subtype. In addition to nAChR subtype, up-regulation may also depend on the host cell. For instance, it was shown that nicotine exposure decreases the functional response of α4β2 and α7 receptors expressed in *Xenopus* oocytes (Peng *et al.*, 1997), but α4β2 receptors stably expressed in HEK293 cells are not desensitised by chronic nicotine exposure (Buisson and Bertrand, 2001).

In vivo studies showed that chronic nicotine treatment does not increase nAChR mRNA levels in mouse brain (Marks *et al.*, 1992), suggesting that up-regulation of the receptors is due to post-transcriptional mechanisms. Studies of the brains of animals chronically treated with nicotine and those of human smokers have shown that the most up-regulated receptor is the α4β2 subtype (Perry *et al.*, 1999; Gentry and Lukas, 2002; Tumkosit *et al.*, 2006). However, the data concerning nicotine up-regulation *in vivo* are contradictory. Studies of α6-containing receptors after nicotine exposure reported upregulation (Parker *et al.*, 2004), downregulation (Lai *et al.*, 2005; Mugnaini *et al.*, 2006) and no change (McCallum *et al.*, 2006). This discrepancy might be due only to the different protocols used, which can lead to different brain nicotine levels and/or kinetics, thus explaining the different results observed in the different studies. A further level of complexity in studying the *in vivo* effects of nicotine is due to the presence of different receptor subtypes that may be differently sensitive to up-regulation.

Most of our knowledge of the up-regulation of nAChRs is based on studies on the α4β2 subtype. Several models have been proposed to explain the up-regulation of this receptor subtypes observed after chronic nicotine treatment: 1) an increase in receptor transport through the secretory pathway to the plasma membrane (Harkness and Millar, 2002); 2) a decrease in surface receptor internalisation due to nicotine-induced conformational modifications that prevent the removal of receptors from the cell surface (Peng *et al.*, 1997); 3) the isomerisation of surface receptors into a more easily activated

high affinity conformation (Buisson and Bertrand, 2001; Vallejo *et al.*, 2005); 4) an increase in subunit assembly and/or a decrease in receptor turnover (Wang *et al.*, 1998; Nashmi *et al.*, 2003; Darsow *et al.*, 2005; Kuryatov *et al.*, 2005). Assembly, trafficking and cell surface expression of the receptors are key steps in nicotine-induced up-regulation. Recent studies by Sallette *et al.* (2004) identified two segments in the extracellular domain of the β2 subunit that are critical for the up-regulation of β2-containing subtypes. The authors suggested that nicotine binding to immature oligomers leads to a conformational reorganisation of these segments, strengthens the interactions between adjacent subunits, and facilitates the maturation process toward high affinity receptors (Sallette *et al.*, 2004; Sallette *et al.*, 2005). These results are in good agreement with the findings of Kurjatov *et al.* (2005), who showed that nicotine acts as a pharmacological chaperone, inducing an active or desensitised conformation, which assembles more efficiently. Another critical factor for receptor assembly and trafficking is subunit availability. Ficklin *et al.* (2005) showed that ubiquilin-1 (an ubiquitin like protein) plays an important role in nicotine-induced up-regulation by sequestering the subunits on proteasomes and thus decreasing their availability. A recent work by Rezvani *et al.* (2007) showed that nicotine, at concentrations achieved by smokers, reduces proteasomal activity, produces accumulation of ubiquitinated synaptic proteins, and increases total protein levels. The authors propose, therefore, that nicotine acts as an inhibitor of proteasome function blocking endoplasmic reticulum-associated degradation of unassembled nAChR subunits, which in turn increases the availability of subunits for assembly into mature receptors that are trafficked to the cell surface.

1.18 nAChRs and nicotine addiction

The VTA has been implicated in the rewarding motivational effects of a wide variety of addictive drugs, including nicotine (Corrigall *et al.*, 2000; Laviolette and van der Kooy, 2003). Within the VTA, both dopaminergic and GABAergic neurons are implicated in signalling pathways or reward (Laviolette and van der Kooy, 2003). Neurons within the VTA have a wide variety of nAChRs (Wooltorton *et al.*, 2003), and nicotine can activate both the dopaminergic and GABAergic neurons of the VTA (Yin and French, 2000; Mansvelder and McGehee, 2002). In the VTA nAChRs are expressed on the soma of dopaminergic neurones (Klink *et al.*, 2001), on GABAergic terminals (Mansvelder *et al.*,

2002) and also on glutamatergic terminals (Mansvelder and McGehee, 2000; Mansvelder *et al.*, 2002). The early acute effects of nicotine predominantly affect GABAergic neurons, where GABA release is modulated by α4β2 nAChRs (Klink *et al.*, 2001). The stimulation and fast subsequent desensitisation of α4β2 receptors produces prolonged stimulation of dopaminergic neurons by removal of the inhibitory GABA input. Nicotine also acts on presynaptic nAChRs located on VTA glutamatergic terminals which show a lower rate of desensitisation after nicotine exposure, eliciting an excitatory glutamatergic input to the dopaminergic neurons (Mansvelder *et al.*, 2002). Several studies have suggested that the presynaptic action of nicotine in the CNS, especially glutamate release is mediated mainly by presynaptic α7 receptors (McGehee *et al.*, 1995; Girod *et al.*, 2000). Finally, dopaminergic neurons express nAChR α4, α3, α5, α6, β2 and β3 subunits (Klink *et al.*, 2001). The somatodendritic nAChRs on dopaminergic neurons of the VTA can directly excite these neurons by receiving cholinergic signals ascending from outside the VTA (Oakman *et al.*, 1995). This process eventually results in transient DA responses that are terminated by nAChR desensitisation (Blaha *et al.*, 1996; Pidoplichko *et al.*, 1997).

Fig. 1.6. Modulation of DA release in the VTA by nAChRs. Native nAChRs modulate DA release in dopaminergic neurons of the mesolimbic and nigrostriatal pathways both directly and indirectly. nAChR agonists exert direct modulation of DA release through presynaptic and preterminal nAChRs. Alternatively, activation of α7 nAChRs on glutamatergic terminals triggers the release of Glu, which in turn stimulates ionotropic Glu receptors on dopaminergic terminals, finally inducing DA release. Additionally, desensitisation of the α4β2 nAChR on GABAergic interneurons can remove the inhibitory GABA input on dopaminergic neurons, thereby indirectly eliciting DA release. (From Kalamida *et al.*, 2007)

1.19 nAChRs in ageing and neurodegenerative diseases

nAChRs numbers in the brain change considerably during development and aging in all animal species. Many studies have demonstrated that the concentration of nicotinic binding sites, particularly the ones with high affinity for agonists, steadily decreases throughout life in nearly all of the studied human brain regions. One exception is the thalamus, in which the binding sites remain constant or increase. In the case of subunit distribution, there is a general agreement that the β2 subunit decreases with age in all brain structures, especially in the neocortex and hippocampus, α4 and α7 decrease in the neocortex, and α3 in the enthorinal cortex. Loss of nAChRs during ageing will tend to predispose brain areas to the consequences of further loss as a result of age-related neurodegeneration.

Initial studies on the cholinergic system in Alzheimer's disease (AD) revealed a severe loss of both cortical innervation and basal forebrain neurons (Perry *et al.*, 2001). Successive studies have reported important deficits of nAChRs in temporal and frontal cortex, hippocampus and various thalamic nuclei of patients with AD, as measured by radiolabelled agonist binding in autopsy tissue and *in vivo* PET analyses (Paterson and Nordberg, 2000). Immunohistochemical studies on temporal cortex indicated reduced staining with both α4 and β2 directed antibodies (Sparks *et al.*, 1998); this decline was also confirmed by western blot analysis (Guan *et al.*, 2000) and additional immunochemical studies (Wevers *et al.*, 1999).

The nicotinic cholinergic system is also involved in Parkinson's disease (PD) (Burghaus *et al.*, 2003). The central feature of this disease is the loss of dopaminergic neurons in the substantia nigra and degeneration of subcortical noradrenergic, serotoninergic and cholinergic nervous pathways. nAChRs are very important in promoting the release of DA in the nigro-striatal pathway, and both the α6β3β2 and the α4β2 subtypes in striatum are responsible for the release of DA from nerve endings (Quik and Kulak, 2002; Champtiaux *et al.*, 2003). In experimental rodent and monkey models of PD, there is a selective decrease in the number of α6-, α4- and β2-containing receptors as detected by means of specific ligand binding or immunoprecipitation experiments (Champtiaux *et al.*, 2003; Kulak *et al.*, 2002; Lai *et al.*, 2004). There is a general consensus that [^{3}H]-nicotine and [^{3}H]-epibatidine binding is decreased in the striatum of PD patients (Court *et al.*, 2000; Guan *et al.*, 2000; Martin-Ruiz *et al.*, 2000). A decrease in nAChRs similar to that reported in AD has also been found in the cerebral cortex of PD patients,

and is mainly due to a decrease in α4- and α7-containing receptors (Burghaus *et al.*, 2003). This reduction of nAChRs in the brain of patients affected by Alzheimer's and Parkinson's diseases can be one of the causes of the mild cognitive impairment associated with these diseases. Targeting presynaptic nAChRs may therefore be advantageous for PD patients. It was recently shown that stimulation of α7 nAChRs protects neuronal cells form degeneration and neuronal death induced by $A\beta_{42}$ amyloid protein that has a high affinity for this subtype (Wang *et al.*, 2000). It has therefore been proposed that the α7 receptor may play a key role in pathological accumulation of $A\beta_{42}$ in neurons that express this subtype.

1.20 nAChRs in schizophrenia and mood and attention disorders

Several lines of evidence suggest the possible involvement of nAChRs in schizophrenia: (1) high prevalence of smoking among schizophrenic patients (90% compared to 33% in the general population (Lohr and Flynn, 1992; Perry *et al.*, 2001); (2) positive correlation between smoking and negative (but not positive) symptoms (Patkar *et al.*, 2002). Recent brain autopsy data indicate that schizophrenic patients have altered nAChRs (Court *et al.*, 2000; Martin-Ruiz *et al.*, 2003). The involvement of heteromeric receptors is doubtful; on the other hand, the involvement of homomeric α7 receptors is much more relevant. Schizophrenic patients have a small, but significant and reproducible decrease in [^{125}I]-αBgtx binding sites and α7 immunoreactivity in the hippocampus (Freedman *et al.*, 1995; Leonard *et al.*, 1996), the reticular nucleus of the thalamus, and the cingulated and frontal cortex (Martin-Ruiz *et al.*, 2003). Genetic linkage analysis also provided evidence of the involvement of α7 receptors; the human α7 gene is in fact partially duplicated in schizophrenic families.

Although to a lesser extent than schizophrenic patients, there is also evidence that nAChR are implicated in mood. Tobacco smoking is higher in depressed individuals than in the normal population (Poirier, 2002) and smoking cessation is associated with depression in individuals with a history of depression. Nicotine was reported to be antidepressive and mood stabiliser in humans (Shytle *et al.*, 2002), and a number of antidepressant inhibit neuronal nAChRs. Moreover, nAChRs were involved in both the anxiolitic and the axiogenic effects of nicotine in experimental animals (Picciotto *et al.*,

2002), although further studies are needed to establish whether nAChRs have a real relevance in the control of mood disorders.

nAChRs are also involved in disorders such as Tourette's syndrome, whose symptoms are ameliorated with administration of nicotine, and attention-deficit hyperactivity, which is often associated with maternal smoking (Leonard *et al.*, 2001) and a potential target for nicotinic ligands-based therapies.

1.21 nAChRs and nociception

Neuronal nAChRs have been shown to play an important role in the antinociceptive pathway. The antinociceptive activity of nicotine is been known since 1932, but interest in nicotinic receptor-mediate analgesia started only after the discovery of the analgesic properties of epibatidine and of its high affinity for the nicotinic receptors. The α4β2 subtype is the main nicotinic receptor involved in the antinociceptive activity, but other subtypes such as α4α5β2 could also contribute (Marubio *et al.*, 1999; Decker *et al.*, 2004).

1.22. Role of nAChRs in epilepsy

Mutations (mainly recurrent and site specific) in the nAChR α4 and β2 subunits are now established causes of autosomal dominant nocturnal frontal lobe epilepsy (ADNFLE) with incomplete penetrance (Steinlein *et al.*, 1995; De Fusco *et al.*, 2000). The cholinergic system is know to have a major effect on sleep modulation (Steriade and Contreras, 1995), therefore a defect in nAChRs is not surprising in this particular form of epilepsy. The mutations lead to increased sensitivity to ACh, a change in Ca^{2+} permeability, thus facilitating the synchronisation of the spontaneous oscillations in the thalamo-cortical circuits and generating seizures (Raggenbass and Bertrand, 2002), and perhaps to a change of receptor stoichiometry (Cagdas *et al.*, 2009). Further evidence of the relevance of the α4-containing receptors in epilepsy come from the finding that mice lacking α4 subunits are more sensitive to the proconvulsant effects of GABA antagonists (McColl *et al.*, 2003) and the fact that anti-nAChRs drugs have antiepileptic activity (Loscher *et al.*, 2003).

1.23 The α4β2 nAChR

The α4β2 nAChR is the predominant nAChR subtype in the mammalian brain. The α4 and β2 subunits represent the most abundant nAChR subunits in chick and rat brains (Whiting *et al.*, 1987; Schoepfer et al, 1988; Wada *et al.*, 1989; Flores *et al.*, 1992), and α4 mRNA is widely detected throughout the human cerebral cortex (Wevers *et al.*, 1994). Rodent brain regions expressing the α4 and β2 subunits show high affinity for (−)-nicotine (Clarke *et al.*, 1985; Deutch *et al.*, 1987: Swanson and Albuquerque, 1987; Marks *et al.*, 1992); moreover, in β2 knock-out mice (−)-nicotine binding to brain slices is fully abolished, demonstrating that β2-containing nAChRs constitute the high affinity binding site for (−)-nicotine (Picciotto *et al.*, 1995). The α4β2 nACh subtype is located mainly presynaptically on GABAergic (Alkondon *et al.*, 1996; Lu *et al.*, 1998; Zhu and Chiappinelli; 1999; Klink *et al.*, 2001) and dopaminergic neurons (Grady *et al.*, 1992; Klink *et al.*, 2001; Champtiaux *et al.*, 2002; Zoli *et al.*, 2002). nAChRs composed of α4 and β2 subunits modulate neurotransmitter release (Dani, 2001) and play a direct role in nicotine addiction (Picciotto *et al.*, 1998; Marubio *et al.*, 1999). In β2 knock-out mice, nicotine fails to elicit striatal DA release, fails to increase discharge frequency of midbrain dopaminergic neurons, and fails to elicit self-administration (Picciotto *et al.*, 1998). This nAChR subtype is elevated in brain tissues from smokers (Benwell *et al.*, 1988; Breese *et al.*, 1997b) and, similarly, in mice chronically exposed to nicotine (Marks *et al.*, 1983). Alterations in the level and/or activity of α4β2 nAChRs have been implicated in different neuropathologies. In the brain of Alzheimer's patients, the nAChR density is markedly reduced (Whitehouse *et al.*, 1986; Aubert *et al.*, 1992), as well as the high affinity binding sites for (−)-nicotine (Perry *et al.*, 1995). α4β2 nAChRs are also thought to be involved in Parkinson's diseases (Rusted *et al.*, 2000) and mutations in both the α4 and the β2 subunits have been linked to autosomal dominant nocturnal frontal lobe epilepsy (Steinlein, 2004) and benign familial neonatal convulsions (Beck *et al.*, 1994).

The stoichiometry of the α4β2 nAChRs in the brain has not yet been elucidated. Several studies showed that this nAChR subtype can exist into at least two different stoichiometries (Zwart and Vijveberg, 1998; Nelson *et al.*, 2003; Zwart *et al.*, 2006). α4 and β2 nAChR subunits expressed heterologously in mammalian cell lines (Buisson and Bertrand, 2001; Nelson *et al.*, 2003; Kuryatov *et al.*, 2005) or *Xenopus* oocytes (Zwart and Vijveberg, 1998; Zwart *et al.*, 2006; Moroni *et al.*, 2006) assemble into a mixture of receptors with high (HS) or low sensitivity (LS) to activation by ACh. HEK293 cells stably

transfected with the α4β2 nAChR have a large majority of receptors with low ACh affinity and slow desensitisation. Metabolic labelling of these cells with [^{35}S]-Methionine showed that the receptors have a stoichiometry of $(\alpha4)_3(\beta2)_2$. Long-term exposure to nicotine, transfection with additional β2 subunits or overnight culture at low temperature (29 °C) result in an increase in the number of receptors characterised by high sensitivity to ACh and a stoichiometry of $(\alpha4)_2(\beta2)_3$ (Nelson et al., 2003). The alternate functional forms of the α4β2 nAChR are not simply a consequence of expressing α4 and β2 subunits in heterologous systems. Several lines of evidence suggest that neurones may also express both α4β2 nAChR forms and that the relative amounts of the two receptor forms influences basal behaviours and sensitivity to acute and chronic exposure to nicotine. Firstly, functional studies showed biphasic agonist concentration-response curve for stimulation of putative α4β2 nAChR function in mouse thalamic preparations (Marks *et al.*, 1999; Butt *et al.*, 2002). Such function is not present in the thalamus of α4-/- or β2-/- knockout mice, which also lack high affinity epibatidine sites (Picciotto *et al.*, 1995). More recent studies from cortical and thalamic synaptosomes of heterozygous α4 ($\alpha4^{+/-}$) and β2 ($\beta2^{+/-}$) mice showed that native α4β2-nAChR very likely have alternative stoichiometries, which can be influenced by the relative level of expression α4 and β2 mRNAs (Gotti *et al.*, 2008). This study showed that partial deletion of α4 induced a large decrease in the response of the component with lower ACh sensitivity and decreased the relative proportion of the α4 subunit in assembled receptors. Similarly, partial deletion of β2 induced a decrease in the component with higher ACh sensitivity and an increase in the relative proportion of the α4 subunit in assembled receptors. These results strongly suggest that α4β2 nAChR with different stoichiometries are expressed in native tissues (Gotti *et al.*, 2008). Secondly, the pharmacological properties of the alternate forms of α4β2 nAChR expressed heterologously in *Xenopus* oocytes closely resemble those of thalamic α4β2 nAChRs (Marks *et al.*, 1999; Butt *et al.*, 2002). Thirdly, a polymorphism in the α4 subunit gene in mice (CHRNA4 A529T) increases the ratio of high to low sensitivity α4β2 nAChRs (Kim *et al.*, 2003) and accounts for mouse strain-specific differences in measures of α4β2 nAChR functions such as sensitivity to nicotine-induced seizures, effects of nicotine on Y-maze activity, respiratory rate, and body temperature (Tritto *et al.*, 2002; Kim *et al.*, 2003).

The α4β2 nAChR represents an important target for drug development and the understanding of its structure-function relationship is a necessary requirement for further advancements in the development of α4β2-selective compounds. Progress in the development of α4β2 nAChR-selective drugs and understanding of the precise roles of this

receptor type in brain functions and diseases, particularly nicotine addiction, has been slowed down by the existence of alternate forms of the α4β2 nAChR and by the difficulties in expressing them separately. Functional and mutational studies showed that it is possible to obtain either the HS $(\alpha4)_2(\beta2)_3$ or the LS $(\alpha4)_3(\beta2)_2$ stoichiometry by injecting the nucleus of *Xenopus* oocytes with 1:10 or 10:1 α4/β2 subunit cDNA ratios, respectively (Moroni *et al.*, 2006). The extreme injection ratio cannot however exclude the presence of other stoichiometries, as demonstrated by the biphasic response of the receptors heterologously expressed in *Xenopus* oocytes to stoichiometry-selective compounds, such as 5I-A85380 (Zwart *et al.*, 2006). Low order concatamers, such as dimers, have been used to express separately the two alternate stoichiometries (Zhou *et al.*, 2003). However, it was shown that dimers of nAChR subunits can assemble improperly, forming pentamers with a dangling subunit, dipentamers or even more complex constructs (Zhou *et al.*, 2003; Groot-Kormelink *et al.*, 2004). An alternate approach is to concatenate the five subunits into pentamers to produce receptors of fixed stoichiometry and subunit order. This thesis describes the use of such approach to express separately functional $(\alpha4)_2(\beta2)_3$ and $(\alpha4)_3(\beta2)_2$ receptors.

1.24 Concatenation of subunit for the study of LGICs

Subunit concatenation by synthetic linkers was first applied succesfully to K^+ channels in order elucidate the architecture and function of the protein (Isacoff *et al.*, 1990). This approach was later used for the study of many other ion channels, such as cyclic nucleotide-gated ion channel (Varnum and Zagotta, 1996), the epithelial Na^+ channel (Firsov *et al.*, 1998), transport proteins (Emerick and Fambrough, 1993).

One of the first application of subunit concatenation to ligand-gated ion channels was to prove the topology for the P2X receptor (Newbolt *et al.*, 1998). This strategy was then applied to the other members of the Cys-loop superfamily of ligand-gated ion channels, such as GABA*A* receptors (Im *et al.*, 1995; Baumann *et al.*, 2001; Baumann *et al.*, 2002), glycine receptors (Grudzinska *et al.*, 2005) and nAChRs (Zhou *et al.*, 2003; Groot-Kormelink *et al.*, 2004; Groot Kormelink *et al.*, 2006; Carbone *et al.*, 2009).

The use of concatenated receptors has proved to be useful for: 1) characterisation of receptor architercture (Newbolt *et al.*, 1998) and stoichiometry (Grudzinska *et al.*, 2005); 2) characterisation of the properties of receptors that contain different subunit isoforms in

specific locations (Minier and Sigel, 2004a; Boileau *et al.*, 2005); 3) selective introduction of mutations into a specific subunit that occurs different times in a receptor , thus facilitating the investigation of positional effects of mutations associated with diseases (Gallaher *et al.*, 2004; Chapter 4 of this thesis); 4) expression of homogenous population of receptors with a fixed stoichiometry and arrangement (Zhou *et al.*, 2003; Tapia *et al.*, 2007; Carbone *et al.*, 2009; Chapter 3 of this thesis).

In order to construct concatenated receptors with functional properties comparable to those of their non-linked counterpart, concatenation of subunit has to follow some important rules: 1) subunit concatenation is possible only if the N-terminus and the C-terminus of the subunit are both on the same side on the membrane; 2) the nature and the length of the synthetic linkers is critical to ensure normal receptor function. A short linker will impair receptor function leading to the formation of non functional receptors (Baumann *et al.*, 2001); a long linker will lead to the formation of dipentameric receptors, monopentamers with a dangling subunit o more complex constructs (Groot-Kormelink *et al.*, 2004; reviewed in Minier and Sigel, 2004b); 3) the signal peptide should be present only in the first subunit and should be removed from all the others to avoid proteolysis of the construct (see Chapter 3 of this thesis); 4) the order of the subunits in the concatenated receptor plays an important role in determining the functional and pharmacological properties of the receptor. As shown in Chapter 3 a specific subunit order is needed for each receptor type to ensure proper function of the receptor.

Thesis synopsis

The findings of this thesis are described in detail in Chapters 3-5. Chapter 3 describes concatenation of $(\alpha4)_2(\beta2)_3$ and $(\alpha4)_3(\beta2)_2$ nAChRs. Chapter 4 describes the localisation of the binding sites in the concatenated receptors and Chapter 5 shows how concatenated receptors can be used for mutational studies. These chapters are divided into four Sections, namely Introduction, Experimental procedures, Results and Discussion. The experimental procedures described in each Chapter are those that were specifically used to examine the issues raised by the studies described in that chapter. Routine experimental procedures used throughout this study are described in Chapter 2. Finally, Chapter 6 briefly summarises the most relevant findings of the work, relating the most recent findings in the nAChRs field to the results presented here.

Aims of the thesis

The overall aim of this study was the engineering and functional characterisation of $(\alpha4)_2(\beta2)_3$ and $(\alpha4)_3(\beta2)_2$ nAChRs expressed in heterologous expression systems. Specific aims were: a) concatenation of α4 and β2 subunits in order to produce pentameric concatenated receptors with defined subunit composition and order and their functional characterisation; b) localisation of the binding sites in concatenated $(\alpha4)_2(\beta2)_3$ and $(\alpha4)_3(\beta2)_2$ nAChRs in order to use them as a tool for mutational studies; c) analysis of the effect of a mutation causing ADNFLE on the two stoichiometries.

CHAPTER 2

Materials and Methods

2.1 Reagents

Standard laboratory chemicals were of Analar grade and were purchase from BDH Ltd., UK. Acetylcholine (ACh), dihydro-β-erythroidine (DHβE), (-) nicotine, A85380, epibatidine, cytisine and $ZnCl_2$ were purchased from Sigma-Aldrich (St Louis, MO, USA). 5I-A85380 was purchased from Tocris (UK). TC2559 was a gift from Targacept Inc. (Winston-Salem, NC, USA) and sazetidine-A from Eli Lilly (Surrey, UK). 5-Br-cytisine (5-Br-Cys) was a gift from Professor Bruce Cassels (University of Chile, Santiago, Chile).

2.2 Animals

Adult female *Xenopus laevis* toads were purchased from Horst Kaehler (Hamburg, Germany). Toads were housed in accordance with Home Office regulations. Briefly, toads were housed in black tanks filled with dechlorinated water (> 15 L per toad) that was kept in a temperature-controlled room (18 °C). The animals were kept under a fixed 12 hour light/dark cycle. Toads were fed twice a week with pellets purchased from the supplier. The water was refreshed weekly.

2.3 Molecular Biology

DNA ligations, maintenance and growth of *Escherichia coli* bacterial strains and the use of restriction enzymes were carried following the procedures described by Maniatis *et al.* (1989). Plasmid isolation and DNA gel purification were carried out using commercially available kits (Qiagen, UK).

The α4 and β2 subunit cDNAs were subcloned into the pCI vector (Promega, UK). The pCI vector is endowed with a 5' and 3' intronic regions flanking the multiple cloning site (MCS). These regions are part of the β-globin gene family and are known to stabilise transcripts and to promote the recruitment of the RNA by polysomes. In order to minimise differences in the transcription of the two cDNAs that may be brought about by different untranslated regions flanking the coding regions of the subunit cDNAs (Briggs *et al.*, 2006), sub-cloning was performed by PCR using primers annealing at the start and end of the translated sequence of the cDNAs. Using these primers, Xba I and Not I restriction

sites were introduced at the 5' and 3' ends respectively of both subunit cDNAs for subsequent cloning into the MCS of the pCI vector. The full-length sequence of the subcloned cDNAs was verified by DNA sequencing (Geneservice, Department of Biochemistry, Oxford University, Oxford, UK).

2.4 Single Point Mutations

Residues of mutant or wild α4 or β2 subunits are numbered in term of the full length, including the signal peptide sequences. To obtain the position in the mature form, subtract 30 from the number for α4 and 25 for β2.

Point mutations were carried out using the QuikChange™ Site-Directed Mutagenesis Kit (Stratagene, La Jolla, CA, USA). Oligonucleotides for PCR reactions were purchased from Eurofins MWG Operon (Germany). In order to increase the number of positive transformants, the protocol used was slightly modified from the manufacturer's instructions, as described below:

1) Oligonucleotides (35 to 45 long, melting temperature (TM) > 80 °C) were synthesised carrying the desired mutation in the middle.
2) Primers were diluted to a final concentration of 150 ng/μl and used in the subsequent PCR.
3) The PCR mix consisted of the following:

1X	reaction buffer
100 ng	plasmid DNA
200 ng	sense primer
200 ng	antisense primer
6 %	dimethyl sulphoxide (DMSO)
0.1 mM	deoxyribonucleotides triphosphate (dNTPs)
2.5 U	Pfu DNA polymerase

nuclease-free water to a final volume of 50 μl

4) The parameters for the PCR run were as follows:

95 °C for 1 minute	1 cycle
95 °C for 45 seconds 55 °C for 1 minute 68 °C for 6 minutes	15 cycles

5) 10 units of the enzyme Dpn I were added to the PCR mixture in order to degrade the parental methylated DNA, which corresponds to the template (non-mutated DNA), and to leave intact only the newly formed DNA (non-methylated and likely containing the desired mutation)

6) X-Gold competent cells were transformed with 30 µl of the digestion product. After overnight incubation, 3 colonies were picked and amplified by growing them in 5 ml of Luria-Bertani (LB) medium at 37 °C. After overnight growth, the cDNA was isolated from the bacteria using commercially available DNA purification kits. The purified plasmid was fully sequenced to confirm the presence of the desired mutation and verified the sequence of the non-mutated regions.

2.5 Construction of concatenated receptors

The strategy used for the construction of concatenated receptors will be described in details in Chapter 3. Briefly, each subunit underwent two sequential PCR steps in order to prepare it for concatenation. The primers used for the PCR reactions are listed in Appendix 1. The first PCR step eliminated the stop codons, inserted the Kozak sequence GCCACC immediately before the signal peptide of the first subunit and added half of the length of the linker upstream and downstream from the 5' and 3' coding regions of each subunit. The second PCR step introduced the second half of the linker and unique restriction sites upstream and downstream of the linker to allow successive subcloning into a modified pcDNA3.1 Hygro (-) plasmid vector (Invitrogen, UK). This plasmid was also used to assemble the concatamers. The restriction sites used for the subcloning are listed in Chapter 3. Subunits were ligated sequentially into pentameric constructs using standard ligation procedures following verification, by full-length cDNA sequencing, that the PCR steps had not introduced any mutation in the constructs sequence. Following assembly, pentameric concatamers were subcloned into a modified pCI vector (Promega, UK). In

addition a SwaI site was inserted downstream the SV40 late region for linearization prior to RNA *in vitro* transcription.

2.6 Insertion of mutations in concatenated receptors

To produce mutant concatenated $(\alpha4)_3(\beta2)_2$ and $(\alpha4)_2(\beta2)_3$ receptors each α4 or β2 subunit was modified separately and subsequently ligated into the pentameric constructs using standard ligation procedures. The full-length sequence of mutant subunit cDNAs was verified by DNA sequencing.

2.7 *In vitro* transcription of concatenated receptors

Concatenated constructs ligated into the pCI modified vector were linearised overnight with Swa I. The restriction digestion was terminated by adding the following:

- $1/20^{th}$ volume 0.5 M EDTA;
- $1/10^{th}$ volume 5M NH_4 acetate;
- 2 volumes of ethanol

and dissolved in TE buffer pH 8 at a concentration of 1 μg/μl. RNA transcription was carried out using the mMessage mMachine kit (Ambion, UK). In order to increase efficiency of the transcription, the protocol used was slightly modified from the manufacturer's instructions, as described below:

1) 1X NTP/CAP mix
   1X reaction buffer
   1 ug linear template DNA
   2 uL enzyme mix
   nuclease-free water to a final volume of 20 uL
2) The mix was incubate at 30 °C for 2 hour.
3) The transcripted RNA was then treated with 2U of TURBO DNase at 37 °C for 15 min in order to remove the template DNA.

RNA was column-purified using the QiaQuick RNA Purification Kit (Qiagen, UK) and stored at -80 °C. RNA was quantified both by gel electrophoresis and by spectrophotometric reading.

2.8 *Xenopus laevis* oocytes preparation

Oocytes were collected from adult female *Xenopus laevis*, anaesthetised and sacrificed according to Home Office guidelines. A visceral incision was made through the skin and body wall. The ovaries were removed and stored in OR2 solution (82 mM NaCl, 2m M KCl, 2 mM $MgCl_2$, 5 mM HEPES adjusted to pH 7.6 with NaOH). Only oocytes at the stage V and VI of maturation were isolated. The theca and epithelial layers were manually removed by using fine forceps. The remaining follicular cell layer was removed by incubating the oocytes for 7 minutes in type IA collagenase (0.5 mg/ml) dissolved in OR2 and placed on a rotating platform. Oocytes were maintained at 18 °C in an incubator in a modified Barth's medium (88 mM NaCl, 1 mM KCl, 2.4 mM $NaHCO_3$, 0.3 mM $Ca(NO_3)_2$, 0.41 mM $CaCl_2$, 0.82 mM $MgSO_4$, 15 mM HEPES and 5 mg/l neomycin, pH 7.6 adjusted to pH 7.6 with NaOH).

2.9 Microinjection of cDNA and cRNA

Needles for microinjection were prepared from glass capillary tubing (Drummond, Broomall, PA, USA), which were pulled in one stage using a horizontal microelectrode puller (Campden Instruments, UK – Model 753). Prior to use the tip of a selected needle was broken using fine forceps to give a narrow tip length of approximately 3 mm with an external ranging from 1.0 to 1.5 μm. The needle was back-filled with light mineral oil and loaded onto a Drummond nanoinjector (Drummond, USA).

For expression of non-linked $(\alpha4)_2(\beta2)_3$ and $(\alpha4)_3(\beta2)_2$ in *Xenopus* oocytes, wild-type or mutant human α4 or β2 subunit cDNAs, ligated into the pCI expression vector, were dissolved in nuclease-free water at a concentration of 1 μg/μl (spectrophotometric and agarose gel electrophoresis determinations). Mixtures of either wild-type or mutated α4 and β2 cDNA at 1:10 or 10:1 ratios (Moroni *et al.*, 2006) were then diluted to reach a concentration of 0.16 μg/μl. The nucleus of oocytes was injected with 18.4 nl, thus the

amount of total cDNA injected was kept constantly equal to 3 ng. To maximise the opportunity of hitting the nucleus, the needle was directed towards the animal pole. The needle tip was assumed to reach the nucleus after penetrating the oocytes for one third of its diameter.

For expression of concatenated $(\alpha4)_2(\beta2)_3$ and $(\alpha4)_3(\beta2)_2$ receptors, the appropriate cRNA was dissolved in nuclease-free water at different concentrations for the different constructs. 50 nl of RNA mix were injected into the cytoplasm of the oocytes. For studies of the effects of chaperone protein 14-3-3 on the functional expression of the pentameric concatamers, 2 ng of cRNA coding for rat 14-3-3 was co-injected with concatamer-cRNA. The cDNA for this protein was kindly provided by Dr. R. Anand (Ohio State University, USA).

Injected oocytes were transferred to a sterile Petri dish containing modified Barth's solution and incubated at 18 °C for a maximum of 5 days. The Barth's solution was changed daily and oocytes that had degraded were removed to minimise enzymatic damage to healthy cells.

2.10 Electrophysiological Recordings

Recordings were performed 2-6 days post-injection. Oocytes were selected according to their appearance; only oocytes with integral membrane and no signs of degradation were chosen for electrophysiological recordings. Oocytes were placed in a 0.1 ml recording chamber and continuously perfused at a rate of 10 ml/min with modified Ringer solution (in mM: NaCl 150, KCl 2.8, HEPES 10, $BaCl_2$ 1.8 and adjusted to pH 7.2 with 5 mM NaOH), unless otherwise stated. Switching between different solutions occurred through manually activated valves. All solutions were freshly made prior to recordings. Unless otherwise mentioned, a nominally Ca^{2+} free solution was chosen in order to minimise the contribution to the response of Ca^{2+}-gated chloride channels which are endogenous to the *Xenopus* oocyte (Barish, 1983) and may be activated by Ca^{2+} entry through the heterologously expressed nAChRs.

Oocytes were impaled by two electrodes connected to a Geneclamp 500B amplifier (Molecular Devices, CA, USA) for standard voltage clamp recordings. Oocytes were voltage-clamped at –60 mV, except for the determination of the reversal potential of the ACh-elicited currents. Electrodes were made from borosilicate capillary glass (GC 150 TF,

Harvard Apparatus, MA, USA) using a vertical two stage electrode puller (Narishige PP-83). The electrodes were back-filled to approximately 5 mm from the top with a solution of 1 mg/ml agarose dissolved in 3 M KCl and stored at room temperature. Prior to recordings electrodes were filled with 3 M KCl and only electrodes with a resistance between 0.5 and 2 MΩ were used for voltage clamping. Typically, traces were filtered at 1 kHz during recording and digitized at 10 kHz using the DigiData 1200 interface (Molecular Devices, CA, USA). All experiments were carried out at room temperature (approximately 20 °C).

2.11 Time course of desensitisation

To study the effect of mutations on receptor desensitisation the decay of currents elicited by 30 s applications of ACh EC_{50} or saturating ACh concentrations was examined. The amplitude of the current measured between peak and plateau was used as an estimate of the fraction of desensitisation occurring during a brief exposure to the agonist. To compare the rate of desensitisation of the wild type and mutant responses, the desensitising phase was fit to a one or two-component exponential, as appropriate (see Section 2.14), obtaining an apparent time desensitisation constant (τ).

2.12 Study of Zn^{2+} sensitivity and Ca^{2+} permeability

The sensitivity to Zn^{2+} was assessed by co-applying a range of Zn^{2+} concentrations with non-desensitising concentration of ACh, 1 μM ACh for linked and non-linked $(\alpha4)_2(\beta2)_3$ nAChRs and 10 μM ACh for linked and non-linked $(\alpha4)_3(\beta2)_2$ receptors. For Zn^{2+} to attain equilibrium around impaled oocytes, Zn^{2+} was pre-applied for 30 s to the cell prior to co-application of ACh and Zn^{2+}. Concentration-response relationships for Zn^{2+} were obtained using this protocol. Peak responses elicited by ACh + Zn^{2+} were normalized to the peak response of the appropriate ACh alone.

The Ca^{2+} permeability of the receptors was determined by constructing current-voltage (I-V) relationships and measuring the shift in the reversal potential of ACh EC_{50} currents in the presence of 1.8 mM Ca^{2+} or 18 mM Ca^{2+} in the perfusing Ringer solution. The I-V relationship characteristics of the ACh-elicited current in wild-type and mutant receptors was determined as follows. First, membrane was held at -60 mV and then the passive cell

properties were measured by steeping the voltage by 10 mV steps from -60 mV to +20 - 30 mV. The membrane was then returned to -60 mV and an EC_{50} concentration of ACh was applied, the holding voltage was then stepped by 10 mV from -60 mV to +20 -30 mV, and EC_{50} ACh was applied at each step. The passive cell properties were then substracted from the ACh-elicited currents. The I-V curve was obtained by plotting the amplitude of the ACh-induced currents as a function of the holding voltage. The reversal potential of the ACh-induced currents was taken as the voltage prior to that at which the ACh-currents became positive.

2.13 Western Blot Assay

Western blot assays were carried out on total membrane homogenates prepared from oocytes expressing heterologously either concatenated or non-linked α4β2 nAChRs. Oocytes were homogenised six days after microinjection with free α4 and β2 subunits cDNAs or concatamer cRNAs. Four batches of oocytes (50 oocytes per batch) were used. Oocytes were homogenised using an ice-cold homogenisation buffer (150 mM NaCl, 2 mM $CaCl_2$, 2% Triton-X100, 20 mM TrisHCl, pH 7.4, supplemented with 1μM pepstatin, 1 mg/ml leupeptin, 2 mM PMSF) at a ratio of 10 μl buffer/oocyte. Homogenates were centrifuged twice at 1000 x g for 5 min at 4 °C to remove the yolk and the supernatants were then re-centrifuged at 10,000 x g for 10 min at 4 °C. Aliquots of the supernatants containing 30 μg of protein were separated by SDS-PAGE electrophoresis (Novex, 7% Tris-acetate gels; Invitrogen, UK). The proteins were subsequently transferred onto nitrocellulose membranes (Optitran BA-S83, Schleider & Schuell, Germany) by electro-blotting (2 h transfer at room temperature at 25 mV). Membranes were blocked for 2 h at room temperature with 5% non-fat dry milk in phosphate buffered saline containing 0.1% Tween 20 (Sigma-Aldrich Co, UK). Membranes were then incubated overnight at 4°C with 0.7 μg/ml of primary antibody (AChRα4 (H-133) or AChRβ2 (H-92), Santa Cruz Biotechnology, USA) and further incubated for 3h at room temperature with 2 μg/ml of secondary antibody (Cy-5-goat anti-rabbit IgG conjugate, Invitrogen, UK). Bound antibodies were visualised on a Typhoon variable mode imager (GE Healthcare, UK). The identity of the bands was determined based on molecular weight of the immunoreactive protein (α4 ≅ 70 kDa; β2 ≅ 50 kDa).

2.14 Data Analysis

Fits to full concentration-response curves for individual oocytes were made independently and then averaged in order to compare significant differences between groups. Concentration-response data for wild type or mutant α4β2 receptors were fitted using one and two components sigmoidal dose-response equations,

$$Y = I/Imax_{Bottom} + (I/Imax_{Top} - I/Imax_{Bottom})/(1 + 10\text{^}((LogEC_{50} - X)*nHill))$$

$$Y = I/Imax_{Bottom} + [(I/Imax_{Top} - I/Imax_{Bottom})*Fraction/(1 + 10\text{^}((LogEC_{50\_1} - X)*nHill_1))] + [I/Imax_{Top} - I/Imax_{Bottom})*(1\text{-}Fraction)/(1 + 10\text{^}((LogEC_{50\_2} - X)*nHill_2))]$$

where X is the logarithm of the agonist concentration, Y is the peak amplitude of the normalized current response, I_{max} is the maximal current and nHill is the Hill slope. An F test determined whether the one-site or two-site model best fit the data; the simpler one-component model was preferred unless the extra sum-of-squares F test had a value of p less than 0.05.

The peak responses elicited by ACh plus Zn^{2+} were normalized to the peak response of the appropriate ACh alone. Where a single component concentration–response relationship was evident, data were fitted to the Hill equation shown above. When Zn^{2+} produced both a potentiating and inhibiting effect, the data were fitted to the following equation designed to account for the potentiating and inhibitory effects of Zn^{2+} on α4β2 receptors assuming this cation binds to two distinct sites on the receptor:

$$I = (1 + ((I_{max} - 1)/(1 + 10\text{^}((logEC_{50} - X) * nHill_{pot}))))/(1 + 10\text{^}((logIC_{50} - X) * nHill_{inh}))$$

where I represents the current responses at a given Zn^{2+} concentration (X), I_{max}, represents the maximally potentiated peak, EC_{50} and IC_{50} are the concentrations of Zn^{2+} inducing half-maximal potentiation or inhibition, respectively, and $nHill_{pot}$ and $nHill_{inh}$ are the Hill coefficients for potentiation and inhibition, respectively. F tests were always performed to assess the fitting of the data; the simpler one-component model was preferred unless the extra sum-of-squares F test had a value of $p < 0.05$.

Current decay data were fit to either the mono-exponential function

$$y = (A_0 * e^{-(t/\tau)}) + B$$

or the bi-exponential equation

$$y = (A_0 * e^{-(\tau 1 - \tau 2)t}) + B$$

where y is the ACh-evoked current, A_0 the amplitude at time zero, t time, τ, $\tau 1$ or $\tau 2$ are the apparent time constant and B the level of current reached at the end of the application.

Data analyses were performed using Graph PAD-Prism software 5 (GraphPad Software, CA, USA). Data were pooled from at least three different batches of oocytes. Statistical significance was determined using one-way analysis of the variance (ANOVA) or Student's *t* test (two-tailed unpaired tests) as appropriate. Values of $p < 0.05$ were considered statistically significant.

CHAPTER 3

Pentameric concatenated $(\alpha4)_2(\beta2)_3$ and $(\alpha4)_3(\beta2)_2$ nicotinic acetylcholine receptors: subunit arrangement determines functional expression

3.1 Introduction

Heterologous co-expression of α4 and β2 nAChR subunits produces high- and low-affinity receptor populations evidenced by biphasic ACh concentration-response curves. High- and low-affinity α4β2 nAChRs result from the assembly of receptors with two distinct stoichiometries: $(\alpha4)_2(\beta2)_3$ (high-affinity subtype) and $(\alpha4)_3(\beta2)_2$ (low-affinity subtype) (Nelson *et al.*, 2003; Moroni *et al.*, 2006; Zwart *et al.*, 2006), although pharmacological studies of α4β2 nAChR expressed heterologously in *Xenopus* oocytes suggest that other stoichiometric arrangements may also occur (Zwart and Vijverberg, 1998; Lopez-Hernandez *et al.*, 2004). $(\alpha4)_2(\beta2)_3$ and $(\alpha4)_3(\beta2)_2$ receptors differ profoundly in sensitivity to activation by agonists, desensitisation kinetics, unitary conductance (Nelson *et al.*, 2003; Moroni *et al.*, 2006), Ca^{2+} permeability (Tapia *et al.*, 2007) and sensitivity to both Zn^{2+} modulation (Moroni *et al.*, 2008) and chronic exposure to nicotine (Nelson *et al.*, 2003; Kuryatov *et al.*, 2005; Moroni *et al.*, 2006). Several studies showed that both $(\alpha4)_2(\beta2)_3$ and $(\alpha4)_3(\beta2)_2$ are likely to be present in the brain (Marks *et al.*, 1999; Butt *et al.*, 2002; Gotti *et al.*, 2008) and it was been suggested that their relative ratio may influence basal behaviours influenced by α4β2 receptors as well as sensitivity to the acute effects of nicotine (Stitzel *et al.*, 2001; Tritto *et al.*, 2002; Kim *et al.*, 2003). Hence, the separate expression of $(\alpha4)_2(\beta2)_3$ and $(\alpha4)_3(\beta2)_2$ in heterologous systems has become an increasingly attractive approach for aiding the characterisation of the properties of these receptors and for the development of stoichiometry-specific α4β2 nAChR drugs.

There has been several attempts at expressing $(\alpha4)_2(\beta2)_3$ and $(\alpha4)_3(\beta2)_2$ nAChRs separately in heterologous systems. These include injection of 1:10 or 10:1 ratios of α4 and β2 subunit cDNAs into the nucleus of *Xenopus* oocytes (Moroni *et al.*, 2006), growing human embryonic kidney 293T cells stably transfected with α4 and β2 subunits at 29 °C or chronically exposed to nicotine (Nelson *et al.*, 2003). Although, as suggested by monophasic ACh concentration-response curves, these approaches yield very homogeneous populations of $(\alpha4)_2(\beta2)_3$ or $(\alpha4)_3(\beta2)_2$ receptors, it is not conclusive that they abolish concurrent expression of multiple forms of the α4β2 receptor. As suggested by the biphasic concentration-response curves produced by agonists such as 5I-A85380 at α4β2 nAChR produced with the 10:1 cDNA ratios (Zwart *et al.*, 2006) the presence of other receptor stoichiometric arrangements cannot be excluded.

Tandem subunit constructs with two subunits attached together by synthetic AGS linkers have also been used to constrain the stoichiometry of α4β2 nAChRs. However, this

approach can lead to the formation of dipentamers (Zhou *et al.*, 2003) or linked subunits may not be fully incorporated into the pentameric structure of the receptor (Groot-Kormelink *et al.*, 2004).

An alternative approach that circumvents the problem of subunit isoforms and stoichiometry heterogeneity is the production of concatenated receptors with forced stoichiometry. In these receptors, the subunit arrangement is fixed by predetermining the order of subunits by fusion at the DNA level. Recently, this strategy was used to produce functional expression of $(\alpha3)_2(\beta4)_3$ nAChR (Groot-Kormelink *et al.*, 2006) and $(\alpha1)_2(\beta2)_2\gamma2$ $GABA_A$ receptors (Baur *et al.*, 2006). As suggested by functional studies, pentameric $(\alpha3)_2(\beta4)_3$ and $(\alpha1)_2(\beta2)_2\gamma2$ $GABA_A$ concatamers are similar to their non-linked counterparts, which shows that concatenation of Cys-loop subunit receptors to pentamers does not alter receptor functions. And, as shown by studies of concatenated $GABA_A$ receptor, this approach offers the unique possibility of studying positional effects of point mutations (Baumann *et al.*, 2003; Baur and Sigel, 2005) and positional effects of subunit isoforms (Minier and Sigel, 2004a; Boileau *et al.*, 2005).

Therefore, in order to facilitate the study of the structural mechanisms underlying the functional properties of the two alternate stoichiometries of the α4β2 nAChR, concatenated $(\alpha4)_2(\beta2)_3$ and $(\alpha4)_3(\beta2)_2$ receptors were engineered. Several strategies have been used to construct pentameric concatamers of Cys-loop receptors. For the concatenation of the $GABA_A$ receptor subunits, linkers of variable lengths and containing three different amino acid residues (glutamine, proline and alanine) were used. Importantly, the signal peptide of every subunit, but the first one, was removed (Baur *et al.*, 2006). By comparison, in the approach used to construct concatenated α3β4 nAChR (Groot-Kormelink *et al.* 2006), the subunit cDNAs were bridged using fixed-length linkers composed of 8 glutamines and the signal peptide was maintained in all five subunits. The choice of polyglutamine linkers was based both on the water-solubility of the sequence and the random coil conformation that acquires in water (Altschuler *et al.*, 1997), making it an ideal linker for this purpose.

This chapter describes the construction of three types of fully concatenated $(\alpha4)_2(\beta2)_3$ and $(\alpha4)_3(\beta2)_2$ nAChRs constructed using different strategies and their expression and functional characterisation in *Xenopus* oocytes. The results obtained suggest that the subunit order plays an important role in the synthesis of concatenated α4β2 nAChRs.

3.2 Experimental procedures

3.2.1 Overall strategy

Three types of α4β2 receptor concatamers were constructed. Because of the homology between the α3β4 and the α4β2 nAChRs, the first type of pentameric concatamers were engineered using the procedure described by Groot-Kormelink *et al.* (2006) to construct the $(\alpha3)_2(\beta4)_3$ nAChR concatamer. Because both subunits expose both C- and N-termini on the extracellular side, the C-terminus of one subunit was covalently linked, at the cDNA level, to the N-terminus of the subsequent subunit. The subunit order for the first type of pentameric concatamers was β2_β2_α4_β2_α4 for the $(\alpha4)_2(\beta2)_3$ receptor and β2_α4_α4_β2_α4 for the $(\alpha4)_3(\beta2)_2$ receptor. The signal peptides were maintained in all subunits which were linked by 8 glutamines (Q8) linkers. For clarity, these constructs are referred to as $\beta2_{(Q8)}\beta2_{(Q8)}\alpha4_{(Q8)}\beta2_{(Q8)}\alpha4$ and $\beta2_{(Q8)}\alpha4_{(Q8)}\alpha4_{(Q8)}\beta2_{(Q8)}\alpha4$, respectively.

The second type of constructs maintained the subunit order of the previous. However, the signal peptide was removed from all the subunits but the first and the subunits were bridged by alanine-glycine-serine linkers (AGS) of variable length to compensate for the differences in the length of the C-terminus of the α4 and the β2 subunits (Zhou *et al.*, 2003). Thus, an $(AGS)_6$ was used to join β2 to the α4 subunit, whereas an $(AGS)_9$ linker bridged the α4 to the β2 subunit. These constructs are referred to as $\beta2_{(AGS)}\beta2_{(AGS)}\alpha4_{(AGS)}\beta2_{(AGS)}\alpha4$ and $\beta2_{(AGS)}\alpha4_{(AGS)}\alpha4_{(AGS)}\beta2_{(AGS)}\alpha4$, respectively.

The third type of constructs used a subunit order of β2_α4_β2_α4_β2 for the $(\alpha4)_2(\beta2)_3$ receptor and β2_α4_β2_α4_α4 for the $(\alpha4)_3(\beta2)_2$ receptor. In these constructs, the signal peptide was removed from all the subunits but the first and the subunits were bridged by AGS linkers of variable length, as in the $\beta2_{(AGS)}\beta2_{(AGS)}\alpha4_{(AGS)}\beta2_{(AGS)}\alpha4$ and $\beta2_{(AGS)}\alpha4_{(AGS)}\alpha4_{(AGS)}\beta2_{(AGS)}\alpha4$ constructs.

Single α4 and β2 subunits were modified by two sequential steps of PCR in order to add the linker and introduce unique restriction sites to allow successive subcloning into a modified pcDNA3.1 Hygro(-) plasmid vector. This plasmid was also used to assemble the concatamers. The pentamers were subsequently assembled using standard ligation reactions following verification, by full-length cDNA sequencing, that the PCR steps had not introduced any mutation in the constructs sequence. Following assembly, pentameric concatamers were subcloned into a modified pCI vector.

3.2.2 Modification of plasmid expression vectors to host pentameric constructs

The expression vector pcDNA3.1 Hygro(-) was chosen for subcloning of single subunits and for assembling the concatameric constructs after linkers and restriction sites were added. The pCI vector was used as expression vector for nuclear injection in *Xenopus* oocytes and for *in vitro* transcription for the reasons explained in Section 2.3. The multiple cloning site (MCS) of both plasmids was modified by oligonucleotides hybridisation in order to introduce restrictions sites for the subcloning of the modified single subunits or the concatenated constructs.

The oligonucleotides used to modify the pcDNA 3.1 vector were:

Nhe I Asc I Swa I Xba I BstB I Age I
Oligo Forward: **CTAGC** GGCGCGCC ATTTAAAT TCTAGA TTCGAA ACCGGT

Pme I Xho I
GTTTAAAC **C**

Xho I Pme I Age I BstB I Xba I Swa I
Oligo Reverse: **TCGAG** GTTTAAAC ACCGGT TTCGAA TCTAGA ATTTAAAT

Asc I Nhe I
GGCGCGCC **G**

After hybridization the resulting double-strand DNA linker was ligated into the pcDNA3.1 Hygro(-) between Nhe I and Xho I (bold and underlined).

The oligonucleotides used to modify the pCI vector were:

Eco RI Asc I Xba I Age I Xho I Swa I
Oligo Forward: **AATTC** GGCGCGCC TCTAGA ACCGGT CTCGAG ATTTAAAT

EcoR V Not I
GATATC **GC**

Not I Eco RV Swa I Xho I Age I Xba I
Oligo Reverse: **GGCCGC** GATATC ATTTAAAT CTCGAG ACCGGT TCTAGA

Asc I Eco RI
GGCGCGCC **G**

After hybridization the resulting double-strand DNA linker was ligated into the pCI vector between Eco RI and Not I (bold and underlined).

The hybridisation of the oligonucleotides was carried out as follows:

1) Forward and reverse oligonucleotides were synthesised in order to carry 3' and 5' overhanging ends.
2) Oligonucleotides were diluted to a final concentration of 1 μg/μl.
3) The hybridisation reaction consisted of the following reagents:

   10 mM Tris HCl pH 8

   10 mM $MgCl_2$

   20 μg Oligo Forward

   20 μg Oligo Reverse

   1 % DMSO

   nuclease-free water to a final volume of 100 μl
4) The reaction mix was placed in a water containing bath at 95 °C for 5 minutes; the bath was then cool slowly to reach room temperature (overnight).
5) The reaction mixture was isopropanol-precipitated and the resulting double stranded DNA was resuspended to a final concentration of 1 μg/μl and used for standard ligations.

The pCI modified vector was also further modified to carry a unique restriction site (Swa I, downstream of the SV40 region) for cDNA linearization, which was needed for *in vitro* RNA transcription. The site was introduced using the QuikChange™ Site-Directed Mutagenesis Kit as described Section 2.4.

3.2.3 Subcloning of single subunits into modified pcDNA3.1 Hygro(-)

Single α4 and β2 subunits underwent two sequential PCR amplification steps. The first PCR step eliminated the stop codons (for all constructs) and signal peptides (for the second and third type of constructs) and inserted the Kozac sequence GCCACC immediately before the signal peptide of the first subunit. Half of the length of the linker (i.e., Q_4, $(AGS)_3$ or $(AGS)_{4/5}$) was added with the first PCR step upstream and downstream from the 5' and 3' coding regions of each subunit. The second PCR step introduced unique restriction sites upstream and downstream of the linkers to allow successive subcloning into modified pcDNA 3.1 Hygro(-) plasmid.

All PCR reactions were performed in the following way:

1) Oligonucletides (35 to 50 bp long), were synthesised in order to pair 20 to 25 bases of the coding region of either the α4 or the β2 subunit (TM 63-65 °C).
2) Primers were diluted to a final concentration of 10 μM and used in the subsequent PCR.
3) The PCR mix consisted of the following:

1X	Thermo Polymerase Buffer II
50 ng	plasmid DNA (either α4 or β2 subunit or product of the first PCR reaction)
1 mM	$MgSO_4$
0.1 μM	forward primer
0.1 μM	reverse primer
6 %	DMSO
0.1 mM	dNTPs
200 U	Vent polymerase
nuclease-free water to a final volume of 50 μl	

4) The parameters for the PCR run were as follows:

95 °C	for 1 minute	1 cycle
95 °C	for 45 seconds	30 cycles
(TM − 10) °C	for 1 minute	
72 °C	for 2 minutes and 30 seconds	

Subsequently, the second PCR reaction was loaded on a 1% agarose gel and isolated from plasmidic template by using a Gel Extraction Kit (Qiagen, UK). The PCR product was eluted in 50 μl of Tris HCl buffer pH 8. Single subunits were subcloned singularly into the pcDNA 3.1 Hygro(-) modified vector using the unique restriction sites added by the second PCR reaction. For all concatamers the subunits were subcloned between the following restrictions sites regardless of the subunit being α4 or β2:

1st subunit: Asc I / Xba I
2nd subunit: Xba I / Age I
3rd subunit: Age I / Xho I
4th subunit: Xho I / Not I
5th subunit: Not I / Eco RV

The absence of unwanted mutations, the correct insertion of the linkers and of the restriction sites flanking the coding region of the subunits were verified by full-length sequencing.

Subunits were ligated sequentially into pentameric constructs using standard ligation procedures as shown in Fig. 3.1.

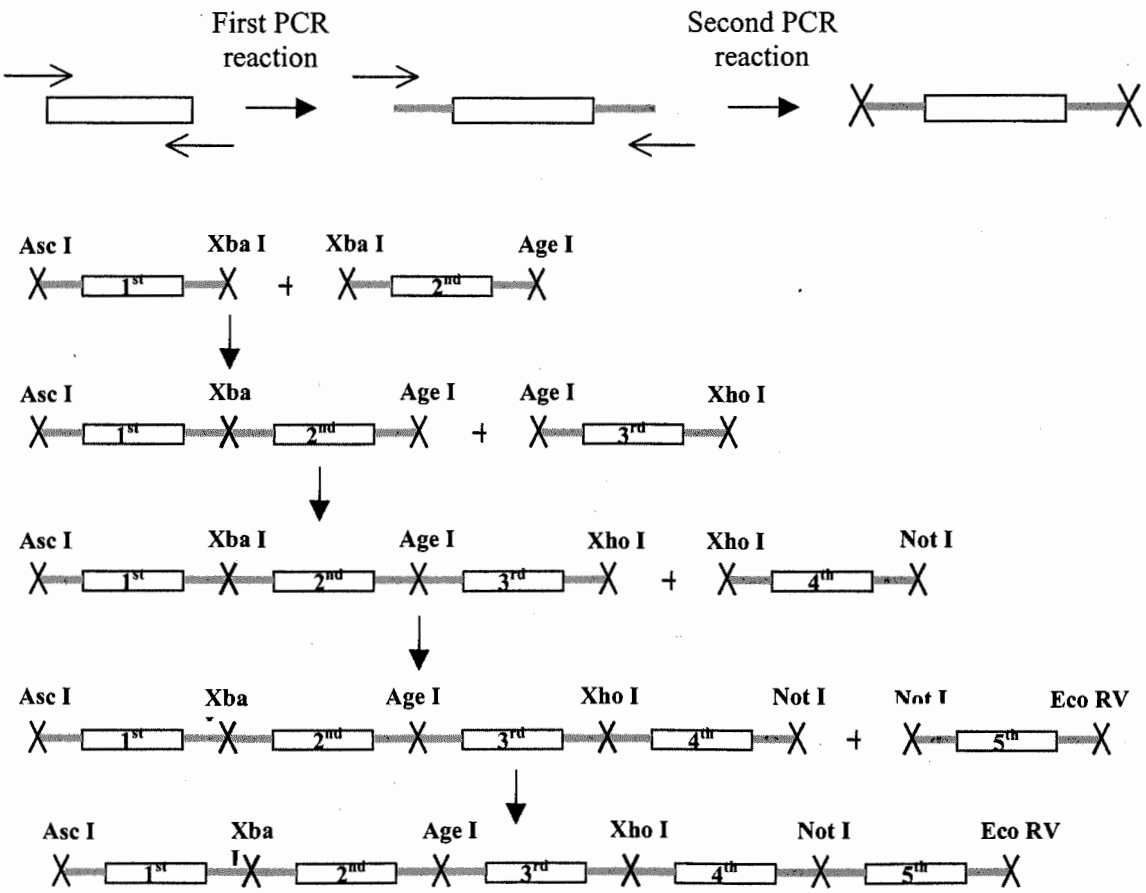

Fig. 3.1 Diagram showing the experimental approach used to create concatenated α4β2 receptors. Starting from wild type α4 and β2 subunits two successive PCR steps were performed to add linkers (grey rectangular box) and unique restriction sites (X). The modified subunits were sequentially ligated into pentameric constructs using standard ligation procedures.

Following assembly, pentameric concatamers were excised from the pcDNA3.1 Hygro(-) modified vector and ligated into the pCI modified vector between Asc I and Eco RV for nuclear injection in *Xenopus* oocytes and *in vitro* transcription.

3.2.4 cDNA and cRNA injection in *Xenopus* oocytes.

Stage V and VI *Xenopus* oocytes were prepared as previously described in Section 2.7 cRNA transcription was carried out as described in Section 2.6. In each oocyte up to 150 ng of cRNAs were injected for the first and second type of constructs in a volume of 50 nl. For the third type 5-10 ng of cRNAs were sufficient to obtain a good level of functional expression.

RESULTS

3.3.1 The pharmacological profile of $\beta2_{(Q8)}\beta2_{(Q8)}\alpha4_{(Q8)}\beta2_{(Q8)}\alpha4$ and $\beta2_{(Q8)}\alpha4_{(Q8)}\alpha4_{(Q8)}\beta2_{(Q8)}\alpha4$ is different from that of their non-linked counterpart

$\beta2_{(Q8)}\beta2_{(Q8)}\alpha4_{(Q8)}\beta2_{(Q8)}\alpha4$ and $\beta2_{(Q8)}\alpha4_{(Q8)}\alpha4_{(Q8)}\beta2_{(Q8)}\alpha4$ constructs were examined to see if they produced functional expression in *Xenopus* oocytes. Fig. 3.2 shows that five days after microinjection with 150 ng or 100 ng of cRNA coding for $\beta2_{(Q8)}\beta2_{(Q8)}\alpha4_{(Q8)}\beta2_{(Q8)}\alpha4$ and $\beta2_{(Q8)}\alpha4_{(Q8)}\alpha4_{(Q8)}\beta2_{(Q8)}\alpha4$ receptors functional expression was markedly and significantly lower than that obtained by injection of non-linked α4 and β2 cRNAs at a 1:10 ratio or 10:1 ratio ($p < 0.001$, Student's t test, n = 8 - 10). Typically, maximal concentrations of ACh induced current responses with an average amplitude of 0.5 ± 0.1 μA or 3.2 ± 1 μA in oocytes expressing $(\alpha4)_2(\beta2)_3$ or $(\alpha4)_3(\beta2)_2$ non-linked receptors, respectively. By comparison, only small currents could be recorded five to six days after injection of more than 150-fold the usual amount of cRNA (150ng for concatamers versus 0.05 - 1 ng for single subunits) (Fig. 3.2 A).

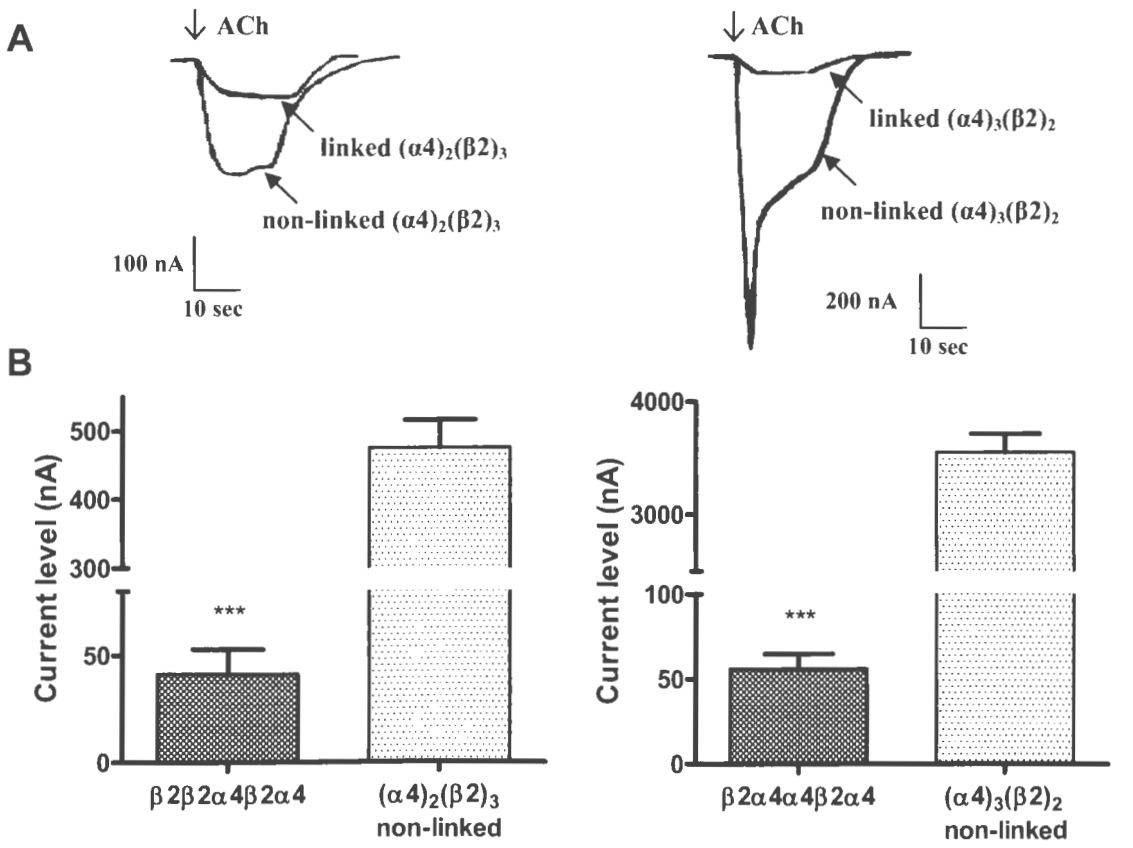

Fig. 3.2. Expression of pentameric $\beta2_{(Q8)}\beta2_{(Q8)}\alpha4_{(Q8)}\beta2_{(Q8)}\alpha4$ and $\beta2_{(Q8)}\alpha4_{(Q8)}\alpha4_{(Q8)}\beta2_{(Q8)}\alpha4$ concatamers in *Xenopus* oocytes. A) ACh evoked small inward currents in oocytes microinjected with 150 ng of $\beta2_{(Q8)}\beta2_{(Q8)}\alpha4_{(Q8)}\beta2_{(Q8)}\alpha4$ (*Left panel*) and $\beta2_{(Q8)}\alpha4_{(Q8)}\alpha4_{(Q8)}\beta2_{(Q8)}\alpha4$ (*Right panel*) cRNAs. Traces evoked in non-linked receptors are superimposed for comparison. **B)** Bar graph comparing the functional expression levels of receptors made of concatenated subunits and expressed by means of extreme transfection ratios. (*** = $p < 0.0001$, Student's t test)

Fig. 3.3 shows ACh current responses from oocytes expressing human neuronal non-linked α4β2 nAChRs following transfection with a 1:10 or 10:1 subunit (α4/β2) injection ratio or with the concatenated constructs. Agonist responses were very similar for the two receptors both in time course and agonist sensitivity. Analysis of the concentration-response curves showed significant differences in EC_{50} values for linked and non-linked receptors ($p < 0.05$, Student's t test, n = 8 - 10) and a slightly different, albeit non significant, value for the Hill slope (data are summarized in Table 3.1)

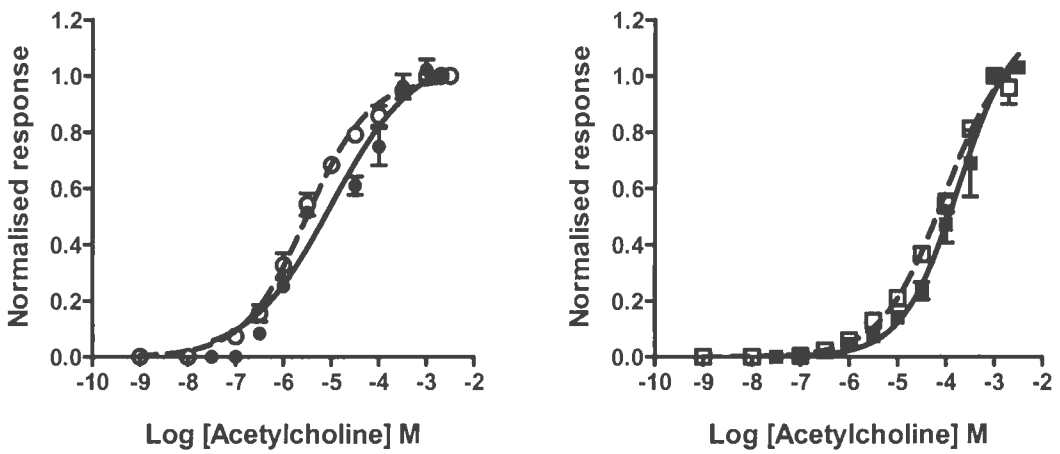

Fig. 3.3. $\beta2_{(Q8)}\beta2_{(Q8)}\alpha4_{(Q8)}\beta2_{(Q8)}\alpha4$ and $\beta2_{(Q8)}\alpha4_{(Q8)}\alpha4_{(Q8)}\beta2_{(Q8)}\alpha4$ receptors have ACh sensitivity similar to that of receptors expressed from monomeric constructs. ACh concentration-response curves for concatenated $(\alpha4)_2(\beta2)_3$ (*Left panel,* ●) and $(\alpha4)_3(\beta2)_2$ (*Right panel,* ■). For comparison ACh concentration response curves for non-linked receptors are shown as dashed lines.

The effects of a range of nicotinic agonists and antagonists were evaluated in order to characterise the pharmacological properties of the concatenated receptors (Figs. 3.4 A, B). Although concentration-response curves for ACh and other ligands were monophasic ($p < 0.001$, F test, n = 8 - 10), suggesting the presence of only one type of receptor population, the pharmacological profile of $\beta2_{(Q8)}\beta2_{(Q8)}\alpha4_{(Q8)}\beta2_{(Q8)}\alpha4$ and $\beta2_{(Q8)}\alpha4_{(Q8)}\alpha4_{(Q8)}\beta2_{(Q8)}\alpha4$ receptors was significantly different from that of the corresponding non-linked receptor ($p < 0.05$, Student's t test, n = 8 - 10). The efficacies of the full agonists epibatidine, A85380 and TC2559 on the concatenated $(\alpha4)_3(\beta2)_2$ receptor were significantly higher than in the non-linked receptor, whereas the partial agonist cytisine was less efficacious on the concatenated receptor than in the non-linked $(\alpha4)_3(\beta2)_2$ receptor (Fig. 3.4 A). Due to the low level of expression, only the full agonists A85380 and TC2559 could be tested on the concatenated $(\alpha4)_2(\beta2)_3$ receptor. Efficacy of A85380 was

slightly higher on the concatenated receptor whilst efficacy of TC2559 was drastically reduced (Fig. 3.4 B). Affinity values of the compounds tested are summarised in Table 3.1.

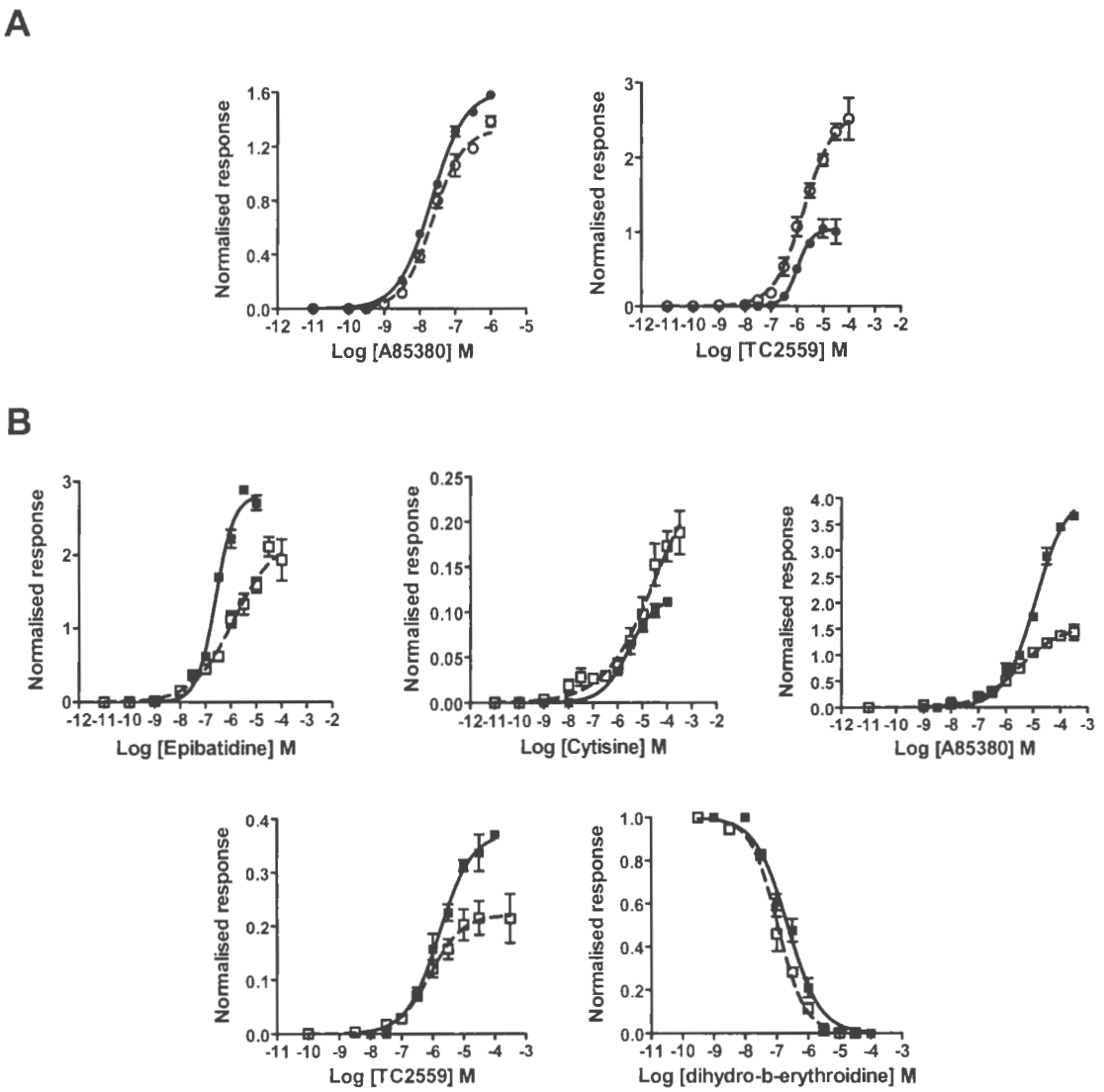

Fig. 3.4. The pharmacological profile of $\beta2_{(Q8)}\beta2_{(Q8)}\alpha4_{(Q8)}\beta2_{(Q8)}\alpha4$ and $\beta2_{(Q8)}\alpha4_{(Q8)}\alpha4_{(Q8)}\beta2_{(Q8)}\alpha4$ receptors is different from that of non-linked α4β2 receptors. **(A)** Concentration-response curves of nicotinic ligands on the function of concatenated and non-linked $(\alpha4)_2(\beta2)_3$ nAChRs (●). **(B)** Concentration-response curves of nicotinic ligands on the function of concatenated and non linked $(\alpha4)_3(\beta2)_2$ nAChRs (■). Responses were normalised to 1mM. Agonist or antagonist data were analysed as described in Methods using a monophasic sigmoidal equation. Data points represent the mean ± SEM of 8 - 10 experiments carried out using at least two different batches of oocytes.

Table 3.1. Functional properties of glutamine-linked $(\alpha4)_2(\beta2)_3$ and $(\alpha4)_3(\beta2)_2$ receptors.

$\beta2_{Q8}\beta2_{Q8}\alpha4_{Q8}\beta2_{Q8}\alpha4$				Non-linked $(\alpha4)_2(\beta2)_3$		
	I/I_{max} ± SEM	EC_{50} μM (95 % CI)	nHill ± SEM	I/I_{max} ± SEM	EC_{50} μM (95 % CI)	nHill ± SEM
ACh	1	3.04 (2.5 – 9.3) *	0.50±0.05	1	3.8 (2.1 - 4.7)	0.84±0.11
A85380	1.58±0.01 *	0.022 (0.02–0.03) *	0.92±0.03	1.38±0.07	0.026 (0.01-0.05)	1.07±0.15
TC2559	1.04±0.03 *	1.04 (0.8 – 2.1)	1.8±0.31 *	2.52±0.2	1.95 (0.8 - 3)	0.82±0.06
$\beta2_{Q8}\alpha4_{Q8}\alpha4_{Q8}\beta2_{Q8}\alpha4$				Non-linked $(\alpha4)_3(\beta2)_2$		
	I/I_{max} ± SEM	EC_{50} μM (95 % CI)	nHill ± SEM	I/I_{max} ± SEM	EC_{50} μM (95 % CI)	nHill ± SEM
ACh	1	158 (128 - 178)	0.8±0.03	1	89 (76 – 120)	0.97±0.1
A85380	3.65±0.1 *	12.13 (11.5–12.7) *	0.78±0.08	1.42±0.1	3.12 (2.3 – 4.8)	0.60±0.07
Cytisine	0.11±0.01 *	4.1 (2.2 – 6.4) *	0.79±0.07 *	0.19±0.02	11.70 (9 – 28)	0.43±0.08
Epibatidine	2.7±0.09 *	25 (17 – 38) *	1.2±0.15 *	2.1±0.28	1.25 (0.8 – 3)	0.50±0.07
TC2559	0.21±0.04 *	1.08 (0.4 – 4.2)	1.03±0.18	0.21±0.04	1.12 (0.5 – 1.8)	0.87±0.08
DhβE	-	0.13 (0.09–0.17)	0.85±0.03	-	0.25 (0.12 – 0.47)	1.06±0.10

All values are means (95 % CI) or means ± SEM from 5-10 cells. Statistical analysis was performed by comparing the agonist EC_{50}, I/I_{max} and nHill of the concatenated receptors to the non-linked receptor using one-way analysis of the variance (ANOVA) to assess significance. The * signifies $p < 0.05$ compared with non-linked $(\alpha4)_2(\beta2)_3$ or $(\alpha4)_3(\beta2)_2$ as appropriate.

3.3.2 $\beta2_{(Q8)}\beta2_{(Q8)}\alpha4_{(Q8)}\beta2_{(Q8)}\alpha4$ and $\beta2_{(Q8)}\alpha4_{(Q8)}\alpha4_{(Q8)}\beta2_{(Q8)}\alpha4$ receptors are degraded during synthesis

The integrity of the concatenated constructs was assessed by Western blotting. Western blot analysis showed concatamer proteins of appropriate size ($\beta2_{(Q8)}\beta2_{(Q8)}\alpha4_{(Q8)}\beta2_{(Q8)}\alpha4$ 290 kD, and $\beta2_{(Q8)}\alpha4_{(Q8)}\alpha4_{(Q8)}\beta2_{(Q8)}\alpha4$..310 kD) but also small amounts of fragments of various sizes that included monomeric and intermediate-sized by-products (Fig. 3.5).

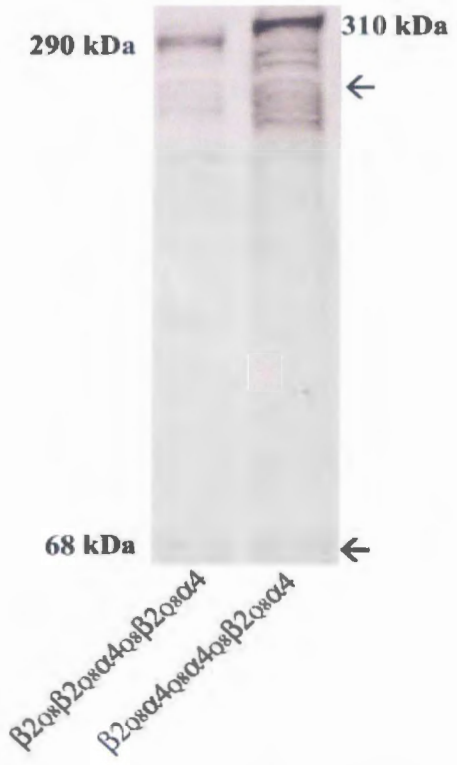

Fig. 3.5. Western blot analysis of $\beta2_{(Q8)}\beta2_{(Q8)}\alpha4_{(Q8)}\beta2_{(Q8)}\alpha4$ and $\beta2_{(Q8)}\alpha4_{(Q8)}\alpha4_{(Q8)}\beta2_{(Q8)}\alpha4$ receptors shows the presence of breakdown products. Membrane homogenates prepared from oocytes injected with $\beta2_{(Q8)}\beta2_{(Q8)}\alpha4_{(Q8)}\beta2_{(Q8)}\alpha4$ and $\beta2_{(Q8)}\alpha4_{(Q8)}\alpha4_{(Q8)}\beta2_{(Q8)}\alpha4$ cRNAs were resolved and then blotted and immunostained as described in Chapter 2. Full length receptors of the expected size ($\beta2_{(Q8)}\beta2_{(Q8)}\alpha4_{(Q8)}\beta2_{(Q8)}\alpha4$ 290 kD, and $\beta2_{(Q8)}\alpha4_{(Q8)}\alpha4_{(Q8)}\beta2_{(Q8)}\alpha4$..310 kD) are produced after injection of linked DNA into oocytes. Smaller fragments (indicated by the arrows) are also present, which suggests cleavage of the pentameric constructs.

These findings suggest proteolytic cleavage of $\beta2_{(Q8)}\beta2_{(Q8)}\alpha4_{(Q8)}\beta2_{(Q8)}\alpha4$ and $\beta2_{(Q8)}\alpha4_{(Q8)}\alpha4_{(Q8)}\beta2_{(Q8)}\alpha4$ proteins. Proteolytic cleavage could have occurred because of the presence of signal peptides between the linked subunits. Signal peptides between tethered receptor subunits favour degradation of concatenated ligand gated ion channel subunits, which subsequently might produce reduced levels of functional expression and/or

incorporation of the breakdown products into receptors of complex and unknown subunit composition (Nicke *et al.*, 2003; Boileau *et al.*, 2005; Baur *et al.*, 2006; Sigel *et al.*, 2006; Ericksen and Boileau, 2007) and possibly novel pharmacological profiles, as found with the $\beta2_{(Q8)}\beta2_{(Q8)}\alpha4_{(Q8)}\beta2_{(Q8)}\alpha4$ or $\beta2_{(Q8)}\alpha4_{(Q8)}\alpha4_{(Q8)}\beta2_{(Q8)}\alpha4$ receptors.

In an attempt to circumvent the problem of concatamer degradation the signal peptide was removed from all the subunits except the first one and the new concatamers $\beta2_{(AGS)}\beta2_{(AGS)}\alpha4_{(AGS)}\beta2_{(AGS)}\alpha4$ and $\beta2_{(AGS)}\alpha4_{(AGS)}\alpha4_{(AGS)}\beta2_{(AGS)}\alpha4$ were constructed.

3.3.3 Functional expression of $\beta2_{(AGS)}\beta2_{(AGS)}\alpha4_{(AGS)}\beta2_{(AGS)}\alpha4$ and $\beta2_{(AGS)}\alpha4_{(AGS)}\alpha4_{(AGS)}\beta2_{(AGS)}\alpha4$ concatamers is very poor

Previous studies on pentameric concatamers of $GABA_A$ receptors (Baur *et al.*, 2006), dimers of $\alpha1\beta$ glycine receptor (Grudzinska *et al.*, 2005) and dimers of $\alpha4\beta2$ nAChR (Zhou *et al.*, 2003) have shown that linkers lengths between 35 and 50 amino acids generally produce good functional expression.

Therefore, in concatamers $\beta2_{(AGS)}\beta2_{(AGS)}\alpha4_{(AGS)}\beta2_{(AGS)}\alpha4$ and $\beta2_{(AGS)}\alpha4_{(AGS)}\alpha4_{(AGS)}\beta2_{(AGS)}\alpha4$, the overall length of the linker (length of synthetic linker plus added restriction enzyme sites and the C-terminus of each subunit) was 43 amino acid residues when bridging $\beta2$ to $\alpha4$ or $\beta2$ to $\beta2$ and 37 amino acid residues when bridging $\alpha4$ to $\beta2$ or $\alpha4$ to $\alpha4$. The linkers were of different lengths to compensate for differences in the length of the C-terminus and N-terminal sequence prior to the first conserved secondary structure element (α-helix A; Brejc *et al.*, 2001) of the $\alpha4$ and $\beta2$ subunits. In addition, to minimise possible amino acid depletion (Sigel *et al.*, 2006), AGS linkers were used, which have been previously used to construct $\alpha4\beta2$ receptor dimers (Zhou *et al.*, 2003). Three – six days after microinjection of up to 150 ng of cRNAs coding for $\beta2_{(AGS)}\beta2_{(AGS)}\alpha4_{(AGS)}\beta2_{(AGS)}\alpha4$ and $\beta2_{(AGS)}\alpha4_{(AGS)}\alpha4_{(AGS)}\beta2_{(AGS)}\alpha4$ concatamers, functional expression amounted to less than 20 nA (not shown). Because of low levels of expression, the pharmacological profile of these receptors was not characterised. Although functional expression was poor, Western blots showed full-length pentameric concatamers without apparent degradation products (Fig. 3.6).

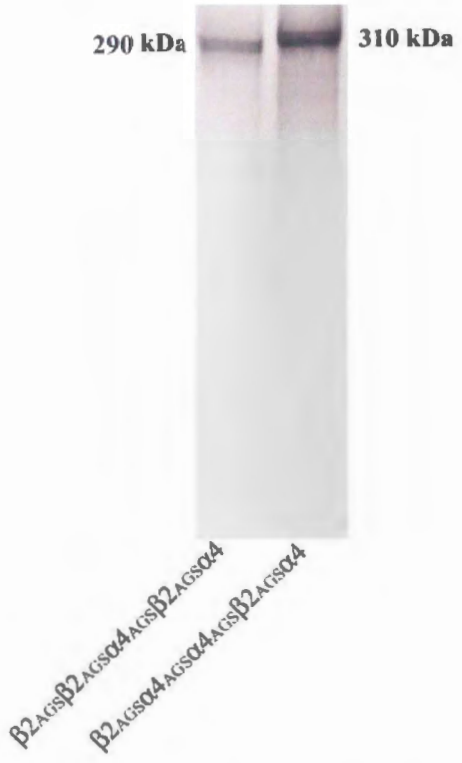

Fig. 3.6. Western blot analysis of $\beta2_{(AGS)}\beta2_{(AGS)}\alpha4_{(AGS)}\beta2_{(AGS)}\alpha4$ and $\beta2_{(AGS)}\alpha4_{(AGS)}\alpha4_{(AGS)}\beta2_{(AGS)}\alpha4$ receptors. Western blot analysis of $\beta2_{(AGS)}\beta2_{(AGS)}\alpha4_{(AGS)}\beta2_{(AGS)}\alpha4$ and $\beta2_{(AGS)}\alpha4_{(AGS)}\alpha4_{(AGS)}\beta2_{(AGS)}\alpha4$ proteins indicated that the pentameric constructs were not cleaved. Total protein from oocytes injected with $\beta2_{(AGS)}\beta2_{(AGS)}\alpha4_{(AGS)}\beta2_{(AGS)}\alpha4$ and $\beta2_{(AGS)}\alpha4_{(AGS)}\alpha4_{(AGS)}\beta2_{(AGS)}\alpha4$ cRNAs was resolved by reducing SDS-PAGE on a NuPage 7% Tris acetate gel. Immunoblot analysis was carried as described in Chapter 2. The molecular mass of the concatenated constructs are shown next to the blots.

3.3.4 β2_α4_β2_α4_β2 and β2_α4_β2_α4_α4 concatamers recapitulate non-linked $(\alpha4)_2(\beta2)_3$ or $(\alpha4)_3(\beta2)_2$ properties

Thus far, it has been shown that even though β2_β2_α4_β2_α4 and β2_α4_α4_β2_α4 concatamers are synthesised and stable in *Xenopus* oocytes, they express very poorly. Previous studies showed that β2-α4 dimers favour the expression of $(\alpha4)_2(\beta2)_3$ or $(\alpha4)_3(\beta2)_2$ receptors when co-expressed with free β2 or α4 subunits, respectively (Zhou *et al.*, 2003). Therefore, concatamers with two consecutive β2-α4 interfaces that were followed by a α4 or β2 subunit, i.e., β2_α4_β2_α4_β2 or β2_α4_β2_α4_α4 to produce $(\alpha4)_2(\beta2)_3$ or $(\alpha4)_3(\beta2)_2$ receptors, respectively, were engineered. In these constructs, only the first subunit included the signal sequence at the N-terminus and the overall length of the linkers was as described above.

Robust functional expression of both constructs was achieved in *Xenopus* oocytes (Fig. 3.7). After four days, maximal ACh (1 mM) evoked up to 200 nA of inward currents

in *Xenopus* oocytes microinjected with 10 ng of β2_α4_β2_α4_β2 cRNA. In the case of the β2_α4_β2_α4_α4 construct, 72 h after injection with 5 ng of cRNA, functional expression was approximately 2 μA. Representative traces evoked by saturating ACh concentrations are shown in Fig. 3.7 A. These expression levels were significantly lower than those obtained by microinjection of non-linked subunit cDNAs (β2_α4_β2_α4_β2 /non linked $(\alpha4)_2(\beta2)_3$ = 66 ± 2% and β2_α4_β2_α4_α4 non-linked $(\alpha4)_3(\beta2)_2$ = 77 ± 1%; $p < 0.01$, Student's t test, n = 10) but markedly higher than the levels achieved with the β2_α4_β2_α4_β2 or β2_α4_β2_α4_α4 constructs ($p < 0.001$, Student's t test, n = 10).

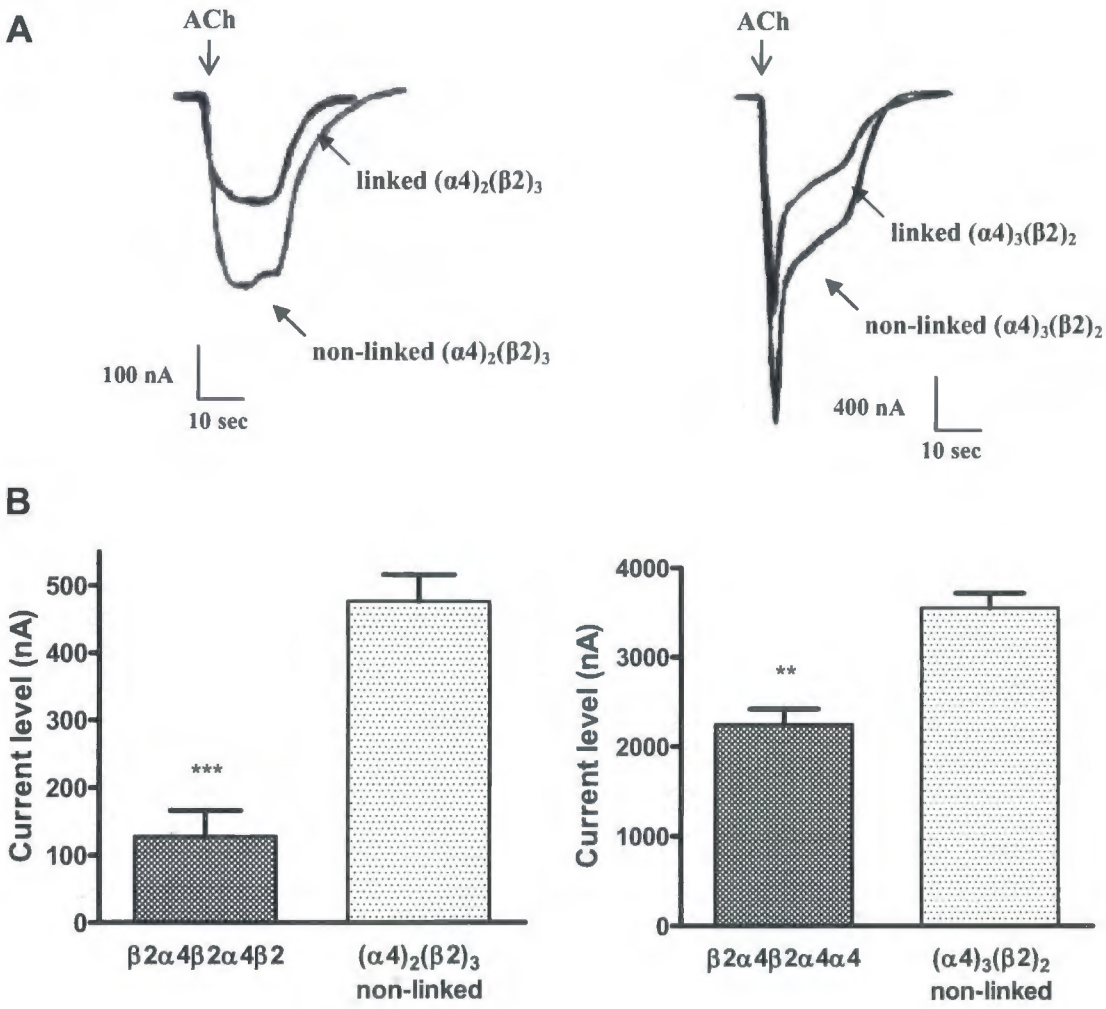

Fig. 3.7. Expression levels of β2_α4_β2_α4_β2 and β2_α4_β2_α4_ α4 pentameric in *Xenopus* oocytes. **A)** Inward currents evoked in oocytes injected with 10 ng of β2_α4_β2_α4_β2 cRNA (*Left*) or 5 ng of β2_α4_β2_α4_α4 cRNA (*Right*) by saturating ACh concentration are shown. Traces evoked in wild type receptors are superimposed for comparison. Arrows indicate the start of the application of ACh. **B)** Bar graph comparing the functional expression levels of HS (*Left*) and LS (*Right*) receptors made of concatenated subunits and expressed by means of extreme transfection ratios. (*** =$p < 0.001$; ** = $p < 0.01$; Student's t test)

It was then tested whether expression of the pentameric concatamers resulted in the synthesis of full-length proteins. Western blot analysis revealed proteins of appropriate size with no apparent breakdown products, suggesting that the pentameric concatamers do not break into fragments or single subunits that could potentially assemble into functional receptors (Fig. 3.8).

Fig. 3.8. Western blot analysis of β2_α4_β2_α4_β2 and β2_α4_β2_α4_α4 expressed in *Xenopus* oocytes. **A)** Western blot analysis indicated that pentameric concatamers β2_α4_β2_α4_β2 and β2_α4_β2_α4_α4 are synthesised and stable when expressed heterologously in *Xenopus* oocytes. Total protein from oocytes injected with either β2_α4_β2_α4_β2 and β2_α4_β2_α4_α4 cRNAs was separated by reducing SDS-PAGE on a NuPage 7% Tris acetate gel.

The functional properties of concatenated receptors were very similar to those of non-concatenated receptors. At the $(\alpha4)_2(\beta2)_3$ receptor concentration-response curves with the agonist ACh indicated that subunit concatenation had little effect on agonist parameters with an EC_{50} of 2.37 ± 2 μM (n = 4) and a Hill coefficient of 1.04 ± 0.06 as compared with non-concatenated subunits with an EC_{50} of 2.8 ± 1 μM (n = 7) and a Hill coefficient of 0.64 ± 0.05 (Fig. 3.9, *Left*) ($p > 0.05$, Student's *t* test, n = 10). Similarly, at the $(\alpha4)_3(\beta2)_2$ receptor subunit concatenation had little effect on the ACh concentration response curve. Analysis of the concentration-response curves showed a small difference, albeit not significant, in EC_{50} values (110 ± 5 versus 90.0 ± 4 μM, for the pentamer and monomer constructs, respectively; $p > 0.05$, Student's *t* test, n = 10) but not in the Hill slope (0.92 ± 0.09 and 0.93 ± 0.08, respectively; $p > 0.05$, Student's *t* test, n = 10) (Fig. 3.9, *Right*).

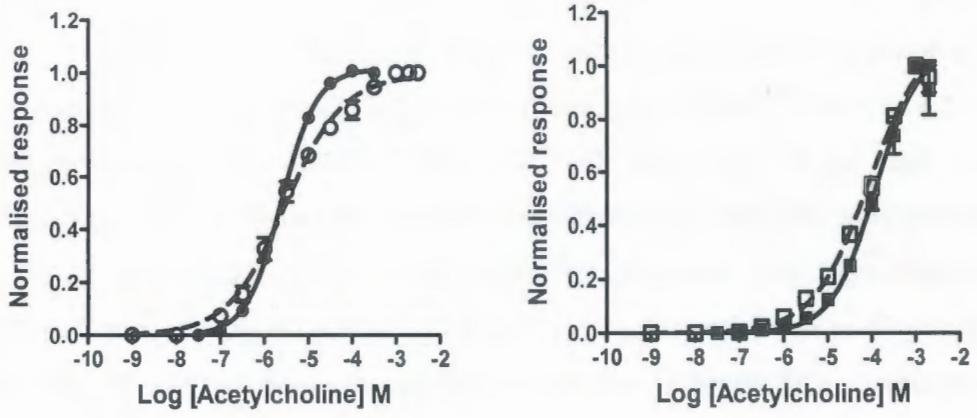

Fig. 3.9. $(\alpha4)_3(\beta2)_2$ and $(\alpha4)_2(\beta2)_3$ nAChRs expressed from the pentameric construct have ACh similar to those of receptors expressed from monomeric constructs. ***Left panel.*** ACh concentration-response curve for concatenated $(\alpha4)_3(\beta2)_2$ (●) compared to non-linked $(\alpha4)_3(\beta2)_2$ receptor (○, dashed line) ***Right panel.*** ACh dose-response curves for concatenated $(\alpha4)_2(\beta2)_3$ (■) and non-linked $(\alpha4)_2(\beta2)_3$ receptors (□, dashed line) The data were best fitted by a one-component sigmoidal equation ($p < 0.0001$, F test, n = 10)

The effects of a range of α4β2-preferring compounds were examined to characterise the functional pharmacology of β2_α4_β2_α4_β2 and β2_α4_β2_α4_α4 receptors in comparison to their non-linked counterparts. Functional pharmacological properties of β2_α4_β2_α4_β2 and β2_α4_β2_α4_α4 receptors were very similar to those that have been previously shown for non-linked $(\alpha4)_2(\beta2)_3$ or $(\alpha4)_3(\beta2)_2$ receptors (Moroni *et al.*, 2006; Zwart *et al.*, 2006; Zwart et al, 2008) (Fig. 3.10). The value of the EC_{50}, I/I_{max} and nHill parameters estimated from concentration-response curves are shown in Tables 3.2 and 3.3. Like the corresponding non-linked receptors β2_α4_β2_α4_β2 and β2_α4_β2_α4_α4 receptors were activated by A85380, 5I-A85380, epibatidine and TC2559 in a concentration-dependent manner. In contrast, cytisine and 5-Br-Cys evoked responses only in oocytes expressing β2_α4_β2_α4_α4 or non-linked $(\alpha4)_3(\beta2)_2$ receptors. At these two types of receptors, cytisine and 5-Br-Cys behaved as partial agonists (Fig. 3.10 B). Sazetidine-A was a full agonist at both β2_α4_β2_α4_β2 and non-linked $(\alpha4)_2(\beta2)_3$ receptors (Fig. 3.10 A), whereas at β2_α4_β2_α4_α4 or non-linked $(\alpha4)_3(\beta2)_2$ receptor it behaved as a poor partial agonist (Fig. 3.10 B). Epibatidine was as potent at β2_α4_β2_α4_β2 as at non-linked $(\alpha4)_2(\beta2)_3$ receptors (Fig. 3.10 A). However, A85380, 5I-A85380 and TC2559 were significantly more potent at β2_α4_β2_α4_β2 than at non-linked $(\alpha4)_2(\beta2)_3$ receptors ($p < 0.001$, Student's t test, n = 7 - 10) (Fig. 3.10 A). The potency of A85380 and TC2559 was lower at β2_α4_β2_α4_α4 than at non-linked $(\alpha4)_3(\beta2)_2$ receptors ($p < 0.001$, Student's t test n = 7 - 10) (Fig. 3.10 B). It is likely that

these differences may be due to mixed expression of both forms of the α4β2 receptor in the case of the non-linked receptors. All agonists produced concentration-response curves that were best fit to a one-component sigmoidal equation ($p < 0.001$, F test, n = 5 - 10). 5I-A85380 produced a monophasic effect on both β2_α4_β2_α4_β2 and non-linked $(\alpha4)_2(\beta2)_3$ (Fig. 3.10 A). However, whereas the effects of 5I-A85380 were monophasic at β2_α4_β2_α4_α4 receptors, at non-linked $(\alpha4)_3(\beta2)_2$ receptors they were clearly biphasic ($p < 0.001$, F test, n = 5 - 10) (Fig. 3.10 B). The EC_{50} for activation of β2_α4_β2_α4_α4 receptors by 5I-A85380 was comparable to the low affinity EC_{50} displayed by this compound at non-linked $(\alpha4)_3(\beta2)_2$, whilst the high-affinity EC_{50} was comparable to that displayed at both β2_α4_β2_α4_β2 and non-linked $(\alpha4)_2(\beta2)_3$. The effect of 5I-A85380 on non-linked $(\alpha4)_3(\beta2)_2$ is similar to the effects that are observed when 5I-A85380 activates a mixed population of high- and low-sensitivity α4β2 receptors expressed in *Xenopus* or mammalian clonal cells (Zwart *et al.*, 2006). This observation suggests that functional expression of non-linked $(\alpha4)_3(\beta2)_2$ is contaminated with a small population, about 10%, of non-linked $(\alpha4)_2(\beta2)_3$ receptors or other possible stoichiometric combinations (Zwart and Vijverberg, 1998; Lopez-Hernandez *et al.*, 2004). Therefore, overall, the findings on the effects of A85380, 5I-A85380 and TC2559 on linked and non-linked α4β2 receptors show that microinjection of oocytes with extreme ratios of α4 and β2 cDNAs to produce either $(\alpha4)_3(\beta2)_2$ or $(\alpha4)_2(\beta2)_3$ does not fully prevent the assembly and expression of multiple forms of the α4β2 nAChR.

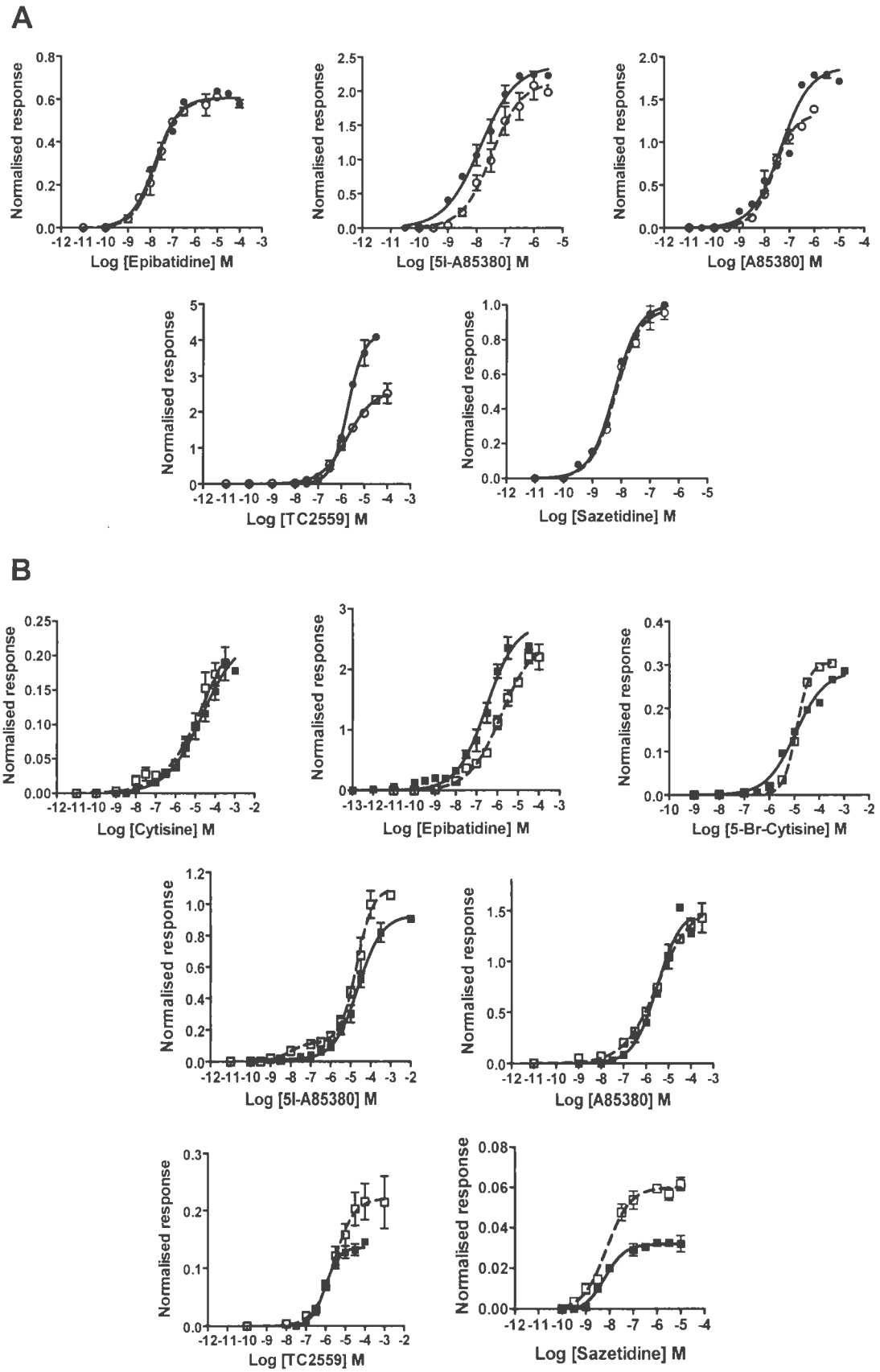

Fig. 3.10. Functional sensitivity of concatenated and non-linked $(\alpha4)_2(\beta2)_3$ and $(\alpha4)_3(\beta2)_2$ nAChR to α4β2-preferring ligands. Concentration-response curves were obtained for the effects of a range of agonists on **(A)** β2_α4_β2_α4_β2 and **(B)** β2_α4_β2_α4_α4 nAChR (filled symbols) expressed heterologously in *Xenopus* oocytes as described in Methods. Responses were normalised to 1 mM ACh. Averaged parameters of best fits to agonist or concentration-response data are given in Tables 2 and 3. For comparison the concentration-response curve constructed for the corresponding non-linked receptors (open symbols, dashed line) have been included in A and B.

Table 3.2. Functional properties of β2_α4_β2_α4_β2 and non-linked $(\alpha4)_2(\beta2)_3$ nAChRs.

	β2_α4_β2_α4_β2			Non-linked $(\alpha4)_2(\beta2)_3$		
	I/I_{max} ± SEM	EC_{50} μM (95% CI)	nHill ± SEM	I/I_{max}± SEM	EC_{50} μM (95% CI)	nHill ± SEM
ACh	1	2.37 (2.1 - 2.7)	1.04±0.06	1	2.8 (2.1 - 3.7)	0.64±0.05
A85380	1.79±0.07 *	0.047 (0.03-0.07)	0.88±0.05	1.38±0.04	0.024 (0.02 - 0.03)	1.02±0.11
5I-A85380	2.23±0.1 *	0.014 (0.009-0.02)	0.71±0.10	2.08±0.16	0.034 (0.02 - 0.06)	0.83±0.1
Cytisine	NE	-	-	NE	-	-
5-Br-Cys	NE	-	-	NE	-	-
Epibatidine	0.61±0.008	0.16 (0.1 - 0.3)	0.82±0.10	0.63±0.01	0.19 (0.1 - 0.4)	0.86±0.12
TC2559	4.08±0.1 *	1.9 (1.6 - 2.3)	1.0±0.14	2.51±0.1	1.86 (1.3 - 2.6)	0.89±0.10
Sazetidine	1.01±0.01	0.0069 (5 - 8 nM)	1.01±0.4	0.98±0.09	0.0065 (4 - 8 nM)	1.03±0.07

All values are means (95 % CI) or means ± SEM from 5-10 cells. Statistical comparisons between the concentration-response curve parameters of the concatenated receptors and those of the non-linked receptors were carried out using one-way analysis of the variance (ANOVA). The * signifies $p < 0.05$ compared with non-linked $(\alpha4)_2(\beta2)_3$ receptors. 5-Br-Cys, 5-Br-cytisine.

Table 3.3. Functional properties of β2_α4_β2_α4_α4 and non-linked $(\alpha4)_3(\beta2)_2$ nAChRs.

	β2_α4_β2_α4_α4			Non-linked $(\alpha4)_3(\beta2)_2$		
	I/I_{max} ± SEM	EC_{50} μM (95% CI)	nHill ± SEM	I/I_{max}± SEM	EC_{50} μM (95% CI)	nHill ± SEM
ACh	1	111 (82 - 151)	0.92±0.09	1	88 (76 - 94)	0.93±0.08
A85380	1.53±0.06 *	2.7 (1.7 - 3.9)	0.80±0.1	1.42±0.06	3.34 (2.3 - 4.8)	0.63±0.06
5I-A85380	0.99±0.06 *	28.20 (17 - 48)	0.73±0.1	0.22±0.04 * 1.05±0.1 *	0.14 (0.1 - 0.2) * 22 (14 - 35)	0.4±0.03 1.2±0.4
Cytisine	0.27±0.04	55 (11 - 150)	0.43±0.05	0.24 ±0.04	15.80 (13 - 88)	0.52±0.1
5Br-Cys	0.28±0.05	11 (10 - 12)	1.3±0.12	0.29±0.01	14 (10 - 19)	0.9±0.1
Epibatidine	2.7±0.01	0.30 (0.2 - 0.6)	0.50±0.1	2.4±0.26	2.3 (0.8 - 7)	0.62±0.07
TC2559	0.15±0.1 *	0.91 (0.63-1.3) *	1.3±0.3	0.21±0.02	2.73 (1.1 - 7.1)	0.85±0.30
Sazetidine	0.008 ± 0.0004	0.0064 (6-10nM)	0.86±0.11	0.0062 ± 0.0004	0.0062 (1 - 8 nM)	0.65±0.1

One-way analysis of variance (ANOVA) compared the level of significance between the values of the parameters of the agonist concentration-response curves of concatenated receptors and those of the non-linked receptors. The * signifies $p < 0.05$ compared with non-linked $(\alpha4)_3(\beta2)_2$ receptor. 5-Br-Cys, 5-Br-cytisine.

Because competitive antagonists bind to a larger domain than their agonist counterparts, they provide a more accurate molecular tool to diagnose the integrity of the α/β agonist binding interface. Therefore, the α4β2 competitive antagonist DhβE was tested on both β2_α4_β2_α4_β2 and β2_α4_β2_α4_α4 receptors (Fig. 3.11). Inward currents elicited by EC_{50} of ACh at either β2_α4_β2_α4_β2 and β2_α4_β2_α4_α4 were inhibited by DhβE in a concentration-dependent and monophasic manner ($p < 0.0001$, F test, n = 6). The IC_{50} for DhβE at β2_α4_β2_α4_β2 was 12 (9 - 15) nM and at β2_α4_β2_α4_α4 was 0.3 (0.25 – 0.35) μM. These values are very similar to those of the corresponding non-linked receptors ($(\alpha4)_2(\beta2)_3$, 17 (14-19) nM; $(\alpha4)_3(\beta2)_2$, 0.2 (0.0.9-0.49) μM) ($p > 0.05$, Student's *t* test, n = 7 - 10).

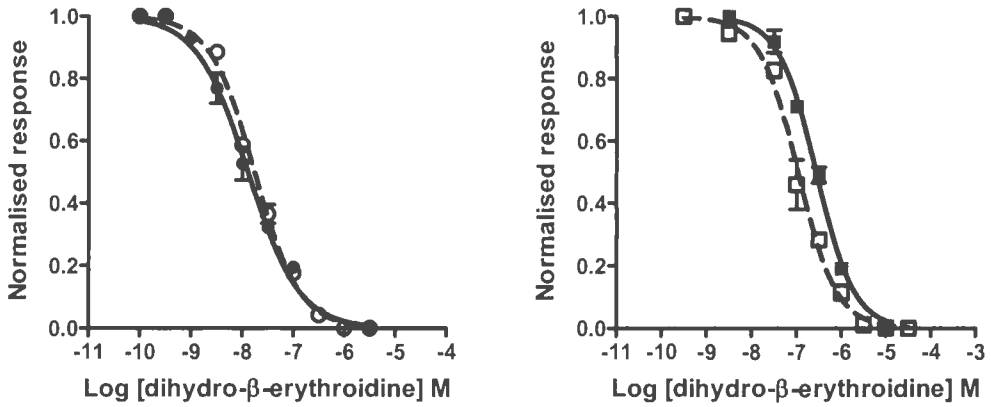

Fig. 3.11 Concentration-response curves of the α4β2-preferring antagonist DhβE on the function of concatenated α4β2 receptors. Concentration-response curves of DhβE on EC_{50} ACh responses of concatenated (continued line) and non-concatenated (dashed line) $(\alpha4)_2(\beta2)_3$ (*Left*, •) and $(\alpha4)_3(\beta2)_2$ (*Right*, ■) nAChRs.

3.3.5 Sensitivity of β2_α4_β2_α4_β2 and β2_α4_β2_α4_α4 concatenated receptors to Zn^{2+} activation and Ca^{2+} permeability

Further studies examined the sensitivity of the β2_α4_β2_α4_β2 and β2_α4_β2_α4_α4 receptors to Zn^{2+} modulation as well as their Ca^{2+} permeability. Non-linked $(\alpha4)_2(\beta2)_3$ and $(\alpha4)_3(\beta2)_2$ receptors differ significantly in their sensitivity to modulation by Zn^{2+} (Moroni *et al.*, 2008) and Ca^{2+} permeability (Tapia *et al.*, 2007). These differences reflect stoichiometry-specific structural signatures. Concentration dependent modulation by Zn^{2+} of currents evoked by ACh revealed that the sensitivity of the α4β2 concatamers was comparable to that of the corresponding non-linked α4β2 receptors (Fig. 3.12) (Moroni *et al.*, 2008). Zn^{2+} inhibited the ACh responses of both β2_α4_β2_α4_β2 and $(\alpha4)_2(\beta2)_3$ monophasically and with similar IC_{50} values (32 (16 – 67) μM and 19 (10 – 36) μM, respectively; Fig. 3.12, *Left panel*). The ACh responses of both β2_α4_β2_α4_α4 and $(\alpha4)_3(\beta2)_2$ receptors were modulated biphasically by Zn^{2+} ($p < 0.01$, F test, n = 5). Zn^{2+} concentrations ranging from 1 to 100 μM potentiated ACh responses at β2_α4_β2_α4_α4 or $(\alpha4)_3(\beta2)_2$ 100 μM. Zn^{2+} increased ACh elicited current to 1.82 ± 0.3 and 1.51 ± 0.5 for β2_α4_β2_α4_α4 or $(\alpha4)_3(\beta2)_2$ respectively (Fig. 3.12, *Right panel*). The EC_{50} for potentiation was 32 (18 – 44) μM for β2_α4_β2_α4_α4 receptors and 19 (17 – 24) μM for non-linked $(\alpha4)_3(\beta2)_2$ receptors. None of these values were significantly different ($p > 0.05$, Student's *t* test, n = 5). Higher concentrations of Zn^{2+} decreased the

degree of potentiation until at concentrations greater than 800 μM Zn^{2+} the amplitudes of the ACh responses elicited in the presence of Zn^{2+} were smaller than those mediated by applications of ACh alone. Zn^{2+} inhibited β2_α4_β2_α4_α4 and non-linked $(\alpha4)_3(\beta2)_2$ nAChR with a similar IC_{50} values of 810 (800 – 819) μM and 803 (799 – 812) μM respectively ($p > 0.05$, Student's t test, n = 5).

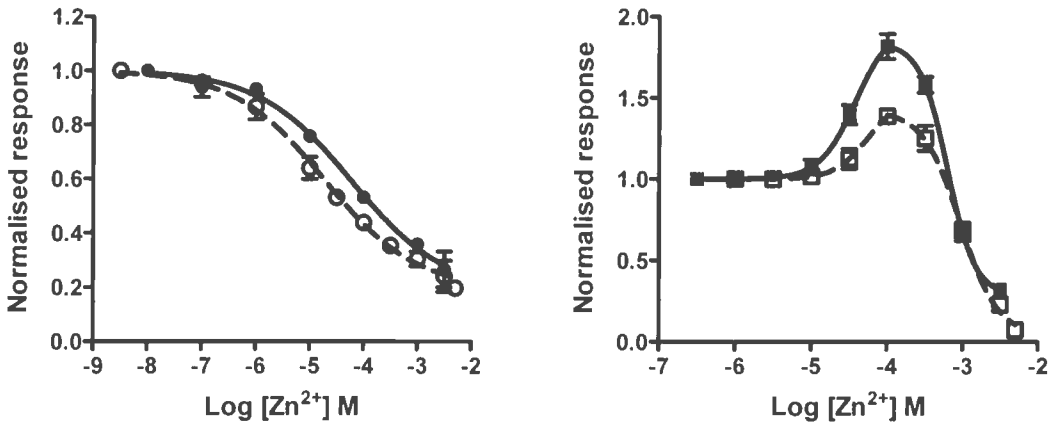

Fig. 3.12. Zn^{2+} sensitivity of concatenated $(\alpha4)_3(\beta2)_2$ and $(\alpha4)_2(\beta2)_3$ nAChRs expressed heterologously in *Xenopus* oocytes. Averaged concentration-response for the effects of Zn^{2+} at concatenated $(\alpha4)_3(\beta2)_2$ (*Left*, ●) and $(\alpha4)_2(\beta2)_3$ (*Right*, ■) nAChRs. The effects of Zn^{2+} on currents activated by EC_{20} or EC_{10} ACh concentrations on concatenated and non-linked $(\alpha4)_3(\beta2)_2$ and $(\alpha4)_2(\beta2)_3$ nAChRs, respectively, were determined as detailed in the Method section.

Ca^{2+} permeability was examined by measuring the reversal potential of I_{ACh} in the presence of 1.8 mM or 18 mM extracellular Ca^{2+} (Tapia *et al.*, 2007). β2_α4_β2_α4_α4 receptors were most permeable to Ca^{2+} than β2_α4_β2_α4_β2 receptors (Fig. 3.13), which would be expected if these receptors replicated the structure and functional properties of non-linked $(\alpha4)_3(\beta2)_2$ and $(\alpha4)_2(\beta2)_3$ receptors, respectively. A 10-fold increase in Ca^{2+} concentration shifted the reversal potential of I_{ACh} in the positive direction by 4 ± 0.1 mV in β2_α4_β2_α4_β2 receptors (Fig. 3.13, *Left*; n = 5-7) and 21 ± 5 mV in β2_α4_β2_α4_α4 receptors (Fig. 3.13, *Right*; n = 7-9).

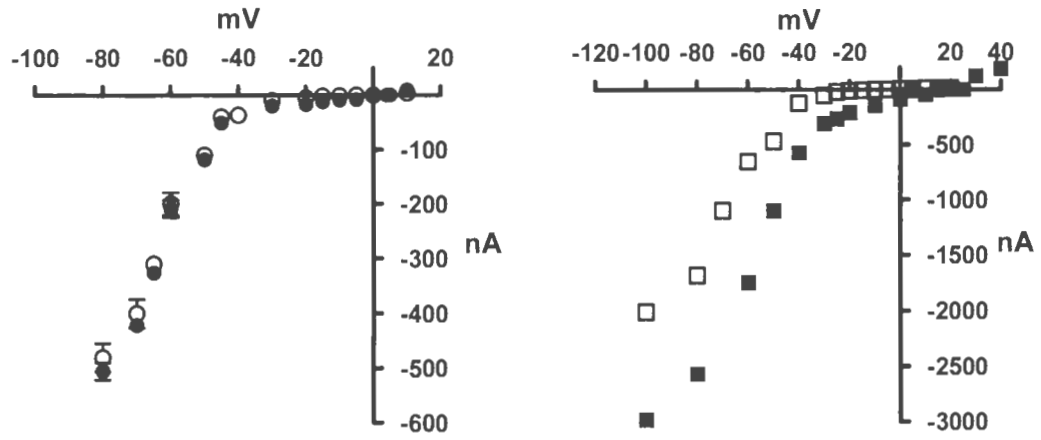

Fig. 3.13. Ca^{2+} permeability of concatenated $(\alpha4)_3(\beta2)_2$ and $(\alpha4)_2(\beta2)_3$ nAChRs expressed heterologously in *Xenopus* oocytes. Current-voltage relationship of β2_α4_β2_α4_β2 (*Left*, ●) and β2_α4_β2_α4_α4 (*Right*, ■) nAChR in the presence of 1.8 mM (non-filled symbols) or 18 mM extracellular (filled symbols) Ca^{2+}. β2_α4_β2_α4_α4 were more permeable to Ca^{2+} as judged by the positive shift of the reversal potential when the external Ca^{2+} was increased by tenfold.

3.3.6 Chaperone 14-3-3 increases functional expression of β2_α4_β2_α4_α4 and β2_α4_β2_α4_β2 constructs

Chaperone protein 14-3-3 interacts with the native (Jeanclos *et al.*, 2001) and recombinant α4 subunit (Jeanclos *et al.*, 2001; Exley *et al.*, 2006) following activation of protein kinase A (PKA). The interaction is dependent on phosphorylation of a serine residue within a PKA consensus sequence (RSLSV; PKA target underlined) in the large cytoplasmic domain of the subunit, which is also a binding motif recognised by 14-3-3 (Jeanclos *et al.*, 2001; O'Kelly *et al.*, 2002; Exley *et al.*, 2006). The interaction significantly increases the steady state levels of α4 subunit alone and α4β2 nAChRs by masking of a dibasic retention signal within the large cytoplasmic domain of α4 subunit (O'Kelly *et al.*, 2002). To investigate the effects of 14-3-3 on functional expression of α4β2 nAChR concatamers, 14-3-3 was co-expressed with β2_α4_β2_α4_β2 or β2_α4_β2_α4_α4. 14-3-3 was found to significantly increase the functional expression of both α4β2 concatamers (Figs. 3.14 A, B). These results indicate that subunit concatenation does not impair the ability of the α4 subunit to interact with chaperone 14-3-3 protein. Interestingly, it was observed that 14-3-3 was more effective at increasing the functional expression of the β2_α4_β2_α4_α4 receptor than that of the β2_α4_β2_α4_β2 receptors. Thus, in the case of the β2_α4_β2_α4_β2 receptor, functional expression was increased by 1.7-fold ($p < 0.05$, Student's t test, n = 6) whereas functional expression of β2_α4_β2_α4_α4 increased by 4-fold ($p < 0.0001$, Student's t test, n = 6).

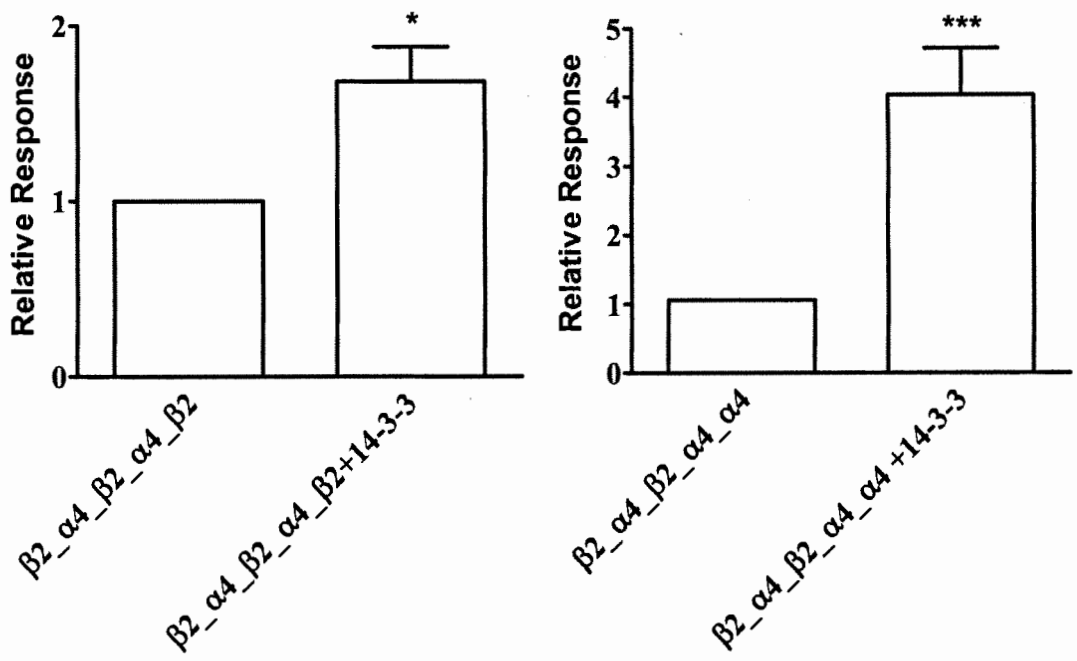

Fig. 3.14. Chaperone 14-3-3 increases functional expression of concatenated $(\alpha4)_3(\beta2)_2$ and $(\alpha4)_2(\beta2)_3$ nAChRs. Bargraph of normalized ACh responses at concatenated β2_α4_β2_α4_β2 *(Left)* or β2_α4_β2_α4_α4 *(Right)* nACh receptors expressed on their own or co-expressed with chaperone protein 14-3-3. Data are given as means ± SEM from five to seven oocytes per column. (* = $p < 0.05$; *** = $p < 0.001$)

DISCUSSION

Characterisation of the α4β2 expressed in heterologous systems is difficult because of the variety of receptor subtypes that can be formed (Zwart and Vijverberg, 1998; Nelson *et al.* 2003; Zhou *et al.*, 2003; Lopez-Hernandez *et al.*, 2004; Moroni *et al.*, 2006). An alternative approach that circumvents this problem is the expression of LGICs with fixed stoichiometry obtained by concatenating subunits in a predefined order and composition.

Three different approaches to constrain the expression of the alternate stoichiometries of the α4β2 receptor were tested. It has been shown here that the pentameric constructs β2_α4_β2_α4_β2 and β2_α4_β2_α4_α4 express functionally well in *Xenopus* oocytes and that these receptors recapitulate the sensitivity to activation by ACh, Ca^{2+} permeability and ability to interact with chaperone protein 14-3-3 of the corresponding non-linked $(\alpha4)_2(\beta2)_3$ or $(\alpha4)_3(\beta2)_2$ receptors, respectively. Using these concatenated receptors, the pharmacological properties of the alternate stoichiometries of the α4β2 nAChR were examined, and from the findings it was concluded that the pentameric concatamers β2_α4_β2_α4_β2 and β2_α4_β2_α4_α4 are valid models of the corresponding non-linked $(\alpha4)_2(\beta2)_3$ and $(\alpha4)_3(\beta2)_2$ receptors, respectively. The sensitivity of β2_α4_β2_α4_β2 and β2_α4_β2_α4_α4 receptors to activation by ACh, sazetidine-A, cytisine, 5-Br-cytisine, and inhibition by DhβE were comparable to those of the corresponding non-linked α4β2 nAChRs. Exceptions were the agonist effects of TC2559, A85380 and 5I-A85380, which activated the concatenated receptors and their non-linked counterparts with significantly different potency and/or efficacy. In addition, 5I-A85380 produced a biphasic concentration response curve at non-linked $(\alpha4)_3(\beta2)_2$ receptors comprising a high and a low affinity components whose respective EC_{50} values were similar to those of the concatenated β2_α4_β2_α4_β2 and β2_α4_β2_α4_α4 receptors, respectively.

A straightforward explanation for these results is that one or more linkers may affect the pharmacological properties of the receptors. However, because the pharmacological profile of non-linked $(\alpha4)_3(\beta2)_2$ receptors resembles that of a mixed population of high- and low-sensitivity α4β2 receptor stoichiometries (Zwart *et al.*, 2006), a more likely explanation is that non-linked α4 and β2 subunits produce multiple receptor stoichiometries, even when the relative abundance of the subunits is manipulated to favour the assembly of only one type of α4β2 receptor, as in the experimental conditions of this study. From the biphasic concentration-response curve produced by 5I-A85380 at α4β2 receptors expressed following microinjection of oocytes with single α4 and β2 cDNAs at a ratio of 10:1, it is clear that approximately 10% of the receptors produced are of the

$(\alpha4)_2(\beta2)_3$ or other possible stoichiometric arrangements. The low levels of receptor contamination shown in this study are revealed by compounds with exceptional high stoichiometry-selectivity, such as 5I-A85380 or pentameric concatenated receptors. These may still confound functional assays and obscure stoichiometry-specific receptor properties (e.g., Zwart *et al.*, 2006). These results indicate that caution should be applied when interpreting functional data produced by non-linked α4β2 receptors expressed heterologously in surrogate cells. The concentration-response curves obtained with ACh and α4β2-preferring agonists indicate that most established α4β2 nAChR ligands distinguish, with varying degrees, the alternate stoichiometries of the α4β2 nAChR. In addition, the receptors clearly differ in their sensitivity to modulation by Zn^{2+} and Ca^{2+} permeability. These findings suggest stoichiometry-specific structural signatures as determinants of the functional behaviour of the $(\alpha4)_2(\beta2)_3$ and $(\alpha4)_3(\beta2)_2$ nAChR. What may be the structural basis for the stoichiometry-dependent properties of the α4β2 nAChR? By analogy to the muscle α1γα1δβ1 nAChR (Unwin, 2005), it is thought that the α4β2 nAChR harbours two functional agonist binding sites, which must be located at the α4(+)/β2(-) interfaces (one per interface). This implies that the subunit order around the channel is α4β2α4β2(α4/β2). This subunit arrangement is supported by the present reported studies on concatenated $(\alpha4)_2(\beta2)_3$ and $(\alpha4)_3(\beta2)_2$ nAChRs.

On both stoichiometries, the agonist sites are both located at the α4(+)/β2(-) interfaces and suggest identical properties. However, one α4(+)/β2(-) interface on both stoichiometries is flanked by non-ACh binding β2(+)/α4(-) interfaces, whereas the other is flanked by a β2(+)/α4(-) interface and depending on the stoichiometry, by a non-agonist binding α4(+)/α4(-) or β2(-)/β2(+) interface. The latter interfaces are stoichiometry-specific and therefore likely candidates for conferring stoichiometry-specific properties to $(\alpha4)_2(\beta2)_3$ and $(\alpha4)_3(\beta2)_2$ nAChR. This view is supported by a recent study on the effect of Zn^{2+} on the alternate forms of the α4β2 receptor, which shows that the signature α4/α4 interface of the $(\alpha4)_3(\beta2)_2$ receptor harbours a Zn^{2+} potentiating site that is absent in the $(\alpha4)_2(\beta2)_3$ stoichiometry (Moroni *et al.*, 2008). Additional support for these findings comes from recent studies that have shown that accessory subunits influence the function of neuronal nAChRs (Kuryatov *et al.*, 2008) and that conserved hydrophobic amino acid residues contribute to an allosteric site on heteromeric nAChRs (Hansen and Taylor, 2007).

Functional expression of both concatamers is increased by co-expression with the chaperone protein 14-3-3, indicating that concatenation does not obliterate the 14-3-3 binding site within the large intracellular loop of α4. The effects of 14-3-3 on the

functional expression of β2_α4_β2_α4_α4 and β2_α4_β2_α4_β2 receptors were strikingly similar to the effects that have been previously observed when the subunits expressed were non-assembled α4 and β2 (Exley *et al.*, 2006). Exley and collaborators (2006) have shown that 14-3-3 favoured expression of low sensitivity (i.e., $(\alpha4)_3(\beta2)_2$) receptors and increased the steady-state levels of the α4 subunit. This effect possibly resulted into greater incorporation of α4 subunits into receptor complexes. This possibility could not account for the differential effects of 14-3-3 on the α4β2 pentameric concatamers, because the subunit composition of these receptors is fixed. A possible explanation is that the higher α4 content of the β2_α4_β2_α4_α4 concatamer enhances the stabilising and up-regulating effects of 14-3-3 in comparison to its actions on β2_α4_β2_α4_β2 receptors. This implies that subunit composition may confer stoichiometry-specific 'receptor maturation' patterns. This view is supported by previous studies that have shown that α4β2 nAChR matures inefficiently in comparison to α4β4 receptors (Sallette *et al.*, 2004), possibly because β2 weakens the process of receptor maturation through inefficient subunit interactions and/or assembly (Sallette *et al.*, 2004; Sallette *et al.*, 2005). Thus, $(\alpha4)_2(\beta2)_3$ receptors may mature less efficiently than $(\alpha4)_3(\beta2)_2$ receptors, which would lower the functional expression of $(\alpha4)_2(\beta2)_3$ relative to that of $(\alpha4)_3(\beta2)_2$ receptors. In this and previous (Moroni *et al.*, 2006; Zwart *et al.*, 2006; Moroni *et al.*, 2008) studies it has been found that the heterologous functional expression of $(\alpha4)_3(\beta2)_2$ receptors in *Xenopus* oocytes is about 30-fold higher than that of $(\alpha4)_2(\beta2)_3$ receptors.

Interestingly, neither β2_β2_α4_β2_α4 nor β2_α4_α4_β2_α4 expressed well in *Xenopus* oocytes, even though both constructs were synthesised and stable. This implies that the constructs were trafficked inefficiently to the cell surface and/or that the constructs did not assemble into properly functional α4β2 receptors. What may influence the functionality of these concatamers? In comparison to β2_α4_β2_α4_β2 or β2_α4_β2_α4_α4 concatamers, the β2-α4 interfaces in the β2_β2_α4_β2_α4 and β2_α4_α4_β2_α4 receptors are preceded by a β2 or are separated by an α4 subunit respectively. Thus, a possible explanation for the low functional expression of β2_β2_α4_β2_α4 and β2_α4_α4_β2_α4 is that their subunit arrangement does not facilitate the subunit interactions that drive the assembly and maturation of α4β2 pentamers (Sallette *et al.*, 2005). Little is known about the elementary steps leading to assembly of pentameric α4β2 complexes, which occurs within the endoplasmic reticulum. By analogy to the assembly of the muscle nAChR (Green and Claudio, 1993), it is likely that the subunits incorporate into pentamers through sequential steps driven by specific subunit-

subunit or subunit-chaperone interactions. Thus, when those subunit interactions are impaired, which might occur if the subunits are not oriented properly or do not acquire appropriate three-dimensional structures, oligomerisation and/or maturation may be inefficient, producing ultimately low expression levels or receptors with altered function. Interestingly, although β4_β4_α3_β4_α3 pentameric concatamers produce functional receptors in *Xenopus* oocytes, the levels of expression were very poor in comparison to the functional expression of non-linked α3β4 receptors (Groot-Kormelink *et al.*, 2006). This suggests that positioning β_α interfaces prior to a β or α subunit may be a strategy that could be applied across the nAChR family to produce concatamers with good functional expression. A subunit domain that may play a critical role in functional expression is the C-terminus. Insertion of fluorescent proteins in the C-terminus of β2 nAChR subunit (Nashmi *et al.*, 2003), ε or γ nAChR subunits (Gensler *et al.*, 2001) or γ2 $GABA_A$ receptor subunit (Kittler *et al.*, 2000) results in partial or complete abolition of function. Although there is evidence that green fluorescent-tagged C-terminus may affect the function of nAChR (Fucile *et al.*, 2002b), recent studies suggest that the effects of the C-terminus on the functional expression of Cys-loop LGIC are likely to reflect its contribution to the process of receptor maturation (Butler *et al.*, 2009). Thus, C-terminus single-point mutants of the $5\text{-}HT_{3A}$ receptor reduce specific radioligand binding and membrane expression, both of which can be partially restored by growing cells expressing the mutant receptors at temperatures lower than 37 °C (Butler *et al.*, 2009). In the case of pentameric concatenated LGIC, poor functional expression could well reflect the fact that the C-terminus of all but one subunit (the fifth) of the concatenated subunits is linked to the N-terminus of the subsequent subunit (Baur *et al.*, 2006; Groot-Kormelink *et al.*, 2006).

In summary, it has been demonstrated here that pentameric concatamers β2_α4_β2_α4_β2 and β2_α4_β2_α4_α4 have pharmacological signatures comparable to those of non-linked $(\alpha4)_2(\beta2)_3$ and $(\alpha4)_3(\beta2)_2$ nAChRs respectively. Thus, this study provides a diagnostic tool for the alternate forms of the α4β2 nAChR. In addition, $(\alpha4)_2(\beta2)_3$ and $(\alpha4)_3(\beta2)_2$ concatamers in combination with mutational and functional experimental approaches can be used to aid the characterisation of other possible stoichiometric arrangements of the α4β2 nAChR. Concatamers with a subunit order of β2_β2_α4_β2_α4 or β2_α4_α4_β2_α4 do not express well in *Xenopus* oocytes nor do they reproduce the pharmacological properties of non-linked receptors. This may be because the subunit arrangement of these constructs hinders interactions between subunits or between subunits and chaperone proteins that are required for receptor assembly and maturation. It

is presently not possible to distinguish between these possibilities because the processes that drive the genesis of functional α4β2 nAChRs are essentially unknown. However, future studies that address this issue may benefit from the availability of pentameric concatenated $(\alpha4)_2(\beta2)_3$ and $(\alpha4)_3(\beta2)_2$ nAChRs whose assembly and maturation, as judged by their functional properties and sensitivity to the chaperone protein 14-3-3, may be comparable to that of the corresponding non-linked α4β2 nAChR.

CHAPTER 4

Identification of agonist binding subunits in linked $(\alpha4)_2(\beta2)_3$ and $(\alpha4)_3(\beta2)_2$ receptors

4.1 Introduction

The advantages of pentameric subunit concatamers as receptor models relative to receptors assembled from free subunits are twofold. Firstly, the stoichiometry and subunit order in concatenated pentamers are fixed. This eliminates the problems encountered in the interpretation of functional data from receptors assembled from free subunits (e.g., Zwart and Vijverberg, 1998; Nelson *et al.*, 2003; Moroni *et al.*, 2006). As mentioned in Chapter 3, the subunit composition of non-linked receptors expressed heterologously in surrogate systems is influenced by the relative availability of exogenous cDNAs or cRNAs introduced into surrogate cells, and often multiple forms of the receptor are co-expressed. Additionally, non-linked subunits may form homomeric (Beato *et al.*, 2002) or heteromeric (Charnet *et al.*, 1992) receptor complexes that do not exist *in vivo*. Secondly, concatenated receptors allow studies that cannot be carried out using non-linked receptors, particularly non-linked receptors with one or two subunits present in multiple copies such as α4β2 nAChRs. For example, a mutation can be introduced into just one subunit to investigate positional effects of single point mutations or positional effects of subunit isoforms. The latter studies can be carried out using lower order concatamers such as dimers and trimers (Baumann *et al.*, 2001; Baumann *et al.*, 2002; Minier and Sigel, 2004a; Gallagher *et al.*, 2004; Boileau *et al.*, 2005; Bollan *et al.*, 2008; Kaur *et al.*, 2009); however, the complication of unknown stoichiometries still remains as dimers and trimers can give rise to several types of receptor ensembles (Bauman *et al.*, 2001).

Although in fully concatenated pentameric receptors, the complication of uncertain stoichiometry and subunit order does not exist, the functional consequences of the incorporation of single point mutations in a given subunit cannot be fully appreciated unless the functional role and the spatial orientation (i.e., orientation of the positive and negative faces) of the subunit are known. Therefore, in this Chapter, in order to identify the function and the spatial orientation of α4 and β2 subunits in β2_α4_β2_α4_β2 and β2_α4_β2_α4_α4 receptors, alanine mutants of conserved aromatic residues predicted to bind agonists in α4β2 nAChRs were incorporated sequentially into the subunits of β2_α4_β2_α4_β2 and β2_α4_β2_α4_α4 and the functional consequences of these mutants were investigated electrophysiologically.

4.2 Experimental procedures

4.2.1 cDNA constructs and mutagenesis

Mutations have been constructed using the QuikChange™ Site-Directed Mutagenesis Kit, as previously described in section 2.4. PCRs have been carried out using the following primers:

$\alpha4^{Y126A}$:	primer forward	GGACATCGTCCTCGCCAACAATGCTGACGG
	primer reverse	CCGTCAGCATTGTTGGCGAGGACGATGTCC
$\alpha4^{W182A}$:	primer forward	CCATGAAATTCGGCTCCGCGACCTACGACAAGGCC
	primer reverse	GGCCTTGTCGTAGGTCGCGGAGCCGAATTTCATGG
$\alpha4^{Y223A}$:	primer forward	CCTACAACACCAGGAAGGCCGAGTGCTGCGCCG
	primer reverse	CGGCGCAGCACTCGGCCTTCCTGGTGTTGTAGG
$\alpha4^{Y230A}$:	primer forward	CGAGTGCTGCGCCGAGATCGCCCCGGACATCACC
	primer reverse	GGTGATGTCCGGGGCGATCTCGGCGCAGCACTCG
$\beta2^{W82A}$:	primer forward	CCACCAATGTCGCGCTGACCCAGGAGTGG
	primer reverse	CCACTCCTGGGTCAGCGCGACATTGGTGG

The full-length sequence of mutant subunit cDNAs was verified by DNA sequencing.

To produce mutant concatenated $(\alpha4)_3(\beta2)_2$ and $(\alpha4)_2(\beta2)_3$ receptors each α4 or β2 subunit was modified separately and subsequently ligated into the pentameric constructs using standard ligation procedures. The full-length sequence of mutant subunit cDNAs was verified by DNA sequencing.

4.2.2 Injection of cDNAs constructs into *Xenopus* oocytes

The effect of the mutation has been firstly analysed in non-linked $(\alpha4)_3(\beta2)_2$ and $(\alpha4)_2(\beta2)_3$ receptors. To express the two α4β2 nAChR stoichiometries, α4 and β2 subunit cDNAs were combined in a ratio of 1:10 to produce a $(\alpha4)_2(\beta2)_3$ stoichiometry, whilst a subunit ratio of 10:1 was used to produce a $(\alpha4)_3(\beta2)_2$ stoichiometry (Moroni et al., 2006). The amount of total cDNA injected per oocyte was kept constantly equal to 3 ng. For

expression of concatenated receptors 10 ng of cDNA per oocyte was injected (see Section 2.9).

4.2.3 Electrophysiological protocols

Concentration-response curves for ACh and epibatidine were obtained by normalizing agonist-induced responses to the control response induced by 1 mM ACh alone. A minimum interval of 4 minutes was allowed between acetylcholine applications as this was found to be sufficient to ensure reproducible recordings. Concentration-response data for wild type or mutant α4β2 receptors were fitted using one component sigmoidal dose-response equations (see Section 2.14).

The sensitivity to Zn^{2+} was assessed by co-applying a range of Zn^{2+} concentrations with 10 μM ACh, the ACh EC_{10} at linked and non-linked $(\alpha4)_3(\beta2)_2$ receptors. For Zn^{2+} to attain equilibrium around impaled oocytes, Zn^{2+} was pre-applied for 30 s to the cell prior to co-application of ACh and Zn^{2+}. Peak responses elicited by ACh + Zn^{2+} were normalized to the peak response of the appropriate ACh alone. Data were fitted to the a two-component equation designed to account for the potentiating and inhibitory effects of Zn^{2+} on α4β2 receptors assuming this cation binds to two distinct sites on the receptor (see Section 2.14).

RESULTS

4.3.1 Effect of mutations implicated in agonist binding on non-linked $(\alpha4)_2(\beta2)_3$ and $(\alpha4)_3(\beta2)_2$ nAChRs

The study of the functional consequences of substituting residues predicted to bind agonists by alanine was initiated to identify the agonist and non-agonist binding subunits in concatenated β2_α4_β2_α4_β2 and β2_α4_β2_α4_α4 nAChRs. As mentioned in Chapter 1, site-directed mutagenesis and biochemical studies (reviewed in Arias, 2000), combined with the structures of the heteromeric *Torpedo* nAChR (Unwin, 2005; Dellisanti *et al.*, 2007), the homomeric prokaryotic proton-gated ion-channels ELIC (Hilf and Dutzler, 2008) and GLIC (Bocquet *et al.*, 2009) and AChBP (Brejc *et al.*, 2001; Celie *et al.*, 2004), have identified several aromatic residues that are mostly conserved among the Cys-loop receptors and that are implicated in agonist binding. In *Torpedo* and muscle nAChR these are α1Tyr93, α1Trp149, α1Tyr190 and α1Tyr198 (the positive face of the binding site), and residues Trp55 and Trp57 located in the complementary ε/γ or δ subunits (the negative face of the binding site). In the α4β2 nAChR the homologous residues are α4Tyr126, α4Trp182, α4Typ223, α4Tyr230, and β2Trp82. (To obtain the position in the mature subunit form, subtract 30 from the number for α4 and 25 for β2). Theoretically, if these residues were substituted by alanine, their contribution to agonist binding would be abolished, which would impact on agonist binding characteristics such as potency and efficacy. It follows then that sequential incorporation of any alanine mutations of any of these residues into the concatenated β2_α4_β2_α4_β2 and β2_α4_β2_α4_α4 nAChRs receptors should lead to the identification of the subunits implicated in agonist binding.

Little is known about the effects of α4Tyr126A ($\alpha4^{Y126A}$), α4Trp182A ($\alpha4^{W182A}$), α4Tyr223A ($\alpha4^{Y223A}$), α4Tyr230A ($\alpha4^{Y230A}$), and β2Trp82A ($\beta2^{W82A}$) on agonist binding in α4β2 nAChRs. Therefore, prior to assaying mutant concatenated receptors, the functional effects of $\alpha4^{Y126A}$, $\alpha4^{W182A}$, $\alpha4^{Y223A}$, $\alpha4^{Y230A}$ and $\beta2^{W82A}$ were investigated on non-linked $(\alpha4)_2(\beta2)_3$ and $(\alpha4)_3(\beta2)_2$ nAChRs. Fig. 4.1 shows that incorporation of mutant subunits $\alpha4^{Y126A}$, $\alpha4^{Y223A}$, $\alpha4^{Y230A}$ or $\beta2^{W82A}$ into non-linked $(\alpha4)_2(\beta2)_3$ or $(\alpha4)_3(\beta2)_2$ receptors caused significant decreases in the level of current evoked by saturating concentration of ACh relative to the values observed in the respective wild-type receptors ($p < 0.05$, Student's *t* test; n = 10 - 15). In contrast, although $\alpha4^{W182A}$ decreased the maximal level of current in $(\alpha4)_2(\beta2)_3$ receptors, its effects on ACh maximal current in $(\alpha4)_3(\beta2)_2$ were not significant. Western blot analysis showed that the reduced level of functional expression

observed in caused not only by impaired gating but also by reduced level of protein expression (data not shown).

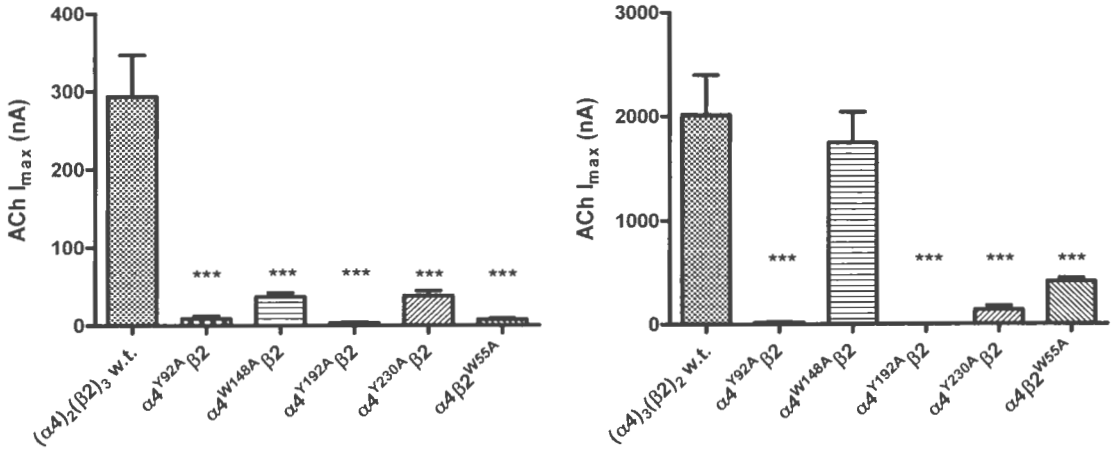

Fig. 4.1. ACh I_{max} currents in wild-type (w.t) or mutant non-linked $(\alpha4)_2(\beta2)_3$ and $(\alpha4)_3(\beta2)_2$ nAChRs. Effect of alanine mutations of the conserved aromatic residues thought to contribute to the agonist binding site of nAChRs on the functional expression of non-linked $(\alpha4)_2(\beta2)_3$ (*Left panel*) and $(\alpha4)_3(\beta2)_2$ (*Right panel*) nAChRs. The data represent the mean ± SEM of 5-10 determinations from individual oocytes from a same batch. (*** = $p < 0.001$, Student's *t* test).

The sensitivity of non-linked $(\alpha4)_2(\beta2)_3$ and $(\alpha4)_3(\beta2)_2$ nAChRs to activation by ACh was significantly decreased by mutants of $\alpha4^{Y126A}$, $\alpha4^{Y230A}$ and $\beta2^{W82A}$ (Fig. 4.2, Table 4.1) ($p < 0.05$; Student's *t* test; n = 10 - 15). $\alpha4^{Y223A}$ completely abolished sensitivity to activation by ACh in both receptor types. Interestingly, a comparison between the extent of the effects of the alanine substitutions in both receptor types showed that non-linked $(\alpha4)_2(\beta2)_3$ receptors were more sensitive to changes in the aromatic residues implicated in agonist binding (Table 4.1). This further confirms that $(\alpha4)_2(\beta2)_3$ and $(\alpha4)_3(\beta2)_2$ nAChRs have significantly different functional properties.

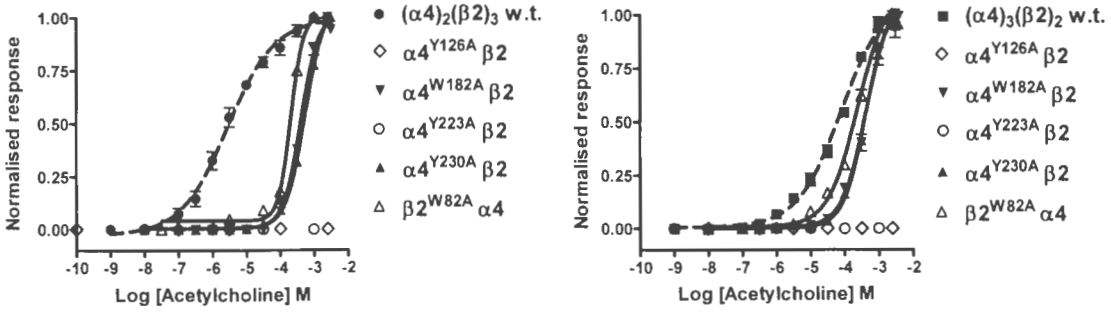

Fig. 4.2. Effects of alanine mutants of conserved aromatic residues on the sensitivity of non-linked to activation by ACh. ACh concentration-response curves obtained from oocytes expressing non-linked wild type or mutant $(\alpha4)_2(\beta2)_3$ (*Left panel*) and $(\alpha4)_3(\beta2)_2$ nAChRs (*Right panel*). Data were normalised to ACh I_{max} for each individual point. The data represent the mean ± SEM from at least 5 oocytes. The concentration-response curve parameters obtained from curve-fitting are summarised in Table 4.1

The results described above support the view that aromatic residues α4Y126, α4W182, α4Y223, α4Y230 and β2W82 are implicated in agonist binding in non-linked $(\alpha4)_2(\beta2)_3$ and $(\alpha4)_3(\beta2)_2$ nAChRs. To further test the involvement of these aromatic residues in agonist binding, their effects on the sensitivity of the receptors to activation by epibatidine, a highly selective agonist of α4β2 nAChR (Moroni *et al.*, 2006) were investigated. Fig. 4.3 shows the effects of $\alpha4^{Y126A}$, $\alpha4^{W182A}$, $\alpha4^{Y223A}$, $\alpha4^{Y230A}$ and $\beta2^{W82A}$ on the potency and efficacy of epibatidine at non-linked $(\alpha4)_2(\beta2)_3$ and $(\alpha4)_3(\beta2)_2$ nAChRs (data summarised in Table 4.1). The potency of epibatidine at mutants $(\alpha4^{Y126A})_3(\beta2)_2$, $(\alpha4^{W182A})_3(\beta2)_2$, $(\alpha4^{Y223A})_3(\beta2)_2$ and $(\alpha4^{Y230A})_3(\beta2)_2$ receptors was significantly reduced ($p < 0.05$; Student's t test; n = 10 - 12), whereas the potency of epibatidine at $(\alpha4)_3(\beta2^{W82A})_2$ was not different from that observed at wild type $(\alpha4)_3(\beta2)_2$ receptors. At non-linked $(\alpha4^{Y126A})_2(\beta2)_3$ and $(\alpha4)_2(\beta2^{W82A})_3$ epibatidine did not activate currents, even at concentrations as high as 3 mM. At non-linked $(\alpha4)_3(\beta2)_2$ nAChRs, $\alpha4^{Y126A}$, $\alpha4^{Y230A}$ and $\beta2^{W82A}$ increased the efficacy of epibatidine in comparison to that observed in their wild-type counterparts. In contrast, the efficacy of epibatidine at $(\alpha4^{W182A})_2(\beta2)_3$ was not different from that observed at the wild type receptor and decreased by about 2-fold at $(\alpha4^{W182A})_3(\beta2)_2$. As for ACh, the incorporation of $\alpha4^{Y223A}$ into non-linked $(\alpha4)_2(\beta2)_3$ or $(\alpha4)_3(\beta2)_2$ receptors abolished sensitivity to activation by epibatidine. The most pronounced effect on epibatidine efficacy was observed on the $\alpha4^{Y230A}$ mutant. Insertion of this mutation in the α4β2 nAChR increased the efficacy of epibatidine by about 4-fold in the $(\alpha4^{Y230A})_2(\beta2)_3$ receptor and about 9-fold in the $(\alpha4^{Y230A})_3(\beta2)_2$ receptor. This effect is likely to be due to changes in receptor gating. The residue Y230 is located in loop C which caps the binding and plays an important role in the activation of the receptor (Sine and Engel, 2006).

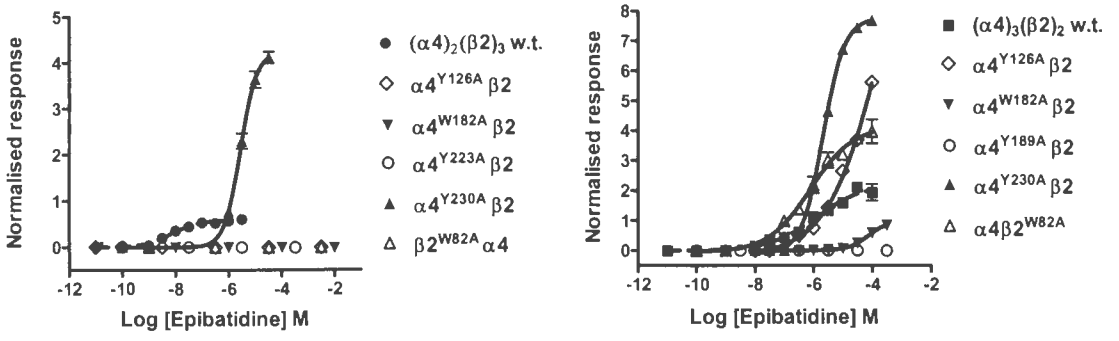

Fig. 4.3. Effects of alanine mutants of conserved aromatic residues on the sensitivity of non-linked α4β2 nAChRs to activation by epibatidine. Epibatidine concentration-response curves obtained from oocytes expressing non-linked wild type or mutant $(\alpha4)_2(\beta2)_3$ *(Left)* and $(\alpha4)_3(\beta2)_2$ *(Right)* nAChRs. Data were normalised to ACh I_{max} for each individual point. The data represent the mean ± SEM from at least 5 oocytes. The concentration-response curve parameters obtained from curve-fitting are summarised in Table 4.1

Table 4.1. Functional effects of alanine mutants of conserved aromatic residues in non-linked $(\alpha4)_2(\beta2)_3$ and $(\alpha4)_3(\beta2)_2$ receptors.

	Non-linked $(\alpha4)_2(\beta2)_3$			Non-linked $(\alpha4)_3(\beta2)_2$		
	I/I_{max} ± SEM	EC_{50} μM (95% CI)	nHill ± SEM	I/I_{max} ± SEM	EC_{50} μM (95% CI)	nHill ± SEM
Acetylcholine						
α4β2 w.t.	1	3.2 (1.4 - 5)	0.7±0.04	1	85 (40 - 130)	0.7±0.03
$\alpha4^{Y126A}$	N.E.	N.D.	N.D.	1	159 (72 - 240) *	1.6±0.02 *
$\alpha4^{W182A}$	1	408 (365-450) *	1.7±0.03 *	1	367 (280-450) *	1.2±0.07 *
$\alpha4^{Y223A}$	N.E.	N.D	N.D.	N.E.	N.D.	N.D.
$\alpha4^{Y230}$A	1	513 (480-550) *	1.7±0.1 *	1	406 (170-640) *	1.3±0.07 *
$\beta2^{W82A}$	1	290 (70 - 513) *	0.86±0.08	1	240 (150-330) *	1±0.01 *
Epibatidine						
w.t. α4β2	0.6±0.02	0.2 (0.01-0.03)	0.72±0.1	2.2±0.2	1.27 (0.4 - 4)	0.54±0.1
$\alpha4^{Y126A}$	N.E.	N.D.	N.D.	4.7±0.09 *	8 (6 - 23)	0.9±0.1
$\alpha4^{W182A}$	0.57±0.01	64 (10 - 100) *	1.2±0.4 *	1±0.1	50 (25 - 125)	1±0.1
$\alpha4^{Y223A}$	N.E.	N.D	N.D.	N.E.	N.D.	N.D.
$\alpha4^{Y230A}$	5.2 ±0.5 *	4.3 (2.4 - 7.5) *	1±0.2	8.1±0.3 *	11 (4 - 70) *	0.7±0.1
$\beta2^{W82A}$	N.E.	N.D.	N.D.	3.9±0.18	0.7 (0.3 - 1.2)	0.7±0.1

All values are means (95 % CI) or means ± SEM from 10 to 15 cells. Statistical comparisons between the concentration-response curve parameters of the wild type and mutant receptors were carried out using Student's *t* tests. The * signifies $p < 0.05$ compared w.t. receptors. Abbreviations: wild type, w.t; no agonist effect. N.E.; not determined, N.D.

The findings of the study described above confirmed that aromatic residues α4Y126, α4W182, α4Y223, α4Y230 and β2W82 are implicated in agonist binding in non-linked $(\alpha4)_2(\beta2)_3$ or $(\alpha4)_3(\beta2)_2$ nAChRs. Therefore, alanine mutants from any of these residues could be used to identify the agonist binding subunits in concatenated β2_α4_β2_α4_β2 and β2_α4_β2_α4_α4 nAChRs. Theoretically, the potency and maximal currents of agonists at β2_α4_β2_α4_β2 and β2_α4_β2_α4_α4 nAChRs should be altered only when alanine mutants of the aromatic agonist binding residues were incorporated into an agonist binding subunit.

4.3.2 Agonist binding β2 subunits in β2_α4_β2_α4_β2 receptors

To identify the agonist binding subunits in β2_α4_β2_α4_β2 receptors, mutant β2W82A was sequentially incorporated into each of the β2 subunits of the concatenated receptor. Mutants of the α4 subunit were not used to identify agonist binding subunits in β2_α4_β2_α4_β2 receptors because, by analogy to *Torpedo* nAChRs, both α4 subunits are presumed to bind agonists in $(\alpha4)_2(\beta2)_3$ receptors. Fig. 4.4 shows average ACh concentration-response curves obtained at wild-type and mutant β2_α4_β2_α4_β2 receptors. The ACh concentration-response curve at $\beta2^{W82A}$_α4_β2_α4_β2 receptors (mutant β2 in the 1st position of the concatamer) was similar to that obtained at wild type in β2_α4_β2_α4_β2 receptors. Thus, at wild type β2_α4_β2_α4_β2 receptors the estimated ACh EC_{50} was 5.22 (2.5 – 10) μM (n = 6) and at $\beta2^{W82A}$_α4_β2_α4_β2 receptors the value of ACh EC_{50} was 4.6 (2.5 – 8.4) μM (n = 10). In contrast, at β2_α4_$\beta2^{W82A}$_α4_β2 (mutation incorporated in 2nd position of concatamer) and β2_α4_β2_α4_$\beta2^{W82A}$ (mutation present on the 5th position of concatamer) receptors, the respective ACh EC_{50} values were significantly decreased to 102 (29 – 353) μM and 124 (37 – 421) μM ($p < 0.05$; Student's t test; n = 5). Although the ACh EC_{50} value obtained at β2_α4_$\beta2^{W82A}$_α4_β2 receptors was lower than that determined for β2_α4_β2_α4_$\beta2^{W82A}$ receptors, statistically they were found to be similar. Together, the findings of this part of the study indicate that the 3rd and 5th β2 subunits in β2_α4_β2_α4_β2 receptors are implicated in agonist binding. In comparison, the 1st subunit does not bind agonists because the agonist sensitivity to ACh was not altered by the incorporation of mutant $\beta2^{W82A}$ into this position.

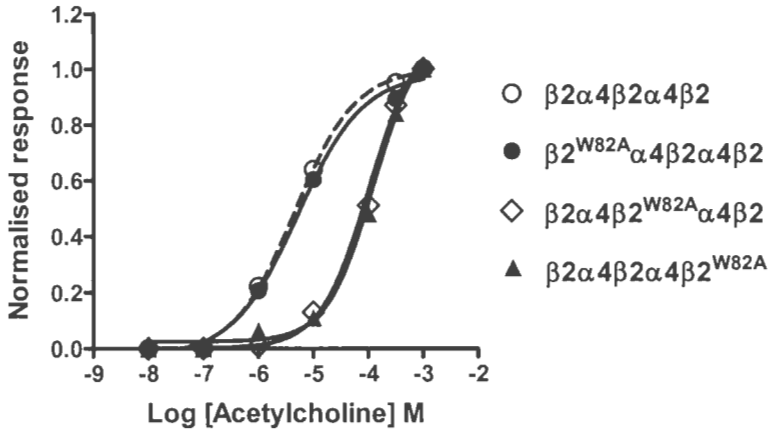

Fig. 4.4. Effects of β2W82A on ACh sensitivity of β2_α4_β2_α4_β2 receptors. Mutant $\beta2^{W82A}$ was incorporated sequentially into the 1st, 3rd and 5th position of concatamer β2_α4_β2_α4_β2 in order to identify the agonist binding β2 subunits of the receptor complex. Data were normalised to ACh I_{max} for each individual point. The data represent the mean ± SEM from at least 5 oocytes.

Since the agonist binding sites are located at the interface between the positive face of α4 and the negative face of β2, and there are only two α4 subunits in β2_α4_β2_α4_β2 concatamers, it is concluded that the agonist binding sites are at located at the interface between the 2nd α4 and 3rd β2 subunits and between the 4th α4 and 5th β2 subunits and that the 1st β2 subunit is the accessory subunit in β2_α4_β2_α4_β2. It follows therefore that the spatial orientation of the subunits in β2_α4_β2_α4_β2 is as illustrated in the following scheme:

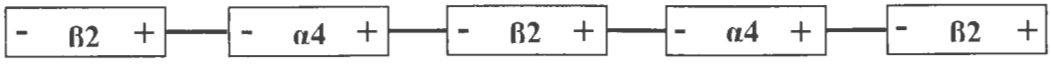

A comparison of the value of the ACh EC_{50} estimated for the corresponding non-linked $(\alpha4)_2(\beta2^{W82A})_3$ receptors (EC_{50} 290 (70 –513) μM and the concatenated β2_α4_$\beta2^{W82A}$_α4_β2 (EC_{50} 102 (29 – 353) μM and β2_α4_β2_α4_$\beta2^{W82A}$ (124 (37 – 421) μM) receptors showed that ACh is more potent, almost twice, at the concatenated receptors. This is likely to be due to the fact that in the non-linked receptors all the β2 subunits are mutated whereas in β2_α4_$\beta2^{W82A}$_α4_β2 and β2_α4_β2_α4_$\beta2^{W82A}$ only one β2 subunit is mutated. Presumably, when the mutation is incorporated simultaneously into the 3rd and 5th β2 subunit the ACh EC_{50} should be similar to that observed at the corresponding non-linked receptors. The sensitivity to activation by agonists could not be

determined in such receptors because the functional expression of the triple-mutated receptors was too low.

4.3.3 Localisation of the agonist binding α4 subunits in β2_α4_β2_α4_α4 nAChRs

The α4 subunit was used to identify the position of the agonist binding sites in β2_α4_β2_α4_α4 receptors. Mutant $\alpha4^{Y230A}$ was chosen to identify the α4 subunits that bind agonists in β2_α4_β2_α4_α4 nAChRs. In the corresponding non-linked $(\alpha4)_3(\beta2)_2$ receptor, $\alpha4^{Y230A}$ decreased sensitivity to activation by ACh or epibatidine, and increased the efficacy of epibatidine by 4-fold (Table 4.1). Thus, theoretically, the sensitivity of β2_α4_β2_α4_α4 receptors to activation by agonists should decrease when agonist binding α4 subunits carry the Y230A mutation. To increase the reliability of the functional assays, the studies that will be described next were carried using epibatidine instead of ACh because the former has higher potency and efficacy than ACh at both non-linked $(\alpha4)_3(\beta2)_2$ (Table 4.1) and β2_α4_β2_α4_α4 (Carbone *et al.*, 2009) receptors.

Incorporation of α4Y230A into the α4 subunit that occupies the 4th position of the concatenated β2_α4_β2_α4_α4 did not alter the sensitivity of the receptor to activation by epibatidine in comparison to that of wild type β2_α4_β2_α4_α4 receptors (β2_α4_β2_$\alpha4^{Y230A}$_α4 epibatidine EC_{50} = 0.29 (0.091 – 0.42) μM (n = 5); β2_α4_β2_α4_α4 epibatidine EC_{50} = 0.47 (0.31 – 0.69) μM) (Fig. 4.5). In contrast, when the mutation was incorporated into the 2nd or 5th position the sensitivity to activation by epibatidine was significantly reduced to respectively 2.92 (1.9 – 4.6) μM and 3.2 (1.5 – 7) μM ($p < 0.05$, Student's *t* test, n = 8 – 9) (Fig. 4.5).

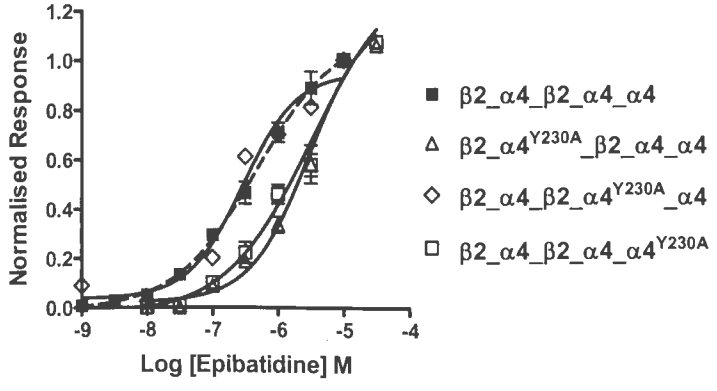

Fig. 4.5. Functional effects of α4Y230A on the sensitivity to activation of β2_α4_β2_α4_α4 concatamers by epibatidine. Mutant $\alpha4^{Y230A}$ was incorporated sequentially into the 2nd, 4th and 5th position of concatamer. β2_α4_β2_α4_α4 in order to identify the agonist binding α4 subunits of the receptor complex. Data were normalised to epibatidine I_{max} for each individual point. The data represent the mean ± SEM from at least 5 oocytes.

Taken together, these results indicate that the α4 subunits that occupy the 2nd and 5th positions in concatamer β2_α4_β2_α4_α4 bind agonists. In contrast, the α4 subunit that is in the 4th position in β2_α4_β2_α4_α4 does not bind agonists and is therefore the accessory subunit. These findings, together with the restrictions imposed by the rule that the agonist binding site is formed at the interface between the positive face of α and the negative face of β, indicate that the spatial orientation of the subunits in this concatamer is as indicated in the following scheme:

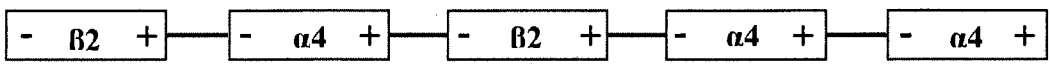

and that the agonist binding sites are at the interface between the 2nd α4 and 3rd β2 subunits and between the 5th α4 and 1st β2 subunit.

So far the findings suggest that the 4th α4 subunit in the concatamer β2_α4_β2_α4_α4 nAChRs does not participate in agonist binding. In order to explore this further, mutant $\alpha4^{E224A}$ was incorporated into the 4th position of the β2_α4_β2_α4_α4 nAChRs. In a previous study it was shown that non-linked $(\alpha4)_3(\beta2)_2$ receptors are selectively potentiated by Zn^{2+} (Moroni *et al.*, 2008). The potentiating Zn^{2+} site resides on the α4(-)/α4(+) interface of the $(\alpha4)_3(\beta2)_2$ nAChR and key residue contributors are α4H195 on the (-) side of the agonist binding α4 subunit and $\alpha4^{E224A}$ on loop C of the accessory α4 subunit of the receptor. Fig. 4.6 shows that incorporating mutant $\alpha4^{E224A}$ into the 4th position of concatamer β2_α4_β2_α4_α4 decreased significantly the potentiating effects of Zn^{2+} on the responses elicited by ACh at this receptor type in comparison to wild type receptors ($p < 0.05$, Student's *t* tests; $n = 10$). Thus, the maximal potentiation achieved by Zn^{2+} at wild type β2_α4_β2_α4_α4 was 1.97 ± 0.1 (normalised response, see Section 2.12; $n = 7$), whereas at mutant receptor β2_α4_β2_$\alpha4^{E224A}$_α4, maximal Zn^{2+} potentiation decreased to 1.40 ± 0.12 ($n = 12$). In contrast when the $\alpha4^{E224A}$ was carried by the 5th α4 subunit, sensitivity to Zn^{2+} potentiation was not different from that of wild type β2_α4_β2_α4_α4 receptors (2.12 ± 0.72; $n = 8$).

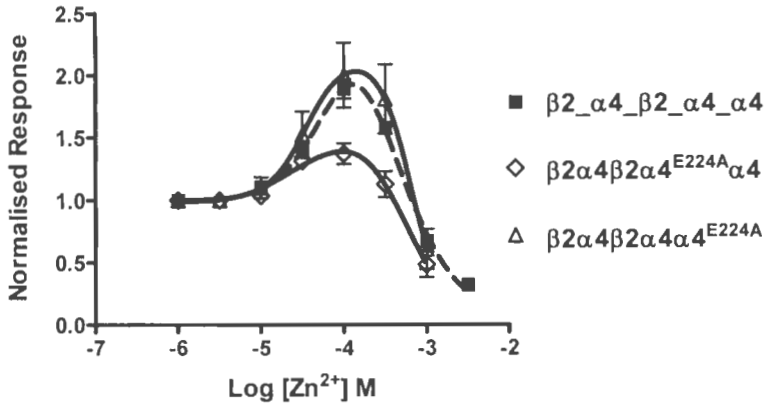

Fig. 4.6. Zn^{2+} sensitivity of wild type and mutant β2_α4_β2_α4_α4 receptors. $\alpha4^{E224A}$ was incorporated into the 4th or 5th position of concatamer β2_α4_β2_α4_α4 to determine the effects of the mutation on the sensitivity of β2_α4_β2_α4_α4 to potentiation by Zn^{2+}. The curves represent averaged concentration-response for the effects of Zn^{2+} at wild type and mutant concatamers. The effects of Zn^{2+} on currents activated by EC_{10} ACh (10 μM) on concatenated receptors were determined as detailed in Chapter 3.

Abolition of Zn^{2+} potentiation by $\alpha4^{E224A}$ in the 4th position of β2_α4_β2_α4_α4 receptors could reflect a perturbation of the general properties of the receptor rather than a specific effect on the Zn^{2+} potentiating site. To analyse this possibility ACh dose-response curves of the mutant β2_α4_β2_α4_α4 receptors were determined. As shown in Fig. 4.7, the ACh sensitivity of β2_α4_β2_$\alpha4^{E224A}$_α4 receptors (ACh EC_{50} = 104 (85 –128) μM) was similar to that of wild type β2_α4_β2_α4_α4 receptors (ACh EC_{50} = 109 (77 – 154) μM). When $\alpha4^{E224A}$ was incorporated into the 5th position of β2_α4_β2_α4_α4 receptors the sensitivity to activation by ACh was slightly decreased (125 (98 – 167) μM; n =5) but this effect was not statistically different from that of wild receptors ($p < 0.05$; Student's *t* test).

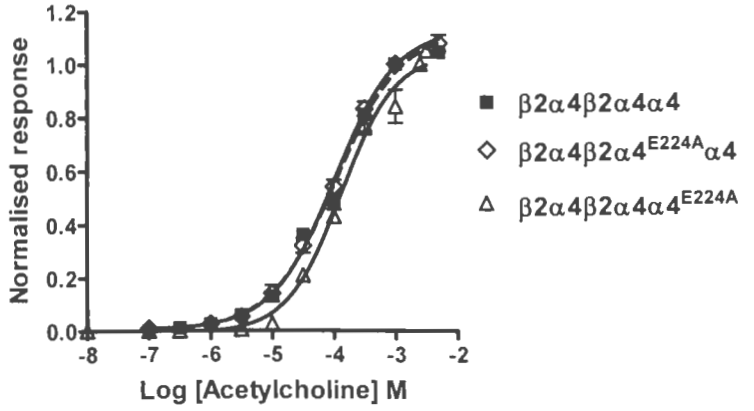

Fig. 4.7. Effects of α4E224A on the ACh sensitivity of wild type and mutant β2_α4_β2_α4_α4 receptors. ACh concentration-response data were obtained from wild type and β2_α4_β2_$\alpha4^{E224A}$_α4 and β2_α4_β2_α4_$\alpha4^{E224A}$ receptors. Data were normalised to ACh I_{max} for each individual point. The data represent the mean ± SEM from at least 5 oocytes.

DISCUSSION

This study has identified the agonist binding subunits in pentameric concatamers β2_α4_β2_α4_β2 and β2_α4_β2_α4_α4. It also established the position of the binding sites within the concatamers and the spatial orientation of the subunits. These findings should increase the insight of studies that seek to understand the positional effects of subunits or mutations in α4β2 nAChRs. In both concatamers, the subunits orientate clockwise; however, the position of the binding sites is concatamer-specific. In the case of the β2_α4_β2_α4_α4 one of the binding sites is assembled at the free α/β interface of the concatamer, whereas in β2_α4_β2_α4_β2 both binding sites are located at subunit interfaces within the concatamer. These differences, together with the subunit order requirement for functional expression of concatenated $(\alpha4)_2(\beta2)_3$ and $(\alpha4)_3(\beta2)_2$ receptors (Chapter 3 and Carbone *et al.*, 2009), suggest that both concatamers regulate subunit assembly differently.

Although the α4β2 nAChR has not been crystallised, the availability of high resolution images of *Torpedo* nAChRs and the crystal structures of the snail (Brejc *et al.*, 2001; Celie *et al.*, 2004), muscle α1 subunit bound to α-Btx (Dellisanti *et al.*, 2007) and proton-gated prokaryotic ELIC (Hilf and Dutzler, 2008) and GLIC (Bocquet *et al.*, 2009) channels, suggests that the agonist binding region of this receptor contains the five aromatic residues that are both highly conserved and implicated in agonist binding in Cys-loop LGICs. In α4β2 nAChRs these residues are α4Y126, α4W182, α4Y223, α4Y230, and β2W82, and this study showed that substitution of these residues by alanine severely handicapped the interaction of agonists with both non-linked α4β2 nAChRs.

In agreement with a role in agonist-receptor interaction, alanine mutants of α4Y126, α4W182, α4Y223, α4Y230, and β2W82 decreased agonist potency, and as judged by ACh I_{max} values they also decreased functional expression. The latter could be a consequence of changes in gating and reduced efficiency in the assembly or trafficking of the receptor ensembles, as suggested by studies in *Torpedo* or muscle nAChR (e.g., Tomaselli *et al.*, 1991; Sine *et al.*, 2002). In muscle and *Torpedo* nAChRs, where these residues have been studied in depth, the most significant changes observed in receptor function by mutants of the conserved aromatic residues of the agonist binding sites, are changes in gating. For example, in muscle nAChRs α1W149 (homologous to α4W182) interacts with agonists through cation-π interactions, which are the most stabilising forces among the agonist-binding cavity interactions described so far, and thus substitutions by alanine or other residues that impair the function of this residue cause a decrease in macroscopic and unitary ACh EC_{50} values (Zhong *et al.*, 1998; Akk, 2001). Similarly,

mutations to residues homologous to α4Y126, α4Y223, α4Y230 and β2W82 were shown to increase macroscopic ACh EC_{50} values and impair gating (Sine *et al.*, 1994; Chen *et al.*, 1995; Auerbach *et al.*, 1996; Akk and Auerbach, 1999; Akk and Steinbach, 2000; Akk, 2001; Bafna *et al.*, 2009).

Although ACh potency was decreased by all of the alanine substitutions assayed in this study, there were clear differences in the extent of the reduction caused by the alanine mutants. For example, unlike $\alpha4^{W182A}$, $\alpha4^{Y230A}$ or $\beta2^{W82A}$, $\alpha4^{Y223A}$ completely abolished sensitivity to ACh in both non-linked $(\alpha4)_2(\beta2)_3$ and $(\alpha4)_3(\beta2)_2$ receptors. These differences have also been observed in *Torpedo* and muscle nAChR (reviewed in Arias, 1997) and reflect the role of each residue in agonist-receptor interaction. Thus, αY190, which is homologous to α4Y223, is a key element in a peripheral loop at the principal face of the agonist binding region, known as loop C, and is close to the pair of adjacent cysteine residues that characterise α subunits. Although αY190 does not interact directly with the agonist, its position in loop C, which caps the entrance to the binding cavity (reviewed in Sine and Engel, 2006) may underlie the profound effects of its alanine mutant on receptor function. The other aromatic residues interact directly with agonists but because within the agonist binding cavity the agonist interacts simultaneously with the other aromatic residues, the absence of one type of these agonist-aromatic residue interactions may not lead to complete disruption of receptor function.

As with other members of the Cys-loop LGIC, α4β2 nAChRs have two agonist binding sites that are located in the extracellular domain of the protein at the α4(+)/β2(-) interfaces of the receptors. Of relevance to α4β2 function, the magnitude of decrease in agonist potency brought about by β2W82A or α4Y230A was similar regardless of the position of the agonist binding subunit carrying the mutated residues. This suggests that each binding site contributes equally to receptor activation. This is in contrast to the muscle nAChR whose agonist binding sites display different properties for agonists and competitive antagonists (Arias, 2000), as expected from binding sites assembled at different subunit interfaces, α1/δ and α1/ε(γ) (Gotti *et al.*, 2006). However, differences in agonist properties have also been reported for α1β2γ $GABA_A$ receptors and in this case both agonist binding sites are assembled from α1 and β2 subunits (Baumann *et al.*, 2003). It could be of interest to test alanine mutants of the other aromatic residues such as α4W182, which provides the strongest stabilising force acting on agonists according to studies of muscle nAChR (Zhong *et al.*, 1998; Brejc *et al.*, 2001; Celie *et al.*, 2004). The

remaining residues interact with agonists by hydrogen bonding and van der Waals interactions, which are, comparatively, of lesser energetic importance.

The identification of the 4th subunit of concatamer β2_α4_β2_α4_α4 as the accessory subunit of the ensemble was confirmed by assaying the effect of Zn^{2+} on the currents elicited by ACh at β2_α4_β2_α4^{E224A}_α4 receptors. α4E224 was suggested by Moroni *et al.*, (2008) to contribute to a potentiating Zn^{2+} binding site that is a functional signature of non-linked $(\alpha4)_3(\beta2)_2$ (Moroni *et al.*, 2008) and concatenated β2_α4_β2_α4_α4 (Carbone *et al.*, 2009). The site was proposed to be contributed by residues located at the α4/α4 interface of $(\alpha4)_3(\beta2)_2$ (Moroni *et al.*, 2008). This interface comprises the (+) side of the accessory α4 subunit and the (-) side of an agonist binding α4 subunit. The findings of this study fully support this proposal.

The decrease of sensitivity to Zn^{2+} potentiation by α4^{E224A} in the 4th α4 subunit could reflect a perturbation of the general properties of the receptor rather than a specific effect on the Zn^{2+} potentiating site. After dismantling of the Zn^{2+} potentiating site located in the α4/α4 interface in β2_α4_β2_α4_α4 receptors, the sensitivity of the receptors to activation by ACh was not affected. Thus, the findings of this study support the suggestion made by Kuryatov *et al.* (2008) that the accessory subunit does not participate in agonist binding. This study and that of Moroni *et al.* (2008) also demonstrate that the accessory subunit confers pharmacological properties, i.e., sensitivity to potentiation by Zn^{2+} to α4β2 nAChRs. This is not a unique characteristic of α4β2 nAChRs. Indeed, the accessory subunit in most Cys-loop receptors plays a key role in the pharmacological signatures of these signalling proteins. Thus, Hansen and Taylor (2007) showed that aromatic residues found in non-ACh-binding interfaces of humanised AChBP contribute to an allosteric binding site sensitive to galanthamine. Also, the γ subunit, the non-agonist binding subunit in αβγ $GABA_A$ receptors, confers sensitivity to potentiation by benzodiazepines (reviewed in Sigel, 2002).

In summary, the findings described in this study clearly identify the functional roles of the subunits of β2_α4_β2_α4_β2 and β2_α4_β2_α4_α4 and confirm the presence of two binding sites in α4β2 nAChRs and the importance of conserved aromatic residues for agonist-receptor interactions.

CHAPTER 5

ADNFLE-linked mutations alter the stoichiometry of α4β2 nAChRs

5.1 Introduction

Autosomal dominant nocturnal frontal lobe epilepsy (ADNFLE) is a rare familial focal epilepsy. It was first described in 1995 and it was the first human epilepsy to be linked to a specific gene defect (Scheffer *et al.*, 1995). ADNFLE is characterised by clusters of frequent brief nocturnal motor seizures arising mainly during stage II of non-REM sleep, which seem to originate in the frontal lobe (Scheffer *et al.*, 1995). Affected individuals are typically of normal intelligence, although psychosis or schizophrenia, behavioural disorders, distinct memory deficits and mental retardation have been reported in some individuals with familial ADNFLE (Khatami *et al.*, 1998; Magnusson *et al.*, 2003; Bertrand *et al.*, 2005; Derry *et al.*, 2008).

Patients affected by ADNFLE often respond well to antiepileptic drugs, especially carbamazepine (CBZ) (Scheffer *et al.*, 1995), which is the drug of choice for nocturnal attacks. One third of the cases, however, commonly patients with a high frequency of seizures, are drug resistant (Oldani *et al.*, 1998; Provini *et al.*, 2000). Recent studies showed that nicotine and tobacco use induce a reduction or complete control of nocturnal seizures (Willoughby *et al.*, 2003; Brodtkorb and Picard, 2006).

ADNFLE is a monogenic epilepsy linked to a specific nAChR subtype, the α4β2 nAChR. So far, four α4 (Steinlein *et al.*, 1995; Steinlein *et al.*, 1997; Hirose *et al.*, 1999; Leniger *et al.*, 2003) and five β2 (De Fusco *et al.*, 2000; Phillips *et al.*, 2001; Bertrand *et al.*, 2005; Hoda *et al.*, 2008) mutations have been linked to ADNFLE. The first six mutations identified are located within or at the C-terminal end of the TM2 domain of the α4 ($\alpha4^{S248F}$; $\alpha4^{776insL}$; $\alpha4^{S252L}$; $\alpha4^{T265I}$) or the β2 ($\beta2^{V287L}$; $\beta2^{V287M}$) nAChR subunit. The M2 domain forms the ion-conducting pathway of the receptor and it is therefore crucial for both ion selectivity and allosteric transitions implicated in receptor function (Miyazawa *et al.*, 2003). Mutations in this region alter the transition of the receptor from the closed to the open state, thus increasing the probability for the receptor of a transition to the active state (Bertrand *et al.*, 1998).

Little is known about the mechanisms that may induce seizures in ADFNLE patients. However, studies on ADNFLE mutated α4β2 nAChRs expressed heterologously in surrogate cells have shown that all of these mutations affect sensitivity to activation by agonists, desensitisation and Ca^{2+} permeability (Weiland *et al.*, 1996; Steinlein *et al.*, 1997; Bertrand *et al.*, 1998; De Fusco *et al.*, 2000; Matshushima *et al.*, 2002; Bertrand *et al.*, 2005), all of which could induce seizures. One hypothesis suggests that the increased ACh

sensitivity displayed by ADNFLE mutant α4β2 receptors could lead to seizures (Bertrand *et al.*, 2002). An alternative hypothesis postulates that the reduced Ca^{2+} permeability of ADNFLE mutant α4β2 receptors decreases the influx of Ca^{2+} into GABAergic presynaptic terminals. This would decrease the release of the inhibitory neurotransmitter GABA, which would shift the brain excitation-inhibition equilibrium towards excitation (Rodrigues-Pinguet *et al.*, 2005). More recently, the discovery that α4β2 nAChRs assemble into two different stoichiometries that are likely to exist in neurones (Marks *et al.*, 1999; Butt *et al.*, 2002; Gotti *et al.*, 2008) and that differ radically in the properties affected by the ADFNLE mutations (e.g., sensitivity to agonists, Ca^{2+} permeability and desensitisation) has suggested another putative mechanism through which ADNFLE-linked mutations can cause the disease. Because ADNFLE α4β2 receptors display properties similar to those of high sensitivity $(\alpha4)_2(\beta2)_3$ nAChRs (i.e., lower Ca^{2+} permeability and higher sensitivity to activation by agonists) (Steinlein *et al.*, 1997; Bertrand *et al.*, 2002; Rodrigues-Pinguet *et al.*, 2005), it may be possible that the mutations promote the formation high sensitivity α4β2 nAChRs. However, a recent study that examined the stoichiometry of ADNFLE mutant α4β2 nAChRs using FRET analysis reported that ADNFLE mutations increased the expression of intracellular $(\alpha4)_3(\beta2)_2$ receptors and that nicotine exposure restored the proportion of the $(\alpha4)_2(\beta2)_3$ stoichiometry to wild type levels.

To address the issue of whether ADNFLE mutations modify the receptor properties or the subunit composition of α4β2 nAChRs, the functional effects of a ADNFLE mutation, $\alpha4^{776insL}$, were investigated in both $(\alpha4)_2(\beta2)_3$ (HS) and $(\alpha4)_3(\beta2)_2$ (LS) receptors. The $\alpha4^{776insL}$ mutation was identified in 1997 in the M2 domain of the CHRNA4 gene in a Norwegian family affected by ADNFLE (Steinlein *et al.*, 1997). Three extra nucleotides are inserted at nucleotide position 776 into the coding region for the C-terminal end of the M2 domain leading to the insertion of a leucine residue in the channel pore region. The $\alpha4^{776insL}$ mutation is the most sensitive mutation to CBZ, which exerts its action on the mutant receptor by acting as an open channel blocker (Picard *et al.*, 1999).

The findings of the studies described in this Chapter on non-linked α4β2 receptors are consistent with a mutation-induced change in receptor stoichiometry. This was therefore further examined by investigating the effects of $\alpha4^{776insL}$ on the properties of the concatenated receptors previously described in Chapter 3. The results obtained support the proposal that ADFNLE mutations alter the stoichiometry of the α4β2 receptors.

5.2 Experimental procedures

5.2.1 cDNA constructs and mutagenesis

Mutations have been constructed using the QuikChange™ Site-Directed Mutagenesis Kit, as previously described in section 2.4. PCRs have been carried out using the following primers:

primer forward:
CGCTCACCGTCTTCCTGCTGCTGCTCATCACCGAGATCATCCCGTCC
primer reverse:
GGACGGGATGATCTCGGTGATGAGCAGCAGCAGGAAGACGGTGAGCG

The full-length sequence of mutant subunit cDNAs was verified by DNA sequencing.

To produce mutant concatenated $(\alpha4)_3(\beta2)_2$ and $(\alpha4)_2(\beta2)_3$ receptors each α4 or β2 subunit was modified separately and subsequently ligated into the pentameric constructs using standard ligation procedures. The full-length sequence of mutant subunit cDNAs was verified by DNA sequencing.

5.2.2 Injection of cDNAs constructs into *Xenopus* oocytes

The effect of the mutation has been firstly analysed in non-linked $(\alpha4)_3(\beta2)_2$ and $(\alpha4)_2(\beta2)_3$ receptors. To express the two α4β2 nAChR stoichiometries, α4 and β2 subunit cDNAs were combined in a ratio of 1:10 to produce a $(\alpha4)_2(\beta2)_3$ stoichiometry, whilst a subunit ratio of 10:1 was used to produce a $(\alpha4)_3(\beta2)_2$ stoichiometry (Moroni et al., 2006). The amount of total cDNA injected per oocyte was kept constantly equal to 3 ng. For expression of concatenated receptors 10 ng of cDNA per oocyte was injected (see Section 2.9).

5.2.3 Electrophysiological protocols

ACh concentration-response curves were obtained by normalizing agonist-induced responses to the control response induced by 1 mM ACh alone. A minimum interval of 4

minutes was allowed between acetylcholine applications as this was found to be sufficient to ensure reproducible recordings. Concentration-response data for wild type or mutant α4β2 receptors were fitted using one component sigmoidal dose-response equations (see Section 2.14).

Ca^{2+} permeability of the concatamers were determined by constructing current-voltage plots relationships and measuring the reversal potential of ACh EC_{50} currents in the presence of 1.8 mM Ca^{2+} or 18 mM Ca^{2+} in the perfusing Ringer solution and measuring the shift in the reversal potential (see Section 2.12).

RESULTS

5.3.1 Effect of a leucine insertion in the M2 domain of the α4 subunit on the expression of α4β2 nAChRs

In order to characterise the effect of the $\alpha4^{776insL}$ mutation in the two alternate stoichiometries of the α4β2 nAChR, the mutant $\alpha4^{776insL}$ subunit was co-injected in *Xenopus* oocytes with the corresponding wild type β2 subunit in a 1:10 or 10:1 α4/β2 cDNAs ratio, which have been shown to produce high sensitivity $(\alpha4)_2(\beta2)_3$ and low sensitivity $(\alpha4)_3(\beta2)_2$ receptors, respectively (Moroni *et al.*, 2006). The mutant receptors expressed with this strategy will be referred to as non-linked $(\alpha4^{776insL})_2(\beta2)_3$ and $(\alpha4^{776insL})_3(\beta2)_2$.

As shown in Fig. 5.1, three days after injection both stoichiometries displayed robust inward currents in response to ACh. Currents evoked by saturating concentration of ACh in the non-linked $(\alpha4^{776insL})_2(\beta2)_3$ receptor were significantly bigger than the wild type (mutant/wild type = 340 ± 10 %, $p < 0.05$, Student's t test, n = 8); the level of expression of the non-linked $(\alpha4^{776insL})_3(\beta2)_2$ receptor was slightly lower than the wild type but not significantly different (mutant/wild type = 60 ± 3%, n = 7).

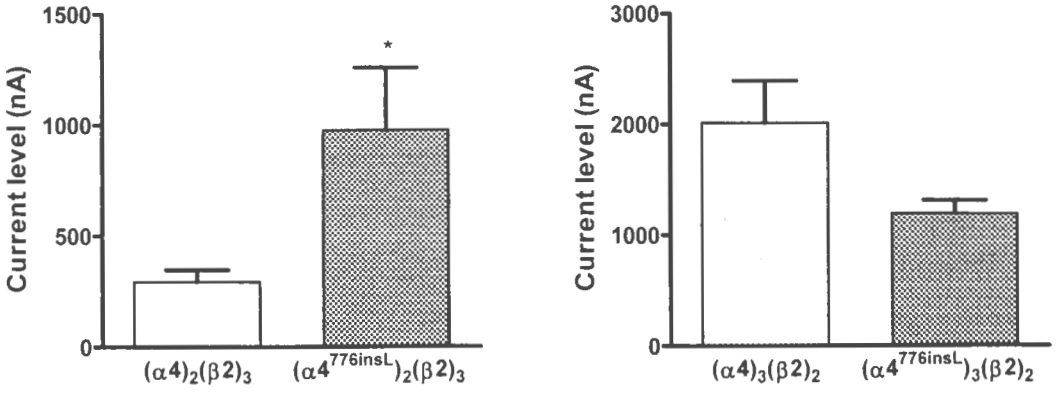

Fig. 5.1. Expression levels of mutant $(\alpha4^{776insL})_2(\beta2)_3$ and $(\alpha4^{776insL})_3(\beta2)_2$ receptors in *Xenopus* oocytes. Bar graph comparing the functional expression levels of mutant and wild type $(\alpha4)_2(\beta2)_3$ (*Left*) and $(\alpha4)_2(\beta2)_3$ (*Right*) receptors. The amplitude of the current responses elicited by maximal concentrations of ACh were 980 ± 200 nA for the mutant $(\alpha4)_2(\beta2)_3$ and 300 ± 50 nA for wild type $(\alpha4)_2(\beta2)_3$ *(Left panel)*. At the $(\alpha4)_3(\beta2)_2$ *(Right panel)* receptor the maximal ACh-elicited current was 1190 ± 100 for mutant receptors versus 2550 ± 165 for wild type receptors. (* $p < 0.05$, Student's t test)

Because mutations in signalling proteins might affect not only functional responses but also receptor assembly and hence the half-life of the subunits, the steady state levels of the subunits in mutant receptors were determined by Western blotting. Immunoblotting

with anti-nAChR α4 or anti-nAChR β2 antibody, showed that $\alpha4^{776insL}$ induced an increase in the steady state levels of both the α4 (Fig. 5.2 A) and the β2 subunits in the non-linked $(\alpha4^{776insL})_2(\beta2)_3$ (Fig. 5.2 B). Surprisingly, the mutation had a different effect on the on the non-linked $(\alpha4^{776insL})_3(\beta2)_2$ receptor. No apparent changes could be observed for the β2 subunit (Fig. 5.2 B), whereas the expression of the α4 subunit was decreased compared to wild type receptors (Fig. 5.2 A). These results are in good agreement with the level of functional expression observed.

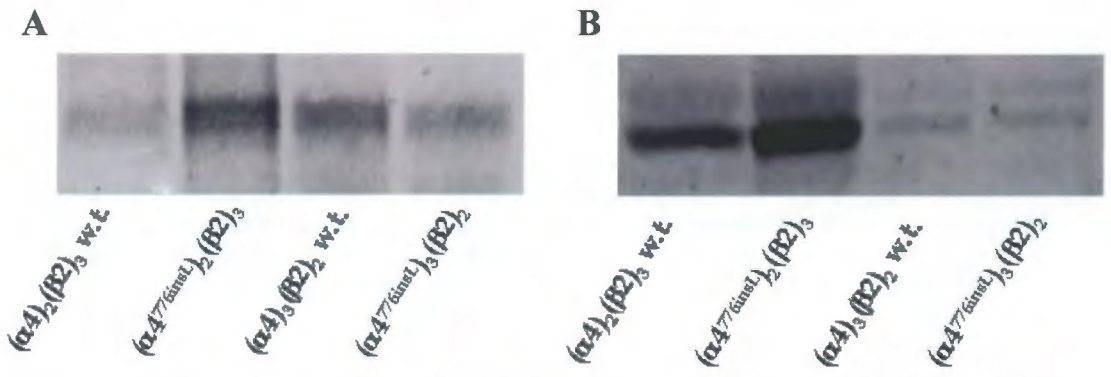

Fig. 5.2. Western blot analysis of total expression levels of α4 and β2 nAChR subunits in wild type and mutant receptors. Membrane homogenates prepared from oocytes injected with 1:10 or 10:1 α4/β2 cDNAs ratio were resolved and then blotted and immunostained as described in Chapter 2. **A)** Immunostaining of wild type and mutant $(\alpha4)_2(\beta2)_3$ and $(\alpha4)_3(\beta2)_2$ with an anti-α4 I Ab showed a specific immunoreactive band at 68 KDa. **B)** Immunostaining of wild type and mutant $(\alpha4)_2(\beta2)_3$ and $(\alpha4)_3(\beta2)_2$ with an anti-β2 I Ab showed a specific immunoreactive band at 52 KDa.

5.3.2 $\alpha4^{776insL}$ mutation increases sensitivity to ACh of the $(\alpha4)_3(\beta2)_2$ stoichiometry

Previous studies showed that mutation 776insL causes a 10-fold increase in sensitivity to agonists in human (Steinlein *et al.*, 1997; Bertrand *et al.*, 1998) and mouse α4β2 receptors (Lipovsek *et al.*, 2008), although no changes were detected in rat α4β2 receptors (Figl *et al.*, 1998). The concentration-response relationship of the mutant receptors for ACh was then analysed. As shown in Fig. 5.3, the mutation had different effects on the ACh concentration-response curve of the two stoichiometries. The non-linked $(\alpha4^{776insL})_3(\beta2)_2$ receptor showed a significant higher sensitivity for the natural agonist than the wild type receptor (Fig. 5.3, *Right panel*). For both receptors the data were fitted to a one-component Hill equation with an EC_{50} of 15 ± 3.37 μM for the mutant receptor and 88 ± 12.2 μM for the wild type receptor ($p < 0.001$, Student's *t* test, n = 8) and a Hill coefficient of 0.44 ± 002 for the mutant receptor and 0.79 ± 0.03 for the wild type receptor ($p < 0.05$, Student's *t* test, n = 8). Neither the sensitivity for ACh nor the nHill

value of the $(\alpha4)_2(\beta2)_3$ stoichiometry were affected by the mutation (Fig. 5.3, *Left panel*). The mutant receptor showed an EC_{50} of 8.1 ± 2.2 μM and a nHill value of 0.59 ± 005, which are not significantly different from the EC_{50} of 3.2 ± 0.7 μM and the Hill coefficient of 0.71 ± 005 of the wild type receptor.

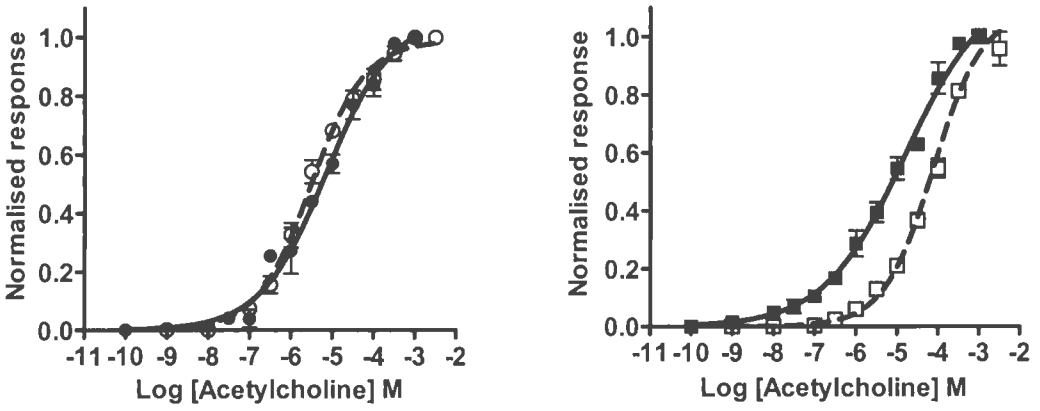

Fig. 5.3. The mutation affect the ACh sensitivity of the two stoichiometries to a different extent. ACh concentration-response curves for mutant $(\alpha4^{776insL})_2(\beta2)_3$ (*Left panel,* ●) and $(\alpha4^{776insL})_3(\beta2)_2$ (*Right panel,* ■). For comparison ACh concentration response curves for non-linked receptors are shown as dashed lines.

5.3.3 Desensitisation of $\alpha4^{776insL}$ mutant α4β2 nAChRs

The $\alpha4^{776insL}$ mutation has been reported to affect the response decay of α4β2 nAChRs (Bertrand *et al.*, 1998; Lipovsek *et al.*, 2008). The rate of decay of the current was measured by applying 10 μM and 600 μM ACh to the wild type and the mutant receptors. Fig. 5.4 shows that the $\alpha4^{776insL}$ mutation caused changes in the rate of decay of the current elicited by saturating concentration of ACh on both $(\alpha4)_2(\beta2)_3$ and $(\alpha4)_3(\beta2)_2$ receptors.

Wild type non-linked $(\alpha4)_2(\beta2)_3$ nAChR did not show significant desensitisation over 30 sec. In contrast, current through the non-linked $(\alpha4^{776insL})_2(\beta2)_3$ receptor decayed rapidly by ~ 80% and then continue to decay slowly in the presence of ACh. The time constants of current decay estimated by curve fitting to the equations described in Section 2.14 are listed in Table 5.1. Currents evoked in both wild type and mutant non-linked $(\alpha4)_3(\beta2)_2$ receptors showed notable desensitisation during application of ACh, with a decay to a plateau level of ~ 30% in the wild type receptor and ~ 50% in the mutant receptor. Current decay during agonist application was best fitted with a one-component exponential in both receptors. Non-linked $(\alpha4^{776insL})_3(\beta2)_2$ receptor displayed a faster

desensitisation rate than wild type. The time constants of the desensitisation are listed in Table 5.1.

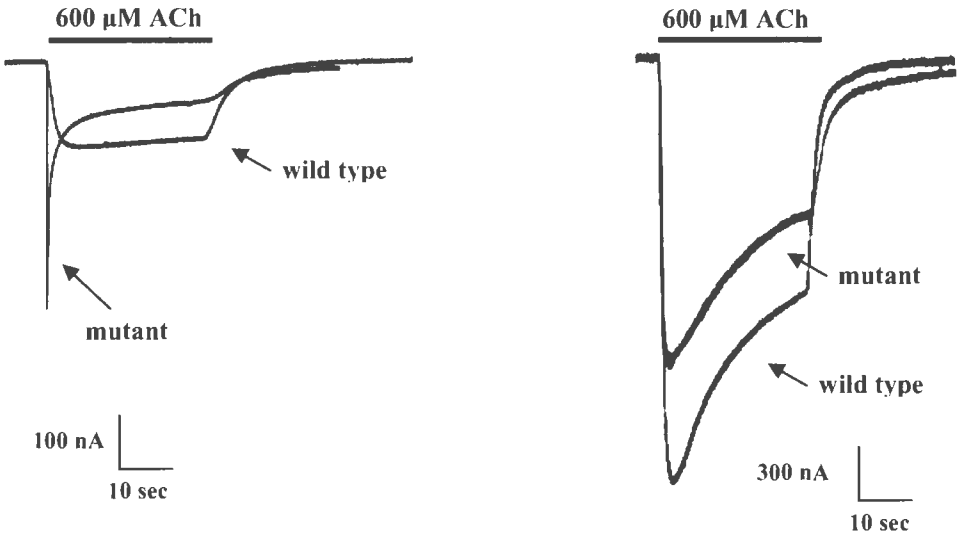

Fig. 5.4. ACh evoked inward currents in wild type and mutant non-linked α4β2 nAChR. Representative traces illustrating the increase in desensitisation induced by the $\alpha4^{776insL}$ mutation in non-linked $(\alpha4)_2(\beta2)_3$ (*Left panel*) and $(\alpha4)_3(\beta2)_2$ (*Right panel*) receptors. Traces evoked in wild type receptors are superimposed for comparison.

Table 5.1. Time constants of current decay of wild type and $\alpha4^{776insL}$ α4β2 nAChRs.

	$(\alpha4)_2(\beta2)_3$ wild type	$(\alpha4^{776insL})_2(\beta2)_3$	$(\alpha4)_3(\beta2)_2$ wild type	$(\alpha4^{776insL})_3(\beta2)_2$
	τ (sec)10 µM ACh			
Fast component		3.6 ± 1.7		
Slow component	32.6 ± 4.2	26.2 ± 3.7	17.5 ± 2.5	13.6 ±4.5
	τ (sec) 600 µM ACh			
Fast component		1.2 ± 0.6		
Slow component	18.9 ± 2.4	10.4 ± 1.9	10.6 ± 2.3	7.4 ± 1.6

Time constants of current decay measured at 10 and 600 µM ACh. Current decay was fitted to a one- or two-component exponential as appropriate. τ values are means ± SEM from 5-10 cells.

5.3.4 $\alpha4^{776insL}$ mutation decreases the Ca^{2+} permeability of the $(\alpha4)_3(\beta2)_2$ nAChR

Steinlein *et al.* (1997) showed that the leucine insertion decreases the Ca^{2+} permeability of α4β2 nAChRs. Ca^{2+} permeability was assessed by measuring the reversal potential of I_{ACh} in the presence of 1.8 mM or 18 mM extracellular Ca^{2+}, as described in Chapter 2 (Tapia *et al.*, 2007). The Ca^{2+} permeability of the two forms of the mutant receptor was differently affected. The permeability of the divalent cation was significantly reduced in the non-linked $(\alpha4^{776insL})_3(\beta2)_2$ receptor, which displayed a 1.7-fold reduction in the shift induced by the 10-fold increase in Ca^{2+} concentration (from 30 ± 5 mV in the wild type receptor to 20 ± 4 mV in the mutant receptor; Fig. 5.5, *Right*) ($p < 0.05$; Student's *t* test, n = 5 - 8). In the non-linked $(\alpha4^{776insL})_2(\beta2)_3$ receptor Ca^{2+} permeability was not affected and the measured shift was 4 ± 0.1 mV in the wild type receptor and 6 ± 0.2 mV in the mutant receptor ($p < 0.05$; Student's *t* test, n = 6 - 9) (Fig. 5.5, *Left*).

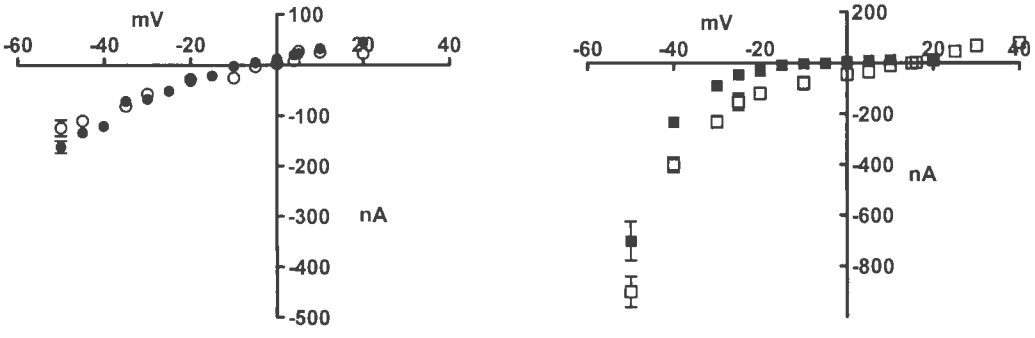

Fig. 5.5 Ca^{2+} permeability of non-linked $(\alpha4^{776insL})_3(\beta2)_2$ and $(\alpha4^{776insL})_2(\beta2)_3$ nAChRs expressed heterologously in *Xenopus* oocytes. Current-voltage relationship of $(\alpha4^{776insL})_2(\beta2)_3$ (*Left,* ●) and $(\alpha4^{776insL})_3(\beta2)_2$ (*Right,* ■) nAChR in the presence of 1.8 mM (non-filled symbols) or 18 mM extracellular (filled symbols) Ca^{2+}. The leucine insertion decreased Ca^{2+} permeability in the $(\alpha4)_3(\beta2)_2$ receptor as judged by the smaller shift of the reversal potential induced in the mutant receptor when the external Ca^{2+} was increased by tenfold.

5.3.5 Agonists efficacy at $\alpha4^{776insL}$ mutant receptors

Previous studies showed that $\alpha4^{776insL}$ affects agonist efficacy (Bertrand *et al.*, 1998). To investigate the effects of this mutation on agonist efficacy at both types of α4β2 nAChRs, wild type and mutant receptors were challenged by maximal concentrations of stoichiometry-selective agonists. The agonists chosen were cytisine, which is a poor partial agonist at the $(\alpha4)_3(\beta2)_2$ receptor (Moroni *et al.*, 2006), and sazetidine-A, which is a full agonist at the $(\alpha4)_2(\beta2)_3$ stoichiometry and a very poor agonist at the $(\alpha4)_3(\beta2)_2$ receptor (Zwart *et al.*, 2008). In the non-linked $(\alpha4^{776insL})_2(\beta2)_3$ receptor the mutation did not

produce significant changes in the efficacy of either agonists (cytisine: 5 ± 2 % in wild type receptors, 5 ± 1 % in mutant receptors; sazetidine A: 93 ± 5 % in wild type receptors, 90 ± 7 % in mutant receptors; Fig. 5.6, *Right*). In contrast, $\alpha4^{776insL}$ caused a significant increase in the efficacy of both agonists at the non-linked $(\alpha4^{776insL})_3(\beta2)_2$ receptor. The efficacy of cytisine increased by 1.6- fold (18 ± 2 % at wild type receptors; 30 ± 5 % at mutant receptor; $p < 0.01$; Student's *t* test, n = 5 - 8) and the efficacy of sazetidine-A was increased by 7.5-fold (6 ± 0.5 % in wild type receptors; 45 ± 0.7 % in mutant receptors; $p < 0.001$; Student's *t* test, n = 5 - 8) (Fig. 5.6, *Left*).

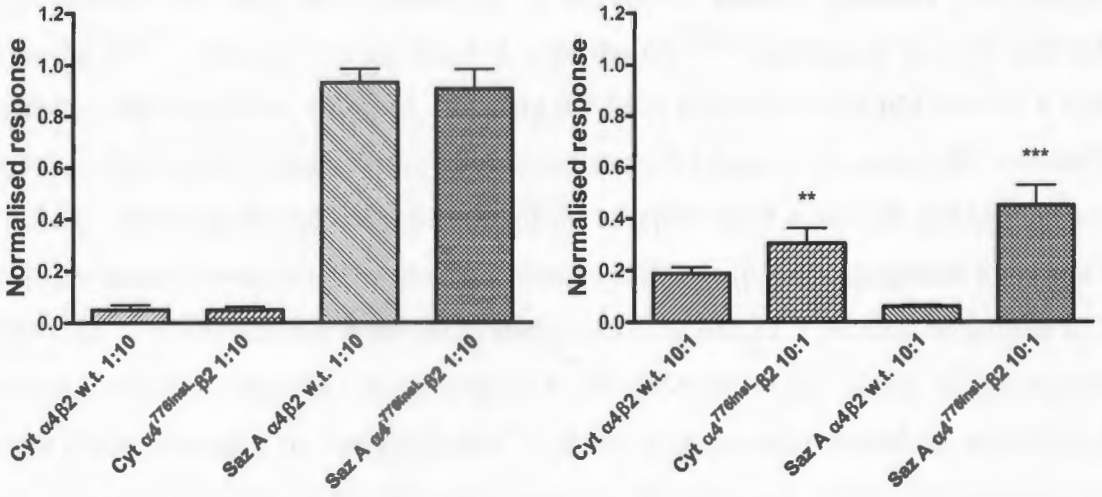

Fig. 5.6. Effect of the $\alpha4^{776insL}$ mutation on agonists efficacies of α4β2 receptors. Bar graph comparing the efficacy of cytisine and sazetidine A on wild type and mutant $(\alpha4)_2(\beta2)_3$ (*Left*) and $(\alpha4)_2(\beta2)_3$ (*Right*) receptors. No changes were observed in the $(\alpha4)_2(\beta2)_3$ receptors (*Left panel*). Both agonist were more efficacious at the $(\alpha4)_3(\beta2)_2$ receptor (*Right panel*). (** = $p < 0.01$; *** = $p < 0001$; Student's *t* test)

5.3.6 Use of the L9'T reporter mutation to determine the stoichiometry of mutant receptors

So far the findings of the studies described above indicate that $\alpha4^{776insL}$ affects the function of $(\alpha4)_3(\beta2)_2$ more markedly than that of its high sensitivity counterpart. As shown by the Western blot $\alpha4^{776insL}$ affects the steady state levels of the subunits and its effect depends on the ratio of subunit cDNAs used to express either $(\alpha4)_2(\beta2)_3$ or $(\alpha4)_3(\beta2)_2$. Because changes in the relative availability of α4 or β2 subunits impact the subunit composition of the receptors (Zwart and Vijverberg, 1998; Nelson *et al.*, 2003; Exley *et al.*, 2006) and because of recent reports that ADNFLE mutations may alter receptor stoichiometry (Son *et al.*, 2009), the subunit composition of both types of mutant

α4β2 receptors was investigated by using the reporter mutation L9'T mutation. Mutating the 9' hydrophobic amino acid in the pore-lining second transmembrane domain of a nicotinic type subunit to a hydrophilic residue makes the resulting receptor more sensitive to agonists (Revah *et al.*, 1991), probably by destabilising the closed state. The extent to which the agonist EC_{50} is reduced is approximately proportional to the number of mutant subunit in the pentamer (Labarca *et al.*, 1995; Chang and Wheiss, 1999). This approach has been previously used to determine the stoichiometry of the α3β4, α3β4bβ3 (Boorman *et al.*, 2000) and α4β2 combinations (Moroni *et al.*, 2006).

The $\alpha4^{776insL}$ subunit was co-expressed with the $\beta2^{L9'T}$ subunit in a 1:10 and 10:1 α4/β2 cDNAs ratio and ACh sensitivity of the double mutant receptors was analysed. When the $\beta2^{L9'T}$ subunit was co-injected with the $\alpha4^{776insL}$ subunit in a 1:10 ratio ACh sensitivity was shifted by 400-fold, reducing the EC_{50} from 4.6 ± 0.6 μM to 0.01 ± 0.004 μM; when the mutant subunits were co-injected in a 10:1 ratio ACh sensitivity was shifted by 7-fold, increasing the apparent affinity of the receptor from 4.3 ± 0.8 μM to 0.59 ± 0.1 μM. If the mutant receptors present a stoichiometry of $(\alpha4)_3(\beta2)_2$ as suggested by Son *et al.* (2009), the $\sqrt[2]{}$ of the potency ratio (EC_{50} α4β2 w.t./EC_{50} α4β2 LT) should be similar to the previously reported data for the LS α4β2 nAChR (Moroni *et al.*, 2006); if the receptors present a stoichiometry of $(\alpha4)_2(\beta2)_3$ the $\sqrt[3]{}$ of the potency ratio should be similar to the previously reported data for the HS α4β2 receptor (Moroni *et al.*, 2006). The expected and experimental values obtained for the $\alpha4^{776insL}\beta2^{LT}$ are listed in Table 5.2. These data are significantly different from those obtained for the wild type receptors by Moroni *et al.* (2006) and are more compatible with receptors with a higher β2 content. However, the presence of five mutations in the channel pore might affect the properties of the receptor and the L9'T mutation might not be and appropriate approach for determining the stoichiometry of α4β2 receptors.

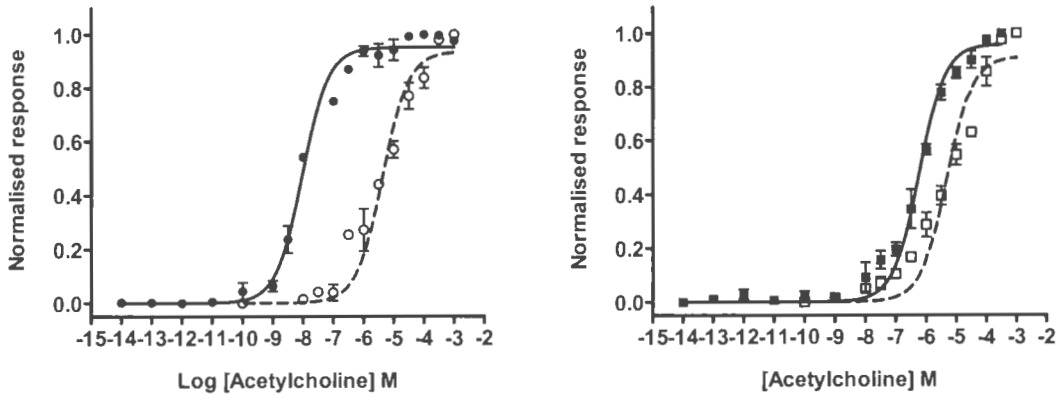

Fig. 5.7. Effect of inserting a L9'T mutation in the β2 subunit in$(\alpha4^{776insL})_3(\beta2)_2$ and $(\alpha4^{776insL})_2(\beta2)_3$ nAChRs. ACh concentration-response curve for $\alpha4^{776insL}\beta2$ (dashed line) and $\alpha4^{776insL}\beta2^{LT}$ (continuous line) are shown. The L9'T mutation caused a left-shift in the ACh dose-response curve in both the non-linked $(\alpha4^{776insL})_2(\beta2)_3$ (*Left panel*) and the $(\alpha4^{776insL})_2(\beta2)_3$ (*Right panel*) receptors. ACh concentration-response data were fitted with the sigmoidal equation under the constraint of equal slopes (nHill = 1) in order to estimate the horizontal distance between the curves as a potency ratio (estimated parameters are shown in Table 5.2). The data were best fitted to a single sigmoidal equation ($p < 0.001$, F test, n = 8 – 10).

Tabke 5.2. Effects of TM2 L9'T mutation on the functional effects of ACh on wild type and mutant $(\alpha4)_2(\beta2)_3$ and $(\alpha4)_3(\beta2)_2$ receptors

	$(\alpha4)_2(\beta2)_3$			$(\alpha4)_3(\beta2)_2$		
	Potency ratio	$^3\sqrt{}$	$^2\sqrt{}$	Potency ratio	$^3\sqrt{}$	$^2\sqrt{}$
$\alpha4\beta2$ w.t./$\alpha4\beta2^{LT}$	18 / 4.2	2.7		465/60		7.7
$\alpha4^{776insL}/\alpha4776^{insL}\beta2^{LT}$	36	3.3	6	8	2	2.8

EC_{50} are the means of EC_{50} estimates obtained by fitting separately each concentration-response curve with a one-component sigmoidal equation, which gave the best fit for all data sets. Potency ratios were calculated from fits in which curves were constrained to slope equal to 1. Values represent data from three to six experiments (n).

5.3.7 Expression of the $\alpha4^{776insL}$ mutation in concatenated $(\alpha4)_2(\beta2)_3$ and $(\alpha4)_3(\beta2)_2$ receptors

A more reliable approach to analyse the effect of the mutation on the stoichiometry of the receptor is the use of concatamers. The mutation has been inserted in all the α4 subunits of the pentameric constructs, thus producing $(\alpha4^{776insL})_3(\beta2)_2$ concatenated

receptors containing three mutations and $(\alpha4^{776insL})_2(\beta2)_3$ concatenated receptors containing two mutations.

The presence of three mutations in the $(\alpha4^{776insL})_3(\beta2)_2$ receptor induced a marked decrease in the level of current from 2200 ± 170 nA in the wild type concatenated receptor to 45 ± 5 nA in the triple mutant concatamer ($p < 0.05$; Student's t test, n = 6) (Fig. 5.8, *Right*). This suggests that the presence of three mutations deeply affects the expression of functional receptors. In contrast, the mutation did not significantly affect the level of current of the concatenated $(\alpha4)_2(\beta2)_3$ receptor (130 ± 40 nA in the wild type receptor; 170 ± 25 nA in the $(\alpha4^{776insL})_2(\beta2)_3$ concatamer; n = 8) (Fig. 5.8, *Left*), suggesting that a receptor containing two mutations is efficiently assembled and trafficked to the membrane.

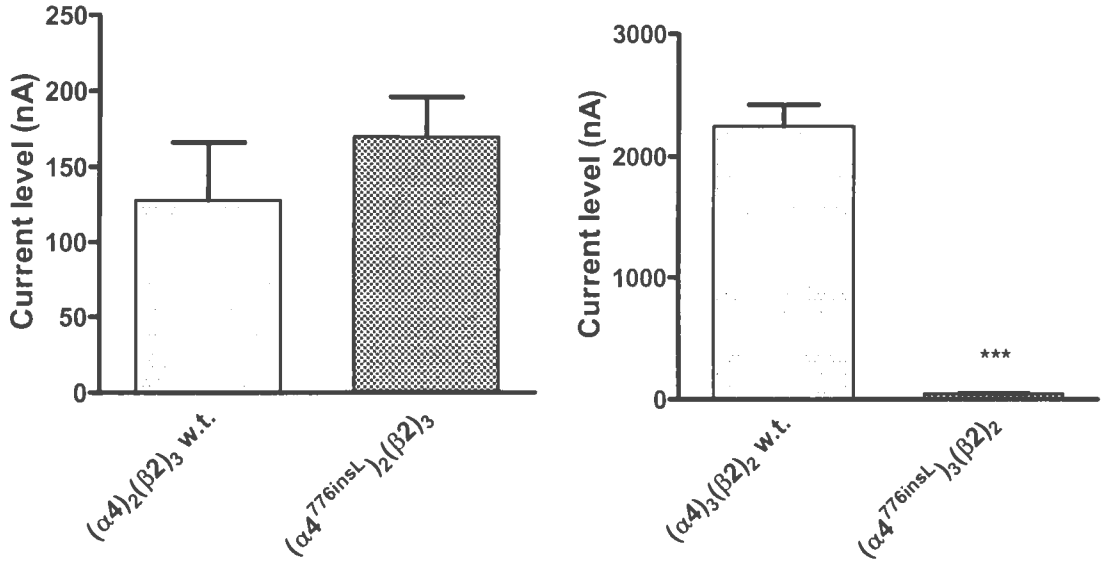

Fig. 5.8. Expression level of concatenated $(\alpha4^{776insL})_2(\beta2)_3$ and $(\alpha4^{776insL})_3(\beta2)_2$ receptors in *Xenopus* oocytes. Bar graph comparing the functional expression levels of mutant and wild type $(\alpha4)_2(\beta2)_3$ (*Left*) and $(\alpha4)_2(\beta2)_3$ (*Right*) concatenated receptors. The amplitude of the current responses elicited by maximal concentrations of ACh were 170 ± 25 nA for the mutant concatenated $(\alpha4)_2(\beta2)_3$ and 130 ± 40 nA for wild type $(\alpha4)_2(\beta2)_3$ (*Left panel*). At the $(\alpha4)_3(\beta2)_2$ (*Right panel*) receptor the maximal ACh-elicited current was 45 ± 5 for mutant receptors versus 2200 ± 170 for wild type receptors. (*** = $p < 0.001$; Student's t test)

ACh concentration-response curves for mutant and wild type concatenated receptors were then determined. For both receptors data were fitted to a one-component Hill equation with an of EC_{50} of 8.3 ± 1.5 μM for the $(\alpha4^{776insL})_2(\beta2)_3$ concatamer and 2.37 ± 2 μM for the wild type $(\alpha4)_2(\beta2)_3$ concatamer ($p < 0.01$, Student's t test, n = 7) and a nHill of 0.62 ± 0.1 for the mutant concatenated receptor and 1.04 ± 0.06 for the wild type receptor ($p < 0.0001$, Student's t test, n = 7) (Fig. 5.9, *Left*). These data are not significantly different from that of the non-linked $(\alpha4^{776insL})_2(\beta2)_3$ receptor (8.1 ± 2.2 μM

and 0.59 ± 005) (see Section 4.3). At the $(\alpha4)_2(\beta2)_3$ receptor ACh concentration-response curves indicated that the insertion of three mutations had little effect on agonist parameters with an EC_{50} of 145 ± 8 μM and a Hill coefficient of 0.9 ± 0.2 (n = 6) for the mutant concatamer as compared with the wild type concatamer with an EC_{50} of 110 ± 5 μM and a Hill coefficient of 0.92 ± 0.09 (n = 9) (Fig. 5.9, *Right*). These values were significantly different from those observed for the non-linked mutant ($p < 0.01$, Student's t test, n = 6 - 7) (see Section 5.3) suggesting that the mutation affects the stoichiometry of the receptor.

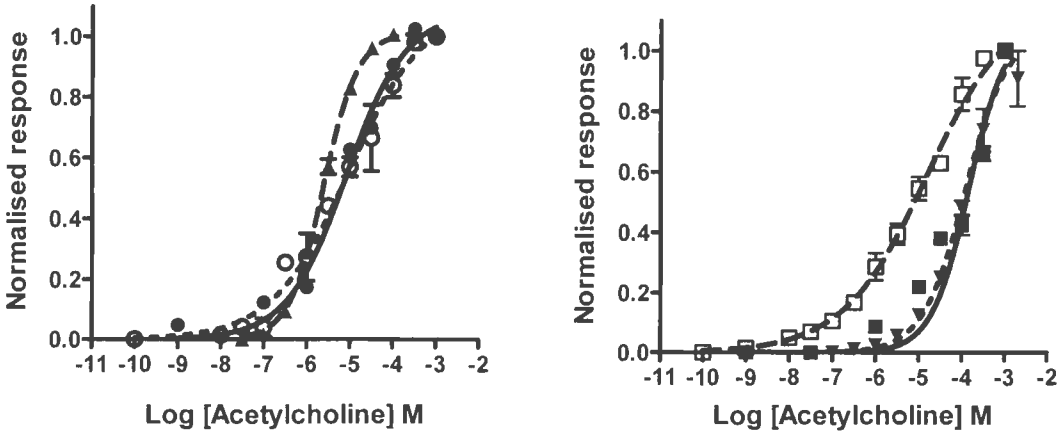

Fig. 5.9. ACh concentration-response curves for concatenated $\alpha4^{776insL}\beta2$ receptors. The *Left panel* shows ACh concentration-response curve for mutant $(\alpha4^{776insL})_2(\beta2)_3$ concatenated receptors (●) and wild type $(\alpha4)_2(\beta2)_3$ concatamers (dashed line, ▲).Curves obtained from non-linked $(\alpha4^{776insL})_2(\beta2)_3$ receptor shown for comparison (dashed line, ○) The *Right panel* shows ACh dose-response curves for concatenated $(\alpha4^{776insL})_3(\beta2)_2$ (■) and wild type $(\alpha4)_3(\beta2)_2$ concatamers (dashed line, ▼). Curves obtained from non-linked $(\alpha4^{776insL})_3(\beta2)_2$ receptor shown for comparison (dashed line, □). The data were best fitted by a one-component sigmoidal equation ($p < 0.0001$, F test, n = 4 - 7).

DISCUSSION

The functional effect of $\alpha4^{776insL}$ on heterologously expressed α4β2 nAChRs has been extensively characterised by several groups. However, most of these studies were carried out in systems expressing a mixture of α4β2 receptors with different stoichiometries (Steinlein *et al.*, 1997; Bertrand *et al.*, 1998; Figl *et al.*, 1998; Rodrigues-Pinguet *et al.*, 2003; Rodrigues-Pinguet *et al.*, 2005). Because α4 and β2 assemble in alternate forms in heterologous systems (Zwart and Vijverberg, 1998; Nelson *et al.*, 2003; Kuryatov *et al.*, 2005; Moroni *et al.*, 2006), which might exist in native tissues (Gotti *et al.* 2008), the study described in this chapter were primarily undertaken to investigate possible stoichiometry-selective effects of $\alpha4^{776insL}$.

One of the most important findings of this study is that $\alpha4^{776insL}$ affects the function of the two alternate forms of the α4β2 receptor differentially. The mutation impacted the agonist sensitivity, desensitisation and Ca^{2+} permeability of $(\alpha4)_3(\beta2)_2$ nAChRs, whereas it only modified, markedly, the desensitisation of $(\alpha4)_2(\beta2)_3$ receptors. The differential effects of the $\alpha4^{776insL}$ mutation on the alternate forms of the α4β2 nAChR can therefore explain why some authors found that $\alpha4^{776insL}$ causes changes in agonist sensitivity and current decay (Steinlein *et al.*, 1997; Bertrand *et al.*, 1998; Lipovsek *et al.*, 2008), whereas others reported no changes in these properties (Figl *et al.*, 1998). As it has been extensively reported in the last 10 years, transfection of expression systems with equal amounts of α4 and β2 cDNAs or cRNAs results in the expression of a variety of different subunit combinations, each with different pharmacological properties (Zwart and Vijverberg, 1998, Buisson and Bertrand, 2001; Houlihan *et al.*, 2001; Nelson *et al.*, 2003; Lopez-Hernandez *et al.*, 2004; Kuryatov *et al.*, 2005; Moroni *et al.*, 2006). Thus, it is most likely that previous studies characterised the effect of $\alpha4^{776insL}$ on a mixed population of α4β2 nAChRs.

Desensitisation was the most affected parameter in both the $(\alpha4)_2(\beta2)_3$ and the $(\alpha4)_3(\beta2)_2$ receptors. Both mutant receptors showed a significant increase in the peak-plateau current, suggesting that the gating equilibrium must be displaced in favour of the desensitised state. The $\alpha4^{776insL}$ mutation also induced an increase in the apparent time constant of desensitisation in both stoichiometries. Moreover, the mutant $(\alpha4)_2(\beta2)_3$ receptor displayed a fast component of desensitisation followed by a slower component, whereas the mutant $(\alpha4)_3(\beta2)_2$ receptor only displayed a slow desensitisation component. The effect of the mutation on the desensitisation properties of the receptor might be one of the main determinants for the dysfunction that causes the epileptic seizures. If the mutant receptors desensitise more rapidly and to a greater extent, as the neurotransmitter

accumulates in the synaptic cleft, excessive desensitisation of receptors occurs. The decreased function of mutant nAChRs may influence other inhibitory pathways such as those mediated by $GABA_A$ receptor (Lena *et al.*, 1993) and could therefore lead to abnormal high frequency spike discharges. High frequency discharges of thalamo-cortical volleys, particular to the frontal lobes, are observed during sleep and could explain the linkage between the sleep and the epileptic syndrome.

The $\alpha4^{776insL}$ mutation changed the ACh sensitivity and Ca^{2+} permeability of $(\alpha4)_3(\beta2)_2$ but not those of $(\alpha4)_2(\beta2)_3$. This implies that if these receptor properties are responsible for seizures in $\alpha4^{776insL}$-linked ADNFLE, then the receptor that mediates this disease is the $(\alpha4)_3(\beta2)_2$ receptor. How could these changes lead to seizures? Changes in agonist potency because of mutations in the channel pore are thought to result from changes in channel gating increasing the probability of transition to the active state (Bertrand *et al.*, 1998; Filatov and White, 1995). The gain of function of the receptor based on the increased ACh sensitivity could not entirely explain the nature of epileptic seizures. If central cholinergic nerve terminals release nearly saturating ACh concentrations (as other types of synapses apparently do (reviewed in Clements, 1996), then increasing the ACh sensitivity of α4β2 nAChRs may only slightly increase the amplitude of nicotinic synaptic potentials. However, in the case of volume transmission (Wonnacott, 1997), which might be the predominant form of transmission by cholinergic neurones in the brain, increased ACh sensitivity could impact significantly the amplitude of nicotinic receptors signals. The presence of low Ca^{2+} permeable receptors only could contribute to ADNFLE seizures with two mechanisms: 1) the reduced function of the mutant receptors could reduce the α4β2-mediated inhibitory transmitter release in the cortex (McNamara, 1999); 2) the reduced Ca^{2+} permeability could shift the balance between α4β2-mediated excitatory and inhibitory neurotransmitter release during bouts of high-frequency cortical synaptic activity, in favour of excitatory transmitter release (Rodrigues-Pinguet *et al.*, 2003).

$\alpha4^{776insL}$ increased the functional expression of $(\alpha4)_2(\beta2)_3$ receptors but decreased that of $(\alpha4)_3(\beta2)_2$. Western blot analysis showed that when the receptors expressed were of the $(\alpha4)_2(\beta2)_3$ type the steady state level of α4 and β2 was increased relative to those seen with the corresponding wild type receptors. This immunoblotting profile is in agreement with the increase in functional expression observed for $\alpha4^{776insL}$ mutant $(\alpha4)_2(\beta2)_3$ receptors. Why would a mutation in the α4 subunit change the steady state level of the β2 subunit? The step-by-step details of how α4β2 nAChRs are assembled is not known. However, recent studies on the effects of chronic exposure to nicotine indicated that the

subunits assemble together into various types of intermediaries as they are synthesised (Kuryatov *et al.*, 2005; Sallette *et al.*, 2005). Thus, if α4 and β2 subunits are mostly present as assembled subunits, then changes in the half-life of one subunit may influence the steady state levels of the other one. An increase in the stability of assembled subunits would lead to an increase in receptor maturation and trafficking, all of which would subsequently lead to higher expression levels. Surprisingly, in comparison to mutant $(\alpha4)_2(\beta2)_3$ receptors, when the receptors expressed were of the $(\alpha4)_3(\beta2)_2$ type immunoblotting assays revealed a decrease in the steady state levels of α4 subunit with no apparent changes in β2 levels and this finding correlates well with the lower functional expression observed for mutant $(\alpha4)_3(\beta2)_2$ receptors. How could the relative availability of subunits affect the pattern of changes in subunit steady state levels caused by $\alpha4^{776insL}$? The different patterns of subunit steady state levels suggest that the assembly of both forms of the α4β2 is handle differently. In the case of the genesis of $(\alpha4)_3(\beta2)_2$ intermediaries with more than one α4 subunit may predominate and the stability of these may be detrimentally affected by the presence of the $\alpha4^{776insL}$ mutation. An obvious consequence of changes in the turnover of receptor intermediaries is changes in the subunit composition of the receptors assembled. A well know example of how changes in turnover time of subunits and receptor intermediaries affect the type of mature receptors expressed is that of the effects of chronic exposure to nicotine. Chronic exposure to nicotine up-regulates the number of high sensitivity α4β2 nAChRs trafficked to the cell surface and this occurs because nicotine stabilises intermediaries that favour the expression of this receptor type (Corringer *et al.*, 2006).

The findings that $\alpha4^{776insL}$ may alter the subunit composition of α4β2 receptors agrees with recent studies by Son *et al.* (2009). In this study it was shown that some ADNFLE-linked mutations, included the one analysed in the present study, increase the expression $(\alpha4)_3(\beta2)_2$ receptors and decrease the expression of the$(\alpha4)_2(\beta2)_3$ stoichiometry. The authors came to this conclusion after having analysed FRET efficiency of mutant receptors in N2A cells. However, FRET analysis only measures intracellular receptor levels without giving any information on surface receptors. It could therefore be possible that the mutant receptors are assembled but they are not trafficked properly to the membrane, thus accumulating in the intracellular space. Also, as stated by the same authors, due to the low level of expression of α4β2 receptors in N2A cells no functional analysis was done, therefore they have no information about the properties of the receptors expressed on the membrane.

To test the stoichiometry-change hypothesis the L9'T mutation was used as a reporter mutation to monitor changes in subunit composition of the surface mutant receptors. Insertion of the L9'T mutation in the β2 subunit of the mutant receptors shifted the ACh dose-response curve as expected but the extent of the shift was not the expected one for a receptor containing three α4 subunits. The shift in the EC_{50} values was in fact more compatible with a higher β2 content in both mutant receptors. However, as already mentioned before, the presence of another mutation in the channel pore domain, might alter the effect of the L9'T mutation on the receptor. Therefore, these findings need to be taken cautiously.

An unambiguous way of studying the effects of mutations on receptor stoichiometry is the use of concatenated receptors. Analysis of the functional properties of $(\alpha4)_3(\beta2)_2$ concatamers containing three mutations showed that the expression of this receptor is problematic, probably because the mutation destabilised the receptor which is therefore not trafficked to the cell surface. In contrast, good levels of expression were achieved after injection of concatenated $(\alpha4)_2(\beta2)_3$ receptors containing two mutations, suggesting that the receptors are stable and that they are trafficked efficiently to the membrane. Analysis of the ACh concentration-response curve of the mutant concatenated receptors clarified the effect of the $\alpha4^{776insL}$ mutation on the stoichiometry of the α4β2 receptor. The EC_{50} of the $(\alpha4)_3(\beta2)_2$ mutant concatamers was not significantly different from the wild type value, suggesting that a receptor with a stoichiometry of $(\alpha4)_3(\beta2)_2$ containing three mutations does not display a high sensitivity behaviour, as observed in the non-linked receptor. The high sensitivity-like properties observed in the mutant non-linked receptor could arise from a change in receptor stoichiometry. This suggestion is supported by the results obtained with the mutant $(\alpha4)_2(\beta2)_3$ concatamer, whose properties were found to be similar to those of the non-linked mutant receptor. A receptor with a stoichiometry of $(\alpha4)_2(\beta2)_3$ containing two mutations displays mutant-like properties, suggesting that the stoichiometry is not altered by the presence of the mutation. However, the non-linked receptors expressed with the extreme injection ratio strategy display some differences in their functional properties (desensitisation and agonist efficacy) suggesting the presence of other stoichiometries. It will be therefore incorrect to say that the mutation shifts the stoichiometry of the receptor from $(\alpha4)_3(\beta2)_2$ to $(\alpha4)_2(\beta2)_3$ in a discrete way. It is more likely that the presence of a mutated α4 subunit biases the subunit composition of the receptor toward a higher β2 content.

This study has shown that ADFNLE mutations affect the alternate forms of the α4β2 receptors differentially. This is important for unravelling the mechanisms underlying the pathophysiology of the disease and also for designing more effective therapeutic strategies. Moreover, given the focal nature of ADNFLE, it might help to understand the subunit composition of the α4β2 receptor not only in the region involved in the epileptic seizures but also in other brain regions. ADNFLE seizures involve thalamo-cortical circuits during sleep. In light of the results presented in this Chapter, it could be suggested that the thalamus has a higher content of $(\alpha4)_3(\beta2)_2$ receptors and it is therefore the most affected area in patients who present ADNFLE-linked mutations. A higher $(\alpha4)_2(\beta2)_3$ receptor content in the other regions might explain why most of the ADNFLE patients do not show any other brain disorder.

FINAL DISCUSSION

The aim of this study was to engineer functional pentameric concatenated $(\alpha4)_2(\beta2)_3$ and $(\alpha4)_3(\beta2)_2$ nAChRs to investigate the functional differences between the two alternate stoichiometries of the α4β2 nAChR. The α4β2 is the most abundant nAChR present in the human brain and its role in physiological and pathological processes is well documented. As shown by several studies, α4 and β2 subunits expressed heterologously assemble into two alternate stoichiometries of the α4β2 nAChR that differ markedly in their functional and pharmacological profile. There is increasing evidence that both forms of the α4β2 receptor exist in neurones and that the ratio between them may impact brain functions, or pathologies, influenced by α4β2 receptors (Kim *et al.*, 2003). Thus, the design of stoichiometry-specific drugs should make it easier to unravel the mechanisms by which this receptor type influence brain functions and would lead to safer and more efficacious drugs. The availability of functional concatenated $(\alpha4)_2(\beta2)_3$ and $(\alpha4)_3(\beta2)_2$ nAChRs should make these tasks easier.

Investigation of the functional and pharmacological properties of concatenated receptors confirmed that the strategies used so far to study the functional properties of a given form of the α4β2 receptor have not solved completely the problem of the expression of multiple receptor forms. As shown in Chapter 3, the presence of a small receptor contamination is clearly visible when comparing the response of linked and non-linked receptors to highly selective compounds, such as TC2559 and 5I-A85380. In contrast, as shown in this study, pentameric concatenated receptors proved to be the ideal tool for the expression of homogenous populations of receptors.

Another important implication of this study is that it provides a tool to express receptors with fixed stoichiometry. The expression of heteromeric proteins in heterologous systems cannot be fully controlled and the subunit composition of the protein may vary for many reasons (e.g., temperature, subunit availability) (Nelson *et al.*, 2003; Lopez-Hernandez *et al.*, 2005; Moroni *et al.*, 2006). The presence of more than one type of stoichiometry often leads to erroneous conclusions. A well-known example is that of the actions of the agonist sazetidine-A on α4β2 receptors. Sazetidine-A was recently reported to bind selectively and with high-affinity to α4β2 nAChRs (Xiao *et al.*, 2006). The functional properties described for this compound were unusual. It was reported that sazetidine-A desensitized α4β2 receptors expressed heterologously in SHEP-1 cells without activating them. However, studies of native α4β2 receptors showed that sazetidine-A acted as a conventional agonist of this receptor type (Xiao *et al.*, 2007; Cucchiaro *et al.*, 2008). These conflicting findings were solved by recent studies that used the drastic 1:10

or 10:1 α4/β2 ratios to express enriched populations of $(\alpha4)_2(\beta2)_3$ or $(\alpha4)_3(\beta2)_2$ nAChRs, respectively (Zwart *et al.*, 2008). This study clearly showed that sazetidine-A has a very low efficacy at $(\alpha4)_3(\beta2)_2$ nAChRs but behaves as a full agonist at $(\alpha4)_2(\beta2)_3$ nAChRs. The mistake of Xiao *et al.* (2006) stemmed directly from the fact that SHEP-1 cells transfected with α4 and β2 subunits express a mixed population of $(\alpha4)_2(\beta2)_3$ and $(\alpha4)_3(\beta2)_2$ nAChRs, which is highly enriched in $(\alpha4)_3(\beta2)_2$ nAChRs, the receptor subtype at which sazetidine A displays poor efficacy.

The reasons for the functional and pharmacological differences between the $(\alpha4)_2(\beta2)_3$ and $(\alpha4)_3(\beta2)_2$ nAChRs are not clear. The distinct functional pharmacology of $(\alpha4)_2(\beta2)_3$ and $(\alpha4)_3(\beta2)_2$ nAChRs might reflect variations in the environment around the two functional ACh binding sites, which are located interfaces between α4 and β2 subunits (Corringer *et al.*, 2000). On both stoichiometries, the agonist sites are both located at the α4(+)/β2(-) interfaces and are thought to contribute equally to agonist binding. However, this may not be so, because of the two binding sites only one is flanked by non-ACh binding β2(+)/α4(-) interfaces on both stoichiometries whereas the other site is flanked by a β2(+)/α4(-) interface and a β2(+)/β2(-) in the $(\alpha4)_2(\beta2)_3$ stoichiometry or a α4(+)/α4(-) interface in the $(\alpha4)_3(\beta2)_2$ stoichiometry. The latter interfaces might confer stoichiometry-specific properties to the receptors, as recently shown for Zn^{2+} modulation (Moroni *et al.*, 2008). Alternatively, residues located at the β2(+)/β2(-), α4(+)/α4(-) or β2(+)/α4(-) interfaces may form additional binding sites that when bound do not activate the protein but modify the properties of the 'classic' ACh binding pocket. Even though there is no evidence that ACh binds any of these interfaces, other allosteric modulators, such as galanthamine (Hansen *et al.* 2007), have been shown to modulate the function of nicotinic receptors by binding non-ACh binding interfaces. These sites represent potential therapeutic targets and will likely prove useful in developing subtype-selective compounds for studying receptor subtypes assembly and localisation. All these questions can now be addressed by using concatenated $(\alpha4)_2(\beta2)_3$ and $(\alpha4)_3(\beta2)_2$ nAChRs. The identification of the role of each subunit in the pentameric concatenated receptors will allow the investigations of the contribution of each binding site to agonist binding as well as investigation of the role of the non-agonist binding interfaces in the two alternate stoichiometries of the α4β2 nAChR.

The functional differences between the $(\alpha4)_2(\beta2)_3$ and $(\alpha4)_3(\beta2)_2$ stoichiometries might lead, as a consequence, to a different involvement of the two receptors in α4β2-linked diseases. This was shown to be true in ADNFLE, where the two stoichiometries are

differentially affected by a specific ADNFLE-linked mutation. The use of concatenated receptors in this study was essential to clarify the changes induced by the mutation in the two alternate forms and that might cause seizures. Given the focal nature of this disease, the finding that some ADNFLE-linked mutations alter the subunit composition of α4β2 nAChRs can help to understand the distribution of the two stoichiometries in specific brain areas. Because the $(\alpha4)_3(\beta2)_2$ stoichiometry is more affected by ADNFLE mutations than the $(\alpha4)_2(\beta2)_3$ stoichiometry and because seizures seem to originate in the thalamus, one might conclude that this region is richer in $(\alpha4)_3(\beta2)_2$ receptors than in $(\alpha4)_2(\beta2)_3$ receptors.

The results obtained in these studies strongly demonstrate that concatenated $(\alpha4)_2(\beta2)_3$ and $(\alpha4)_3(\beta2)_2$ receptors not only can be employed for a finer and more detailed dissection of receptor properties and architecture and for the design of stoichiometry-specific drugs but that they also provide the pharmacological tools for the identification of the α4β2 subunit arrangement present in neurones. There is, however, one problem that needs to be solved for concatenated receptors to realise their full potential. In comparison to receptors assembled from free subunits, concatenated receptors have poor levels of functional expression (Baur *et al.*, 2006; this study). Undoubtedly, the size of the constructs must operate against efficacious transcription, protein synthesis, receptor assembly and trafficking to the cell surface. One possible way to minimize low transcription or translation is to improve the quality of the codons of the cDNAs. The tremendous development in recombinant protein expression that have occurred in the last 10 years have highlighted that codon usage (frequency of codons in host cells), GC content, *cis* elements and repeated sequences determine how efficiently proteins are expressed in expression systems. Perhaps, optimisation of the sequences of α4 and β2 cDNAs should aid to increase the functional expression of the concatenated constructs described in this study.

References

Absalom, N. L., T. M. Lewis, *et al.* (2003). "Role of charged residues in coupling ligand binding and channel activation in the extracellular domain of the glycine receptor." J Biol Chem **278**(50): 50151-7.

Adem, A., S. S. Jossan, *et al.* (1988). "Distribution of nicotinic receptors in human thalamus as visualized by 3H-nicotine and 3H-acetylcholine receptor autoradiography." J Neural Transm **73**(1): 77-83.

Adem, A., B. Synnergren, *et al.* (1987). "[3H]acetylcholine nicotinic recognition sites in human brain: characterization of agonist binding." Neurosci Lett **83**(3): 298-302.

Akk, G. (2001). "Aromatics at the murine nicotinic receptor agonist binding site: mutational analysis of the alphaY93 and alphaW149 residues." J Physiol **535**(Pt 3): 729-40.

Akk, G. and A. Auerbach (1999). "Activation of muscle nicotinic acetylcholine receptor channels by nicotinic and muscarinic agonists." Br J Pharmacol **128**(7): 1467-76.

Akk, G. and J. H. Steinbach (2000). "Structural elements near the C-terminus are responsible for changes in nicotinic receptor gating kinetics following patch excision." J Physiol **527 Pt 3**: 405-17.

Albuquerque, E. X., E. F. Pereira, *et al.* (1996). "Nicotinic acetylcholine receptors on hippocampal neurons: cell compartment-specific expression and modulatory control of channel activity." Prog Brain Res **109**: 111-24.

Albuquerque, E. X., E. F. Pereira, *et al.* (1998). "Neuronal nicotinic receptors modulate synaptic function in the hippocampus and are sensitive to blockade by the convulsant strychnine and by the anti-Parkinson drug amantadine." Toxicol Lett **102-103**: 211-8.

Alkondon, M., E. F. Pereira, *et al.* (1996). "Mapping the location of functional nicotinic and gamma-aminobutyric acidA receptors on hippocampal neurons." J Pharmacol Exp Ther **279**(3): 1491-506.

Alkondon, M., E. F. Pereira, *et al.* (1998). "Alpha-bungarotoxin- and methyllycaconitine-sensitive nicotinic receptors mediate fast synaptic transmission in interneurons of rat hippocampal slices." Brain Res **810**(1-2): 257-63.

Alkondon, M., E. F. Pereira, *et al.* (1997). "Neuronal nicotinic acetylcholine receptor activation modulates gamma-aminobutyric acid release from CA1 neurons of rat hippocampal slices." J Pharmacol Exp Ther **283**(3): 1396-411.

Alkondon, M., E. F. Pereira, *et al.* (1992). "Blockade of nicotinic currents in hippocampal neurons defines methyllycaconitine as a potent and specific receptor antagonist." Mol Pharmacol **41**(4): 802-8.

Altschuler, E. L., N. V. Hud, *et al.* (1997). "Random coil conformation for extended polyglutamine stretches in aqueous soluble monomeric peptides." J Pept Res **50**(1): 73-5.

Anand, R., W. G. Conroy, *et al.* (1991). "Neuronal nicotinic acetylcholine receptors expressed in *Xenopus* oocytes have a pentameric quaternary structure." J Biol Chem **266**(17): 11192-8.

Arias, H. R. (1997). "Topology of ligand binding sites on the nicotinic acetylcholine receptor." Brain Res Brain Res Rev **25**(2): 133-91.

Arias, H. R. (2000). "Localization of agonist and competitive antagonist binding sites on nicotinic acetylcholine receptors." Neurochem Int **36**(7): 595-645.

Ascher, P., W. A. Large, *et al.* (1979). "Studies on the mechanism of action of acetylcholine antagonists on rat parasympathetic ganglion cells." J Physiol **295**: 139-70.

Aubert, I., D. M. Araujo, *et al.* (1992). "Comparative alterations of nicotinic and muscarinic binding sites in Alzheimer's and Parkinson's diseases." J Neurochem **58**(2): 529-41.

Auerbach, A. (2005). "Gating of acetylcholine receptor channels: Brownian motion across a broad transition state." Proc Natl Acad Sci USA **102**(5): 1408-12.

Auerbach, A., W. Sigurdson, *et al.* (1996). "Voltage dependence of mouse acetylcholine receptor gating: different charge movements in di-, mono- and unliganded receptors." J Physiol **494 (Pt 1)**: 155-70.

Badio, B., H. M. Garraffo, *et al.* (1997). "Pseudophrynaminol: a potent noncompetitive blocker of nicotinic receptor-channels." Biochem Pharmacol **53**(5): 671-6.

Bafna, P. A., A. Jha, *et al.* (2009). "Aromatic residues εTrp-55 and δTrp-57 and the activation of acetylcholine receptor channels." J Biol Chem **284**(13): 8582-8.

Barish, M. E. (1983). "A transient calcium-dependent chloride current in the immature *Xenopus* oocyte." J Physiol **342**: 309-25.

Baumann, S. W., R. Baur, *et al.* (2001). "Subunit arrangement of gamma-aminobutyric acid type A receptors." J Biol Chem **276**(39): 36275-80.

Baumann, S. W., R. Baur, *et al.* (2002). "Forced subunit assembly in alpha1beta2gamma2 GABAA receptors. Insight into the absolute arrangement." J Biol Chem **277**(48): 46020-5.

Baumann, S. W., R. Baur, *et al.* (2003). "Individual properties of the two functional agonist sites in GABA(A) receptors." J Neurosci **23**(35): 11158-66.

Baur, R., F. Minier, *et al.* (2006). "A GABA(A) receptor of defined subunit composition and positioning: concatenation of five subunits." FEBS Lett **580**(6): 1616-20.

Baur, R. and E. Sigel (2005). "Benzodiazepines affect channel opening of GABA A receptors induced by either agonist binding site." Mol Pharmacol **67**(4): 1005-8.

Beato, M., P. J. Groot-Kormelink, *et al.* (2002). "Openings of the rat recombinant alpha 1 homomeric glycine receptor as a function of the number of agonist molecules bound." J Gen Physiol **119**(5): 443-66.

Beck, C., B. Moulard, *et al.* (1994). "A nonsense mutation in the alpha4 subunit of the nicotinic acetylcholine receptor (CHRNA4) cosegregates with 20q-linked benign neonatal familial convulsions (EBNI)." Neurobiol Dis **1**(1-2): 95-9.

Beckstein, O. and M. S. Sansom (2006). "A hydrophobic gate in an ion channel: the closed state of the nicotinic acetylcholine receptor." Phys Biol **3**(2): 147-59.

Bencherif, M. and R. J. Lukas (1993). "Cytochalasin modulation of nicotinic cholinergic receptor expression and muscarinic receptor function in human TE671/RD cells: a possible functional role of the cytoskeleton." J Neurochem **61**(3): 852-64.

Benwell, M. E., D. J. Balfour, *et al.* (1988). "Evidence that tobacco smoking increases the density of (-)-[3H]nicotine binding sites in human brain." J Neurochem **50**(4): 1243-7.

Bertrand, D., F. Elmslie, *et al.* (2005). "The CHRNB2 mutation I312M is associated with epilepsy and distinct memory deficits." Neurobiol Dis **20**(3): 799-804.

Bertrand, D., J. L. Galzi, *et al.* (1993). "Mutations at two distinct sites within the channel domain M2 alter calcium permeability of neuronal alpha 7 nicotinic receptor." Proc Natl Acad Sci USA **90**(15): 6971-5.

Bertrand, D., F. Picard, *et al.* (2002). "How mutations in the nAChRs can cause ADNFLE epilepsy." Epilepsia **43 Suppl 5**: 112-22.

Bertrand, D., S. Valera, *et al.* (1991). "Steroids inhibit nicotinic acetylcholine receptors." Neuroreport **2**(5): 277-80.

Bertrand, S., S. Weiland, *et al.* (1998). "Properties of neuronal nicotinic acetylcholine receptor mutants from humans suffering from autosomal dominant nocturnal frontal lobe epilepsy." Br J Pharmacol **125**(4): 751-60.

Blaha, C. D., L. F. Allen, *et al.* (1996). "Modulation of dopamine efflux in the nucleus accumbens after cholinergic stimulation of the ventral tegmental area in intact, pedunculopontine tegmental nucleus-lesioned, and laterodorsal tegmental nucleus-lesioned rats." J Neurosci **16**(2): 714-22.

Blount, P. and J. P. Merlie (1989). "Molecular basis of the two nonequivalent ligand binding sites of the muscle nicotinic acetylcholine receptor." Neuron **3**(3): 349-57.

Blount, P. and J. P. Merlie (1990). "Mutational analysis of muscle nicotinic acetylcholine receptor subunit assembly." J Cell Biol **111**(6 Pt 1): 2613-22.

Blount, P., M. M. Smith, *et al.* (1990). "Assembly intermediates of the mouse muscle nicotinic acetylcholine receptor in stably transfected fibroblasts." J Cell Biol **111**(6 Pt 1): 2601-11.

Bocquet, N., H. Nury, *et al.* (2009). "X-ray structure of a pentameric ligand-gated ion channel in an apparently open conformation." Nature **457**(7225): 111-4.

Bohler, S., S. Gay, *et al.* (2001). "Desensitization of neuronal nicotinic acetylcholine receptors conferred by N-terminal segments of the beta 2 subunit." Biochemistry **40**(7): 2066-74.

Boileau, A. J., R. A. Pearce, *et al.* (2005). "Tandem subunits effectively constrain GABAA receptor stoichiometry and recapitulate receptor kinetics but are insensitive to GABAA receptor-associated protein." J Neurosci **25**(49): 11219-30.

Bollan, K. A., R. Baur, *et al.* (2008). "The promiscuous role of the epsilon subunit in GABAA receptor biogenesis." Mol Cell Neurosci **37**(3): 610-21.

Boorman, J. P., P. J. Groot-Kormelink, *et al.* (2000). "Stoichiometry of human recombinant neuronal nicotinic receptors containing the b3 subunit expressed in *Xenopus* oocytes." J Physiol **529 Pt 3**: 565-77.

Boulter, J., J. Connolly, *et al.* (1987). "Functional expression of two neuronal nicotinic acetylcholine receptors from cDNA clones identifies a gene family." Proc Natl Acad Sci USA **84**(21): 7763-7.

Bouzat, C., F. Gumilar, *et al.* (2002). "Subunit-selective contribution to channel gating of the M4 domain of the nicotinic receptor." Biophys J **82**(4): 1920-9.

Bouzat, C., F. Gumilar, *et al.* (2004). "Coupling of agonist binding to channel gating in an ACh-binding protein linked to an ion channel." Nature **430**(7002): 896-900.

Breese, C. R., C. Adams, *et al.* (1997a). "Comparison of the regional expression of nicotinic acetylcholine receptor alpha7 mRNA and [125I]-alpha-bungarotoxin binding in human postmortem brain." J Comp Neurol **387**(3): 385-98.

Breese, C. R., M. J. Marks, *et al.* (1997b). "Effect of smoking history on [3H]nicotine binding in human postmortem brain." J Pharmacol Exp Ther **282**(1): 7-13.

Brejc, K., W. J. van Dijk, *et al.* (2001). "Crystal structure of an ACh-binding protein reveals the ligand-binding domain of nicotinic receptors." Nature **411**(6835): 269-76.

Briggs, C. A., E. J. Gubbins, *et al.* (2006). "Untranslated region-dependent exclusive expression of high-sensitivity subforms of alpha4beta2 and alpha3beta2 nicotinic acetylcholine receptors." Mol Pharmacol **70**(1): 227-40.

Broad, L. M., R. Zwart, *et al.* (2006). "Identification and pharmacological profile of a new class of selective nicotinic acetylcholine receptor potentiators." J Pharmacol Exp Ther **318**(3): 1108-17.

Broadbent, S., P. J. Groot-Kormelink, *et al.* (2006). "Incorporation of the beta3 subunit has a dominant-negative effect on the function of recombinant central-type neuronal nicotinic receptors." Mol Pharmacol **70**(4): 1350-7.

Brodtkorb, E. and F. Picard (2006). "Tobacco habits modulate autosomal dominant nocturnal frontal lobe epilepsy." Epilepsy Behav **9**(3): 515-20.

Broide, R. S. and F. M. Leslie (1999). "The alpha7 nicotinic acetylcholine receptor in neuronal plasticity." Mol Neurobiol **20**(1): 1-16.

Bruggmann, D., K. S. Lips, *et al.* (2003). "Rat arteries contain multiple nicotinic acetylcholine receptor alpha-subunits." Life Sci **72**(18-19): 2095-9.

Buisson, B. and D. Bertrand (2001). "Chronic exposure to nicotine upregulates the human (alpha)4((beta)2 nicotinic acetylcholine receptor function." J Neurosci **21**(6): 1819-29.

Buisson, B. and D. Bertrand (2002). "Nicotine addiction: the possible role of functional upregulation." Trends Pharmacol Sci **23**(3): 130-6.

Burghaus, L., U. Schutz, *et al.* (2003). "Loss of nicotinic acetylcholine receptor subunits alpha4 and alpha7 in the cerebral cortex of Parkinson patients." Parkinsonism Relat Disord **9**(5): 243-6.

Burzomato, V., M. Beato, *et al.* (2004). "Single-channel behavior of heteromeric alpha1beta glycine receptors: an attempt to detect a conformational change before the channel opens." J Neurosci **24**(48): 10924-40.

Butler, A. S., S. A. Lindesay, *et al.* (2009). "Importance of the C-terminus of the human 5-HT3A receptor subunit." Neuropharmacology **56**(1): 292-302.

Butt, C. M., S. R. Hutton, *et al.* (2002). "Bovine serum albumin enhances nicotinic acetylcholine receptor function in mouse thalamic synaptosomes." J Neurochem **83**(1): 48-56.

Carbone, A. L., M. Moroni, *et al.* (2009). "Pentameric concatenated (alpha4)(2)(beta2)(3) and (alpha4)(3)(beta2)(2) nicotinic acetylcholine receptors: subunit arrangement determines functional expression." Br J Pharmacol **156**(6): 970-81.

Cartier, G. E., D. Yoshikami, *et al.* (1996). "A new alpha-conotoxin which targets alpha3beta2 nicotinic acetylcholine receptors." J Biol Chem **271**(13): 7522-8.

Castelan, F., J. Mulet, *et al.* (2007). "Cytoplasmic regions adjacent to the M3 and M4 transmembrane segments influence expression and function of alpha7 nicotinic acetylcholine receptors. A study with single amino acid mutants." J Neurochem **100**(2): 406-15.

Castro, N. G. and E. X. Albuquerque (1995). "Alpha-bungarotoxin-sensitive hippocampal nicotinic receptor channel has a high calcium permeability." Biophys J **68**(2): 516-24.

Celie, P. H., I. E. Kasheverov, *et al.* (2005). "Crystal structure of nicotinic acetylcholine receptor homolog AChBP in complex with an alpha-conotoxin PnIA variant." Nat Struct Mol Biol **12**(7): 582-8.

Celie, P. H., S. E. van Rossum-Fikkert, *et al.* (2004). "Nicotine and carbamylcholine binding to nicotinic acetylcholine receptors as studied in AChBP crystal structures." Neuron **41**(6): 907-14.

Chakrapani, S., T. D. Bailey, *et al.* (2004). "Gating dynamics of the acetylcholine receptor extracellular domain." J Gen Physiol **123**(4): 341-56.

Champtiaux, N., C. Gotti, *et al.* (2003). "Subunit composition of functional nicotinic receptors in dopaminergic neurons investigated with knock-out mice." J Neurosci **23**(21): 7820-9.

Champtiaux, N., Z. Y. Han, *et al.* (2002). "Distribution and pharmacology of alpha 6-containing nicotinic acetylcholine receptors analyzed with mutant mice." J Neurosci **22**(4): 1208-17.

Chang, Y. and D. S. Weiss (1998). "Substitutions of the highly conserved M2 leucine create spontaneously opening rho1 gamma-aminobutyric acid receptors." Mol Pharmacol **53**(3): 511-23.

Changeux, J. P., D. Bertrand, *et al.* (1998). "Brain nicotinic receptors: structure and regulation, role in learning and reinforcement." Brain Res Brain Res Rev **26**(2-3): 198-216.

Changeux, J. P. and S. J. Edelstein (2001). "Allosteric mechanisms in normal and pathological nicotinic acetylcholine receptors." Curr Opin Neurobiol **11**(3): 369-77.

Charnet, P., C. Labarca, *et al.* (1992). "Pharmacological and kinetic properties of alpha 4 beta 2 neuronal nicotinic acetylcholine receptors expressed in Xenopus oocytes." J Physiol **450**: 375-94.

Chavez, R. A. and Z. W. Hall (1992). "Expression of fusion proteins of the nicotinic acetylcholine receptor from mammalian muscle identifies the membrane-spanning regions in the alpha and delta subunits." J Cell Biol **116**(2): 385-93.

Chavez-Noriega, L. E., J. H. Crona, *et al.* (1997). "Pharmacological characterization of recombinant human neuronal nicotinic acetylcholine receptors h alpha 2 beta 2, h alpha 2 beta 4, h alpha 3 beta 2, h alpha 3 beta 4, h alpha 4 beta 2, h alpha 4 beta 4 and h alpha 7 expressed in *Xenopus* oocytes." J Pharmacol Exp Ther **280**(1): 346-56.

Che, D., T. Wegge, *et al.* (2001). "exo-2-(Pyridazin-4-yl)-7-azabicyclo[2.2.1]heptanes: syntheses and nicotinic acetylcholine receptor agonist activity of potent pyridazine analogues of (+/-)-epibatidine." J Med Chem **44**(1): 47-57.

Chen, D. and J. W. Patrick (1997). "The alpha-bungarotoxin-binding nicotinic acetylcholine receptor from rat brain contains only the alpha7 subunit." J Biol Chem **272**(38): 24024-9.

Chen, J., Y. Zhang, *et al.* (1995). "Activation kinetics of recombinant mouse nicotinic acetylcholine receptors: mutations of alpha-subunit tyrosine 190 affect both binding and gating." Biophys J **69**(3): 849-59.

Cheng, X., I. Ivanov, *et al.* (2007). "Nanosecond-timescale conformational dynamics of the human alpha7 nicotinic acetylcholine receptor." Biophys J **93**(8): 2622-34.

Cheng, X., B. Lu, *et al.* (2006). "Channel opening motion of alpha7 nicotinic acetylcholine receptor as suggested by normal mode analysis." J Mol Biol **355**(2): 310-24.

Cheng, X., H. Wang, *et al.* (2006). "Targeted molecular dynamics study of C-loop closure and channel gating in nicotinic receptors." PLoS Comput Biol **2**(9): e134.

Chiappinelli, V. A. (1985). "Actions of snake venom toxins on neuronal nicotinic receptors and other neuronal receptors." Pharmacol Ther **31**(1-2): 1-32.

Chiara, D. C., R. E. Middleton, *et al.* (1998). "Identification of tryptophan 55 as the primary site of [3H]nicotine photoincorporation in the gamma-subunit of the Torpedo nicotinic acetylcholine receptor." FEBS Lett **423**(2): 223-6.

Cho, C. H., W. Song, *et al.* (2005). "Rapid upregulation of alpha7 nicotinic acetylcholine receptors by tyrosine dephosphorylation." J Neurosci **25**(14): 3712-23.

Clarke, P. B. (1993). "Nicotinic receptors in mammalian brain: localization and relation to cholinergic innervation." Prog Brain Res **98**: 77-83.

Clarke, P. B., R. D. Schwartz, *et al.* (1985). "Nicotinic binding in rat brain: autoradiographic comparison of [3H]acetylcholine, [3H]nicotine, and [125I]-alpha-bungarotoxin." J Neurosci **5**(5): 1307-15.

Clements, J. D. (1996). "Transmitter timecourse in the synaptic cleft: its role in central synaptic function." Trends Neurosci **19**(5): 163-71.

Cohen B.N., C. Labarca *et al.* (1992)."Tris+/Na+ permeability ratios of nicotinic acetylcholine receptors are reduced by mutations near the intracellular end of the M2 region." J Gen Physiol. 99(4):545-72.

Colledge, M. and S. C. Froehner (1997). "Tyrosine phosphorylation of nicotinic acetylcholine receptor mediates Grb2 binding." J Neurosci **17**(13): 5038-45.

Cooper, E., S. Couturier, *et al.* (1991). "Pentameric structure and subunit stoichiometry of a neuronal nicotinic acetylcholine receptor." Nature **350**(6315): 235-8.

Corrigall, W. A., K. M. Coen, *et al.* (2000). "Response of nicotine self-administration in the rat to manipulations of mu-opioid and gamma-aminobutyric acid receptors in the ventral tegmental area." Psychopharmacology (Berl) **149**(2): 107-14.

Corringer, P. J., S. Bertrand, *et al.* (1999a). "Molecular basis of the charge selectivity of nicotinic acetylcholine receptor and related ligand-gated ion channels." Novartis Found Symp **225**: 215-24; discussion 224-30.

Corringer, P. J., S. Bertrand, *et al.* (1999b). "Mutational analysis of the charge selectivity filter of the alpha7 nicotinic acetylcholine receptor." Neuron **22**(4): 831-43.

Corringer, P. J., J. L. Galzi, *et al.* (1995). "Identification of a new component of the agonist binding site of the nicotinic alpha 7 homooligomeric receptor." J Biol Chem **270**(20): 11749-52.

Corringer, P. J., N. Le Novere, *et al.* (2000). "Nicotinic receptors at the amino acid level." Annu Rev Pharmacol Toxicol **40**: 431-58.

Corringer, P. J., J. Sallette, *et al.* (2006). "Nicotine enhances intracellular nicotinic receptor maturation: a novel mechanism of neural plasticity?" J Physiol Paris **99**(2-3): 162-71.

Corriveau, R. A., S. J. Romano, *et al.* (1995). "Expression of neuronal acetylcholine receptor genes in vertebrate skeletal muscle during development." J Neurosci **15**(2): 1372-83.

Court, J. and F. Clementi (1995). "Distribution of nicotinic subtypes in human brain." Alzheimer Dis Assoc Disord **9 Suppl 2**: 6-14.

Court, J. A., S. Lloyd, *et al.* (1997). "Nicotinic and muscarinic cholinergic receptor binding in the human hippocampal formation during development and aging." Brain Res Dev Brain Res **101**(1-2): 93-105.

Court, J. A., C. Martin-Ruiz, *et al.* (2000). "Nicotinic receptors in human brain: topography and pathology." J Chem Neuroanat **20**(3-4): 281-98.

Court, J. A., E. K. Perry, *et al.* (1995). "The role of the cholinergic system in the development of the human cerebellum." Brain Res Dev Brain Res **90**(1-2): 159-67.

Couturier, S., D. Bertrand, *et al.* (1990). "A neuronal nicotinic acetylcholine receptor subunit (alpha 7) is developmentally regulated and forms a homo-oligomeric channel blocked by alpha-BTX." Neuron **5**(6): 847-56.

Cucchiaro, G., Y. Xiao, *et al.* (2008). "Analgesic effects of Sazetidine-A, a new nicotinic cholinergic drug." Anesthesiology **109**(3): 512-9.

Curtis, L., B. Buisson, *et al.* (2002). "Potentiation of human alpha4beta2 neuronal nicotinic acetylcholine receptor by estradiol." Mol Pharmacol **61**(1): 127-35.

Cymes, G. D., Y. Ni, *et al.* (2005). "Probing ion-channel pores one proton at a time." Nature **438**(7070): 975-80.

Dani, J. A. (1989). "Open channel structure and ion binding sites of the nicotinic acetylcholine receptor channel." J Neurosci **9**(3): 884-92.

Dani, J. A. (2001). "Overview of nicotinic receptors and their roles in the central nervous system." Biol Psychiatry **49**(3): 166-74.

Darsow, T., T. K. Booker, *et al.* (2005). "Exocytic trafficking is required for nicotine-induced up-regulation of alpha 4 beta 2 nicotinic acetylcholine receptors." J Biol Chem **280**(18): 18311-20.

Decker, M. W., J. D. Brioni, *et al.* (1995). "Diversity of neuronal nicotinic acetylcholine receptors: lessons from behavior and implications for CNS therapeutics." Life Sci **56**(8): 545-70.

Decker, M. W., L. E. Rueter, *et al.* (2004). "Nicotinic acetylcholine receptor agonists: a potential new class of analgesics." Curr Top Med Chem **4**(3): 369-84.

Decker, E. R. and J. A. Dani (1990). "Calcium permeability of the nicotinic acetylcholine receptor: the single-channel calcium influx is significant." J Neurosci **10**(10): 3413-20.

De Fusco, M., A. Becchetti, *et al.* (2000). "The nicotinic receptor beta 2 subunit is mutant in nocturnal frontal lobe epilepsy." Nat Genet **26**(3): 275-6.

Dellisanti, C. D., Y. Yao, *et al.* (2007). "Crystal structure of the extracellular domain of nAChR alpha1 bound to alpha-bungarotoxin at 1.94 A resolution." Nat Neurosci **10**(8): 953-62.

Demuro, A., E. Palma, *et al.* (2001). "Inhibition of nicotinic acetylcholine receptors by bicuculline." Neuropharmacology **41**(7): 854-61.

Dennis, M., J. Giraudat, *et al.* (1988). "Amino acids of the *Torpedo marmorata* acetylcholine receptor alpha subunit labeled by a photoaffinity ligand for the acetylcholine binding site." Biochemistry **27**(7): 2346-57.

Derry, C. P., S. E. Heron, *et al.* (2008). "Severe autosomal dominant nocturnal frontal lobe epilepsy associated with psychiatric disorders and intellectual disability." Epilepsia **49**(12): 2125-9.

Deutch, A. Y., J. Holliday, *et al.* (1987). "Immunohistochemical localization of a neuronal nicotinic acetylcholine receptor in mammalian brain." Proc Natl Acad Sci USA **84**(23): 8697-701.

Di Angelantonio, S., R. Giniatullin, *et al.* (2003). "Modulation of neuronal nicotinic receptor function by the neuropeptides CGRP and substance P on autonomic nerve cells." Br J Pharmacol **139**(6): 1061-73.

Drisdel, R. C. and W. N. Green (2000). "Neuronal alpha-bungarotoxin receptors are alpha7 subunit homomers." J Neurosci **20**(1): 133-9.

Duvoisin, R. M., E. S. Deneris, *et al.* (1989). "The functional diversity of the neuronal nicotinic acetylcholine receptors is increased by a novel subunit: beta 4." Neuron **3**(4): 487-96.

Eaton, J. B., J. H. Peng, *et al.* (2003). "Characterization of human alpha 4 beta 2-nicotinic acetylcholine receptors stably and heterologously expressed in native nicotinic receptor-null SH-EP1 human epithelial cells." Mol Pharmacol **64**(6): 1283-94.

Eccles J. C., (1964) "The physiology of synapses." Springer

Elgoyhen, A. B., D. S. Johnson, *et al.* (1994). "Alpha 9: an acetylcholine receptor with novel pharmacological properties expressed in rat cochlear hair cells." Cell **79**(4): 705-15.

Elgoyhen, A. B., D. E. Vetter, *et al.* (2001). "alpha10: a determinant of nicotinic cholinergic receptor function in mammalian vestibular and cochlear mechanosensory hair cells." Proc Natl Acad Sci USA **98**(6): 3501-6.

Emerick M. C. and D. M Fambrough (1993)."Intramolecular fusion of Na pump subunits assures exclusive assembly of the fused alpha and beta subunit domains into a functional enzyme in cells also expressing endogenous Na pump subunits." J Biol Chem. **268(31)**:23455-9.

England, P. M., Y. Zhang, *et al.* (1999). "Backbone mutations in transmembrane domains of a ligand-gated ion channel: implications for the mechanism of gating." Cell **96**(1): 89-98.

Ericksen, S. S. and A. J. Boileau (2007). "Tandem couture: Cys-loop receptor concatamer insights and caveats." Mol Neurobiol **35**(1): 113-28.

Exley, R., M. Moroni, *et al.* (2006). "Chaperone protein 14-3-3 and protein kinase A increase the relative abundance of low agonist sensitivity human alpha 4 beta 2 nicotinic acetylcholine receptors in *Xenopus* oocytes." J Neurochem **98**(3): 876-85.

Fairclough, R. H., R. Josephs, *et al.* (1993). "Imaging ligand binding sites on the *Torpedo* acetylcholine receptor." Ann N Y Acad Sci **681**: 113-25.

Fenster, C. P., M. L. Beckman, *et al.* (1999). "Regulation of alpha4beta2 nicotinic receptor desensitization by calcium and protein kinase C." Mol Pharmacol **55**(3): 432-43.

Ficklin, M. B., S. Zhao, *et al.* (2005). "Ubiquilin-1 regulates nicotine-induced up-regulation of neuronal nicotinic acetylcholine receptors." J Biol Chem **280**(40): 34088-95.

Figl, A., N. Viseshakul, *et al.* (1998). "Two mutations linked to nocturnal frontal lobe epilepsy cause use-dependent potentiation of the nicotinic ACh response." J Physiol **513 (Pt 3)**: 655-70.

Filatov, G. N. and M. M. White (1995). "The role of conserved leucines in the M2 domain of the acetylcholine receptor in channel gating." Mol Pharmacol **48**(3): 379-84.

Firsov D., I. Gautschi, et al. (1998). "The heterotetrameric architecture of the epithelial sodium channel (ENaC)." EMBO J. 1998 Jan 15;17(2):344-52.

Flores, C. M., S. W. Rogers, *et al.* (1992). "A subtype of nicotinic cholinergic receptor in rat brain is composed of alpha 4 and beta 2 subunits and is up-regulated by chronic nicotine treatment." Mol Pharmacol **41**(1): 31-7.

Forster, I. and D. Bertrand (1995). "Inward rectification of neuronal nicotinic acetylcholine receptors investigated by using the homomeric alpha 7 receptor." Proc Biol Sci **260**(1358): 139-48.

Francis, M. M., E. Y. Cheng, *et al.* (2001). "Specific activation of the alpha 7 nicotinic acetylcholine receptor by a quaternary analog of cocaine." Mol Pharmacol **60**(1): 71-9.

Frazier, C. J., A. V. Buhler, *et al.* (1998). "Synaptic potentials mediated via alpha-bungarotoxin-sensitive nicotinic acetylcholine receptors in rat hippocampal interneurons." J Neurosci **18**(20): 8228-35.

Freedman, R., M. Hall, *et al.* (1995). "Evidence in postmortem brain tissue for decreased numbers of hippocampal nicotinic receptors in schizophrenia." Biol Psychiatry **38**(1): 22-33.

Fu, X. W., C. A. Nurse, *et al.* (2003). "Expression of functional nicotinic acetylcholine receptors in neuroepithelial bodies of neonatal hamster lung." Am J Physiol Lung Cell Mol Physiol **285**(6): L1203-12.

Fucile, S., B. Barabino, *et al.* (1997). "Alpha 5 subunit forms functional alpha 3 beta 4 alpha 5 nAChRs in transfected human cells." Neuroreport **8**(11): 2433-6.

Fucile, S., J. M. Matter, *et al.* (1998). "The neuronal alpha6 subunit forms functional heteromeric acetylcholine receptors in human transfected cells." Eur J Neurosci **10**(1): 172-8.

Fucile, S., E. Palma, *et al.* (2002a). "Serotonin antagonizes the human neuronal alpha7 nicotinic acetylcholine receptor and becomes an agonist after L248T alpha7 mutation." Neuroscience **110**(1): 169-79.

Fucile, S., E. Palma, *et al.* (2002b). "The single-channel properties of human acetylcholine alpha 7 receptors are altered by fusing alpha 7 to the green fluorescent protein." Proc Natl Acad Sci USA **99**(6): 3956-61.

Gallagher, M. J., L. Song, *et al.* (2004). "The juvenile myoclonic epilepsy GABA(A) receptor alpha1 subunit mutation A322D produces asymmetrical, subunit position-dependent reduction of heterozygous receptor currents and alpha1 subunit protein expression." J Neurosci **24**(24): 5570-8.

Galzi, J. L., D. Bertrand, *et al.* (1991). "Functional significance of aromatic amino acids from three peptide loops of the alpha 7 neuronal nicotinic receptor site investigated by site-directed mutagenesis." FEBS Lett **294**(3): 198-202.

Galzi, J. L. and J. P. Changeux (1995). "Neuronal nicotinic receptors: molecular organization and regulations." Neuropharmacology **34**(6): 563-82.

Galzi, J. L., A. Devillers-Thiery, *et al.* (1992). "Mutations in the channel domain of a neuronal nicotinic receptor convert ion selectivity from cationic to anionic." Nature **359**(6395): 500-5.

Galzi, J. L., F. Revah, *et al.* (1990). "Identification of a novel amino acid alpha-tyrosine 93 within the cholinergic ligands-binding sites of the acetylcholine receptor by photoaffinity labeling. Additional evidence for a three-loop model of the cholinergic ligands-binding sites." J Biol Chem **265**(18): 10430-7.

Gandia, L., M. Villarroya, *et al.* (1996). "Inhibition of nicotinic receptor-mediated responses in bovine chromaffin cells by diltiazem." Br J Pharmacol **118**(5): 1301-7.

Gao, F., N. Bren, *et al.* (2005). "Agonist-mediated conformational changes in acetylcholine-binding protein revealed by simulation and intrinsic tryptophan fluorescence." J Biol Chem **280**(9): 8443-51.

Garcia-Colunga, J. and R. Miledi (1999). "Modulation of nicotinic acetylcholine receptors by strychnine." Proc Natl Acad Sci USA **96**(7): 4113-8.

Gensler, S., A. Sander, *et al.* (2001). "Assembly and clustering of acetylcholine receptors containing GFP-tagged epsilon or gamma subunits: selective targeting to the neuromuscular junction *in vivo*." Eur J Biochem **268**(8): 2209-17.

Gentry, C. L. and R. J. Lukas (2002). "Regulation of nicotinic acetylcholine receptor numbers and function by chronic nicotine exposure." Curr Drug Targets CNS Neurol Disord **1**(4): 359-85.

Gerzanich, V., R. Anand, *et al.* (1994). "Homomers of alpha 8 and alpha 7 subunits of nicotinic receptors exhibit similar channel but contrasting binding site properties." Mol Pharmacol **45**(2): 212-20.

Gerzanich, V., A. Kuryatov, *et al.* (1997). ""Orphan" alpha6 nicotinic AChR subunit can form a functional heteromeric acetylcholine receptor." Mol Pharmacol **51**(2): 320-7.

Gerzanich, V., F. Wang, *et al.* (1998). "alpha 5 Subunit alters desensitization, pharmacology, Ca^{++} permeability and Ca^{++} modulation of human neuronal alpha 3 nicotinic receptors." J Pharmacol Exp Ther **286**(1): 311-20.

Giniatullin, R. A., M. Talantova, *et al.* (1997). "Desensitization shortens the high-quantal-content endplate current time course in frog muscle with intact cholinesterase." J Physiol **502 (Pt 3)**: 641-8.

Giniatullin, R. A., M. V. Talantova, *et al.* (2001). "The role of desensitisation in decay time of miniature endplate currents in frogs *Rana ridibunda* and *Rana temporaria*." Neurosci Res **39**(3): 287-92.

Giraudat, J., M. Dennis, *et al.* (1986). "Structure of the high-affinity binding site for noncompetitive blockers of the acetylcholine receptor: serine-262 of the delta subunit is labeled by [^{3}H]chlorpromazine." Proc Natl Acad Sci USA **83**(8): 2719-23.

Girod, R., N. Barazangi, *et al.* (2000). "Facilitation of glutamatergic neurotransmission by presynaptic nicotinic acetylcholine receptors." Neuropharmacology **39**(13): 2715-25.

Gotti, C. and F. Clementi (2004). "Neuronal nicotinic receptors: from structure to pathology." Prog Neurobiol **74**(6): 363-96.

Gotti, C., D. Fornasari, *et al.* (1997). "Human neuronal nicotinic receptors." Prog Neurobiol **53**(2): 199-237.

Gotti, C., M. Moretti, *et al.* (2008). "Partial deletion of the nicotinic cholinergic receptor alpha 4 or beta 2 subunit genes changes the acetylcholine sensitivity of receptor-mediated 86Rb+ efflux in cortex and thalamus and alters relative expression of alpha 4 and beta 2 subunits." Mol Pharmacol **73**(6): 1796-807.

Gotti, C., M. Moretti, *et al.* (2005). "Heterogeneity and selective targeting of neuronal nicotinic acetylcholine receptor (nAChR) subtypes expressed on retinal afferents of the superior colliculus and lateral geniculate nucleus: identification of a new native nAChR subtype alpha3beta2(alpha5 or beta3) enriched in retinocollicular afferents." Mol Pharmacol **68**(4): 1162-71.

Gotti, C., M. Zoli, *et al.* (2006). "Brain nicotinic acetylcholine receptors: native subtypes and their relevance." Trends Pharmacol Sci **27**(9): 482-91.

Grady, S., M. J. Marks, *et al.* (1992). "Characterization of nicotinic receptor-mediated [3H]dopamine release from synaptosomes prepared from mouse striatum." J Neurochem **59**(3): 848-56.

Grady, S. R., N. M. Meinerz, *et al.* (2001). "Nicotinic agonists stimulate acetylcholine release from mouse interpeduncular nucleus: a function mediated by a different nAChR than dopamine release from striatum." J Neurochem **76**(1): 258-68.

Graham, A. J., M. A. Ray, *et al.* (2003). "Differential nicotinic acetylcholine receptor subunit expression in the human hippocampus." J Chem Neuroanat **25**(2): 97-113.

Grando, S. A., B. D. Zelickson, *et al.* (1995). "Keratinocyte muscarinic acetylcholine receptors: immunolocalization and partial characterization." J Invest Dermatol **104**(1): 95-100.

Grando S. A., K. Kawashima, et al. (2007). "Recent progress in understanding the non-neuronal cholinergic system in humans."Life Sci. 80(24-25): 2181-5.

Green, W. N. and T. Claudio (1993). "Acetylcholine receptor assembly: subunit folding and oligomerization occur sequentially." Cell **74**(1): 57-69.

Green, W. N. and C. P. Wanamaker (1997). "The role of the cystine loop in acetylcholine receptor assembly." J Biol Chem **272**(33): 20945-53.

Groot-Kormelink, P. J., S. Broadbent, *et al.* (2004). "Incomplete incorporation of tandem subunits in recombinant neuronal nicotinic receptors." J Gen Physiol **123**(6): 697-708.

Groot-Kormelink, P. J., S. Broadbent, *et al.* (2006). "Constraining the expression of nicotinic acetylcholine receptors by using pentameric constructs." Mol Pharmacol **69**(2): 558-63.

Groot-Kormelink, P. J., W. H. Luyten, *et al.* (1998). "A reporter mutation approach shows incorporation of the "orphan" subunit beta3 into a functional nicotinic receptor." J Biol Chem **273**(25): 15317-20.

Grosman, C., M. Zhou, *et al.* (2000). "Mapping the conformational wave of acetylcholine receptor channel gating." Nature **403**(6771): 773-6.

Grudzinska, J., R. Schemm, *et al.* (2005). "The beta subunit determines the ligand binding properties of synaptic glycine receptors." Neuron **45**(5): 727-39.

Grun, E. A., J. R. Pauly, *et al.* (1992). "Adrenalectomy reverses chronic injection-induced tolerance to nicotine." Psychopharmacology (Berl) **109**(3): 299-304.

Guan, Z. Z., X. Zhang, *et al.* (2000). "Decreased protein levels of nicotinic receptor subunits in the hippocampus and temporal cortex of patients with Alzheimer's disease." J Neurochem **74**(1): 237-43.

Haghighi, A. P. and E. Cooper (2000). "A molecular link between inward rectification and calcium permeability of neuronal nicotinic acetylcholine alpha3beta4 and alpha4beta2 receptors." J Neurosci **20**(2): 529-41.

Han, Z. Y., N. Le Novere, *et al.* (2000). "Localization of nAChR subunit mRNAs in the brain of *Macaca mulatta*." Eur J Neurosci **12**(10): 3664-74.

Hansen, S. B., G. Sulzenbacher, *et al.* (2005). "Structures of *Aplysia* AChBP complexes with nicotinic agonists and antagonists reveal distinctive binding interfaces and conformations." Embo J **24**(20): 3635-46.

Hansen, S. B. and P. Taylor (2007). "Galanthamine and non-competitive inhibitor binding to ACh-binding protein: evidence for a binding site on non-alpha-subunit interfaces of heteromeric neuronal nicotinic receptors." J Mol Biol **369**(4): 895-901.

Hansen, S. B., H. L. Wang, *et al.* (2008). "An ion selectivity filter in the extracellular domain of Cys-loop receptors reveals determinants for ion conductance." J Biol Chem **283**(52): 36066-70.

Harkness, P. C. and N. S. Millar (2002). "Changes in conformation and subcellular distribution of alpha4beta2 nicotinic acetylcholine receptors revealed by chronic nicotine treatment and expression of subunit chimeras." J Neurosci **22**(23): 10172-81.

Harvey, S. C., J. M. McIntosh, *et al.* (1997). "Determinants of specificity for alpha-conotoxin MII on alpha3beta2 neuronal nicotinic receptors." Mol Pharmacol **51**(2): 336-42.

Hefft, S., S. Hulo, *et al.* (1999). "Synaptic transmission at nicotinic acetylcholine receptors in rat hippocampal organotypic cultures and slices." J Physiol **515 (Pt 3)**: 769-76.

Heidmann, T. and J. P. Changeux (1984). "Time-resolved photolabeling by the noncompetitive blocker chlorpromazine of the acetylcholine receptor in its transiently open and closed ion channel conformations." Proc Natl Acad Sci USA **81**(6): 1897-901.

Hiel, H., A. E. Luebke, *et al.* (2000). "Cloning and expression of the alpha9 nicotinic acetylcholine receptor subunit in cochlear hair cells of the chick." Brain Res **858**(1): 215-25.

Hilf, R. J. and R. Dutzler (2008). "X-ray structure of a prokaryotic pentameric ligand-gated ion channel." Nature **452**(7185): 375-9.

Hilf, R. J. and R. Dutzler (2009). "Structure of a potentially open state of a proton-activated pentameric ligand-gated ion channel." Nature **457**(7225): 115-8.

Hirose, S., H. Iwata, *et al.* (1999). "A novel mutation of CHRNA4 responsible for autosomal dominant nocturnal frontal lobe epilepsy." Neurology **53**(8): 1749-53.

Hoda, J. C., W. Gu, *et al.* (2008). "Human nocturnal frontal lobe epilepsy: pharmocogenomic profiles of pathogenic nicotinic acetylcholine receptor beta-subunit mutations outside the ion channel pore." Mol Pharmacol **74**(2): 379-91.

Hogg, R. C., M. Raggenbass, *et al.* (2003). "Nicotinic acetylcholine receptors: from structure to brain function." Rev Physiol Biochem Pharmacol **147**: 1-46.

Horiuchi, Y., R. Kimura, *et al.* (2003). "Evolutional study on acetylcholine expression." Life Sci **72**(15): 1745-56.

Houghtling, R. A., M. I. Davila-Garcia, *et al.* (1995). "Characterization of (+/-) (-)[^{3}H]epibatidine binding to nicotinic cholinergic receptors in rat and human brain." Mol Pharmacol **48**(2): 280-7.

Houlihan, L. M., Y. Slater, *et al.* (2001). "Activity of cytisine and its brominated isosteres on recombinant human alpha7, alpha4beta2 and alpha4beta4 nicotinic acetylcholine receptors." J Neurochem **78**(5): 1029-43.

Hucho, F., W. Oberthur, *et al.* (1986). "The ion channel of the nicotinic acetylcholine receptor is formed by the homologous helices M II of the receptor subunits." FEBS Lett **205**(1): 137-42.

Huganir, R. L., A. H. Delcour, *et al.* (1986). "Phosphorylation of the nicotinic acetylcholine receptor regulates its rate of desensitization." Nature **321**(6072): 774-6.

Im W. B., J. F. Pregenzer, *et al.* (1995). "Chloride channel expression with the tandem construct of alpha 6-beta 2 GABAA receptor subunit requires a monomeric subunit of alpha 6 or gamma 2." J Biol Chem. **270(44)**:26063-6.

Imoto, K., C. Busch, *et al.* (1988). "Rings of negatively charged amino acids determine the acetylcholine receptor channel conductance." Nature **335**(6191): 645-8.

Inoue, M. and H. Kuriyama (1991). "Somatostatin inhibits the nicotinic receptor-activated inward current in guinea pig chromaffin cells." Biochem Biophys Res Commun **174**(2): 750-7.

Isacoff E.Y., Y. N. Jan *et al.* (1990). "Evidence for the formation of heteromultimeric potassium channels in Xenopus oocytes." Nature **345(6275)**:530-4.

Jackson, M. B. (1986). "Kinetics of unliganded acetylcholine receptor channel gating." Biophys J **49**(3): 663-72.

Jeanclos, E. M., L. Lin, *et al.* (2001). "The chaperone protein 14-3-3eta interacts with the nicotinic acetylcholine receptor alpha 4 subunit. Evidence for a dynamic role in subunit stabilization." J Biol Chem **276**(30): 28281-90.

Jha, A., D. J. Cadugan, *et al.* (2007). "Acetylcholine receptor gating at extracellular transmembrane domain interface: the cys-loop and M2-M3 linker." J Gen Physiol **130**(6): 547-58.

Ji, D. and J. A. Dani (2000). "Inhibition and disinhibition of pyramidal neurons by activation of nicotinic receptors on hippocampal interneurons." J Neurophysiol **83**(5): 2682-90.

Johnson, D. S., J. Martinez, *et al.* (1995). "Alpha-conotoxin ImI exhibits subtype-specific nicotinic acetylcholine receptor blockade: preferential inhibition of homomeric alpha 7 and alpha 9 receptors." Mol Pharmacol **48**(2): 194-9.

Jones, A. K. and D. B. Sattelle (2006). "The cys-loop ligand-gated ion channel superfamily of the honeybee, *Apis mellifera*." Invert Neurosci **6**(3): 123-32.

Jones, S., S. Sudweeks, *et al.* (1999). "Nicotinic receptors in the brain: correlating physiology with function." Trends Neurosci **22**(12): 555-61.

Kalamida, D., K. Poulas, *et al.* (2007). "Muscle and neuronal nicotinic acetylcholine receptors. Structure, function and pathogenicity." Febs J **274**(15): 3799-845.

Kandel E. R., J. H. Schwartz, T. .M.J essell (2000). "Principles of neural science." 4th ed. McGraw-Hill, New York

Kao, P. N. and A. Karlin (1986). "Acetylcholine receptor binding site contains a disulfide cross-link between adjacent half-cystinyl residues." J Biol Chem **261**(18): 8085-8.

Karlin, A. (2002). "Emerging structure of the nicotinic acetylcholine receptors." Nat Rev Neurosci **3**(2): 102-14.

Karlin, A. and M. H. Akabas (1995). "Toward a structural basis for the function of nicotinic acetylcholine receptors and their cousins." Neuron **15**(6): 1231-44.

Kash, T. L., A. Jenkins, *et al.* (2003). "Coupling of agonist binding to channel gating in the GABA(A) receptor." Nature **421**(6920): 272-5.

Kash, T. L., J. R. Trudell, *et al.* (2004). "Structural elements involved in activation of the gamma-aminobutyric acid type A (GABAA) receptor." Biochem Soc Trans **32**(Pt3): 540-6.

Katz B., (1966). "Nerve, muscle, and synapse." McGraw-Hill

Katz, E., A. B. Elgoyhen, *et al.* (2004). "Developmental regulation of nicotinic synapses on cochlear inner hair cells." J Neurosci **24**(36): 7814-20.

Kaur, K. H., R. Baur, *et al.* (2009). "Unanticipated structural and functional properties of delta-subunit-containing GABAA receptors." J Biol Chem **284**(12): 7889-96.

Kawashima, K. and T. Fujii (2000). "Extraneuronal cholinergic system in lymphocytes." Pharmacol Ther **86**(1): 29-48.

Kawashima, K., K. Yoshikawa, *et al.* (2007). "Expression and function of genes encoding cholinergic components in murine immune cells." Life Sci **80**(24-25): 2314-9.

Ke, L. and R. J. Lukas (1996). "Effects of steroid exposure on ligand binding and functional activities of diverse nicotinic acetylcholine receptor subtypes." J Neurochem **67**(3): 1100-12.

Keller, S. H., J. Lindstrom, *et al.* (2001). "Adjacent basic amino acid residues recognized by the COP I complex and ubiquitination govern endoplasmic reticulum to cell surface trafficking of the nicotinic acetylcholine receptor alpha-Subunit." J Biol Chem **276**(21): 18384-91.

Kelley, S. P., J. I. Dunlop, *et al.* (2003). "A cytoplasmic region determines single-channel conductance in 5-HT3 receptors." Nature **424**(6946): 321-4.

Keramidas, A., A. J. Moorhouse, *et al.* (2002). "Cation-selective mutations in the M2 domain of the inhibitory glycine receptor channel reveal determinants of ion-charge selectivity." J Gen Physiol **119**(5): 393-410.

Keramidas, A., A. J. Moorhouse, *et al.* (2004). "Ligand-gated ion channels: mechanisms underlying ion selectivity." Prog Biophys Mol Biol **86**(2): 161-204.

Keyser, K. T., L. R. Britto, *et al.* (1993). "Three subtypes of alpha-bungarotoxin-sensitive nicotinic acetylcholine receptors are expressed in chick retina." J Neurosci **13**(2): 442-54.

Khatami, R., M. Neumann, *et al.* (1998). "A family with autosomal dominant nocturnal frontal lobe epilepsy and mental retardation." J Neurol **245**(12): 809-10.

Khiroug, L., R. Giniatullin, *et al.* (2003). "Functional mapping and Ca2+ regulation of nicotinic acetylcholine receptor channels in rat hippocampal CA1 neurons." J Neurosci **23**(27): 9024-31.

Khiroug, L., E. Sokolova, *et al.* (1998). "Recovery from desensitization of neuronal nicotinic acetylcholine receptors of rat chromaffin cells is modulated by intracellular calcium through distinct second messengers." J Neurosci **18**(7): 2458-66.

Khiroug, S. S., P. C. Harkness, *et al.* (2002). "Rat nicotinic ACh receptor alpha7 and beta2 subunits co-assemble to form functional heteromeric nicotinic receptor channels." J Physiol **540**(Pt 2): 425-34.

Kim, H., B. A. Flanagin, *et al.* (2003). "The mouse Chrna4 A529T polymorphism alters the ratio of high to low affinity alpha 4 beta 2 nAChRs." Neuropharmacology **45**(3): 345-54.

Kittler, J. T., J. Wang, *et al.* (2000). "Analysis of GABAA receptor assembly in mammalian cell lines and hippocampal neurons using gamma 2 subunit green fluorescent protein chimeras." Mol Cell Neurosci **16**(4): 440-52.

Klink, R., A. de Kerchove d'Exaerde, *et al.* (2001). "Molecular and physiological diversity of nicotinic acetylcholine receptors in the midbrain dopaminergic nuclei." J Neurosci **21**(5): 1452-63.

Kracun, S., P. C. Harkness, *et al.* (2008). "Influence of the M3-M4 intracellular domain upon nicotinic acetylcholine receptor assembly, targeting and function." Br J Pharmacol **153**(7): 1474-84.

Kreienkamp, H. J., R. K. Maeda, *et al.* (1995). "Intersubunit contacts governing assembly of the mammalian nicotinic acetylcholine receptor." Neuron **14**(3): 635-44.

Kukhtina, V., D. Kottwitz, *et al.* (2006). "Intracellular domain of nicotinic acetylcholine receptor: the importance of being unfolded." J Neurochem **97 Suppl 1**: 63-7.

Kulak, J. M., J. M. McIntosh, *et al.* (2002). "Loss of nicotinic receptors in monkey striatum after 1-methyl-4-phenyl-1,2,3,6-tetrahydropyridine treatment is due to a decline in alpha-conotoxin MII sites." Mol Pharmacol **61**(1): 230-8.

Kulak, J. M., J. M. McIntosh, *et al.* (2001). "Nicotine-evoked transmitter release from synaptosomes: functional association of specific presynaptic acetylcholine receptors and voltage-gated calcium channels." J Neurochem **77**(6): 1581-9.

Kuo, Y. P., L. Xu, *et al.* (2005). "Roles for nicotinic acetylcholine receptor subunit large cytoplasmic loop sequences in receptor expression and function." J Pharmacol Exp Ther **314**(1): 455-66.

Kuryatov, A., J. Luo, *et al.* (2005). "Nicotine acts as a pharmacological chaperone to up-regulate human alpha4beta2 acetylcholine receptors." Mol Pharmacol **68**(6): 1839-51.

Kuryatov, A., F. A. Olale, *et al.* (2000). "Acetylcholine receptor extracellular domain determines sensitivity to nicotine-induced inactivation." Eur J Pharmacol **393**(1-3): 11-21.

Kuryatov, A., J. Onksen, *et al.* (2008). "Roles of accessory subunits in alpha4beta2(*) nicotinic receptors." Mol Pharmacol **74**(1): 132-43.

Labarca, C., M. W. Nowak, *et al.* (1995). "Channel gating governed symmetrically by conserved leucine residues in the M2 domain of nicotinic receptors." Nature **376**(6540): 514-6.

Lai, A., N. Parameswaran, *et al.* (2005). "Long-term nicotine treatment decreases striatal alpha 6* nicotinic acetylcholine receptor sites and function in mice." Mol Pharmacol **67**(5): 1639-47.

Lai, A., J. Sum, *et al.* (2004). "Selective recovery of striatal 125I-alpha-conotoxinmii nicotinic receptors after nigrostriatal damage in monkeys." Neuroscience **127**(2): 399-408.

Langenbuch-Cachat, J., C. Bon, *et al.* (1988). "Photoaffinity labeling of the acetylcholine binding sites on the nicotinic receptor by an aryldiazonium derivative." Biochemistry **27**(7): 2337-45.

Lape, R., D. Colquhoun, *et al.* (2008). "On the nature of partial agonism in the nicotinic receptor superfamily." Nature **454**(7205): 722-7.

Laviolette, S. R. and D. van der Kooy (2003). "The motivational valence of nicotine in the rat ventral tegmental area is switched from rewarding to aversive following blockade of the alpha7-subunit-containing nicotinic acetylcholine receptor." Psychopharmacology (Berl) **166**(3): 306-13.

Law, R. J., R. H. Henchman, *et al.* (2005). "A gating mechanism proposed from a simulation of a human alpha7 nicotinic acetylcholine receptor." Proc Natl Acad Sci USA **102**(19): 6813-8.

Lee, W. Y., C. R. Free, *et al.* (2009). "Binding to gating transduction in nicotinic receptors: Cys-loop energetically couples to pre-M1 and M2-M3 regions." J Neurosci **29**(10): 3189-99.

Lee, W. Y. and S. M. Sine (2004). "Invariant aspartic Acid in muscle nicotinic receptor contributes selectively to the kinetics of agonist binding." J Gen Physiol **124**(5): 555-67.

Lee, W. Y. and S. M. Sine (2005). "Principal pathway coupling agonist binding to channel gating in nicotinic receptors." Nature **438**(7065): 243-7.

Lena, C., J. P. Changeux, *et al.* (1993). "Evidence for "preterminal" nicotinic receptors on GABAergic axons in the rat interpeduncular nucleus." J Neurosci **13**(6): 2680-8.

Leniger, T., C. Kananura, *et al.* (2003). "A new Chrna4 mutation with low penetrance in nocturnal frontal lobe epilepsy." Epilepsia **44**(7): 981-5.

Le Novere, N. and J. P. Changeux (2001). "The ligand gated ion channel database: an example of a sequence database in neuroscience." Philos Trans R Soc Lond B Biol Sci **356**(1412): 1121-30.

Le Novere, N., P. J. Corringer, *et al.* (1999). "Improved secondary structure predictions for a nicotinic receptor subunit: incorporation of solvent accessibility and experimental data into a two-dimensional representation." Biophys J **76**(5): 2329-45.

Le Novere, N., P. J. Corringer, *et al.* (2002). "The diversity of subunit composition in nAChRs: evolutionary origins, physiologic and pharmacologic consequences." J Neurobiol **53**(4): 447-56.

Leonard, R. J., C. G. Labarca, *et al.* (1988). "Evidence that the M2 membrane-spanning region lines the ion channel pore of the nicotinic receptor." Science **242**(4885): 1578-81.

Leonard, S., C. Adams, *et al.* (1996). "Nicotinic receptor function in schizophrenia." Schizophr Bull **22**(3): 431-45.

Leonard, S., L. E. Adler, *et al.* (2001). "Smoking and mental illness." Pharmacol Biochem Behav **70**(4): 561-70.

Lewis T. M., P. C. Harkness, *et al.* (1997). "The ion channel properties of a rat recombinant neuronal nicotinic receptor are dependent on the host cell type." J Physiol. **505 (Pt 2)**:299-306.

Lindstrom, J. (1997). "Nicotinic acetylcholine receptors in health and disease." Mol Neurobiol **15**(2): 193-222.

Lindstrom, J. M. (2000). "Acetylcholine receptors and myasthenia." Muscle Nerve **23**(4): 453-77.

Lipovsek, M., P. Plazas, *et al.* (2008). "Properties of mutated murine alpha4beta2 nicotinic receptors linked to partial epilepsy." Neurosci Lett **434**(2): 165-9.

Lohr, J. B. and K. Flynn (1992). "Smoking and schizophrenia." Schizophr Res **8**(2): 93-102.

Lopez, M. G., R. I. Fonteriz, *et al.* (1993). "The nicotinic acetylcholine receptor of the bovine chromaffin cell, a new target for dihydropyridines." Eur J Pharmacol **247**(2): 199-207.

Lopez-Hernandez, G. Y., J. Sanchez-Padilla, *et al.* (2004). "Nicotine-induced up-regulation and desensitization of alpha4beta2 neuronal nicotinic receptors depend on subunit ratio." J Biol Chem **279**(36): 38007-15.

Loscher, W., H. Potschka, *et al.* (2003). "Are neuronal nicotinic receptors a target for antiepileptic drug development? Studies in different seizure models in mice and rats." Eur J Pharmacol **466**(1-2): 99-111.

Lu, Y., S. Grady, *et al.* (1998). "Pharmacological characterization of nicotinic receptor-stimulated GABA release from mouse brain synaptosomes." J Pharmacol Exp Ther **287**(2): 648-57.

Luetje, C. W. and J. Patrick (1991). "Both alpha- and beta-subunits contribute to the agonist sensitivity of neuronal nicotinic acetylcholine receptors." J Neurosci **11**(3): 837-45.

Luetje, C. W., K. Wada, *et al.* (1990). "Neurotoxins distinguish between different neuronal nicotinic acetylcholine receptor subunit combinations." J Neurochem **55**(2): 632-40.

Lummis, S. C., D. L. Beene, *et al.* (2005). "Cis-trans isomerization at a proline opens the pore of a neurotransmitter-gated ion channel." Nature **438**(7065): 248-52.

Luo, S., J. M. Kulak, *et al.* (1998). "Alpha-conotoxin AuIB selectively blocks alpha3 beta4 nicotinic acetylcholine receptors and nicotine-evoked norepinephrine release." J Neurosci **18**(21): 8571-9.

Lyford, L. K., A. D. Sproul, *et al.* (2003). "Agonist-induced conformational changes in the extracellular domain of alpha 7 nicotinic acetylcholine receptors." Mol Pharmacol **64**(3): 650-8.

Macklin, K. D., A. D. Maus, *et al.* (1998). "Human vascular endothelial cells express functional nicotinic acetylcholine receptors." J Pharmacol Exp Ther **287**(1): 435-9.

Maelicke, A. Schrattenholz and E.X. Albuquerque (2000). "Neuronal nicotinic acetylcholine receptors in non-neuronal cells, expression and renaturation of ligand binding domain, and modulatory control by allosterically acting ligands." In: F. Clementi, D. Fornasari and C. Gotti, Editors, Handbook of Experimental Pharmacology Vol. Neuronal Nicotinic Receptors, Springer, Berlin (2000), pp. 477–496.

Magnusson, A., E. Stordal, *et al.* (2003). "Schizophrenia, psychotic illness and other psychiatric symptoms in families with autosomal dominant nocturnal frontal lobe epilepsy caused by different mutations." Psychiatr Genet **13**(2): 91-5.

Mansvelder, H. D., J. R. Keath, *et al.* (2002). "Synaptic mechanisms underlie nicotine-induced excitability of brain reward areas." Neuron **33**(6): 905-19.

Mansvelder, H. D. and D. S. McGehee (2000). "Long-term potentiation of excitatory inputs to brain reward areas by nicotine." Neuron **27**(2): 349-57.

Mansvelder, H. D. and D. S. McGehee (2002). "Cellular and synaptic mechanisms of nicotine addiction." J Neurobiol **53**(4): 606-17.

Marks, M. J., J. B. Burch, *et al.* (1983). "Effects of chronic nicotine infusion on tolerance development and nicotinic receptors." J Pharmacol Exp Ther **226**(3): 817-25.

Marks, M. J., J. R. Pauly, *et al.* (1992). "Nicotine binding and nicotinic receptor subunit RNA after chronic nicotine treatment." J Neurosci **12**(7): 2765-84.

Marks, M. J., P. Whiteaker, *et al.* (1999). "Two pharmacologically distinct components of nicotinic receptor-mediated rubidium efflux in mouse brain require the beta2 subunit." J Pharmacol Exp Ther **289**(2): 1090-103.

Martin, M., C. Czajkowski, *et al.* (1996). "The contributions of aspartyl residues in the acetylcholine receptor gamma and delta subunits to the binding of agonists and competitive antagonists." J Biol Chem **271**(23): 13497-503.

Martin-Ruiz, C., J. Court, *et al.* (2000). "Nicotinic receptors in dementia of Alzheimer, Lewy body and vascular types." Acta Neurol Scand Suppl **176**: 34-41.

Martin-Ruiz, C. M., V. H. Haroutunian, *et al.* (2003). "Dementia rating and nicotinic receptor expression in the prefrontal cortex in schizophrenia." Biol Psychiatry **54**(11): 1222-33.

Marubio, L. M., M. del Mar Arroyo-Jimenez, *et al.* (1999). "Reduced antinociception in mice lacking neuronal nicotinic receptor subunits." Nature **398**(6730): 805-10.

Marutle, A., U. Warpman, *et al.* (1998). "Regional distribution of subtypes of nicotinic receptors in human brain and effect of aging studied by (+/-)-[^{3}H]epibatidine." Brain Res **801**(1-2): 143-9.

Matsushima, N., S. Hirose, *et al.* (2002). "Mutation (Ser284Leu) of neuronal nicotinic acetylcholine receptor alpha 4 subunit associated with frontal lobe epilepsy causes faster desensitization of the rat receptor expressed in oocytes." Epilepsy Res **48**(3): 181-6.

McCallum, S. E., N. Parameswaran, *et al.* (2006). "Increases in alpha4* but not alpha3*/alpha6* nicotinic receptor sites and function in the primate striatum following chronic oral nicotine treatment." J Neurochem **96**(4): 1028-41.

McColl, C. D., M. K. Horne, *et al.* (2003). "Electroencephalographic characterisation of pentylenetetrazole-induced seizures in mice lacking the alpha 4 subunit of the neuronal nicotinic receptor." Neuropharmacology **44**(2): 234-43.

McGehee, D. S., M. J. Heath, *et al.* (1995). "Nicotine enhancement of fast excitatory synaptic transmission in CNS by presynaptic receptors." Science **269**(5231): 1692-6.

McGehee, D. S. and L. W. Role (1995). "Physiological diversity of nicotinic acetylcholine receptors expressed by vertebrate neurons." Annu Rev Physiol **57**: 521-46.

McIntosh, J. M., A. D. Santos, *et al.* (1999). "Conus peptides targeted to specific nicotinic acetylcholine receptor subtypes." Annu Rev Biochem **68**: 59-88.

McNamara, J. O. (1999). "Emerging insights into the genesis of epilepsy." Nature **399**(6738 Suppl): A15-22.

Meyer, E. L., Y. Xiao, *et al.* (2001). "Agonist regulation of rat alpha 3 beta 4 nicotinic acetylcholine receptors stably expressed in human embryonic kidney 293 cells." Mol Pharmacol **60**(3): 568-76.

Middleton, R. E. and J. B. Cohen (1991). "Mapping of the acetylcholine binding site of the nicotinic acetylcholine receptor: [3H]nicotine as an agonist photoaffinity label." Biochemistry **30**(28): 6987-97.

Mike, A., N. G. Castro, *et al.* (2000). "Choline and acetylcholine have similar kinetic properties of activation and desensitization on the alpha7 nicotinic receptors in rat hippocampal neurons." Brain Res **882**(1-2): 155-68.

Millar, N. S. and C. Gotti (2009). "Diversity of vertebrate nicotinic acetylcholine receptors." Neuropharmacology **56**(1): 237-46.

Minier, F. and E. Sigel (2004a). "Positioning of the alpha-subunit isoforms confers a functional signature to gamma-aminobutyric acid type A receptors." Proc Natl Acad Sci USA **101**(20): 7769-74.

Minier, F. and E. Sigel (2004b). "Techniques: use of concatenated subunits for the study of ligand-gated ion channels." Trends Pharmacol Sci **25**(9): 499-503.

Mitra, A., T. D. Bailey, *et al.* (2004). "Structural dynamics of the M4 transmembrane segment during acetylcholine receptor gating." Structure **12**(10): 1909-18.

Miyazawa, A., Y. Fujiyoshi, *et al.* (2003). "Structure and gating mechanism of the acetylcholine receptor pore." Nature **423**(6943): 949-55.

Moretti, M., S. Vailati, *et al.* (2004). "Nicotinic acetylcholine receptor subtypes expression during rat retina development and their regulation by visual experience." Mol Pharmacol **66**(1): 85-96.

Moroni, M., R. Zwart, *et al.* (2006). "Alpha4beta2 nicotinic receptors with high and low acetylcholine sensitivity: pharmacology, stoichiometry, and sensitivity to long-term exposure to nicotine." Mol Pharmacol **70**(2): 755-68.

Moroni, M., R. Vijayan, *et al.* (2008). "Non-agonist-binding subunit interfaces confer distinct functional signatures to the alternate stoichiometries of the alpha4beta2 nicotinic receptor: an alpha4-alpha4 interface is required for Zn^{2+} potentiation." J Neurosci **28**(27): 6884-94.

Mugnaini, M., M. Garzotti, *et al.* (2006). "Selective down-regulation of [(125)I]Y0-alpha-conotoxin MII binding in rat mesostriatal dopamine pathway following continuous infusion of nicotine." Neuroscience **137**(2): 565-72.

Mukhtasimova, N., C. Free, *et al.* (2005). "Initial coupling of binding to gating mediated by conserved residues in the muscle nicotinic receptor." J Gen Physiol **126**(1): 23-39.

Mukhtasimova, N. and S. M. Sine (2007). "An intersubunit trigger of channel gating in the muscle nicotinic receptor." J Neurosci **27**(15): 4110-9.

Mulle, C., C. Lena, *et al.* (1992). "Potentiation of nicotinic receptor response by external calcium in rat central neurons." Neuron **8**(5): 937-45.

Nashmi, R., M. E. Dickinson, *et al.* (2003). "Assembly of alpha4beta2 nicotinic acetylcholine receptors assessed with functional fluorescently labeled subunits: effects of localization, trafficking, and nicotine-induced upregulation in clonal mammalian cells and in cultured midbrain neurons." J Neurosci **23**(37): 11554-67.

Nelson, M. E., A. Kuryatov, *et al.* (2003). "Alternate stoichiometries of alpha4beta2 nicotinic acetylcholine receptors." Mol Pharmacol **63**(2): 332-41.

Newbolt A., R. Stoop, *et al.* (1998) "Membrane topology of an ATP-gated ion channel (P2X receptor)." J Biol Chem. **273(24)**:15177-82.

Nicke, A., J. Rettinger, *et al.* (2003). "Monomeric and dimeric byproducts are the principal functional elements of higher order P2X1 concatamers." Mol Pharmacol **63**(1): 243-52.

Nowak, M. W., P. C. Kearney, *et al.* (1995). "Nicotinic receptor binding site probed with unnatural amino acid incorporation in intact cells." Science **268**(5209): 439-42.

Oakman, S. A., P. L. Faris, *et al.* (1995). "Distribution of pontomesencephalic cholinergic neurons projecting to substantia nigra differs significantly from those projecting to ventral tegmental area." J Neurosci **15**(9): 5859-69.

O'Kelly, I., M. H. Butler, *et al.* (2002). "Forward transport. 14-3-3 binding overcomes retention in endoplasmic reticulum by dibasic signals." Cell **111**(4): 577-88.

Oldani, A., M. Zucconi, *et al.* (1998). "Autosomal dominant nocturnal frontal lobe epilepsy. A video-polysomnographic and genetic appraisal of 40 patients and delineation of the epileptic syndrome." Brain **121 (Pt 2)**: 205-23.

Oswald, R. E. and J. P. Changeux (1982). "Crosslinking of alpha-bungarotoxin to the acetylcholine receptor from *Torpedo marmorata* by ultraviolet light irradiation." FEBS Lett **139**(2): 225-9.

Paas, Y., G. Gibor, *et al.* (2005). "Pore conformations and gating mechanism of a Cys-loop receptor." Proc Natl Acad Sci USA **102**(44): 15877-82.

Pacheco, M. A., T. E. Pastoor, *et al.* (2003). "Phosphorylation of the alpha4 subunit of human alpha4beta2 nicotinic receptors: role of cAMP-dependent protein kinase (PKA) and protein kinase C (PKC)." Brain Res Mol Brain Res **114**(1): 65-72.

Panicker, S., H. Cruz, *et al.* (2002). "Evidence for a centrally located gate in the pore of a serotonin-gated ion channel." J Neurosci **22**(5): 1629-39.

Papke, R. L., J. Boulter, *et al.* (1989). "Single-channel currents of rat neuronal nicotinic acetylcholine receptors expressed in *Xenopus* oocytes." Neuron **3**(5): 589-96.

Papke, R. L. and S. F. Heinemann (1994). "Partial agonist properties of cytisine on neuronal nicotinic receptors containing the beta 2 subunit." Mol Pharmacol **45**(1): 142-9.

Paradiso, K. G. and J. H. Steinbach (2003). "Nicotine is highly effective at producing desensitization of rat alpha4beta2 neuronal nicotinic receptors." J Physiol **553**(Pt 3): 857-71.

Parker, S. L., Y. Fu, *et al.* (2004). "Up-regulation of brain nicotinic acetylcholine receptors in the rat during long-term self-administration of nicotine: disproportionate increase of the alpha6 subunit." Mol Pharmacol **65**(3): 611-22.

Paterson, D. and A. Nordberg (2000). "Neuronal nicotinic receptors in the human brain." Prog Neurobiol **61**(1): 75-111.

Patkar, A. A., R. Gopalakrishnan, *et al.* (2002). "Relationship between tobacco smoking and positive and negative symptoms in schizophrenia." J Nerv Ment Dis **190**(9): 604-10.

Paulson, H. L., A. F. Ross, *et al.* (1991). "Analysis of early events in acetylcholine receptor assembly." J Cell Biol **113**(6): 1371-84.

Pauly, J. R. and A. C. Collins (1993). "An autoradiographic analysis of alterations in nicotinic cholinergic receptors following 1 week of corticosterone supplementation." Neuroendocrinology **57**(2): 262-71.

Pedersen, S. E. and J. B. Cohen (1990). "d-Tubocurarine binding sites are located at alpha-gamma and alpha-delta subunit interfaces of the nicotinic acetylcholine receptor." Proc Natl Acad Sci USA **87**(7): 2785-9.

Pedersen, S. E., S. D. Sharp, *et al.* (1992). "Structure of the noncompetitive antagonist-binding site of the *Torpedo* nicotinic acetylcholine receptor. [3H]meproadifen mustard reacts selectively with alpha-subunit Glu-262." J Biol Chem **267**(15): 10489-99.

Peng, X., V. Gerzanich, *et al.* (1997). "Chronic nicotine treatment up-regulates alpha3 and alpha7 acetylcholine receptor subtypes expressed by the human neuroblastoma cell line SH-SY5Y." Mol Pharmacol **51**(5): 776-84.

Pereira, E. F., S. Reinhardt-Maelicke, *et al.* (1993). "Identification and functional characterization of a new agonist site on nicotinic acetylcholine receptors of cultured hippocampal neurons." J Pharmacol Exp Ther **265**(3): 1474-91.

Perry, D. C., M. I. Davila-Garcia, *et al.* (1999). "Increased nicotinic receptors in brains from smokers: membrane binding and autoradiography studies." J Pharmacol Exp Ther **289**(3): 1545-52.

Perry, E. K., J. A. Court, *et al.* (1992). "Autoradiographic distribution of [3H]nicotine binding in human cortex: relative abundance in subicular complex." J Chem Neuroanat **5**(5): 399-405.

Perry, E. K., C. M. Martin-Ruiz, *et al.* (2001). "Nicotinic receptor subtypes in human brain related to aging and dementia." Alcohol **24**(2): 63-8.

Perry, E. K., C. M. Morris, *et al.* (1995). "Alteration in nicotine binding sites in Parkinson's disease, Lewy body dementia and Alzheimer's disease: possible index of early neuropathology." Neuroscience **64**(2): 385-95.

Phillips, H. A., I. Favre, *et al.* (2001). "CHRNB2 is the second acetylcholine receptor subunit associated with autosomal dominant nocturnal frontal lobe epilepsy." Am J Hum Genet **68**(1): 225-31.

Picard, F., S. Bertrand, *et al.* (1999). "Mutated nicotinic receptors responsible for autosomal dominant nocturnal frontal lobe epilepsy are more sensitive to carbamazepine." Epilepsia **40**(9): 1198-209.

Picciotto, M. R. (2003). "Nicotine as a modulator of behavior: beyond the inverted U." Trends Pharmacol Sci **24**(9): 493-9.

Picciotto, M. R., D. H. Brunzell, *et al.* (2002). "Effect of nicotine and nicotinic receptors on anxiety and depression." Neuroreport **13**(9): 1097-106.

Picciotto, M. R., M. Zoli, *et al.* (1995). "Abnormal avoidance learning in mice lacking functional high-affinity nicotine receptor in the brain." Nature **374**(6517): 65-7.

Picciotto, M. R., M. Zoli, *et al.* (1998). "Acetylcholine receptors containing the beta2 subunit are involved in the reinforcing properties of nicotine." Nature **391**(6663): 173-7.

Pidoplichko, V. I., M. DeBiasi, *et al.* (1997). "Nicotine activates and desensitizes midbrain dopamine neurons." Nature **390**(6658): 401-4.

Placzek, A. N., F. Grassi, *et al.* (2004). "A single point mutation confers properties of the muscle-type nicotinic acetylcholine receptor to homomeric alpha7 receptors." Mol Pharmacol **66**(1): 169-77.

Plazas, P. V., E. Katz, *et al.* (2005). "Stoichiometry of the alpha9alpha10 nicotinic cholinergic receptor." J Neurosci **25**(47): 10905-12.

Poirier, J. (2002). "Evidence that the clinical effects of cholinesterase inhibitors are related to potency and targeting of action." Int J Clin Pract Suppl(127): 6-19.

Provini, F., G. Plazzi, *et al.* (2000). "The wide clinical spectrum of nocturnal frontal lobe epilepsy." Sleep Med Rev **4**(4): 375-386.

Pugh, P. C. and D. K. Berg (1994). "Neuronal acetylcholine receptors that bind alpha-bungarotoxin mediate neurite retraction in a calcium-dependent manner." J Neurosci **14**(2): 889-96.

Purohit, P., A. Mitra, *et al.* (2007). "A stepwise mechanism for acetylcholine receptor channel gating." Nature **446**(7138): 930-3.

Quick, M. W. and R. A. Lester (2002). "Desensitization of neuronal nicotinic receptors." J Neurobiol **53**(4): 457-78.

Quik M., J. M.Kulak (2002). "Nicotine and nicotinic receptors; relevance to Parkinson's disease." Neurotoxicology. **23(4-5)**:581-94.

Raggenbass, M. and D. Bertrand (2002). "Nicotinic receptors in circuit excitability and epilepsy." J Neurobiol **53**(4): 580-9.

Ragozzino, D., S. Fucile, *et al.* (1997). "Functional properties of neuronal nicotinic acetylcholine receptor channels expressed in transfected human cells." Eur J Neurosci **9**(3): 480-8.

Ramirez-Latorre, J., C. R. Yu, *et al.* (1996). "Functional contributions of alpha5 subunit to neuronal acetylcholine receptor channels." Nature **380**(6572): 347-51.

Ramón y Cajal, S. (1888). "Estructura de los centros nerviosos de las aves." Rev. Trim. Histol. Norm. Patol. 1, pp. 1–10.

Ren, X. Q., S. B. Cheng, *et al.* (2005). "Structural determinants of alpha4beta2 nicotinic acetylcholine receptor trafficking." J Neurosci **25**(28): 6676-86.

Revah, F., D. Bertrand, *et al.* (1991). "Mutations in the channel domain alter desensitization of a neuronal nicotinic receptor." Nature **353**(6347): 846-9.

Rezvani, K., Y. Teng, *et al.* (2007). "Nicotine regulates multiple synaptic proteins by inhibiting proteasomal activity." J Neurosci **27**(39): 10508-19.

Robinson, S. F., E. U. Grun, *et al.* (1996). "Changes in sensitivity to nicotine and brain nicotinic receptors following chronic nicotine and corticosterone treatments in mice." Pharmacol Biochem Behav **54**(3): 587-93.

Roccamo, A. M. and F. J. Barrantes (2007). "Charged amino acid motifs flanking each extreme of the alphaM4 transmembrane domain are involved in assembly and cell-surface targeting of the muscle nicotinic acetylcholine receptor." J Neurosci Res **85**(2): 285-93.

Rodrigues-Pinguet, N., L. Jia, *et al.* (2003). "Five ADNFLE mutations reduce the Ca2+ dependence of the mammalian alpha4beta2 acetylcholine response." J Physiol **550**(Pt 1): 11-26.

Rodrigues-Pinguet, N. O., T. J. Pinguet, *et al.* (2005). "Mutations linked to autosomal dominant nocturnal frontal lobe epilepsy affect allosteric Ca^{2+} activation of the alpha 4 beta 2 nicotinic acetylcholine receptor." Mol Pharmacol **68**(2): 487-501.

Roerig, B., D. A. Nelson, *et al.* (1997). "Fast synaptic signaling by nicotinic acetylcholine and serotonin 5-HT3 receptors in developing visual cortex." J Neurosci **17**(21): 8353-62.

Rogers, S. W., A. Mandelzys, *et al.* (1992). "The expression of nicotinic acetylcholine receptors by PC12 cells treated with NGF." J Neurosci **12**(12): 4611-23.

Role, L. W. and D. K. Berg (1996). "Nicotinic receptors in the development and modulation of CNS synapses." Neuron **16**(6): 1077-85.

Rubboli, F., J. A. Court, *et al.* (1994). "Distribution of nicotinic receptors in the human hippocampus and thalamus." Eur J Neurosci **6**(10): 1596-604.

Rusted, J. M., P. A. Newhouse, *et al.* (2000). "Nicotinic treatment for degenerative neuropsychiatric disorders such as Alzheimer's disease and Parkinson's disease." Behav Brain Res **113**(1-2): 121-9.

Sala, C., I. Kimura, *et al.* (1996). "Expression of two neuronal nicotinic receptor subunits in innervated and denervated adult rat muscle." Neurosci Lett **215**(2): 71-4.

Sala, F., J. Mulet, *et al.* (2005). "Charged amino acids of the N-terminal domain are involved in coupling binding and gating in alpha7 nicotinic receptors." J Biol Chem **280**(8): 6642-7.

Sallette, J., S. Bohler, *et al.* (2004). "An extracellular protein microdomain controls up-regulation of neuronal nicotinic acetylcholine receptors by nicotine." J Biol Chem **279**(18): 18767-75.

Sallette, J., S. Pons, *et al.* (2005). "Nicotine upregulates its own receptors through enhanced intracellular maturation." Neuron **46**(4): 595-607.

Sambrook, J., Fritsch, E.F., and Maniatis, T. (1989). "Molecular cloning: a laboratory manual." Cold Spring Harbor Laboratory Press, NY, Vol. 1, Chapter 1, 5

Scheffer, I. E., K. P. Bhatia, *et al.* (1995). "Autosomal dominant nocturnal frontal lobe epilepsy. A distinctive clinical disorder." Brain **118 (Pt 1)**: 61-73.

Schoepfer, R., P. Whiting, *et al.* (1988). "cDNA clones coding for the structural subunit of a chicken brain nicotinic acetylcholine receptor." Neuron **1**(3): 241-8.

Seerden, J. P., M. T. Tulp, *et al.* (1998). "Synthesis and structure-activity data of some new epibatidine analogues." Bioorg Med Chem **6**(11): 2103-10.

Sgard, F., E. Charpantier, *et al.* (2002). "A novel human nicotinic receptor subunit, alpha10, that confers functionality to the alpha9-subunit." Mol Pharmacol **61**(1): 150-9.

Sharma, G. and S. Vijayaraghavan (2002). "Nicotinic receptor signaling in nonexcitable cells." J Neurobiol **53**(4): 524-34.

Sharma, G. and S. Vijayaraghavan (2003). "Modulation of presynaptic store calcium induces release of glutamate and postsynaptic firing." Neuron **38**(6): 929-39.

Sherrington, C.S. (1897) in Textbook of Physiology (Foster, M., ed.), p. 60

Shoop, R. D., N. Yamada, *et al.* (2000). "Cytoskeletal links of neuronal acetylcholine receptors containing alpha 7 subunits." J Neurosci **20**(11): 4021-9.

Shytle, R. D., A. A. Silver, *et al.* (2002). "Neuronal nicotinic receptor inhibition for treating mood disorders: preliminary controlled evidence with mecamylamine." Depress Anxiety **16**(3): 89-92.

Sigel, E. (2002). "Mapping of the benzodiazepine recognition site on GABA(A) receptors." Curr Top Med Chem **2**(8): 833-9.

Sigel, E., R. Baur, *et al.* (2006). "Impact of subunit positioning on GABAA receptor function." Biochem Soc Trans **34**(Pt 5): 868-71.

Sihver, W., P. G. Gillberg, *et al.* (1998). "Laminar distribution of nicotinic receptor subtypes in human cerebral cortex as determined by [3H](-)nicotine, [3H]cytisine and [^{3}H]epibatidine in vitro autoradiography." Neuroscience **85**(4): 1121-33.

Sine, S. M. (2002). "The nicotinic receptor ligand binding domain." J Neurobiol **53**(4): 431-46.

Sine, S. M. and T. Claudio (1991). "Gamma- and delta-subunits regulate the affinity and the cooperativity of ligand binding to the acetylcholine receptor." J Biol Chem **266**(29): 19369-77.

Sine, S. M. and A. G. Engel (2006). "Recent advances in Cys-loop receptor structure and function." Nature **440**(7083): 448-55.

Sine, S. M., P. Quiram, *et al.* (1994). "Conserved tyrosines in the alpha subunit of the nicotinic acetylcholine receptor stabilize quaternary ammonium groups of agonists and curariform antagonists." J Biol Chem **269**(12): 8808-16.

Skok, M., E. Lykhmus, *et al.* (2001). "Structure of epitopes recognized by the antibodies to alpha(181-192) peptides of neuronal nicotinic acetylcholine receptors: extrapolation to the structure of acetylcholine-binding domain." J Neuroimmunol **121**(1-2): 59-66.

Slater, Y. E., L. M. Houlihan, *et al.* (2003). "Halogenated cytisine derivatives as agonists at human neuronal nicotinic acetylcholine receptor subtypes." Neuropharmacology **44**(4): 503-15.

Smit, A. B., N. I. Syed, *et al.* (2001). "A glia-derived acetylcholine-binding protein that modulates synaptic transmission." Nature **411**(6835): 261-8.

Smith, M. M., J. Lindstrom, *et al.* (1987). "Formation of the alpha-bungarotoxin binding site and assembly of the nicotinic acetylcholine receptor subunits occur in the endoplasmic reticulum." J Biol Chem **262**(9): 4367-76.

Smulders, C. J., R. Zwart, *et al.* (2005). "Cholinergic drugs potentiate human nicotinic alpha4beta2 acetylcholine receptors by a competitive mechanism." Eur J Pharmacol **509**(2-3): 97-108.

Soliakov, L. and S. Wonnacott (1996). "Voltage-sensitive Ca^{2+} channels involved in nicotinic receptor-mediated [^{3}H]dopamine release from rat striatal synaptosomes." J Neurochem **67**(1): 163-70.

Son, C. D., F. J. Moss, *et al.* (2009). "Nicotine normalizes intracellular subunit stoichiometry of nicotinic receptors carrying mutations linked to autosomal dominant nocturnal frontal lobe epilepsy." Mol Pharmacol **75**(5): 1137-48.

Sparks, D. L., T. G. Beach, *et al.* (1998). "Immunohistochemical localization of nicotinic beta2 and alpha4 receptor subunits in normal human brain and individuals with Lewy body and Alzheimer's disease: preliminary observations." Neurosci Lett **256**(3): 151-4.

Spande T. F, Martin-Garraffo H., Edwards M. W., *et al.* (1992). "Epibatidine: a novel (chloropyridyl)azabicycloheptane with potent analgesic activity from an Ecuadoran poison frog." J Am Chem Soc **114**(9): 3475–78.

Spurden, D. P., J. A. Court, *et al.* (1997). "Nicotinic receptor distribution in the human thalamus: autoradiographical localization of [3H]nicotine and [125I] alpha-bungarotoxin binding." J Chem Neuroanat **13**(2): 105-13.

Steinlein, O. K. (2004). "Nicotinic receptor mutations in human epilepsy." Prog Brain Res **145**: 275-85.

Steinlein, O. K., A. Magnusson, *et al.* (1997). "An insertion mutation of the CHRNA4 gene in a family with autosomal dominant nocturnal frontal lobe epilepsy." Hum Mol Genet **6**(6): 943-7.

Steinlein, O. K., J. C. Mulley, *et al.* (1995). "A missense mutation in the neuronal nicotinic acetylcholine receptor alpha 4 subunit is associated with autosomal dominant nocturnal frontal lobe epilepsy." Nat Genet **11**(2): 201-3.

Steriade, M. and D. Contreras (1995). "Relations between cortical and thalamic cellular events during transition from sleep patterns to paroxysmal activity." J Neurosci **15**(1 Pt 2): 623-42.

Stitzel, J. A., P. Dobelis, *et al.* (2001). "Long sleep and short sleep mice differ in nicotine-stimulated $^{86}Rb^{+}$ efflux and alpha4 nicotinic receptor subunit cDNA sequence." Pharmacogenetics **11**(4): 331-9.

Swanson, K. L. and E. X. Albuquerque (1987). "Nicotinic acetylcholine receptor ion channel blockade by cocaine: the mechanism of synaptic action." J Pharmacol Exp Ther **243**(3): 1202-10.

Swanson, K. L. and E. X. Albuquerque (1992). "Progress in understanding the nicotinic acetylcholine receptor function at central and peripheral nervous system synapses through toxin interactions." Md Med J **41**(7): 623-31.

Taly, A., M. Delarue, *et al.* (2005). "Normal mode analysis suggests a quaternary twist model for the nicotinic receptor gating mechanism." Biophys J **88**(6): 3954-65.

Tapia, L., A. Kuryatov, *et al.* (2007). "Ca^{2+} permeability of the $(alpha4)_3(beta2)_2$ stoichiometry greatly exceeds that of $(alpha4)_2(beta2)_3$ human acetylcholine receptors." Mol Pharmacol **71**(3): 769-76.

Temburni, M. K., R. C. Blitzblau, *et al.* (2000). "Receptor targeting and heterogeneity at interneuronal nicotinic cholinergic synapses *in vivo*." J Physiol **525 Pt 1**: 21-9.

Thomas, P., M. Stephens, *et al.* (1993). "(+)-Anatoxin-a is a potent agonist at neuronal nicotinic acetylcholine receptors." J Neurochem **60**(6): 2308-11.

Timmermann, D. B., J. H. Gronlien, *et al.* (2007). "An allosteric modulator of the alpha7 nicotinic acetylcholine receptor possessing cognition-enhancing properties *in vivo*." J Pharmacol Exp Ther **323**(1): 294-307.

Tomaselli, G. F., J. T. McLaughlin, *et al.* (1991). "Mutations affecting agonist sensitivity of the nicotinic acetylcholine receptor." Biophys J **60**(3): 721-7.

Triggle D. J., C. R. Triggle (1976). "Chemical pharmacology of the synapse." Academic Press

Tritto, T., J. A. Stitzel, *et al.* (2002). "Variability in response to nicotine in the LSxSS RI strains: potential role of polymorphisms in alpha4 and alpha6 nicotinic receptor genes." Pharmacogenetics **12**(3): 197-208.

Tumkosit, P., A. Kuryatov, *et al.* (2006). "Beta3 subunits promote expression and nicotine-induced up-regulation of human nicotinic alpha6* nicotinic acetylcholine receptors expressed in transfected cell lines." Mol Pharmacol **70**(4): 1358-68.

Turner, T. J. (2004). "Nicotine enhancement of dopamine release by a calcium-dependent increase in the size of the readily releasable pool of synaptic vesicles." J Neurosci **24**(50): 11328-36.

Tzartos, S. J., T. Barkas, *et al.* (1998). "Anatomy of the antigenic structure of a large membrane autoantigen, the muscle-type nicotinic acetylcholine receptor." Immunol Rev **163**: 89-120.

Ulens, C., R. C. Hogg, *et al.* (2006). "Structural determinants of selective alpha-conotoxin binding to a nicotinic acetylcholine receptor homolog AChBP." Proc Natl Acad Sci USA **103**(10): 3615-20.

Unwin, N. (1995). "Acetylcholine receptor channel imaged in the open state." Nature **373**(6509): 37-43.

Unwin, N. (2005). "Refined structure of the nicotinic acetylcholine receptor at 4A resolution." J Mol Biol **346**(4): 967-89.

Unwin, N., A. Miyazawa, *et al.* (2002). "Activation of the nicotinic acetylcholine receptor involves a switch in conformation of the alpha subunits." J Mol Biol **319**(5): 1165-76.

Unwin, N., C. Toyoshima, *et al.* (1988). "Arrangement of the acetylcholine receptor subunits in the resting and desensitized states, determined by cryoelectron microscopy of crystallized *Torpedo* postsynaptic membranes." J Cell Biol **107**(3): 1123-38.

Valor, L. M., A. Campos-Caro, *et al.* (2002). "Transcription factors NF-Y and Sp1 are important determinants of the promoter activity of the bovine and human neuronal nicotinic receptor beta 4 subunit genes." J Biol Chem **277**(11): 8866-76.

Vallejo Y. F., B. Buisson et al. (2005). "Chronic nicotine exposure upregulates nicotinic receptors by a novel mechanism." J Neurosci. **25(23)**:5563-72.

Varnum M. D., W. N. Zagotta (1996). "Subunit interactions in the activation of cyclic nucleotide-gated ion channels." Biophys J. **70(6)**:2667-79.

Verrall, S. and Z. W. Hall (1992). "The N-terminal domains of acetylcholine receptor subunits contain recognition signals for the initial steps of receptor assembly." Cell **68**(1): 23-31.

Vetter, D. E., E. Katz, *et al.* (2007). "The alpha10 nicotinic acetylcholine receptor subunit is required for normal synaptic function and integrity of the olivocochlear system." Proc Natl Acad Sci USA **104**(51): 20594-9.

Vetter, D. E., M. C. Liberman, *et al.* (1999). "Role of alpha9 nicotinic ACh receptor subunits in the development and function of cochlear efferent innervation." Neuron **23**(1): 93-103.

Villarroel, A. and B. Sakmann (1992). "Threonine in the selectivity filter of the acetylcholine receptor channel." Biophys J **62**(1): 196-205; discussion 205-8.

Wada, E., K. Wada, *et al.* (1989). "Distribution of alpha 2, alpha 3, alpha 4, and beta 2 neuronal nicotinic receptor subunit mRNAs in the central nervous system: a hybridization histochemical study in the rat." J Comp Neurol **284**(2): 314-35.

Wanamaker, C. P., J. C. Christianson, *et al.* (2003). "Regulation of nicotinic acetylcholine receptor assembly." Ann N Y Acad Sci **998**: 66-80.

Wang, F., V. Gerzanich, *et al.* (1996). "Assembly of human neuronal nicotinic receptor alpha5 subunits with alpha3, beta2, and beta4 subunits." J Biol Chem **271**(30): 17656-65.

Wang, F. and K. Imoto (1992). "Pore size and negative charge as structural determinants of permeability in the *Torpedo* nicotinic acetylcholine receptor channel." Proc Biol Sci **250**(1327): 11-7.

Wang, H., M. Yu, *et al.* (2003). "Nicotinic acetylcholine receptor alpha7 subunit is an essential regulator of inflammation." Nature **421**(6921): 384-8.

Wang, H. L., X. Cheng, *et al.* (2008). "Control of cation permeation through the nicotinic receptor channel." PLoS Comput Biol **4**(2): e41.

Wang, H. Y., D. H. Lee, *et al.* (2000). "Amyloid peptide Abeta(1-42) binds selectively and with picomolar affinity to alpha7 nicotinic acetylcholine receptors." J Neurochem **75**(3): 1155-61.

Wang, K., J. T. Hackett, *et al.* (2004). "Regulation of the neuronal nicotinic acetylcholine receptor by SRC family tyrosine kinases." J Biol Chem **279**(10): 8779-86.

Wang, Z. Y., D. K. Okita, *et al.* (1998). "T-cell recognition of muscle acetylcholine receptor subunits in generalized and ocular myasthenia gravis." Neurology **50**(4): 1045-54.

Wang, Z. Z., C. Fuhrer, *et al.* (1996). "The nicotinic acetylcholine receptor at the neuromuscular junction: assembly and tyrosine phosphorylation." Cold Spring Harb Symp Quant Biol **61**: 363-71.

Weiland, S., V. Witzemann, *et al.* (1996). "An amino acid exchange in the second transmembrane segment of a neuronal nicotinic receptor causes partial epilepsy by altering its desensitization kinetics." FEBS Lett **398**(1): 91-6.

Wessler, I., H. Kilbinger, *et al.* (2001). "The biological role of non-neuronal acetylcholine in plants and humans." Jpn J Pharmacol **85**(1): 2-10.

Wessler, I., H. Kilbinger, *et al.* (2003). "The non-neuronal cholinergic system in humans: expression, function and pathophysiology." Life Sci **72**(18-19): 2055-61.

Wessler, I., C. J. Kirkpatrick, *et al.* (1999). "The cholinergic 'pitfall': acetylcholine, a universal cell molecule in biological systems, including humans." Clin Exp Pharmacol Physiol **26**(3): 198-205.

Wevers, A., A. Jeske, *et al.* (1994). "Cellular distribution of nicotinic acetylcholine receptor subunit mRNAs in the human cerebral cortex as revealed by non-isotopic in situ hybridization." Brain Res Mol Brain Res **25**(1-2): 122-8.

Wevers, A., L. Monteggia, *et al.* (1999). "Expression of nicotinic acetylcholine receptor subunits in the cerebral cortex in Alzheimer's disease: histotopographical correlation with amyloid plaques and hyperphosphorylated-tau protein." Eur J Neurosci **11**(7): 2551-65.

Whaley, K., D. Lappin, *et al.* (1981). "C2 synthesis by human monocytes is modulated by a nicotinic cholinergic receptor." Nature **293**(5833): 580-3.

Whitehouse, P. J., A. M. Martino, *et al.* (1986). "Nicotinic acetylcholine binding sites in Alzheimer's disease." Brain Res **371**(1): 146-51.

Whiting, P. and J. Lindstrom (1987). "Purification and characterization of a nicotinic acetylcholine receptor from rat brain." Proc Natl Acad Sci USA **84**(2): 595-9.

Whiting, P., R. Schoepfer, *et al.* (1991). "Structural and pharmacological characterization of the major brain nicotinic acetylcholine receptor subtype stably expressed in mouse fibroblasts." Mol Pharmacol **40**(4): 463-72.

Whiting, P. J. and J. M. Lindstrom (1986). "Purification and characterization of a nicotinic acetylcholine receptor from chick brain." Biochemistry **25**(8): 2082-93.

Whiting, P. J. and J. M. Lindstrom (1988). "Characterization of bovine and human neuronal nicotinic acetylcholine receptors using monoclonal antibodies." J Neurosci **8**(9): 3395-404.

Whiting, P. J., R. Liu, *et al.* (1987). "Structurally different neuronal nicotinic acetylcholine receptor subtypes purified and characterized using monoclonal antibodies." J Neurosci **7**(12): 4005-16.

Wiesner, A. and C. Fuhrer (2006). "Regulation of nicotinic acetylcholine receptors by tyrosine kinases in the peripheral and central nervous system: same players, different roles." Cell Mol Life Sci **63**(23): 2818-28.

Williams, B. M., M. K. Temburni, *et al.* (1998). "The long internal loop of the alpha 3 subunit targets nAChRs to subdomains within individual synapses on neurons in vivo." Nat Neurosci **1**(7): 557-62.

Willoughby, J. O., K. J. Pope, *et al.* (2003). "Nicotine as an antiepileptic agent in ADNFLE: an N-of-one study." Epilepsia **44**(9): 1238-40.

Wilson, G. and A. Karlin (1998). "The location of the gate in the acetylcholine receptor channel." Neuron **20**(6): 1269-81.

Wilson, G. and A. Karlin (2001). "Acetylcholine receptor channel structure in the resting, open, and desensitized states probed with the substituted-cysteine-accessibility method." Proc Natl Acad Sci USA **98**(3): 1241-8.

Wong, E. T., S. G. Holstad, *et al.* (1995). "Pharmacological and physiological properties of a putative ganglionic nicotinic receptor, alpha 3 beta 4, expressed in transfected eucaryotic cells." Brain Res Mol Brain Res **28**(1): 101-9.

Wonnacott, S. (1997). "Presynaptic nicotinic ACh receptors." Trends Neurosci **20**(2): 92-8.

Wooltorton, J. R., V. I. Pidoplichko, *et al.* (2003). "Differential desensitization and distribution of nicotinic acetylcholine receptor subtypes in midbrain dopamine areas." J Neurosci **23**(8): 3176-85.

Xiao Y, Fan H, *et al.* (2006). "Sazetidine-A, a novel ligand that desensitizes alpha4beta2 nicotinic acetylcholine receptors without activating them." Mol Pharmacol. **70**(4):1454-60.

Xiu, X., A. P. Hanek, *et al.* (2005). "A unified view of the role of electrostatic interactions in modulating the gating of Cys loop receptors." J Biol Chem **280**(50): 41655-66.

Xu, J., Y. Zhu, *et al.* (2006). "Identification of sequence motifs that target neuronal nicotinic receptors to dendrites and axons." J Neurosci **26**(38): 9780-93.

Yin, R. and E. D. French (2000). "A comparison of the effects of nicotine on dopamine and non-dopamine neurons in the rat ventral tegmental area: an *in vitro* electrophysiological study." Brain Res Bull **51**(6): 507-14.

Yu, X. M. and Z. W. Hall (1994). "A sequence in the main cytoplasmic loop of the alpha subunit is required for assembly of mouse muscle nicotinic acetylcholine receptor." Neuron **13**(1): 247-55.

Zhong, W., J. P. Gallivan, *et al.* (1998). "From *ab initio* quantum mechanics to molecular neurobiology: a cation-pi binding site in the nicotinic receptor." Proc Natl Acad Sci USA **95**(21): 12088-93.

Zhou, Y., M. E. Nelson, *et al.* (2003). "Human alpha4beta2 acetylcholine receptors formed from linked subunits." J Neurosci **23**(27): 9004-15.

Zhou, Y., J. E. Pearson, *et al.* (2005). "Phi-value analysis of a linear, sequential reaction mechanism: theory and application to ion channel gating." Biophys J **89**(6): 3680-5.

Zhu, P. J. and V. A. Chiappinelli (1999). "Nicotine modulates evoked GABAergic transmission in the brain." J Neurophysiol **82**(6): 3041-5.

Zia, S., A. Ndoye, *et al.* (1997). "Nicotine enhances expression of the alpha 3, alpha 4, alpha 5, and alpha 7 nicotinic receptors modulating calcium metabolism and regulating adhesion and motility of respiratory epithelial cells." Res Commun Mol Pathol Pharmacol **97**(3): 243-62.

Zoli, M., M. Moretti, *et al.* (2002). "Identification of the nicotinic receptor subtypes expressed on dopaminergic terminals in the rat striatum." J Neurosci **22**(20): 8785-9.

Zoli, M., M. R. Picciotto, *et al.* (1999). "Increased neurodegeneration during ageing in mice lacking high-affinity nicotine receptors." Embo J **18**(5): 1235-44.

Zwart, R., L. M. Broad, *et al.* (2006). "5-I A-85380 and TC-2559 differentially activate heterologously expressed alpha4beta2 nicotinic receptors." Eur J Pharmacol **539**(1-2): 10-7.

Zwart, R., A. L. Carbone, *et al.* (2008). "Sazetidine-A is a potent and selective agonist at native and recombinant alpha 4 beta 2 nicotinic acetylcholine receptors." Mol Pharmacol **73**(6): 1838-43.

Zwart, R. and H. P. Vijverberg (1998). "Four pharmacologically distinct subtypes of alpha4beta2 nicotinic acetylcholine receptor expressed in *Xenopus laevis* oocytes." Mol Pharmacol **54**(6): 1124-31.

APPENDIX 1

Table A.1. Primers used for concatenation of $\beta2_{(Q8)}\beta2_{(Q8)}\alpha4_{(Q8)}\beta2_{(Q8)}\alpha4$ and $\beta2_{(Q8)}\alpha4_{(Q8)}\alpha4_{(Q8)}\beta2_{(Q8)}\alpha4$ receptors

$\beta2_{(Q8)}\beta2_{(Q8)}\alpha4_{(Q8)}\beta2_{(Q8)}\alpha4$		
Subunit		**Primer sequence**
1st subunit β2	**1st step F**	Asc I Kozak β2 F **GGCGCGCC** GCCACC ATGGCCCGGCGCTGCGGCC TM = 64 °C
	1st step R	Linker β2 R TTGCTGCTGTTGCTGCTGTTGCTG ATTTAT CTTGGAGCTGGGGGCTGAGTGGTC TM = 64 °C
	2nd step F	Asc I kozak β2 F TTTAAA **GGCGCGCC** GCCACC ATGGCC TM = 66 °C
	2nd step R	Xba I Linker β2 R TTTAAA **TCTAGA** TTGCTGCTGTTGCTGCTGTTGCTG ATTTAT CTTGGAG TM = 66 °C
2nd subunit β2	**1st step F**	Xba I β2 F TTTAAA **TCTAGA** ATGGCCCGGCGCTGCGG TM = 59 °C
	1st step R	Linker β2 R TTGCTGCTGTTGCTGCTGTTGCTG TTCGAA CTTGGAGCTGGGGGCTGAGT TM = 58 °C
	2nd step F	Xba I β2 F TTTAAA **TCTAGA** ATGGCCCGGCGCTGCGG TM = 61 °C
	2nd step R	Age I Linker TTTAAA **ACCGGT** TTGCTGCTGTTGCTGCTGTTGCTG TT TM = 60 °C
3rd subunit α4	**1st step F**	Age I α4 F TTTAAA **ACCGGT** ATGGAGCTAGGGGGCCCCGG TM = 60 °C
	1st step R	Xho I Linker α4 R **CTCGAG** TTGCTGCTGTTGCTGCTGTTGCTG ATTTATGATCATGCCAGCCAGCCAGG TM = 60 °C

	2nd step F	Linker Age I TTCGAA CAGCAACAGCAGCAACAGCAGCAA **ACCGGT** TM = 60 °C
	2nd step R	Xho I Linker α4 R TTTAAA **CTCGAG** TTGCTGCTGTTGCTGCTGTTGCTG ATT TM = 61 °C
4th subunit β2	**1st step F**	Xho I β2 F TTTAAA **CTCGAG** ATGGCCCGGCGCTGCGGCCC TM = 59 °C
	1st step R	Linker β2 R TTGCTGCTGTTGCTGCTGTTGCTG ATTTAT CTTGGAGCTGGGGGCTGAGTGGTC TM = 58 °C
	2nd step F	Xho I β2 F TTTAAA **CTCGAG** ATGGCCCGGCGCTGCGGCCC TM = 61 °C
	2nd step R	Not I Linker β2 R TTTAAA **GCGGCCGC** TTTGCTGCTGTTGCTGCTGTTGCTG ATTTATCTTG TM = 60 °C
5th subunit α4	**1st step F**	Not I α4 F **GCGGCCGC** ATGGAGCTAGGGGGCCCCGGAG TM = 58 °C
	1st step R	Eco RV α4 R **GATATC** TTAGATCATGCCAGCCAGCCAGGGCG TM = 58 °C
	2nd step F	Not I α4 F TTTAAA **GCGGCCGC** ATGGAGCTAGGGGGCCCC TM = 58 °C
	2nd step R	Eco RV α4 R TTTAAA **GATATC** TTAGATCATGCCAGCCAGCCAGGGC TM = 58 °C

$\beta2_{(Q8)}\alpha4_{(Q8)}\alpha4_{(Q8)}\beta2_{(Q8)}\alpha4$		
Subunit		**Primer sequence**
2nd subunit α4	**1st step F**	Xba I α4 F TTTAAA **TCTAGA** ATGGAGCTAGGGGGCCCCGGAG TM = 59 °C
	1st step R	Linker α4 R TTGCTGCTGTTGCTGCTGTTGCTG TTCGAA GATCATGCCAGCCAGCCAGGGCG TM = 58 °C
	2nd step F	Xba I α4 F TTTAAA **TCTAGA** ATGGAGCTAGG GGGCCCCGGA TM = 61 °C
	2nd step R	Age I Linker α4 R TTTTCC **ACCGGT** TTGCTGCTGTTGCTGCTGTTGCTG TTCGAAGATCAT TM = 60 °C

Primers used for the subunit concatenation of the pentameric constructs $\beta2_{(Q8)}\beta2_{(Q8)}\alpha4_{(Q8)}\beta2_{(Q8)}\alpha4$ and $\beta2_{(Q8)}\alpha4_{(Q8)}\alpha4_{(Q8)}\beta2_{(Q8)}\alpha4$ described in Chapter 3. Linkers are underlined whereas restriction sites are shown in bold. Melting temperature (TM) of each primer is shown.

Table A.2. Primers for concatenation of $\beta2_{(AGS)}\beta2_{(AGS)}\alpha4_{(AGS)}\beta2_{(AGS)}\alpha4$ and $\beta2_{(AGS)}\alpha4_{(AGS)}\alpha4_{(AGS)}\beta2_{(AGS)}\alpha4$ receptors

$\beta2_{(AGS)}\beta2_{(AGS)}\alpha4_{(AGS)}\beta2_{(AGS)}\alpha4$		
Subunit		**Primer sequence**
1st subunit β2	**1st step F**	Asc I Kozak β2 F **GGCGCGCC** GCCACC ATGGCCCGGCGCTGCGGCC TM = 64 °C
	1st step R	Linker β2 R TTGCTGCTGTTGCTGCTGTTGCTG ATTTAT CTTGGAGCTGGGGGCTGAGTGGTC TM = 64 °C
	2nd step F	Asc I kozak β2 F TTTAAA **GGCGCGCC** GCCACC ATGGCC TM = 66 °C
	2nd step R	Xba I Linker β2 R TTTAAA **TCTAGA** TTGCTGCTGTTGCTGCTGTTGCTG ATTTAT CTTGGAG TM = 66 °C
2nd subunit β2	**1st step F**	Linker β2 F AGCGCTGGAAGTGCTGGTAGC ACGGATACAGAGGAG CGGCTGGTGG TM = 64 °C
	1st step R	Linker β2 R GGCACTTCCAGCGCTACCAGC CTTGGAGCTGGGGGCTGAGTGGTCT TM = 64 °C
	2nd step F	Xba I Linker β2 F TTTAAA **TCTAGA** GCGGGCAGCGCTGGAAGTGCTGGTAGC ACGG TM = 64 °C
	2nd step R	Age I Linker β2 R TTTAAA **ACCGGT** ACTACCGGCACTTCCAGCGCTACCAGC CTTG TM = 64 °C
3rd subunit α4	**1st step F**	Linker α4 F AGCGCTGGAAGTGCTGGTAGC CGGGCCCACGCCGAGGAGCG TM = 66 °C
	1st step R	Linker α4 R TCCAGCGCTGCCCGCACTACCGGC GATCATGCCAGCCAGCCAGGGCGG TM = 66 °C

	2nd step F	Age I Linker α4 F TTTAAA **ACCGGT** GCGGGCAGCGCTGGAAGTGCTGGTAGC CGGG TM = 66 °C
	2nd step R	Xho I Linker TTTAAA **CTCGAG** GCTACCAGCACTTCCAGCGCTGCCCGCACTACCGG TM = 66 °C
4th subunit β2	**1st step F**	Linker β2 F GCTGGAAGTGCTGGTAGCGCTGGAAGT ACGGATACAGAGGAGCGGCTGGTG TM = 63 °C
	1st step R	Linker β2 R AGCACTTCCAGCGCTGCCCGC CTTGGAGCTGGGGGCTGAGTGGTC TM = 64 °C
	2nd step F	Xho I Linker AAATTT **CTCGAG** GCCGGTAGTGCGGGCAGCGCTGGAAGTGCTGGTAGCGCTGGAAG TM=64°C
	2nd step R	Not I Linker TTTAAA **GCGGCCGC** GCTACCAGCACTTCCAGCGCTGCCCGCC TM = 64 °C
5th subunit α4	**1st step F**	Linker α4 F AGCGCTGGAAGTGCTGGTAGC CGGGCCCACGCCGAGGAGC TM = 64 °C
	1st step R	Eco RV α4 R **GATATC** TTAGATCATGCCAGCCAGCCAGGGCG TM = 64 °C
	2nd step F	Not I Linker α4 F AAATTT **GCGGCCGC** TGCGGGCAGCGCTGGAAGTGCTGGTAGC CGG TM = 64 °C
	2nd step R	Eco RV α4 R TTTAAA **GATATC** TTAGATCATGCCAGCCAGCCAGGG TM = 64 °C

$\beta2_{(AGS)}\alpha4_{(AGS)}\alpha4_{(AGS)}\beta2_{(AGS)}\alpha4$		
Subunit		**Primer sequence**
2nd subunit α4	**1st step F**	Linker α4 F AGCGCTGGAAGTGCTGGTAGC CGGGCCCACGCCGAGGAGC TM = 64 °C
	1st step R	Linker α4 R TCCAGCGCTGCCCGCACTACCGGC GATCATGCCAGCCAGCCAGGGCG TM = 64 °C
	2nd step F	Xba I Linker α4 F AAATTT **TCTAGA** GCGGGCAGCGCTGGAAGTGCTGGTAGC CGG TM = 64 °C
	2nd step R	Age I Linker AAATTT **ACCGGT** GCTACCAGCACTTCCAGCGCTGCCCGCACTACCG TM = 64 °C
3rd subunit α4	**1st step F**	Linker α4 F GCTGGAAGTGCTGGTAGCGCTGGAAGT CGGGCCCACGCCGAGGAG TM = 64 °C
	1st step R	Linker α4 R TCCAGCGCTGCCCGCACTACCGGC GATCATGCCAGCCAGCCAGGGCG TM = 64 °C
	2nd step F	Age I Linker TTTAAA **ACCGGT** GCCGGTAGTGCGGGCAGCGCTGGAAGTGCTGGTAGCGCTGGAAGT TM=64°C
	2nd step R	Xho I Linker TTTAAA **CTCGAG** GCTACCAGCACTTCCAGCGCTGCCCGCACTACCG TM = 64 °C

Primers used for the subunit concatenation of the pentameric constructs $\beta2_{(AGS)}\beta2_{(AGS)}\alpha4_{(AGS)}\beta2_{(AGS)}\alpha4$ and $\beta2_{(AGS)}\alpha4_{(AGS)}\alpha4_{(AGS)}\beta2_{(AGS)}\alpha4$ described in Chapter 3. Linkers are underlined whereas restriction sites are shown in bold. Melting temperature (TM) of each primer is shown.

Table A.3. Primers for concatenation of $\beta2_{(AGS)}\alpha4_{(AGS)}\beta2_{(AGS)}\alpha4_{(AGS)}\beta2$ and $\beta2_{(AGS)}\alpha4_{(AGS)}\beta2_{(AGS)}\alpha4_{(AGS)}\alpha4$ receptors

$\beta2_{(AGS)}\beta2_{(AGS)}\alpha4_{(AGS)}\beta2_{(AGS)}\alpha4$		
Subunit		**Primer sequence**
1st subunit β2	**1st step F**	Asc I Kozak β2 F **GGCGCGCC** GCCACC ATGGCCCGGCGCTGCGGCC TM = 64 °C
	1st step R	Linker β2 R GGCACTTCCAGCGCTACCAGC CTTGGAGCTGGGGGCTGAGTGGTC TM = 64 °C
	2nd step F	Asc I kozak β2 F TTTAAA **GGCGCGCC** GCCACC ATGGCC TM = 66 °C
	2nd step R	Xba I Linker β2 R TTTAAA **TCTAGA** ACTACCGGCACTTCCAGCGCTACCAGC CTTGG TM = 66 °C
2nd subunit α4	**1st step F**	Linker α4 F AGCGCTGGAAGTGCTGGTAGC CGGGCCCACGCCGAGGAGC TM = 64 °C
	1st step R	Linker α4 R TCCAGCGCTGCCCGCACTACCGGC GATCATGCCAGCCAGCCAGGGCG TM = 64 °C
	2nd step F	Xba I Linker α4 F AAATTT **TCTAGA** GCGGGCAGCGCTGGAAGTGCTGGTAGC CGG TM = 64 °C
	2nd step R	Age I Linker AAATTT **ACCGGT** GCTACCAGCACTTCCAGCGCTGCCCGCACTACCG TM = 64 °C
3rd subunit β2	**1st step F**	Linker β2 F GCTGGAAGTGCTGGTAGCGCTGGAAGT ACGGATACAGAGGAGCGGCTGGTG TM = 63 °C
	1st step R	Linker β2 R ACTTCCAGCGCTGCCCGC CTTGGAGCTGGGGGCTGAGTGGTC TM = 64 °C

	2nd step F	Age I Linker TTTAAA **ACCGGT** GCCGGTAGTGCGGGCAGCGCTGGAAGTGCTGGTAGCGCTGGAAGT TM=64°C
	2nd step R	Xho I Linker β2 R TTTAAA **CTCGAG** GCTACCAGCACTTCCAGCGCTGCCCGC CTTGG TM = 64 °C
4th subunit α4	**1st step F**	Linker α4 F AGCGCTGGAAGTGCTGGTAGC CGGGCCCACGCCGAGGAGC TM = 64 °C
	1st step R	Linker α4 R TCCAGCGCTGCCCGCACTACCGGC GATCATGCCAGCCAGCCAGGGCG TM = 64 °C
	2nd step F	Xho I Linker α4 F AAATTT **CTCGAG** GCGGGCAGCGCTGGAAGTGCTGGTAGC CGG TM = 64 °C
	2nd step R	Not I Linker AAATTT **GCGGCCGC** GCTACCAGCACTTCCAGCGCTGCCCGCACTACCG TM = 64 °C
5th subunit β2	**1st step F**	Linker β2 F CAGCGCTGGAAGTGCTGGTAGCGCTGGAAGT ACGGATACAGAGGAGCGGCTGGTGG TM =64°C
	1st step R	Eco RV β2 R GCGGCCGC **GATATC** TTACTTGGAGCTGGGGGCTGAGTGGTC TM = 64 °C
	2nd step F	Not I Linker β2 F TTTAAA **GCGGCCGC** TGCCGGTAGTGCGGGCAGCGCTGGAAGTGCTGGTAGCGCT TM = 64 °C
	2nd step R	Eco RV β2 R TTTAAA **GCGGCCGC** GATATCTTACTTGGAGCTG TM = 64 °C

$\beta2_{(AGS)}\alpha4_{(AGS)}\beta2_{(AGS)}\alpha4_{(AGS)}\alpha4$		
Subunit		**Primer sequence**
5th subunit α4	**1st step F**	Linker α4 F GCTGGAAGTGCTGGTAGCGCTGGAAGT CGGGCCCACGCCGAG GAGC TM = 64 °C
	1st step R	Eco RV α4 R **GATATC** TTAGATCATGCCAGCCAGCCAGGGCG TM = 64 °C
	2nd step F	Not I Linker TTTAAA **GCGGCCGC** TGCCGGTAGTGCGGGCAGCGCTGGAAGTGCTGGTAGCGCT TM = 64 °C
	2nd step R	Eco RV α4 R TTTAAA **GATATC** TTAGATCATGCCAGCCAGCCAGGG TM = 64 °C

Primers used for the subunit concatenation of the pentameric constructs $\beta2_{(AGS)}\alpha4_{(AGS)}\beta2_{(AGS)}\alpha4_{(AGS)}\beta2$ and $\beta2_{(AGS)}\alpha4_{(AGS)}\beta2_{(AGS)}\alpha4_{(AGS)}\alpha4$ described in Chapter 3. Linkers are underlined whereas restriction sites are shown in bold. Melting temperature (TM) of each primer is shown.